The role of Merlin in Cardiovascular Disease.

Chun Xu Shan, B.Sc, M.Sc

Thesis Submitted to Dublin City University (DCU) for the Degree of Doctor of Philosophy (Ph.D)

Research was carried out in the School of Health and Human Performance, DCU under the supervision of Doctor Ronan Murphy.

School of Health and Human Performance

July 2013

Dublin City University

Declaration

I hereby certify that this material, which I now submit for assessment on the programme of study leading to the award of Doctor of Philosophy is entirely my own work, that I have exercised reasonable care to ensure that the work is original and does not to the best of my knowledge breach any law of copyright, and has not been taken from the work of others save and to the extent that such work has been cited and acknowledged within the text of my work.

Signature: _____   **I.D.**___58120866____

Poster Presentations

Chun. Shan, Andrew. Murphy, Philip. Cummins, Ronan. Murphy. Merlin and the ERM-Vascular Wizardry or just old fashioned Rac n' Rho. (Bio) pharmaceutical & Pharmacological Sciences research day 2011, Dublin City University.

Chunxu Shan, Andrew Murphy, Brian McDonnell, Paul Dowling, Ciaran McGinn, Philip Cummins, Ronan Murphy. The role of Merlin in Haemodynamic Regulation of Cytoskeleton Organization and Cell Adhesion in Endothelial Cells. North American Vascular Biology Organization (NAVBO) Workshop: Vascular Matrix Biology and Bioengineering Workshop 2011; Hyannis MA, USA.

Chunxu Shan, Andrew Murphy, Brian McDonnell, Ciaran McGinnis, Paul Dowling, Philip Cummins, Ronan Murphy. Molecular and Cellular Dynamics of Merlin in Vascular Cells via Mechamotransduction. Arteriosclerosis, Thrombosis, Vascular Biology (ATVB). Workshop: Vascular Cells, Inflammation and Thrombosis 2012; Chicago - Chicago, IL, USA.

Chunxu Shan, Brian McDonnell, Paul Dowling4, Ciaran McGinn, Philip Cummins, Ronan Murphy. The Role of the Actin binding proteins Merlin, in the pathogenesis of Cardiovascular disease. The 8th international symposium on Biomechanics in Vascular Biology and Cardiovascular Disease. 2013; Rotterdam, Holland.

Contents

Chapter 2

Abbreviations

2-D-DIGE	2-D Fluorescence Difference Gel Electrophoresis
aa	Amino Acid
ABP	Actin Binding Protein
Abl	Abelson Tyrosine Kinase
ACE	Angiotensin converting enzyme
ADP	Adenosine Di-phosphate
Ang	Angiotensin
APS	Ammonium Persulphate
Arp2/3	Actin related protein 2/3
ATP	Adenosine Tri-Phosphate
BCA	Bicinchoninic acid
BSA	Bovine Serum Albumin
cDNA	Complimentary DNA
C-Terminal	Carboxyl Terminal
CVD	Cardiovascular disease
DAG	Diacylglycerol
DMSO	Dimethlysulphoxide
DNA	Deoxyribonucleic acid
dNTP	Deoxy nucleotide tri-phosphate

EC	Endothelial Cells
ECM	Extracellular matrix
EDTA	Ethylenediaminetetraacetic acid
EDRF	Endothelial derived relaxing factor
EGFR	Epidermal Growth Factor
eNOS	Endothelial nitric oxide synthase
ERK	Extracellular signal-regulated kinase
ERM	Ezrin/Radixin/Moesin
F-actin	Filamentous − Actin
FAK	Focal Adhesion Kinase
FBS	Foetal Bovine Serum
FD40	FITC-Dextran 40kDa
FERM	(F for 4.1 protein, E for ezrin, R for radixin and M for moesin)
FITC	Fluorescein isothiocyanate
G-Actin	Globular - Actin
GDP	Guanine Di-Phosphate
GEF	Guanine nucleotide exchange factor
GFP	Green Fluorescent Protein
GST	Gluthione S-Transferase
GTP	Guanine Tri-Phosphate
HAEC	Human Aortic Endothelial Cell

ICAM	Intracellular Adhesion Molecule
IGF	Insulin like growth factor
LASP	LIM And SH3 Protein
LSS	Laminar Shear Stress
MAPK	Mitogen Activated Protein Kinase
MLCK	Myosin light chain kinase
$MgCl_2$	Magnesium Chloride
Mn	Manganese
NaCl	Sodium Chloride
NaOH	Sodium Hydroxide
NFκB	Nuclear factor $-$ κB
NO	Nitric oxide
PAGE	Polyacrylamide gel electrophoresis
PAK	p21-activated kinase
PBS	Phosphate buffered saline
PCR	Polymerase chain reaction
PDGF	Platelet derived growth factor
PECAM	Platelet Endothelial Cell Adhesion Molecule
PI3K	Phosphatidylinositol-3-kinase
PKC	Protein kinase C
P/S	Penicillin/Streptomycin
qRT-PCR	Quantitative Real-Time - PCR

Raf	Receptor associated factors
RAP	Ras like Protein
Rho Ras	Homology gene family
RNA	Ribonucleic acid
ROS	Reactive oxygen species
Rpm	Rotations per minute
RT-PCR	Reverse transcriptase $-$ PCR
SDS	Sodium dodecyl sulphate
SSB	Sample Solubilisation Buffer
ss	Single stranded
siRNA	Small interfering RNA
SRSRY	(S for serine, R for arginine and Y for tyrosine) peptide
TAE	Tris acetate EDTA
TE	Tris $-$ EDTA
TEE	Trans-Endothelial Exchange
TEMED	N,N,N', N'-Tetramethylethlylenediamine
TF	Tissue Factor
TGF-β	Transforming growth factor $-$ β
t-PA	Tissue Plasminogen activator
uPA	Urokinase
uPAR	Urinokinase plaminogen activator receptor
VASP	Vasodilator Stimulated Phosphoprotein

VE	Vascular Endothelial
VEGF	Vascular Endothelial growth factor
VEGFR	VEGF - Receptor
VSMC	Vascular Smooth Muscle Cells
VWF	Von Willebrand Factor
WASP	Wiskott-Aldrich syndrome protein
WAVE	WASP family verpolin-homologous protein

Units

bp	Base pairs
cm	Centimetre
^{o}C	Degree Celsius
kDa	KiloDaltons
µg	Microgram
µl	Microlitre
µM	Micromolar
g	Grams
hr	Hours
kg	Kilogram
L	Litre
M	Molar
mA	Milliamperes
mg	Milligrams
min	Minutes
ml	Millilitres
mM	Millimolar
ng	Nanograms
nm	Nanometres
pmol	Picomolar

Sec	Seconds
w/v	Weight per volume
V	Volts

Index of Tables and Figures

Tables

This table displays the results of merlin CO-IP elution sampled. The results pointed that compared with controls, merlin protein binding to many proteins include tubulin, myosin light chain 6B, annexin and actin. This result further confirmed our last co-localisation study that merlin present at numerous functional sites of stress fibres, focal adhesion, at sites of cell-cell contact and the leading cell edge in lamellipodial regions.

Chapter 5

Figures

Chapter1

Figure 1.1: The structure of human heart.

Human heart consists of four chambers: right and left atria and right and left ventricles. The atria and ventricles are separated by atrioventricular valves (AVs); the atria and arteries are separated by semilunar valves.

Figure 1.2: Anatomical structure of vasculature system.

This imagines showing the three layers of blood vessel and how the blood flow basically circulates within the vascular system.

Figure 1.3: The pie charts showing the percentage of all global death in different diseases.

The red part represents the death number of cardiovascular disease which occupies about 30% of all global death.

Figure 1.4: The progression of atherosclerosis

A) Activated EC increase its permeability that allow diffusion of LDL inside vascular wall which in turn attract adhesion and migration monocytes and macrocytes. B) Fatty streak is the first sign of an atherosclerotic plaque which can be observed in children age 10 to 14. At early stage fatty streaks appear as yellow grease which running along the artery wall. C) As fatty streaks progress to intermediate lesions, they form a fibrous cap that isolate the lesion form blood flow. D) The complicated lesion occurs when the fibrous cap breaks and expose sub-endothelial layer to platelets and complement factors triggers a thrombotic response.

Figure 1.5:   The Cytoskeleton

Figure 1.6:   Structural comparison of Merlin and ERM proteins.

(A) The amino acid sequence of the erythrocyte protein 4.1 superfamily. Varies colour bars show the location of different domains. The oval blue shapes represent FERM membrane protein binding domains (also called N-ERMAD). The yellow and golden region represent α-helix domain. The actin binding domains on C-terminal are depicted by green box which is absent on merlin. (B) Showing the varies binding site of ERM and their binding partners.

Figure 1.7:   Crystal structure and superposition of the FERM domains.

A, colour 3D crystal structure represent the merlin FERM domain. Merlin FERM contains three subdomains, subdomain A is colour as green, subdomain B is colour as blue-green and subdomain C is colour blue respectively. Gray represents the C-terminal α-helical segment that is linked to FERM domain by linker region (brown). B, Comparison of the FERM domain in merlin (blue) with radixin (brown). The arrow shows the deletion site of merlin.

Figure 1.8:   Haemodynamic force

Shear stress: the frictional force of blood flow against the endothelium. Cyclic strain: the physical stretch to the vessel generated by the circulating blood pressure.

Figure 1.9:   Endothelial mechanosensors.

The figure shows the endothelial mechanosensors and their localizations. Ion channels, ATP channels, heterotrimeric G proteins, glyocalyx and G-protein-coupled receptors (GPCRs) exist on apical surface and transfer various mechanical stimuli. PECAM-1, VE-Cadherin and ECAM-1 present at literally cell membrane and involved in cell communication. Integrins, meanwhile connect the cell to ECM.

while cells on the bottom and left side were counted. This procedure prevented the accidental double-counting of cells.

Figure 2.2:   (A) The ADAMTM counter and (B) loading of an AccuChip.

To count cells, cell suspensions were mixed with both solutions at a 1:1 ratio and 20 μl of each mixture loaded into an AccuChip cell count chip. Once inside the ADAMTM instrument, the chip was then processed, with the result displayed on the LCD screen.

Fig. 2.3:   Illustration of the orbital shaker and its operation during shear stress studies

Fig.2.4:   Ibidi® flow system used in laminar shear studies.

(A): Ibidi® pressure pump connected to Ibidi® flow unit and Y-shaped slide. (B): Illustration of Y-shaped and straight Ibidi® μ-slides, which allow different forms of shear stress to be investigated.

Figure 2.5:   Illustration of the computer-controlled Flexercell system apparatus, and its mechanism of operation in vascular cyclic strain simulation.

Figure 2.6:   Wet transfer cassette assembly

The cassette was inserted into the Trans Blot Module with the black side facing to the same colour. Proteins were transferred at 100 V for 2 hrs. or overnight at 4°C in the cold room at 50V while stirring.

Figure 2.9:   Microporator apparatus

A) The base unit generates electrical parameters necessary for transfection of DNA and siRNA into cells. B) The apparatus utilises a tube (containing the electroporation buffer) and custom pipette used to deliver the electroporation parameters to the cells

suspended within a gold-plated pipette tip. C) The microporation kit containing the necessary microporation solutions, tips and microporation tubes.

Fig 2.7:   xCELLigence® system

The xCELLigence® system (Roche, Basal, Switzerland) is a novel system that allows monitoring of cell migration, adhesion and proliferation in real time without any labeling A) xCELLigence® system used for cell adhesion and migration assays. B) CIM- plate for migration assay. C) E-plate for adhesion and proliferation assay.

Chapter 3

Figure 3.1:   Human Aortic Endothelial cell (HAECs) morphological a lterations in response to LSS and DSS compared to static control cells.

HAECs were sheared at 10 dynes for 24 hrs. using the Ibidi® system.   B) Compared with the static control (A), HAECs realigned in the direction of LSS. White arrows indicate the direction of flow.   No uniform F-actin realignment was observed under DSS conditions.   Images are representative.   C) Site of curvature.   D) Site of bifurcation.

Figure 3.2:   F-actin staining.

Confluent HAECs were exposed to LSS (10 dynes/cm^2, 24 hrs.), and monitored for F-actin realignment using confocal microscopy (phalloidin stain for F-actin). Results indicated that HAEC F-actin filaments realigned in the direction of flow under shear stress. The white arrows show the directions of LSS.

Figure 3.3:   The effect of shear stress on Merlin protein expression

Following exposure of 10 dynes/10cm^2 of physiological, laminar, shear stress over a 24 hr. time period using the orbital rotator, cell lysates were analysed by Western blot.   Studies A) were conducted on sub-confluent cells seeded at 10^4cells/cm^2. Studies B) were conducted on fully-confluent cells seeded at a

density of 10^5cells/cm^2.   C) Histograms represent fold change in band intensity relative to un-sheared controls and are averaged from three independent experiments.   All values were controlled for equal loading by equalising for corresponding GAPDH protein.

Figure 3.4:   The effect of shear stress on Phosphorylated Merlin protein expression

Following exposure of to 10 dynes/10cm^2 of laminar shear stress over a 24 hr. time period using an orbital rotator, both sub-confluent cells (seeded at 10^4 cells/cm^2) and fully-confluent cells (seeded at 10^5 cells/cm^2) were lysed and analysed by Western blotting.   Histograms represent fold change in band intensity relative to un-sheared controls and were averaged from three independent experiments.   All values were controlled for equal loading by equalising for corresponding GAPDH protein.

Figure 3.5:   The effect of cyclic strain on Merlin protein expression

Following exposure of to 5% and 10% cyclic strain over a 24 hr. time period using the Flexercell Tension Plus™ FX-4000T™ system, cell lysates were analysed by Western blotting. A) Histograms represent fold change in band intensity relative to un-strained controls and were averaged from three independent experiments. B) Western blot analysis of Merlin expression (75KD) in HAECs following 24 hr. cyclic strain.   All values were controlled for equal loading by equalising for corresponding GAPDH.

Figure 3.6:   The effect of cyclic strain on Phosphorylated Merlin protein expression

Following exposure of to 5% and 10% cyclic strain over a 24 hours period using a Flexercell Tension Plus™ FX-4000T™ system, cell lysates were analysed by Western blot.   Histograms represent fold change in band intensity relative to unstrained controls and were averaged from three independent experiments. All values were controlled for equal loading by equalising for corresponding GAPDH.

Figure 3.7:   The effect of 20% cyclic stretch on Phosphorylated Merlin
                    protein expression

                    Following exposure of 20% cyclic stretch at time point of 1
                    minute, 5 minute and 10 minute using the Flexercell Tension
                    Plus™ FX-4000T™ system, cell lysates were analysed by
                    Western blot.   A) Western blot analysis of Phosphorylated
                    Merlin expression (75KD) in HAECs after exposure to 20%
                    cyclic strain at different time points.   B) Histograms
                    represent fold change in band intensity relative to
                    un-stretched controls and were averaged from three
                    independent experiments.   All values were controlled for
                    equal loading by equalising for corresponding GAPDH.

Figure 3.8:   Merlin mRNA expression change under haemodynamic
                    stimulus.

                    A) Following exposure of 10 dynes/10cm^2 of laminar shear
                    stress over a 24 hr. time period using the orbital rotator, and
                    B) following exposure of 5% and 10% cyclic strain over a
                    24 hr. time period using the Flexercell Tension Plus™
                    FX-4000T™ system, Merlin mRNA was extracted and a
                    two-step QRT-PCR carried out using specific primer sets for
                    the measurement of Merlin gene expression.   Results were
                    normalised to the housekeeping gene, 18s, and histograms
                    represent normalised values relative to the un-sheared
                    control.

Figure 3.9:   The effect of shear stress on vascular endothelial cells and
                    Merlin co-localisation with F-actin

                    HAECs were exposed to static and 10 dynes/cm^2 laminar
                    shear stress for 24 hrs. Cellular localisation of Merlin was
                    analysed by immunofluorescent imaging, co-staining for
                    F-actin and monitoring of Merlin (green) with F-actin
                    (yellow) by standard fluorescent microscopy.   HAEC
                    F-actin filaments realigned in the direction of flow under
                    LSS while and no F-actin filaments realignments were
                    observed under static conditions.   (Arrow showing the
                    direction of blood flow).

Figure 3.10:   Merlin localisation by immunofluorescence microscopy.

Cellular localisation of Merlin was analysed by immunofluorescent imaging. Arrows indicate Merlin localisation with action at the stress fibres (A), focal adhesions (B), cell-cell junction (C), and lamellipodia leading edges (D).

Chapter 4

Figure 4.3:   Optimisation of Merlin siRNA concentrations.

HAECs were transfected with Merlin siRNA at different concentration using microporator (Digital Bio), and cells were then incubated at 37oC for 48 hr. Cell lysates were analysed by western blot. A) Western blot analysis of Merlin (75KD) expression change after transfected with siRNA. B) Histograms represent fold change in band intensity relative to scrambled controls. . All values were controlled for equal loading by equalising for corresponding GAPDH.

Figure 4.4:   The effect of ECM on Merlin absent HAECs adhesion

The effect of ECM on Merlin absent HAECs adhesion was studied using xCelligence system. Merlin knock down HAECs were seeded into E-plate which was pre-coated with fibronectin (Green), fibrinogen (Blue), Laminin (Pink) and Vitronectin (Cyan), at a concentration of 30,000 cells/well. Plate with no coating (Red) was set as control. Results appear to indicate that: the graphs shows merlin absent HAECs preferential adhesion to VN and Histograms represent slope changes according with CI value of ECMs related to no-coating control.

Figure 4.5:   The role of Merlin absence on HAECs –ECM adhesion.

The role of Merlin absence on HAECs –ECM adhesion was studied using xCelligence system. Merlin knock down HAECs were seeded into E-plate which was pre-coated with fibronectin (A), fibrinogen (B), Laminin (C) and Vitronectin (D), at a concentration of 30,000 cells/well. Graphs illustrate that absent of Merlin (Red) increase HAECs adhesion to all ECM compared with scrambled control (Green).

Figure4.6:   The role of Merlin absence on HAECs' migration.

The role of Merlin absence on HAECs migration was studied using xCelligence system. Merlin knock down HAECs were seeded into CIM-plate at a concentration of 30,000 cells/well. Graphs illustrate that absent of Merlin (Green) increase HAECs migration compared with scrambled control (Blue). Histograms represent slope change according with CI values related to scrambled control.

Figure 4.7:   The role of laminar shear stress on Merlin absent HAECs adhesion.

The role of laminar shear stress on HAECs adhesion was studied using xCelligence system. Following 10 dynes/cm^2 24 hours shear, both scrambled and merlin absent cells were seeded into E-plate at concentration of 30,000cells/well. Graphs illustrate that the effect of LSS on absent of Merlin HAECs adhesion. Green: scrambled control; Blue: merlin knock-down; Pink: sheared; Cyan: merlin knok-downed+sheared. Histograms represent slope change according with CI values.

Figure 4.8:   The role of laminar shear stress on Merlin absent HAECs migration.

The role of laminar shear stress on HAECs adhesion was studied using xCelligence system. Following 10 dynes/cm^2 24 hours shear, both scrambled and merlin absent cells were seeded into E-plate at concentration of 30,000cells/well. Graphs illustrate that the effect of LSS on absent of Merlin HAECs migration. Cyan: scrambled control; Pink: sheared; Green: merlin knock-down; Blue: merlin knok-downed+sheared. Histograms represent slope change according with CI values.

Figure 4.9:   The role of cyclic strain on Merlin absent HAECs adhesion.

The role of cyclic strain on HAECs adhesion was studied using xCelligence system. Following 10% 24 hours strain, both scrambled and merlin absent cells were seeded into E-plate at concentration of 30,000cells/well. Graph illustrate that the effect of cyclic strain on merlin absent HAECs adhesion: Green: scrambled control; Blue: merlin knock-down; Pink: strained; Cyan: merlin knok-downed+sheared. Histograms represent the slope change according to the CI value.

Figure 4.10:   The role of cyclic strain on Merlin absent HAECs migration.

The role of cyclic strain on HAECs adhesion was studied using xCelligence system. Following 10% 24 hours strain, both scrambled and merlin absent cells were seeded into E-plate at concentration of 30,000cells/well. Graph illustrate that the effect of cyclic strain on merlin absent HAECs migration: Green:

scrambled control; Blue: merlin knock-down; Pink: strained; Cyan: merlin knok-downed+sheared. Histograms represent the slope change according to the CI value.

Figure 4.11:   The model of merlin "open and close conformation".

Xu demonstrated that merlin binding to polymerized actin at its N-terminal domain mapping to residues 178–367. This interaction is not affected folding of merlin which is considered as "close conformation". The "closed conformation" may serve as a docking site that allows merlin interacts with its critical effector proteins that fail of merlin growth suppressor function. In contrast, interaction of merlin with microtubules exists in an ''open conformation". Merlin is unable to associate with microtubules in the ''closed conformation", due to the losses of the correct conformation necessary for this association.

Figure 4.12:   Crosstalk between actin filaments and microtubule, and their interaction with focal adhesion.

Microtubules are stabilized at the plus ends and oriented towards to the leading edge of migrating cell where it interacts with FA. Several proteins are involved in the processes, including cross-linker proteins which possess both actin- and microtubule-binding domains and actin-based motor protein myosin. The local targeting of microtubules modulates the activities of Rho family GTPases, resulting in the regulation of focal adhesion turnover

Chapter 5

Figure 5.1:   uPA-uPAR and their interacting receptors

Figure 5.2:   The role of RGDs mediated integrin inhibition on the HAECs adhesion

The role of RGDs mediated integrin inhibition on wild type HAECs adhesion was studied using xCelligence system. HAECs were seeded into E-plate which was pre-treated with either RGD1, RGD2, or RGD3, at a concentration of 30,000cells/well.

Untreated cells were used for control. Graphs illustrate that compared with untreated control; RGD inhibitors significantly decrease HAEC's adhesion. The histogram represents slope changes according with CI value change of RGDS treated HACEs related to no-treated control.

Figure 5.3:   The inhibitions of RGD inhibitors on uPA mediated HAECs adhesion

The inhibition of RGDs inhibitors on uPA mediated wild type HAECs adhesion was studied using xCelligence system. HAECs were seeded into E-plate which was pretreated with uPA and either RGD1, RGD2, or RGD3 (the concentration is described in material and method), at a concentration of 30,000cells/well. Untreated cells were used for control. Graphs illustrate that compared with untreated control; uPA increases HAECs' adhesion which is significantly inhibited by addition of RGD inhibitors. The histogram represents slope changes according with CI value change.

Figure 5.4:   The inhibition of RGDs inhibitors on D2A mediated wild type HAECs adhesion

The inhibition of RGDs inhibitors on D2A mediated wild type HAECs adhesion was studied using xCelligence system. HAECs were seeded into E-plate which was pretreated with D2A and either RGD1, RGD2, or RGD3 (the concentration is described in material and method), at a concentration of 30,000cells/well. Untreated cells were used for control. Graphs illustrate that compared with untreated control; D2A increases HAECs' adhesion which is significantly inhibited by addition of RGD inhibitors. The histogram represents slope changes according with CI value change.

Figure 5.5:   The inhibition of RGD inhibitors on SRSRY peptide mediated HAECs adhesion.

The inhibition of RGDs inhibitors on SRSRY mediated wild type HAECs adhesion was studied using xCelligence system. HAECs were seeded into E-plate which was pretreated with SRSRY and either RGD1, RGD2, or RGD3 (the concentration is described in material and method), at a concentration of 30,000cells/well. Untreated cells were used for control. Graphs illustrate that

compared with untreated control; SRSRY increases HAECs' adhesion which is significantly inhibited by addition of RGD inhibitors. The histogram represents slope changes according with CI value change.

Figure 5.6:   The role of RGD-1 mediated integrin inhibition on the merlin absent HAECs adhesion

The role of RGD1 mediated integrin inhibition on the merlin absent HAECs adhesion was studied using xCelligence system. Both Merlin absent and scrambled control HAECs were seeded into E-plate which was pre-treated with RGD1 at a concentration of 30,000cells/well. Untreated scrambled control HAECs were used as control. Graphs illustrate that compared with untreated control, the treatment of RGD 1 inhibitor significantly reduce the effect of merlin absence on HAECs adhesion. The histogram represents slope changes according with CI value change.

Figure 5.7:   The role of RGD-2 mediated integrin inhibition on the merlin absent HAECs adhesion

The role of RGD2 mediated integrin inhibition on the merlin absent HAECs adhesion was studied using xCelligence system. Both Merlin absent and scrambled control HAECs were seeded into E-plate which was pre-treated with RGD2 at a concentration of 30,000cells/well. Untreated scrambled control HAECs were used as control. Graphs illustrate that compared with untreated control, the treatment of RGD 2 inhibitor reduce the effect of merlin absence on HAECs adhesion. The histogram represents slope changes according with CI value change.

Figure 5.8:   The role of RGD-3 mediated integrin inhibition on the merlin absent HAECs adhesion

The role of RGD-3 mediated integrin inhibition on the merlin absent HAECs adhesion was studied using xCelligence system. Both Merlin absent and scrambled control HAECs were seeded into E-plate which was pre-treated with RGD3 at a concentration of 30,000cells/well. Untreated scrambled control HAECs were used as control. Graphs illustrate that compared with untreated control, the treatment of RGD3 inhibitor significantly reduce the effect of merlin absence on HAECs adhesion. The histogram

represents slope changes according with CI value change.

Figure 5.9:   The role of RGD-1 mediated integrin inhibition on the merlin absent HAECs migration

The role of RGD-1 mediated integrin inhibition on the merlin absent HAECs adhesion was studied using xCelligence system. Both Merlin absent and scrambled control HAECs were seeded into upper chamber of CIM-plate at a concentration of 30,000cells/well. The lower chamber was pre-treated with RGD-1 inhibitor. Graphs illustrate that compared with untreated control; RGD-1 inhibitors significantly reduce merlin absent HAEC's migration. The histogram represents slope changes according with CI value change.

Figure 5.10:   The role of RGD-2 mediated integrin inhibition on the merlin absent HAECs migration

The role of RGD-2 mediated integrin inhibition on the merlin absent HAECs adhesion was studied using xCelligence system. Both Merlin absent and scrambled control HAECs were seeded into upper chamber of CIM-plate at a concentration of 30,000cells/well. The lower chamber was pre-treated with RGD-1 inhibitor. Graphs illustrate that compared with untreated control; RGD-2 inhibitors reduce merlin absent HAEC's migration slightly. The histogram represents slope changes according with CI value change.

Figure 5.11:   The role of RGD-3 mediated integrin inhibition on the merlin absent HAECs migration

The role of RGD-3 mediated integrin inhibition on the merlin absent HAECs adhesion was studied using xCelligence system. Both Merlin absent and scrambled control HAECs were seeded into upper chamber of CIM-plate at a concentration of 30,000cells/well. The lower chamber was pre-treated with RGD-1 inhibitor. Graphs illustrate that compared with untreated control; RGD-3 inhibitors significantly reduce merlin absent HAEC's migration. The histogram represents slope changes according with CI value change.

loss of merlin activity results free of integrin binding site that promote interaction between integrin and the integrin–actin linkage proteins including talin, vinculin, Kindlins and α-actinin. The Rac, CDC42 and Rho pathways are then activated following the binding of above proteins to integrin which in turn lead to formation of various functional migration structures such as filopodia, lamellipodia and stress fiber.

Abstract

Atherosclerosis is a disease characterised by the development and progression of many physiological changes within the vessel walls of the cardiovascular system. The principle hallmark change is thickening and loss of elasticity of the arterial wall. Atherosclerosis normally occurs at large and medium-sized muscular elastic arteries; the aorta, coronary and cerebra, principally at the site of arterial bifurcation and regions of high curvature. At such sites, the more complex blood flow pattern such as disturbed shear stress pattern forms which contributes to the development of atherosclerosis. Endothelial integrity plays a pivotal role in normal blood vessel function and the disruption of which will lead to the initiation and progression of atherosclerosis. The actin cytoskeleton and its dynamics, provides endothelial structural integrity and well as playing a pivotal role in many cellular processes, such as gene transcription, signal transduction, and cell cycle. Cytoskeletal homeostasis can be greatly disrupted by many factors, such as inflammation and haemodynamic forces. Altered actin dynamics underpins many (patho-) physiological processes in endothelial cells such as migration, differentiation, proliferation and adhesion.

Merlin, an actin adaptor proteins which belong to the ERM protein family, has been well characterised as a tumour suppressor. In this study, we utilized various novel techniques including for hemodynamic modelling of biomechanical forces to subject human aortic endothelial cells to specific shear stress and cyclic strain at both biological and pathological levels. We demonstrated that merlin is highly sensitive to haemodynamic stimuli including shear stress and cyclic strain. Merlin is seen to localise at many sites of dynamic actin such as focal adhesion, cell-cell contact, stress fibre and leading edge of migrating cell. This study has also demonstrated that merlin plays an important role in the regulation of HAEC adhesion and migration through integrin

mediated pathways. Knock-down of merlin greatly increased HAEC adhesion and migration. By using various ECMs, it has been show that merlin knock-down HAECs preferentially adhere to vitronectin and Fibronectin; both of them contain the adhesive sequence (RGD) that selectively binds to integrins such as $\alpha v \beta 3$. This was further illustrated using various specific RGD inhibitors, which demonstrated that merlin orchestrated migration was principally mediated by $\alpha v \beta 3$. Moreover, we also discovered another cell surface receptor-uPAR is involved during merlin-integrin mediated mechano-transduction. Overall, we have demonstrated for the first time that merlin plays a crucial role in the vasculature.

Chapter One

Introduction

1.0 Introduction.

1.1 The vascular system.

The vascular system is a closed transport system composed of the heart, blood vessels, and capillaries, as well as the lymphatic system. The rhythmic and endless heart beatings promote unidirectional blood flow cycle within the cardiovascular system which provides humoral materials for cells in the body, including nutrients, and oxygen. The blood flow also removes cellular metabolic waste products, such as carbon dioxide for excretion. Meanwhile, through the blood transport, many hormones and other information materials reach their target organs which function to coordinate whole body functions and homeostasis, including the immune system, hemostasis and regulation of vascular tone.

Blood circulation was first described by William Harvey in 1628 (Fishman 1982). However, he did not fully understand how blood flow exchange through tissue due to the technological limitations. In 1661, following the development of the microscope, an Italian scientist, Marcello Malpighi discovered capillaries between the artery and vein, supporting Harvey's hypothesis (Toffoletto 1965). Since then, intensive studies have contributed to our current knowledge and understanding of the cardiovascular system and hemostasis.

Any imbalance in the homeostasis of blood circulation can give rise to many patho-physiological conditions and metabolism disorders. In oxygen sensitive organs, such as the brain, unconsciousness may occur as soon as 3 minutes upon the loss of brain blood supply. More than half of patients suffer irreversible brain and heart damage after 10 minutes of blood circulation insufficiency.

1.1.1 The basic structure of the cardiovascular system.

1.1.1.1 Heart.

The heart is an organ comprised principally of cardiac muscle, which plays a pivotal role in the cardiovascular system. It is essentially a pump, which not only keeps the blood circulating, but also ensures it flows in the right direction. The heart may be divided into two sides, right sides and left sides; the right side of the heart pumps blood to the lungs, while the left side pumps blood to the rest of the body (Figure 1). Each side of the heart can also be further divided into two chambers: the two upper chambers are named as the atria, and two lower chambers are named as the ventricles.

The right atrium collects the deoxygenated blood from all around the body and passes it into the right ventricle. The deoxygenated blood is then pumped to the lungs by the right ventricle, where the blood is oxygenated. The oxygenated blood flows into the left atrium, and is transferred into the left ventricle, which pumps the oxygenated blood to the whole body. The atrium, ventricles and arteries are separated by a fibrous tissue structures, termed atrioventricular (AV) and semilunar valves, which ensure the correct, unidirectional flow of blood.
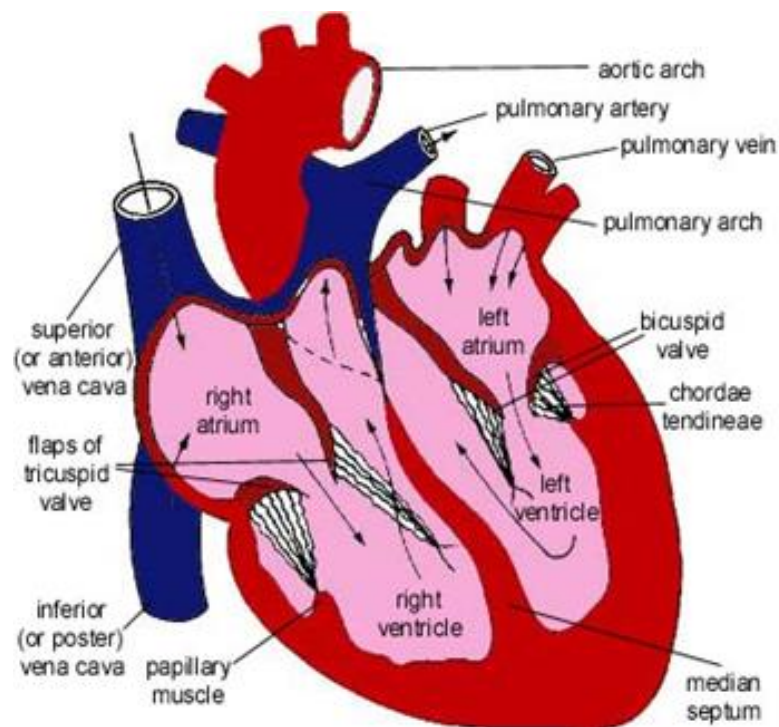
Figure 1.1:   Structure of the human heart.

The human heart consist of four chambers: right and left atria and right and left ventricles.   The chambers are separated by atrioventricular valves (AVs), while the atria and arteries are separated by semilunar valves. (www.library.thinkquest.org/.../structure.htm)

1.1.1.2 Blood vessels.

Blood vessels can be basically divided to three separate subclasses: arteries, capillaries and veins. With the exception of capillaries, artery and vein share a common three layer structures: tunica adventitia, tunica media and tunica intima.

(i) Tunica adventitia.

As the outmost layer, the tunica adventitia is mainly comprised of loose elastic connective tissue and collagen fibres, which separates blood vessels from surrounding tissues and prevents over dilation of vessels during heart contraction. The main components of the connective tissue are fibroblasts, which have the ability to repair adventitia during injury. In some large vessels, tunica adventitia also contains tiny vessels that supply the essential nutrients to the vessel walls.

(ii) Tunica media.

The layer between tunica adventitia and tunica intima is named as tunica media that composed of elastic fibres and smooth muscle cells. The thickness and composition of this layer varies depending on the function and diameters of the vessels. For example, the large arteries which transport blood under high pressure contain proportionally more elastic fibres than SMCs, which therefore permit the vessels to dilate during heart contractions that reducing the resistance of circulation. The middle and small arteries, known as arterioles, contain more SMCs that play an important role in regulation of vascular tone. Many scientists believe that vascular smooth muscle is a subtype of fibroblasts, due to its ability to product extracellular matrix (ECM) such as collagen fibres and elastic fibres during the development of the artery. Under pathological conditions, SMCs migrate into the intima where they secret additional ECMs which in turn cause development of fatty streaks leading to atherogenesis.

(iii) Tunica intima.

The intima (tunica intima) is both the innermost and thinnest layer of the vascular wall, and may be further divided into endothelial and sub-endothelial layers. The

sub-endothelium is a thin layer of connective tissue located between the endothelium and the internal elastic lamina, containing a small amount of collagen fibres, elastic fibres, and a small amount of vertically parallel smooth muscle in some cases. The sub-endothelial layer provides a physical support for the endothelium, preventing the endothelium from experiencing overstretch and recoil. It also serves to regulate transportation of molecules between SMCs and the endothelium.
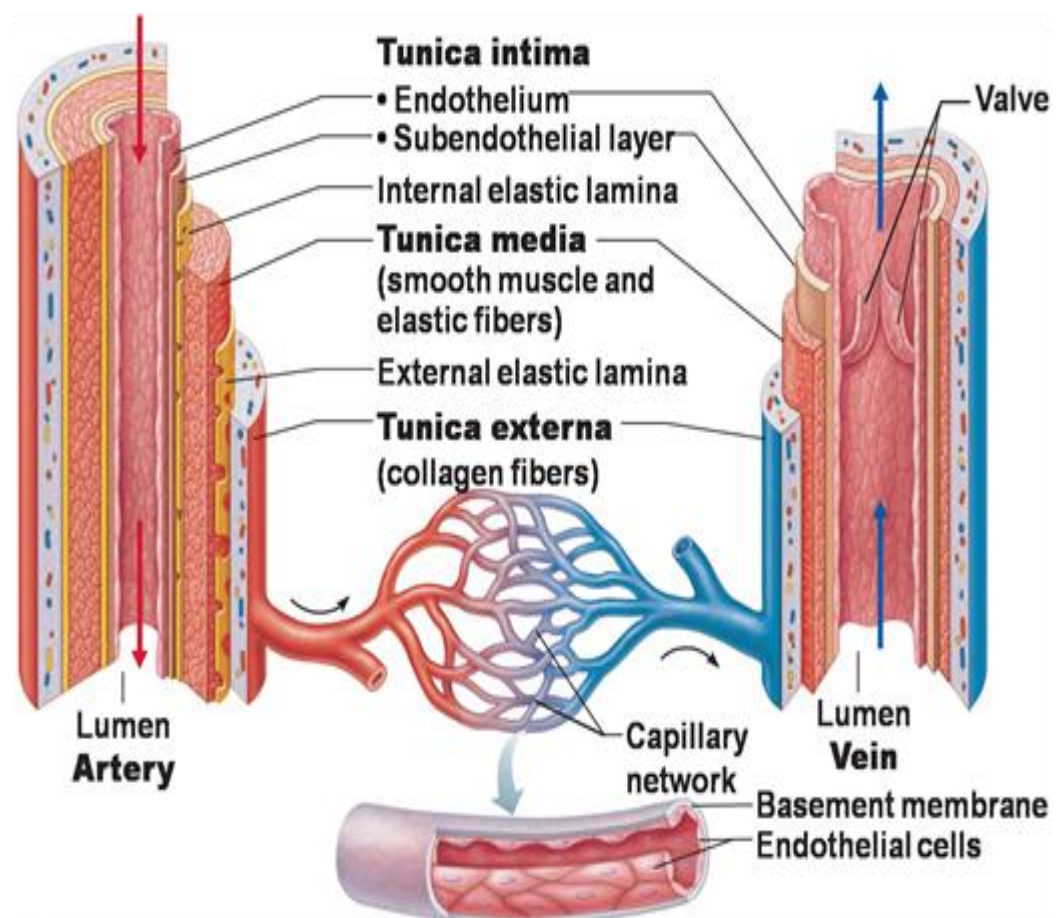
Figure 1.2:   Anatomical structure of the vasculature system.

This image illustrates the three-layered structure of blood vessels and the direction of blood flow as it circulates throughout the vascular system.

(fhttp://legacy.owensboro.kctcs.edu/gcaplan/anat2/notes/APIINotes5%20Circulatory%20Anatomy.htm)

1.1.1.3 The endothelium.

The endothelium is the mono inner layer of blood vessels and a basic component of the vasculature, which was originally considered to compartmentalise blood flow from the underlying tissues and matrix (Cines, et al. 1998). Intensive stud in the field of EC biology over the past three decades has shed much light on its complex function and role in the (patho)-physiology of the cardiovascular system. Located between the blood flow and, smooth muscle cells, and also surrounded by connective tissue and (ECM), endothelial cells are constantly exposed to physical and chemical stimuli, and act as a paracrine and endocrine organ to secrete many factors involved in the regulation of blood vessel tone, blood cell trafficking, hemostasis, permeability, proliferation, immunity, cholesterol level, and lipid homeostasis (Grover-Páez and Zavalza-Gómez 2009a) (Vanhoutte, et al. 2009).

Under physiological conditions, the EC layer is referred to as "quiescent or inactive" and provides an anti-vasospasm, anti-inflammatory and, anti-coagulation environment, preventing aggregation of platelet (Aird, W.C. 2008). The "coble stone" morphology of endothelial cells form an intact barrier and elongate at the direction of blood flow providing a hemodynamically optimal surface for blood flow, reducing friction. Under normal blood flow, the endothelial barrier releases vaso-dilative substances including NO and PGI_2 to relax vessel walls. The production of an endothelium-derived relaxing factor (EDRF) by ECs was first described by Gurchaott and Zawadzhi in the early 1980s, which was later identified as NO by two research group (Palmer RM,1987. Ignarro LJ, 1987). NO is the main vaso-dilative factor that produced by endothelial nitric oxide synthase (eNOS), which then can easily diffuse into underlying SMCs due to its small size and thus induce vascular relaxation by modulating the calcium signaling in SMCs (Loscalzo and Welch 1995).

The release of NO and PGI$_2$ also breaks down the pro-aggregating mediator ADP that in turn inhibits leukocyte and platelets interaction with the EC surface (Gryglewski 1995). Although the mechanism of NO release is complex, it is well established that hemodynamic forces are a major stimuli and regulator (Rubanyi, Romero and Vanhoutte 1986). Capable of sensing acute change in shear stress and mechanotransduction in the vessel wall tense, ECs undergo cellular and molecular adaption and release NO promptly. The action is particularly potent in larger arteries, which consist of thicker layer of SMCs.

Under pathological conditions, endothelial cells constantly strive to achieve homeostasis, modulate leukocyte adhesion, tethering and transmigration, as well as regulating various cell fate and functions such as adhesion, migration, permeability and proliferation. Endothelial dysfunction occurs as a result of the "activation" of the endothelium caused by the imbalance of vascular regulatory mechanisms; which induce the damage to the arterial wall (Davignon and Ganz 2004). Change in EC morphology and phenotype is considered as the first sign of dysfunction, leading to the initiation development and progression of cardiovascular disease (Montecucco and Mach 2009). At athero-prone areas, ECs are exposed to cardiovascular risk factors, which change pattern of synthesis and secretion of various bioactive substances. These alterations include change in EC surface charge, losing their non-thrombogenic ability and, accumulation of lipid droplets, which turn into foam cells latterly. Chronic exposure to cardiovascular risk factors can utterly exhaust the protective system of EC and cause inflammation. As a consequence, ECs may lose integrity and detach into circulation (Sima, Stancu and Simionescu 2009b) (Sima, Stancu and Simionescu 2009a). The dysfunctional ECs process anti-hemostatic properties, including abnormal vascular tone, increase affinity to leukocytes and over production of cytokines and growth factors (Aird 2007).

1.1.2 Cardiovascular disease.

The cardiovascular system comprises of the heart, arteries, veins and lymphatic system. As a result, cardiovascular diseases (CVD) are a class of diseases which involve heart and blood vessels and consequently include heart failure, arrhythmia, angina, hypertension, high cholesterol, and stoke amongst others.

1.1.2.1 The epidemic of cardiovascular disease.

The function of the cardiovascular system is so important that any pathological change can be vital. According to the World Health Organisation (WHO), CVD is the leading cause of global death *(www.who.int/mediacentre/factsheets/fs317/en/)*. Cardiovascular disease causes more American deaths than cancer and this number is rapidly increasing each year. It is also estimated that 17.3 million people died from CVD around the world in 2008 which representing 30% of all global deaths and this number is expected to rise to 23.6 million in 2030. In Ireland, this Figure is even higher; approximately 10,000 people die from CVD annually; including coronary heart disease (CHD), stroke and other circulatory diseases. CVD is the most common cause of death in Ireland, accounting for 36% of all deaths. The largest number of these deaths relate to CHD - mainly heart attack - at 5,000. 22% of premature deaths (under age 65) are due to CVD (http://www.irishheart.ie/iopen24/about-us-t-1.html).
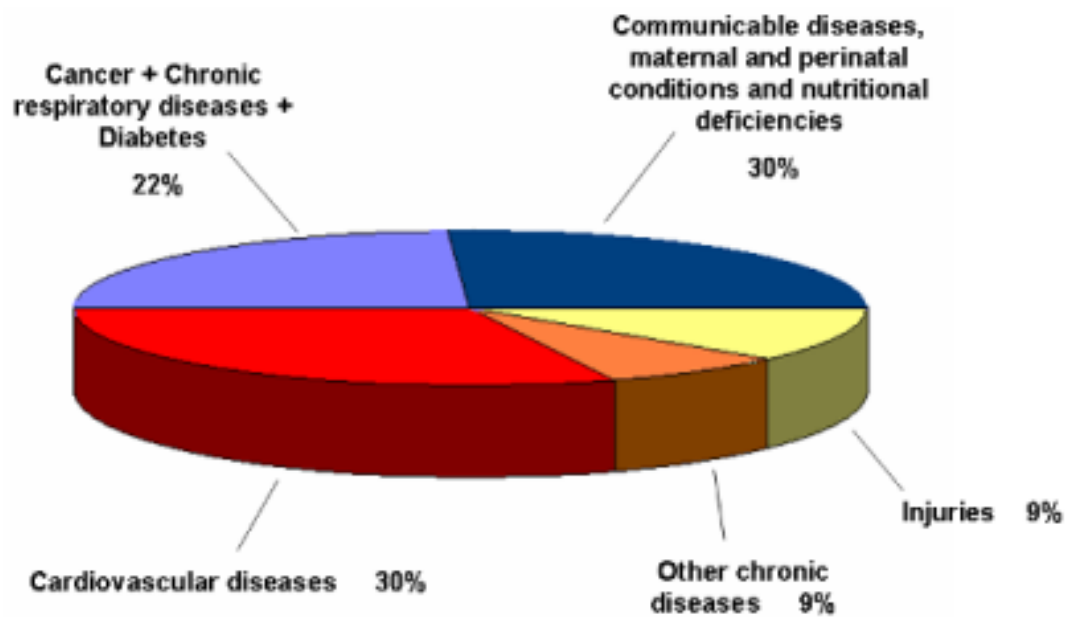
Figure 1.3: The pie charts showing the percentage of all global death from different diseases.

The red section represents the number of deaths from CVD, which makes up approximately 30% of all global deaths. *(http://www.who.int/cardiovascular_diseases/en/)*

1.1.2.2 The risk factors of cardiovascular disease.

The pathophysiology of CVD is varied and complex, hence there are many cellular and molecular mechanisms which contribute to the diseases. General risk factors of CVD include unhealthy diet (high cholesterol diet and salt intake), physical inactivity, over-consumption of alcohol and tobacco. Prolonged exposure to such unhealthy habits leads to intermediate risk factors, which includes high blood pressure, high serum cholesterol, raised blood glucose levels and obesity, which increases chances of developing CVD in the future. Among these risk factors, high serum cholesterol and unhealthy diet are the major causes of CVD, and as a result the principle focus for the of heart disease is mainly focused on reducing the level of serum cholesterol. Some studies have also shown that reduction of the amount of

daily salt intake led to over 25% of patients having a reduced chance of developing CVDs (Cook, et al. 2007).

1.1.2.3 Atherosclerosis.

Atherosclerotic disease is a condition whose physiological hallmark is the thickening and loss of elasticity of arterial wall. Underpinning this condition, is the excessive deposition of lipid, accompanied by a proliferation, migration and apoptosis of smooth muscle cells, unparalleled with altered ECM dynamics and fibrous matrix turnover, which gradually develop to necrotic cores with cholesterol crystals and calcification at a later stage.

Atherosclerosis normally occur at large and medium-sized muscular elastic arteries; the aorta, coronary and cerebra, especially at the site of arterial bifurcation and regions of high curvature that results in complex blood flow patterns (Hahn and Schwartz 2009). At such sites, disturbed blood flow occurs, leads to formation of atherosclerotic plaques which in turn cause narrowing of blood vessels and luminal occlusion or even wall rupture at advanced stages (Orr, et al. 2006). In summary, pro-atherosclerosis risky factors include increased plasma lipids, hypertension, high glucose, obesity, lack of physical exercise and exposure to cigarette smoke (Hahn and Schwartz 2009).

1.1.2.3.1 Pathogenesis of atherosclerosis.

The pathogenesis of this disease is not fully elucidated. Despite dramatic progress in the field of cardiovascular research in recent years, the pathogenesis of atherosclerosis is still based on a variety of theories or hypotheses. Among these

theories, lipid metabolism and biology as well as endothelial dysfunction are commonly accepted as being important in the initiation, development and progression of this condition.

The lipid infiltration paradigm believes that the mechanism of disease is closely related to the lipid metabolism disorders. As atherosclerosis is characterized by excessive deposition and accumulation of lipids, especially low-density lipoprotein (LDL) cholesterol, the major pathological hallmark of the disease is the formation of the arterial wall plaques in which cholesterol and cholesteryl ester constitute the main components. Although the arterial wall is also capable of synthesizing cholesterol and other lipids, recent studies indicate that lipid in atherosclerotic plaques is mainly originates from plasma. Facilitated by lipoprotein, plasma cholesterol, is taken up into the intima of vascular walls and is then deposited on SMCs, causing their proliferation and migration. The excessive LDL can be engulfed by macrophages to generate foam cells. The accumulation of foam cells, together with SMCs, lipid-laden monocytes and T lymphocyte in the intima slowly leads to the development and progression of an early fatty streak which is the first stage of atherosclerosis. However, despite the improvement of pharmacological intervention to lower blood cholesterol, the number of deaths due to atherosclerosis is still increasing, suggests that there additional and more complicated molecular mechanism behind it.

As previously mentioned, long term exposure to many stimuli such as hypercholesterolemia and perturbed/oscillatory shear stress, leads to significant alteration of normal vascular functions (Endemann and Schiffrin 2004) (Grover-Páez and Zavalza-Gómez 2009b). It is well accepted that loss of endothelial integrity is one of the first steps in development of atherosclerosis. Activated ECs increase their permeability, allowing circulating LDL diffuse through the endothelial monolayer. The constant accumulation of LDL leads to attachment and migration of

monocytes and macrophages (Figure 1.4 A). The dysfunctional ECs also secret adhesion molecules and chemoattractants that result in the adhesion, tethering and transmigration of leukocyte. All these factors contribute the initiation of atherosclerosis.

1.1.2.3.2 Pathological changes.

Atherosclerosis can be classified into three different stages: formation if fatty streaks, development of fibrous plaques, and finally establishment of complicated lesions.

Formation of fatty streaks is the earliest change and becoming more common in young people, even being observed in children as young as aged 10 to 14. Fatty streaks are usually confined within the arterial intima, and appear as fat depositions, a few millimeters to a few centimeters in length, which running along the artery wall (Figure 1.4 B). At the early stage, the fatty streaks consist of only monocytes and macrophages. Adhesion of monocytes and macrophages to Ecs is driven and potentiated by excessive oxidized lipoprotein particles which contain mainly cholesterol and cholesterol esters, as well as phospholipids and triglycerides. Dysfunctional EC contribute to atherosclerotic development due to increased permeability, allowing LDL diffuse into the arterial wall (Hadi, Carr and Al Suwaidi 2005). Prolonged exposure of macrophages with LDL leads to formation of foam cells (Zhou, et al. 1999). Fatty streaks are latterly linked by lipid-filled SMCs which may undergo apoptosis and develop into a necrotic core. SMCs are also important in the formation of fibrous caps, and contribute in maintaining plaque stability (Arroyo and Lee 1999). Fatty streaks are flat or only slightly higher than the endothelium; therefore it does not affect local circulation and is present well before a clinical threshold.

Fatty streaks may be reversible or alternatively be the foundation of an atherosclerotic plaque. Fibrous plaques are also located within the arterial intima which results in thickening and expansion of the arterial wall (Figure 1.4 C). As the lesion progresses to the intermediate stage, fatty streaks develop into fibrous plaques and form a fibrous wall which isolates the lesion from blood flow. These contain a mixture of collagen fibers, as well as a large numbers of lipid-laden SMCs, macrophages and lymphocytes. Activated ECs release chemoattractants and adhesion molecules leading to adhesion of leukocytes (Springer 1994). These adhesion molecules mainly belong to the selectin and integrin families, along with the IG superfamily (Carlos and Harlan 1994). As fibrous plaque grows, it occludes the arterial lumen and may cause stenosis. Some research has indicated that less than 50% stenosis will result in acute myocardial infarctions (Ambrose, et al. 1988b) (Ambrose, et al. 1988a).

The complicated lesion occurs when the fibrous cap ruptures (Figure 1.4 D). Although atherosclerosis is progresses slowly over time, it sometimes takes ten years to develop, but this stage can be vital. The exposure of the sub-endothelial layer of the arterial wall (made of collagen, elastin fibers and SMC) to platelets and complement factors triggers a thrombotic response. Fibrous plaques may be classified as either stable or vulnerable. Stable plaques consist of more SMC and collagen, while vulnerable plaques consist of more lymphocytes. Although stable plaques cause stenosis, it leads to less serious clinical problems such as stroke and heart attack due to its stability (Stoneman and Bennett 2004).
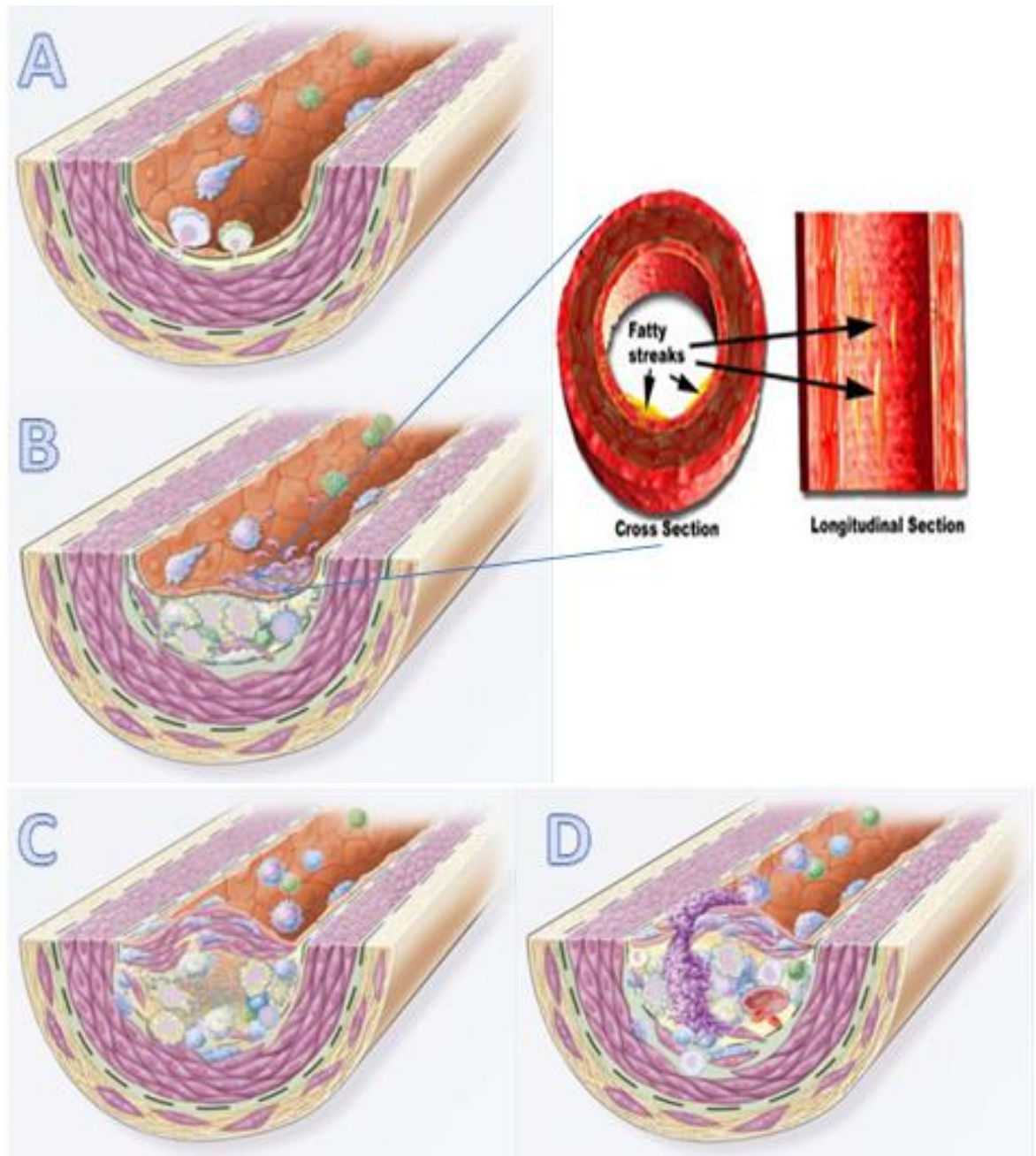
Figure 1.4:   The progression of atherosclerosis

A) Activated ECs increase permeability, allowing diffusion of LDL inside the vascular wall, which in turn attract adhesion and migratory monocytes and macrocytes.   B) Fatty streaks are the first sign of an atherosclerotic plaque, and may be observed in children aged 10 to 14.   At the early stage, fatty streaks appear as yellow grease running along the artery wall.   C) As fatty streaks progress to intermediate lesions, they form a fibrous cap, which isolates the lesion from blood flow.   D) Complicated lesions occur when fibrous caps break and expose the sub-endothelial layer to platelets and complement factors, triggering a thrombotic response (Montecucco and Mach 2009).

(http://www.heartsite.com/AMI_slides/html/aSlide_07.html)

1.2 The cytoskeleton.

The cytoskeleton is a filamentous protein network in cells, which maintains the cell's shape, and its functional polarity. It extends throughout the cell and attaches to the plasma membrane and cell organelles, regulating their organization. Cytoskeleton is composed of three filamentous systems; microfilament, microtubules and intermediate filaments, which occupy about 20–30 percent of the cytosol weight. Instead of a fixed structure, the cytoskeleton is very dynamic – it can be assembled within 1 minute and can last from few minutes to few hours, depending on physical and biochemical stimuli. The three sub structures of the system can be easily distinguished by their size and components; microfilaments are constituted by actin and actin binding proteins (ABPs), 8–9 nm in diameter, and are organized into a two-stranded twisted structure. Microtubules are stiff hollow tubes comprised by protein tubulin and microtubule-associated proteins (MAPs). The diameter of microtubules is much larger than microfilaments (approximately 24nm long). Intermediate filaments are slightly larger than microfilaments, approximately 10 nm in diameter, and have a rope-like structure (figure 1.5). Essentially, each of the filament systems has its own distinct function; microfilaments normally accumulate at the edge of migrating cells and generate functional structures such as lamellipodia, filopodia and stress fibers, with the aid of actin-binding proteins, as well as acting as tracks for ATP-powered myosin motor proteins, which underpins the mechanism for muscle contraction. Microtubules form the basic framework throughout the cell, providing scaffold support for organelles and also form contractile rings during cell mitosis. One of the functions of EC cytoskeleton is to provide cellular structural integrity, and does so by regulating endothelium permeability, cell-cell and cell-substratum adhesion, in addition to cell migration (Lee and Gotlieb 2002) (Lee and Gotlieb 2003). Endothelial integrity plays a pivotal role in normal blood vessel function, disruption of which can lead to initiation and progression of atherosclerosis.
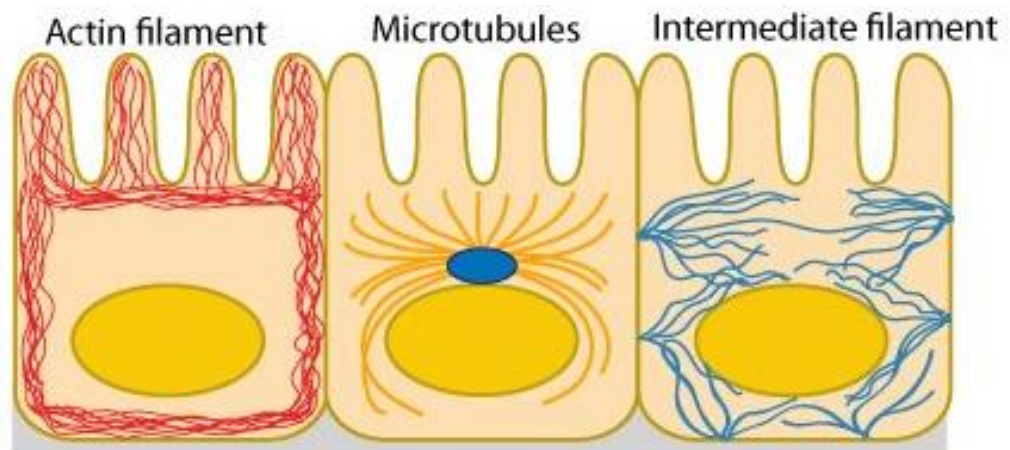
Figure 1.5: The Cytoskeleton.

Cytoskeleton is composed of three filamentous systems; microfilament, microtubules and intermediate filaments. Composed of actin and actin binding proteins (ABPs), microfilament are 8–9 nm in diameter, and are organized into a two-stranded twisted structure that normally accumulate at the edge of migrating cells and generate functional structures such as lamellipodia, filopodia and stress fibers. Microtubules are stiff hollow tubes comprised by protein tubulin and microtubule-associated proteins (MAPs). The diameter of microtubules is much larger than microfilaments (approximately 24nm long) and forms the basic framework throughout the cell, providing scaffold support for organelles and also form contractile rings during cell mitosis. Intermediate filaments are slightly larger than microfilaments, approximately 10 nm in diameter, and have a rope-like structure (Goldman et al., 1999).

1.2.1   Actin and actin binding proteins.

Actin is the basic building block of microfilaments, and is an abundant intracellular protein in eukaryotic cells.   In vertebrates, three isoforms of actin (α, β, and γ) are found.   Only expressed in muscle cells, α-actin is involved in muscle contraction in association with myosin. In contrast, β and γ are found together in almost all non-muscle cells.   Actin is highly conserved, and arose from an ancestral bacterial gene.   Actin exists in two forms; a globular monomer G-actin, and a filamentous polymer, comprising of G-actin subunits, F-actin.   G-actin polymerizes into F-actin filaments when cations are added in solution.   When ionic strength is lowered,

F-actin depolymerizes.   G-subunits assemble in the same direction causing the filament to become polarized.   Hence, addition of subunits is favored at the (+) end and dissociation at the (-) end.

Two actin-related proteins play crucial roles in polymerization. ARP2 and APR3 nucleate, and cause branching of G-actin into F-actin (Pollard and Beltzner 2002) (Dyche Mullins and Pollard 1999).   Capping proteins, gelsolin and cofilin, regulate growth by covering an end of the F-actin filament (Pottiez, et al. 2009) (Carlier, et al. 1997).   Filaments assemble into two helices of actin subunits.   Actin filaments are found in a variety of different structures, such as filament bundles in microvilli, or in the meshwork of the leading edge, but mainly in the cell cortex (Chesarone and Goode 2009) (Mallavarapu and Mitchison 1999). These structures are organized by cross-linking proteins, which have one or two F-actin binding sites, and form a dimer with a similar molecule.   Dimers can result in linkages bonds that are further apart, such as α-actinin (McGough, Way and DeRosier 1994), found in stress fibers and filopodia.   Different cross-linking proteins give different structure and function to actin.   Filamin is highly flexible and is found stabilizing cross-links in meshwork (Stossel, et al. 2001).   Spectrin extends large distances and is found in the cell cortex (Viel and Branton 1996).   Actin filaments interact with the plasma membrane either laterally or at their end.   This is achieved through actin-binding proteins, such as ERM proteins in microvilli (as mentioned above).   Changes in actin structure are of great importance to its function, as it affects the shape of the cell, in addition to driving intracellular movements.   Actin filaments provide support and organisation in the cell cortex underneath the plasma membrane.   They make up the core of microvilli.   In epithelial cells they form the adherens belt that provides cellular strength.   Actin is also involved in cell migration (Ridley, et al. 2003b).   It is initiated by formation of a large, broad membrane protrusion at the leading edge of the cell, referred to as a "lamellipodium".   Actin filaments are rapidly cross-linked into bundles and networks here. Slender membrane projections

called "filopodia" stabilize the leading edge, preventing retraction. Movement of the cell is controlled by actin polymerization (Parsons, Horwitz and Schwartz 2010c). Migration is needed for processes such as fibroblast migration during wound healing, morphogenetic movements during embryonic development and chemotactic movements of immune cells. Cells have contractile microfilaments that attach to the substratum through specialized regions referred to as "focal adhesions". These microfilaments form a contractile ring during cytokinesis which constricts to form two daughter cells.

1.2.1.1 Actin in the Nucleus.

Actin has been observed in the nucleus in several studies dating back to the 1970's and 80's, however, results were subject to scepticism due to perceived contamination with cytoplasmic actin, or it was thought to simply diffuse in and out of the nucleus. These findings were largely forgotten about and little attention or research was carried out in this area until, recently. However, a large number of papers have since been published on the subject in the last 5 years, highlighting the importance of actin in the nucleus. The paradigm of nuclear actin is now accepted, the quest is to decipher the function, organization and location of actin and its binding partners. In the cytoplasm, actin is present in either the G or F-actin form, but in the nucleus, there may be different forms, involved in the various functions and cell fate decisions (Jockusch, et al. 2006a). Cytoplasmic actin F-actin can be identified by labeling with fluorescent phalloidin. Phalloidin interacts with sites of actin monomer-monomer contacts found in F-actin but is usually not found in the nucleus (Olave, Reck-Peterson and Crabtree 2002). Using monoclonal mouse antibodies against actin, 2G2 and 1C7 (which also recognize an epitope on G-actin and lower dimer, dimeric forms of actin observed in actin polymerization) it was found to stain the nucleus of many mammalian nuclei. It recognized two different unconventional forms of actin

(Gonsior, et al. 1999) (Schoenenberger, et al. 2005). It is now thought "Actin can assume a variety of oligomeric or polymeric forms" (Jockusch, et al. 2006b). Actin-binding proteins could act to stabilize these unconventional forms of actin and could participate in specific nuclear activities, such as chromatin remodeling or RNA synthesis (Jockusch, et al. 2006a). In chromatin modifications, nuclear actin functions are clearly linked to the nuclear actin-related proteins APR's; see table 1.1 (Blessing, Ugrinova and Goodson 2004). Nuclear pores, which will be discussed below, are wide enough to allow monomers of actin into the nucleus. In addition, actin-binding proteins, which contain nuclear localization signals, could transport other forms of actin into the nucleus (Jockusch, et al. 2006a). Actin has been found at the nucleoplasmic filaments of the Nuclear Pore Complex and so may have a role in nuclear export (Hofmann, et al. 2001). The presence of actin-binding proteins in the nucleus has only recently been elucidated and the dynamic between cytoplasmic and unclear cytoskeletal moieties will be an intense focus of research in the future.

Table 1.1: Nuclear actin-binding proteins

Actin subfamily	Phylogenetic range[b]	Localization[c]	pI[d]	Function	Complexes
Actin	Humans to *Giardia*	Cytoplasm, nucleus	5.31 (h) 5.44 (y)	Cell motility or transport, chromatin remodeling Nuclear assembly? Transcription?	Microfilaments, dynactin, ARP2/3 SWI2/SNF2-containing CRCs INO80-containing CRCs SWR1-containing CRCs A/B group hnRNPs NuA4 histone acetyltransferase
ARP1	Humans to yeast	Cytoplasm	5.98 (h) 5.40 (y)	Dynein motor activity	Dynactin
ARP2	Humans to plants	Cytoplasm	6.29 (h) 5.54 (y)	Actin polymerization	ARP2/3
ARP3	Humans to plants	Cytoplasm	5.61 (h) 5.57 (y)	Actin polymerization	ARP2/3
ARP4	Human to plants	Nucleus	5.48 (h) 5.34 (y)	Chromatin remodeling	SWI2/SNF2-containing CRCs INO80-containing CRCs SWR1-containing CRCs NuA4 histone acetyltransferase
ARP5	Humans to plants	Nucleus	5.17 (h) 5.32 (y)	Chromatin remodeling	INO80-containing CRCs
ARP6	Humans to plants	Nucleus	4.92 (h) 5.33 (y)	Chromatin remodeling	SWR1-containing CRCs
ARP7	Yeast	Nucleus	5.35 (y)	Chromatin remodeling	Yeast SWI2/SNF2-containing CRCs (SWI/SNF, RSC)
ARP8	Humans to plants	Nucleus	4.69 (h) 8.08 (y)	Chromatin remodeling	INO80-containing CRCs
ARP9	Yeast	Nucleus	5.03 (y)	Chromatin remodeling	Yeast SWI2/SNF2-containing CRCs (SWI/SNF, RSC complex)
ARP10 and ARP11	Humans to yeast (?)[e]	Cytoplasm	7.06 (h) 8.01 (y)	Dynein motor activity	Dynactin

*PI: the abbreviation of Isoelectric Points.
(Blessing, Ugrinova and Goodson 2004)

1.2.2 ERM family (Ezrin, Radixin, Moesin).

A common function of actin cytoskeletal structures is to support or to change the shape of the plasma membrane. ERM proteins are members of the erythrocyte protein 4.1 superfamily that are much conserved in evolution. They are found in all metazoan genomes, but not in unicellular organisms, suggesting that they evolved in response to cell-cell communication (Saotome, Curto and McClatchey

2004). They are paralogs that probably arose due to gene duplication, and so have functional redundancy in vertebrates, which makes it hard to study them by gene knockout. They appear to function widely as linker proteins that link microfilaments to the plasma membrane (Sato, et al. 1992). ERM proteins shear a common structure. C-terminal domain which attaches to the actin filaments and the N-terminal FERM domain attaches to the cytosolic face of transmembrane glycoprotein's e.g. integrins. ERM proteins come in an active actin-binding form, and an inactive folded conformation. Extracellular signals cause conformational changes through the binding of PIP2 or phosphorylation. ERM proteins play an important role in maintaining cellular architecture and integrity.

1.2.2.1 Merlin.

Merlin (also called Schwannomin), a relatively new member of ERM family, was identified in 1993 (Rouleau, et al. 1993) (Trofatter, et al. 1993). It was found to be mutated or deleted in Neurofibromatosis type 2 (NF2) syndromes. NF2 is an autosomal-dominantly inherited disease affecting central and peripheral nerves and causes schwannomas, meningiomas, and ependymomas (Ramesh 2004). The NF2 gene was mapped to chromosome 22q12 (Scoles 2008), is approximately 100kb long and transcribes a protein 590 (isoform 2) or 595 (isoform 1) amino acids in length with a 60-75 KDa molecular weight (Shimizu, et al. 2002) (Shimizu, et al. 2002). At present, 10 Merlin isoforms have been identified; among which, isoform type 1 and isoform type 2 are most common and best characterized. Merlin isoform I consists of 595 amino acids, while Merlin isoform II contains 590 amino acids, due to their slight different C-terminal. However, unlike isoform 1, isoform 2 is believed to lack tumor suppressor function (Gutmann, et al. 1999).

Merlin also belongs to band 4.1 superfamily, which includes ezrin, radixin, moesin and talin and are collectively known as ERM proteins (Trofatter, et al. 1993). ERM proteins interact with actin and membrane proteins, regulating cell membrane organization. Merlin shares a common structure with this protein family; a tri-lobe N-terminal domain, a charged C-terminal, and is linked by a long α-helical region (Scoles 2008) (Figure 1.6). However, unlike other ERM proteins that consist of the C-terminal actin binding sites, Merlin contains a low affinity actin-binding domain on the FERM domain at its N-terminal (Huang, et al. 1998) (Xu and Gutmann 1998). The structural similarity of Merlin with ERM proteins indicates that Merlin also functions as a scaffolding protein, connecting F-actin to trans-membrane proteins through the FERM domain. The FERM domain contains three globular sub-domains sharing 60-70% of the same sequences with other members of the ERM family (Figure 1.7) (Berryman, Gary and Bretscher 1995). The FERM region can also interact with the C-terminal of Merlin to form a homodimer, or interact with other ERM proteins to form heterodimers, resulting in an active state required for its tumor suppressor function. In this process, the C-terminal of Merlin acts as cap inhibiting the FERM domain bond to trans-membrane proteins (Huang, et al. 1998).

The head to tail intra/inter molecular association does not exist in Merlin isoform 2, and may explain why isoform 2 lacks tumor suppressor function and associates with F-actin more efficiently. The actin-binding site of Merlin is located at residues 178-367 on the N-terminal. Merlin can bind with F-actin directly through this domain, or indirectly via the other ERM proteins. Phosphorylation of Merlin is the other important regulatory mechanism of its function. Merlin can be phosphorylated at serine 518 in the C-terminal by either p21-activated kinase (PAK) or cAMP dependent protein kinase A (PKA), resulting in disassociation of the C-terminal from FERM (Kissil, et al. 2002) which is required for its tumour suppressor activity and exist a inactivate state. Interestingly, some studies have shown that Merlin can only interact with F-actin while ERM proteins are able to bind both G and F-actin;

suggesting a unique functional role for Merlin.
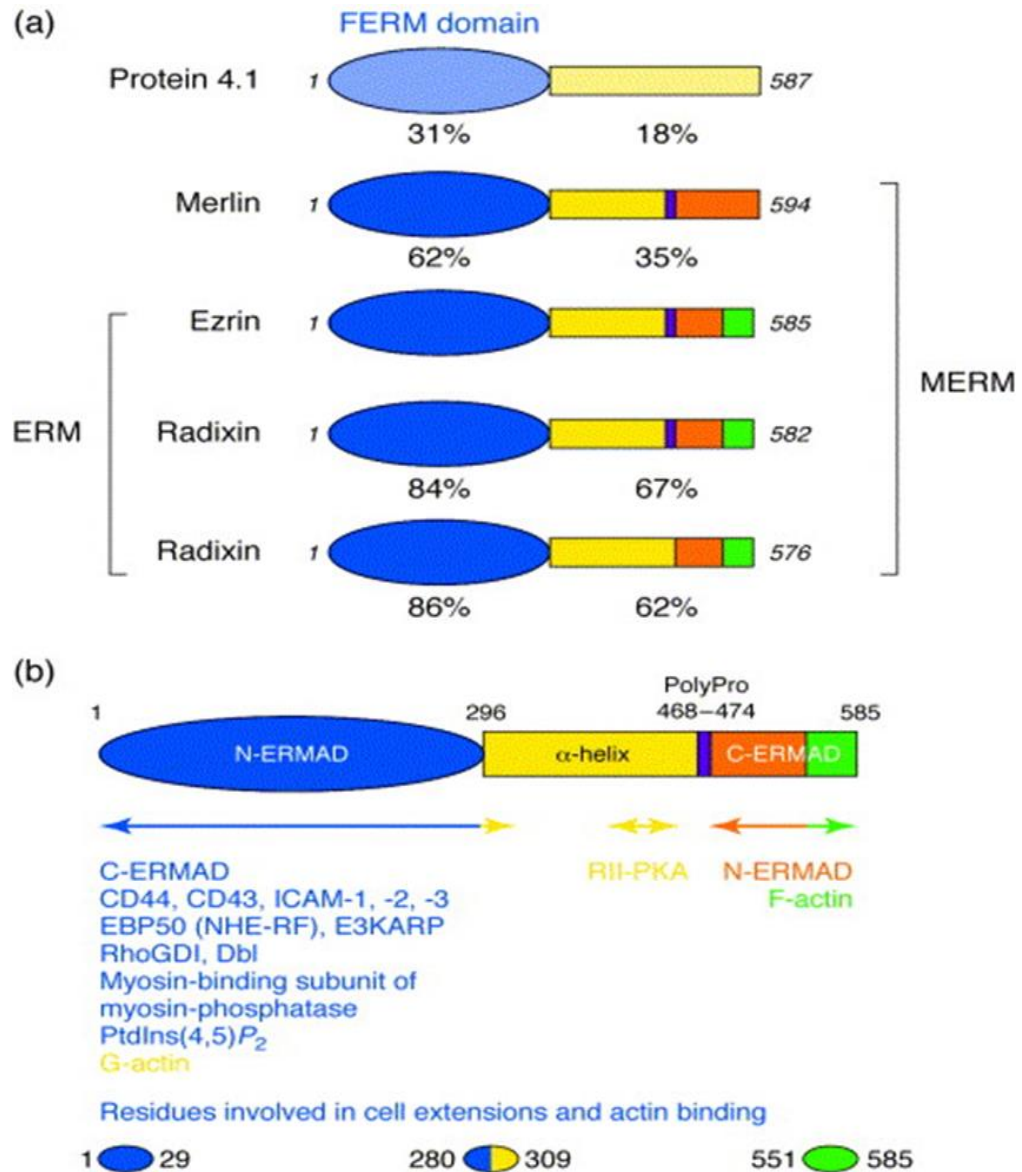
Figure 1.6: Structural comparison of Merlin and ERM proteins.

(A) The amino acid sequence of the erythrocyte protein 4.1 superfamily. Various colored bars show the location of different domains. The oval blue shapes represent FERM membrane protein binding domains (also called N-ERMAD). The yellow and golden regions represent α-helix domains. The actin-binding domains on C-terminal are depicted by a green box, absent on Merlin. (B) Illustration of various binding sites of ERM and their binding partners. (Mangeat, Roy and Martin 1999)
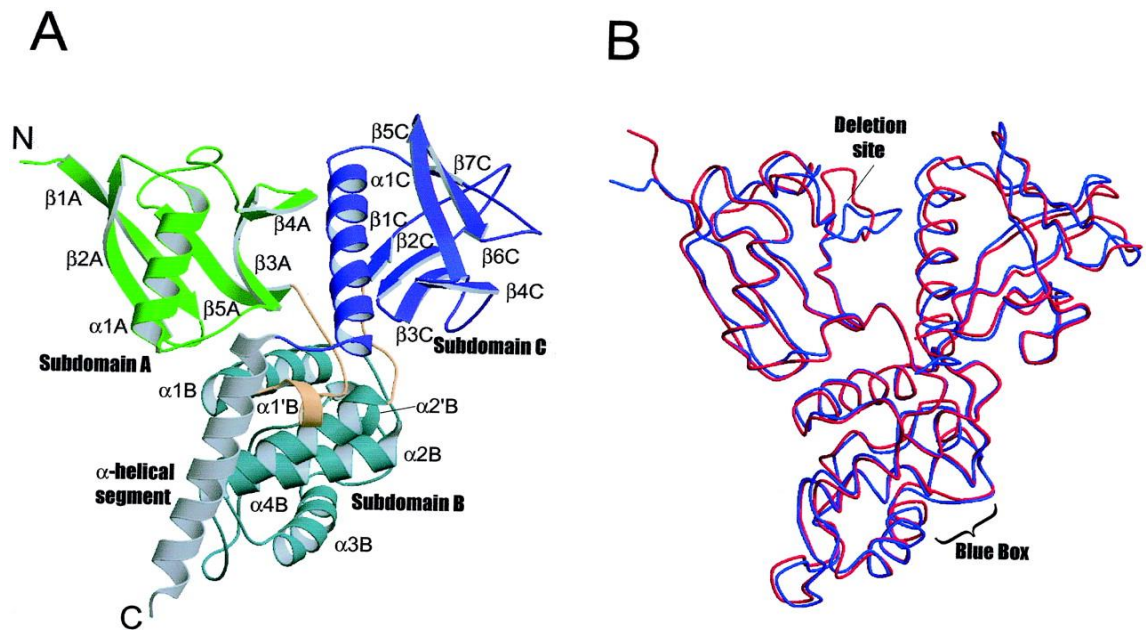
Figure 1.7: Crystal structure and superposition of the FERM domains.

A) Colored 3D crystal structure representing the Merlin FERM domain. Merlin FERM contains three sub-domains; sub-domain A (green), sub-domain B (blue-green) and sub-domain C (blue). Gray represents the C-terminal α-helical segment, linked to the FERM domain by a linker region (brown). B) Comparison of the FERM domain in Merlin (blue) with radixin (brown). The arrow shows the deletion site of Merlin.(Shimizu, et al. 2002)

Increasing evidence indicates that Merlin is a key regulator in actin polymerization, cytoskeleton remodeling, cell motility and cell proliferation. Loss of Merlin results in disorganized stress fibers and cell adhesion. Merlin also plays an important role during early embryonic development; loss of Merlin is embryonic lethal in both murine and fly models (Stamenkovic and Yu 2010).

1.2.2.2 Ezrin.

Ezrin is the only ERM protein detected in developing intestinal epithelial cells. Saotome and his colleagues found that in the absence of ezrin, abnormal villus

morphogenesis occurs (Saotome, Curto and McClatchey 2004). Villi were found not to separate correctly during morphogenesis and leading to abnormal apical tension and, incomplete secondary lumen formation. It also resulted in disorganization of apical junctions between cells, and of the terminal web from which microvilli project. Ezrin knock-down in mice caused a loss of gastric acid secretion in parietal cells, which are normally rich in ezrin (Tamura, et al. 2005), caused by defects in the formation/expansion of canalicular apical membranes. Ezrin is present both in retinal pigment epithelium apical microvilli and basal infoldings and Müller microvilli. In knockout mice, reductions in apical microvilli and basal infoldings in retinal pigment epithelium cells and Müller cells microvilli were seen, as well as microvilli inclusions in the cytoplasm of these cells which is not normally observed in the wild type but is found in microvillus inclusion disease (Bonilha, et al. 2006). Also retardation in the photoreceptor development was seen in knock out mice.

1.2.2.3 Radixin.

Radixin was originally identified as a constituent of adherence junctions in rat liver. Knockout mice were used to investigate the role played by radixin (Kikuchi, et al. 2002). They found that mice which did not express radixin were normal at birth, but after 8 weeks, presented with liver injury, and morphology of bile canalicular apical cell surfaces became abnormal. In radixin-absent mice, MRP2 protein was no longer present in bile canalicular membranes, indicating that radixin, which interacts with MRP2, may be necessary for localization/anchoring of the protein to the apical surface of the cells (Kikuchi, et al. 2002). Radixin is also highly expressed in the cochlear and vestibular stereocilia (Kitajiri, et al. 2004). There are two types of stereocilia, cochlear and vestibular stereocilia, which are essential for the transduction of acoustic and acceleration stimuli, respectively, into electrical signals.

Mice defective in radixin suffered from deafness but did not lose their balance. Ezrin was up-regulated and maintained in vestibular stereocilia but was not in cochlear stereocilia. The former is an example of structural and functional compensation of one ERM protein by another and an example of an advantage in having functional redundancy (Kitajiri, et al. 2004).

1.2.2.4   Moesin.

Moesin is found primarily in endothelial cells, but is also co-expressed with ezrin in a few subsets of epithelial cells. Moesin is the single ERM orthologue in Drosophila. DMoesin gene was inactivated during oogenesis and actin filament attachment to the oocyte cortex was shown to be impaired (Jankovics, et al. 2002). It was also shown to disrupt cell shape and antero-posterior polarity by impairing the localization of maternal determinants caused by incorrect attachment of actin to the cortex (Polesello, et al. 2002). Speck, Hughes, Noren, Kulikauskas and Fehon showed that moesin functions in maintaining epithelial integrity by regulating cell-signaling events which affect actin organization and polarity by activating GTPase Rho using negative feedback (Speck, et al. 2003).

DMoesin also has a structural role in photoreceptor morphogenesis. Rhabdomeres (actin-rich) are columns of closely packed photosensitive microvilli. Down-regulation of moesin causes disruption of the membrane cytoskeleton that builds the rhabdomere. (Karagiosis and Ready 2004). The effect, again, is only to be seen in Drosophila as tests on mice showed little effect most likely due to functional redundancy (Doi, et al. 1999).

1.2.2.5 Lasp-1 (Lim and SH3 protein 1).

Human MLN50 gene was found to be over-expressed in some breast carcinomas (Tomasetto, et al. 1995). The 261 amino acid sequence contained an N-terminal LIM motif and a C-terminal SH3 binding domain and is so now termed "lasp-1" and was the first in a new family of LIM proteins (Tomasetto, et al. 1995). Lasp-1 also contains two nebulin-like actin binding repeats which have been shown to bind to actin, and have possible roles in organization of the actin cytoskeleton *(Schreiber, Moog-Lutz and RÃ 1998)* (Chew, et al. 2002). No specific function has been attached to lasp-1. The different binding motifs suggest that it mediates many different protein-protein interactions as a scaffold for the formation of higher order complexes. Lasp-1 is a ubiquitously expressed protein that is found in varying degrees in non-muscle tissues. Lasp-1 localizes in F-actin rich ion-transporting cells such as pancreatic and salivary duct cells and it was shown to be focused around the cortical regions and leading edges of lamellae of parietal cells, as well as being a cytosolic protein its has recently been found in the nucleus (Chew, et al. 2000a) (Grunewald, et al. 2007a). Lasp-1, along with Ezrin, is phosphorylated in response to increases in cAMP, both have a SH3 domain plus similar intercellular localization, suggesting the functions are interdependent (Chew, et al. 1998). Phosphorylation of lasp-1 by an antagonist in parietal cells through the cAMP pathway increases acid secretary responses (Chew, et al. 2000b). "Lasp-1 is a dynamic protein that transits from the cell periphery to focal adhesions upon stimulation with growth factors" (Lin, et al. 2004). Another example of the possible role of lasp-1 is the interaction with zyxin which is found in the focal adhesions of fibroblast cells and is a regulator of actin filament assembly (Li, Zhuang and Trueb 2004). Interesting findings about cell migration and adhesion were found *by Lin, Park, Lin, et al., 2004*, as they stated that "depletion of lasp-1 protein from cells strongly inhibits cell migration in response to ECM proteins". However it did not diminish cell attachment and spreading occurred normally. Also they found that over amplification of lasp-1 has the same effect on

migration, cell attachment and spreading. This shows that for normal migration lasp-1 expression must remain within specific limits. The inhibition of lasp-1 in breast cancer cells has shown a decrease in zyxin expression in focal contacts. Furthermore, over-expression of lasp-1 in kidney cells results in higher migratory rates. Lasp-1 has also been shown to be absent from benign breast gland epithelial cells and to very high levels in breast carcinoma and lymph node metastasis (Grunewald, et al. 2006). Clearly, lasp-1 has important roles in proliferation, migration and signaling in cells. It is likely that a focus on lasp-1 expression in cancers will be seen as a recent study found that it was highly expressed in 55.4% of malign breast carcinoma cells suggesting it may be used as a marker for cancer in the future (Grunewald, et al. 2007b).

1.3 Haemodynamic force.

The major function of the vascular system is to transport blood to tissues. As a consequence, endothelial cells are constantly exposed to haemodynamic forces which are some of the most important extracellular stimuli that regulate endothelial function (Traub and Berk 1998). Cobblestone-shaped ECs elongate and align in the direction of blood flow. At the site of athero-prone areas, disturbed flow will interrupt EC alignment, NF-κb activation and subsequent inflammatory response (Orr, et al. 2006), adhesion and chemokine receptor expressions, leading to re-organisation of the cytoskeleton and cell-cell/cell-matrix junctional/adaptor protein expression change. Several pro-thrombotic factors such as vWF are also released at regions of disturbed flow (Resnick, et al. 2003).

Shear stress and cyclic strain are two forms of haemodynamic force. As blood flow drag through the vessel walls, the fiction force is called "shear stress", and is described by fictional force per area squared (Figure 3). In a region of straight

blood vessels, the direction, force and pattern of blood flow is always the same and is referred to as "laminar shear stress". Under laminar shear stress, endothelial cells elongate in the same direction as blood flow. At regions of arterial bifurcation and curvature, more complex flow patterns (e.g. disturbed flow, turbulent and oscillatory flow) are experience by the vessel wall. Under physiological conditions, shear stress is controlled by arterial elasticity, and the value of shear stress is around 10-15 dyne/cm^2 (Lehoux and Tedgui 2003). Three factors influence the value of shear stress; blood flow rate, blood viscosity and vessel radius. The equation below describes the relationship between these factors:

$$\textbf{Shear stress (dyne/cm}^2\textbf{)} = \textbf{4}\mu\textbf{Q/}\pi * \textbf{(r)}^3$$

Where: μ = blood flow rate, π = blood viscosity, r = vessel radius. (Hunt et al. 2002)

Cyclic strain is generated by circulating blood pressure against vessel walls, and results in a physical stretch to ECs (Figure 3). Blood pressure is generated by periodic heart contraction; the driving force for blood flow. Unlike shear stress, which is higher in smaller vessels, cyclic strain is most prominent in larger arteries due to its high blood pressure and decreases as it travels further. In response to cyclic strain decrease, SMCs in peripheral smaller arteries contract to maintain physiological blood pressure (Hahn and Schwartz 2009). The relationship between cyclic strain and vessel dimension can be described by following equation:

T=Pr/h

Where: P= the blood pressure, r= the radius of the vessel, T =wall tension,

h= the thickness of the wall (Lehoux and Tedgui 2003) (Folkow 1993).
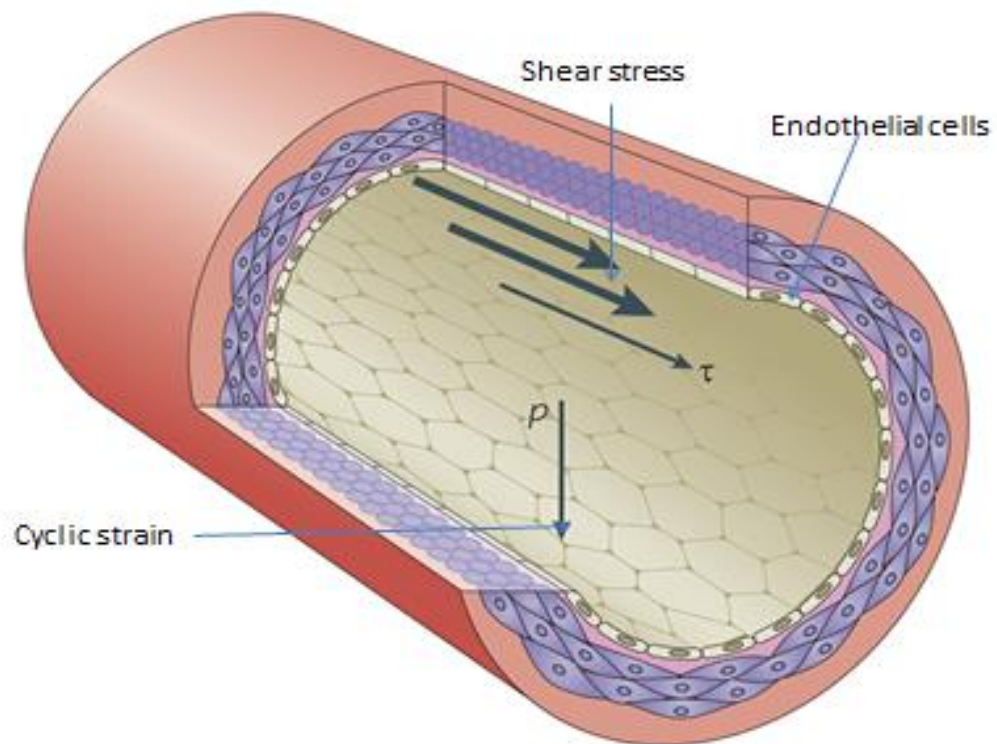
Figure 1.8:   Haemodynamic force

Shear stress: frictional force of blood flow against the endothelium. Cyclic strain: physical stretch to the vessel generated by the circulating blood pressure (Hahn and Schwartz 2009).

1.4   Vascular Mechano-regulation.

1.4.1 Mechanotransduction.

Mechanotransduction is defined as the process by which cells convert mechanical factors into biochemical signals, which in turn results in change in cellular signaling, gate and function, including structural stability and morphogenetic movements. Shear stress and cyclic strain are the two main forms of stimuli which act on ECs, influencing their overall biology (Orr, et al. 2006). Acute hemodynamic changes include blood flow increase, elevated NO levels and induced relaxation of SMC. Over time, shear stress regulates expression changes of many genes that encode for adhesion molecules, growth factors, coagulation factors and chemoattractants (Chien, Li and Shyy 1998). Many studies have also shown the effect of cyclic stretch on vascular remodeling through integrin mediated pathways (Katsumi, et al. 2004). Cell membrane adhesion receptors and cytoskeletal structure are two important factors involved in Mechanotransduction (Hoffman, Grashoff and Schwartz 2011). Many mechanotransducers have been implicated in sensing flow, including integrins, ion channels, receptor tyrosine kinases, heterotrimeric G proteins, platelet and endothelial cell-adhesion molecule-1 (PECAM-1) and vascular endothelial (VE)-cadherin (Hahn and Schwartz 2009).
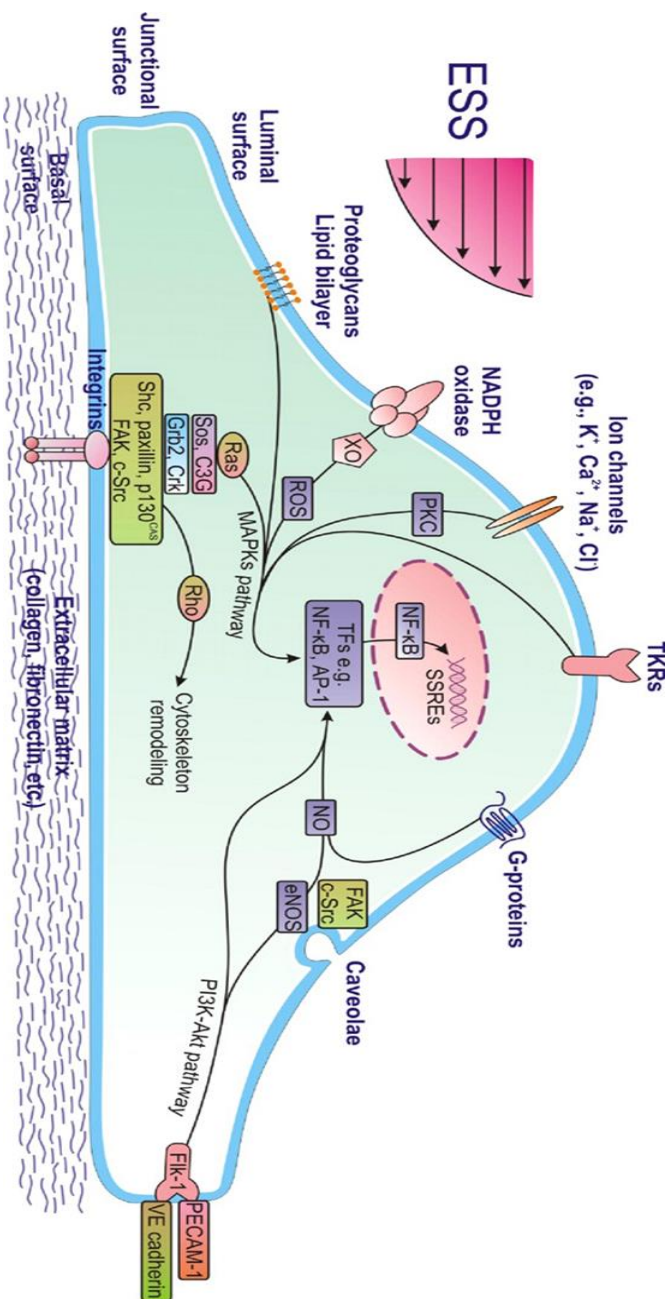
Figure 1.9: Endothelial mechanosensors.

This figure shows endothelial mechanosensors and their localizations. Ion channels, ATP channels, heterotrimeric G proteins, glyocalyx and G-protein-coupled receptors (GPCRs) exist on apical surface and transfer various mechanical stimuli. PECAM-1, VE-Cadherin and ECAM-1 present at the cell membrane and are involved in cell communication. Integrins, meanwhile connect the cell to ECM. (*Chatzizisis, Y. S. et al. J Am Coll Cardiol 2007:0:j.jacc.2007.02.059v1-12962*)

1.4.2 Mechanotransducers.

1.4.2.1 Integrins.

Many cell surface receptors are involved in cell adhesion, migration and mechanotransduction, among which, integrins are the best studied and characterized due to their importance in a multitude of cellular functions. Integrins are a family of transmembrane, cell-surface receptors that mediate interactions between the cytoskeleton and the extracellular matrix, and play an important role in cell "outside-in" and "inside-out" signaling, as well as in the regulation of cell morphology and function, such as cell motility, proliferation, apoptosis and differentiation (Schwartz and Assoian 2001a). Integrin consists of α and β subunits (Figure.1.10) and to date, at least 18 alpha (α) subunits and 8 beta (β) subunits in humans have been identified, generating 24 heterodimers. This diversity of integrin allows integrin binding to specific ECMs and the same ECM-induced adhesions through different integrins, and as such, can differentially affect adhesion dynamics and cell motility (Table.1.2). For example, on fibronectin a5b1 integrin-mediated adhesions are more dynamic than avb3-mediated adhesions that are associated with more persistent migration (Huttenlocher and Horwitz 2011a).
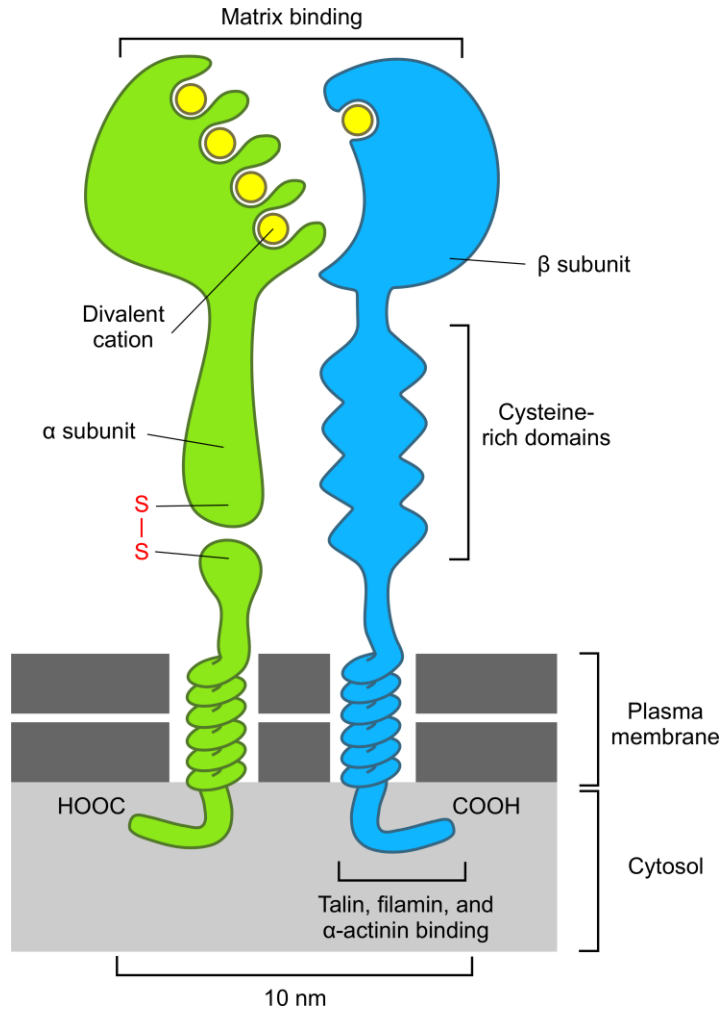
Figure1.10. General structure of an integrin molecule

Integrins are heterodimers that consists of α and β subunits and to date, at least 18 alpha (α) subunits and 8 beta (β) subunits in humans have been identified, generating 24 heterodimers. The diversity of integrin allows integrin binding to specific ECMs and the same ECM-induced adhesions through different integrins, and as such, can differentially affect adhesion dynamics and cell motility
http://personalpages.manchester.ac.uk/staff/j.gough/lectures/the_cell/cell_adhesion/page23.html

Integrins transduce signals into the cell interior upon ligand binding. Intracellular signals regulate ligand binding affinity through a process called "integrin activation". Integrin activation is involved in such processes as platelet aggregation, leukocyte extravasation, and cell adhesion and migration, thus influencing such processes as hemostasis, inflammation and angiogenesis (Ratnikov, Partridge and Ginsberg 2005).

The actin binding protein, talin, plays an important role in integrin activation (Critchley and Gingras 2008). Talin binds the integrin β subunit cytoplasmic tail to the actin cytoskeleton. The arginine-glycine-aspartic acid (RGD) sequence in fibronectin was identified as a general integrin-binding motif (Takada, Ye and Simon 2007). Integrins also recognize other non-RGD sequences in ligands and may be categorized into groups based on ligand-binding specificity; laminin-binding, collagen-binding, leukocyte and RGD-recognizing integrins (Takada, Ye and Simon 2007). Gene deletion studies have demonstrated the essential roles for almost all integrins, with defects suggesting widespread contributions both maintenance of tissue integrity and promotion of cellular migration (Humphries, et al. 2000).

Table 1.2: Different types of integrins and their specific binding proteins

SUBUNIT COMPOSITION	PRIMARY CELLULAR DISTRIBUTION	LIGANDS
α1β1	Many types	Mainly collagens
α2β1	Many types	Mainly collagens; also laminins
α3β1	Many types	Laminins
α4β1	Hematopoietic cells	Fibronectin; VCAM-1
α5β1	Fibroblasts	Fibronectin
α6β1	Many types	Laminins
αLβ2	T lymphocytes	ICAM-1, ICAM-2
αMβ2	Monocytes	Serum proteins (e.g., C3b, Fibrinogen, Factor X); ICAM-1
αIIbβ3	Platelets	serum proteins (e.g., Fibrinogen, von Willebrand factor, vitronectin); fibronectin
α6β4	Epithelial cells	Laminins

(Hynes 1992)

1.4.2.2 G-proteins.

G-proteins are another group of mechanotransducers that belong to GTPase superfamily. They act as molecular switcher and are capable of binding GTP promoting the "on" condition while being turned "off" by changing GTP to GDP. G-proteins are critical in many endothelial functions, including control of endothelial permeability, proliferation and migration (Wieland and Mittmann 2003) (Knezevic, et al. 2009) (Hamm 1998). Up until now, two classes of GTPase have been identified which are involved in cell signaling; small and large G-proteins. The small G-proteins (also referred to as Monomeric G-proteins) include Ras and Ras-like protein. During the last few decades, members of Ras-like proteins have been intensively studied due to their important role in regulation cell motility. Ras-like proteins consist of Rac, Rho and Cdc 42. Rac is known to be involved in control of microfilament organization, which in turn regulates lamellipodia formation on the leading edge of migrating cell. Rho is involved in regulation of stress fiber formation, while Cdc 42 is known involved in control filopodia formation (Etienne-Manneville and Hall 2002) (Burridge and Wennerberg 2004).

Large G-proteins are heterotrimers composed of Gα Gβ and Gγ subunits which are located at the inner surface of the plasma membrane. G-proteins are activated by transmembrane G-protein coupled receptors (GPCRs) and different GPCRs activate specific G-proteins inducing distinct cellular reactions. The large G-proteins contain seven transmembrane domains; the Gβγ dimer secures the tight binding of protein to the cytoplasmic membrane and the Gα chain involved in changing GDP to GTP upon GPCR activation (Papadaki and Eskin 1997). Activation of G-protein releases the Gα sub-domain from Gβγ sub-domain; both of these sub-domains are then free to act on specific downstream effectors (Wieland and Mittmann 2003).

Many studies have demonstrated that in response to shear stress, G-proteins are

involved in regulating vascular tone by regulating the secretion of NO, PGI_2 and endothelin (Ohno, et al. 1993) (Berthiaume and Frangos 1992) (Kuchan and Frangos 1993). Some studies have also shown that inhibition of G-protein blocked shear induced Ras activity (Gudi, Clark and Frangos 1996) (Gudi, et al. 2003). G-protein expression also changed under physiological shear stress in co-cultured ECS and SMCs (Redmond, Cahill and Sitzmann 1998). All these studies pointed to the fact that G-proteins play an important role in regulation of mechanotransduction.

1.4.2.3 Ion channels.

Among all cell membrane channels, ion channels are the simplest, due to their less ability to hydrolyze ATP. They are trans-membrane proteins that control ion transportation across the membrane. The "in and out flux" of ions establishes small voltage gradients cross the membrane. Ions channels allow the fluxes of ions cross membrane much faster; for 10^6 to 10^8 ions per second while only 10^2 to 10^5 ions per second for the other channels. Selectivity and gating are two basic characteristics of ion channels. Selectivity allows only one or a few types of ion to pass through the distinct channels, while gating is responsible for cells maintaining the resting membrane potential.

Many ions channels have been shown to be involved in control of vascular functions (Martinac 2004) and among these channels, K^+ and Cl^- have been intensively studied as they are responsible for machanotransduction. Olesen, Claphamt and Davies have demonstrated the activation of K^+ channels response to shear flow in endothelial cells (Olesen, Claphamt and Davies 1988). This influx of K^+ decreases the contraction of VSMCs, and in turn, dilates vessel walls. Shear stress also activates Cl^- channels, which in turn induce out-rectifying of Cl^- and cause membrane depolarisation (Barakat, et al. 1999).

1.5 Cell migration.

Cell migration is an important biological event that is crucial in maintaining cell morphogenesis. Indeed, abnormal cell migrations contribute to many human diseases, including cancer, immunodeficiency disorders and cardiovascular disease. Under physiological conditions, cell migration is required for immune surveillance, angiogenesis and tissue regeneration and repair (Huttenlocher and Horwitz 2011b) (Brakebusch, et al. 2002). Under pathological conditions such as infections, leukocytes are attracted by inflammatory signals and move towards to the infectious site. The migration of ECs also helps repair injured vessel wall thus maintaining endothelial integrity.

1.5.1 Mechanism of cell migration.

1.5.1.1 The Lamellipodium.

The adhesion of cell membrane integrins into extracellular matrices seems to be the first step in cellular migration. By staining β3 subunits of integrin with green fluorescence protein, studies have illustrated that migrating cells form a functional protrusion region on the leading edge was initiated by polarization of cytoskeleton (Laukaitis, et al. 2001) (Ballestrem, et al. 2001). Lamellipodia, filopodia and membrane ruffles are distinct functional structures on cell membrane which are essential for cell migration. In 1980, Abercrombie observed a protruded cell membrane structure at the front of migrating cells approximately 0.2 μm thick. This structure was subsequently termed "lamellipodium", and termed "ruffles" when curled upwards (Abercrombie 1980). Later, J.P. Heath and B.F. Holifield demonstrated that these structures were based on actin polymerization (Heath and Holifield 1992). Currently, we have a clearer idea about these protrusion structures. The lamellipodium is a thin membrane protrusion about 0.2 μm in height at the front

of spreading and migrating cells or the cells leading edge (Small 1994). They are then described as membrane ruffles when they curl upward. Filopodia are small bundles that projected beyond the cell edge. Lamellipodia contains highly dynamic actin filaments and plays an important role in the development of adhesion complexes. With the helps of many proteins such as Arp2/3, filamin, VASP and WAVE, these protruding structures adhere to underlying ECM, which is then stabilised and form another structure called a "focal complex".

1.5.1.2 Focal complex.

Migrating cells first form transitional adhesions to the lamellipodium, which is mediated by cell membrane adhesion receptors. To date, many cell surface adhesion receptors have been demonstrated to be involved in cell adhesion. Among these receptors, integrins are best characterised. In response to adhesion cues, the extracellular domain of an integrin firmly attaches to their specific ligand which in turn causes conformational change of their cytoplasmic tails inducing its linkage to the cytoskeleton. Large numbers of proteins are known to promote interaction of integrins to the cytoskeleton, among which talin, vinculin, kindlins and α-actinin are the most well studied and therefore characterised. The initial adhesion (focal contact) then mature to large dot-like adhesions termed "focal complexes". A focal complex is a dynamic multiprotein macro-structure approximately 1 μm in diameter and located directly behind the leading edge. A focal complex can further stabilise and mature into a relatively more stable elongated plaque like structure known as a focal adhesion, approximately 2 μm in wide and 3-10 μm in length (Zimerman, Volberg and Geiger 2004). Focal complexes are widely distributed from the front of leading edge to the rear of the cell. Due to its highly dynamic and transient nature, the components of focal adhesions are difficult to study. Structural proteins in focal adhesion are listed in table1.3.
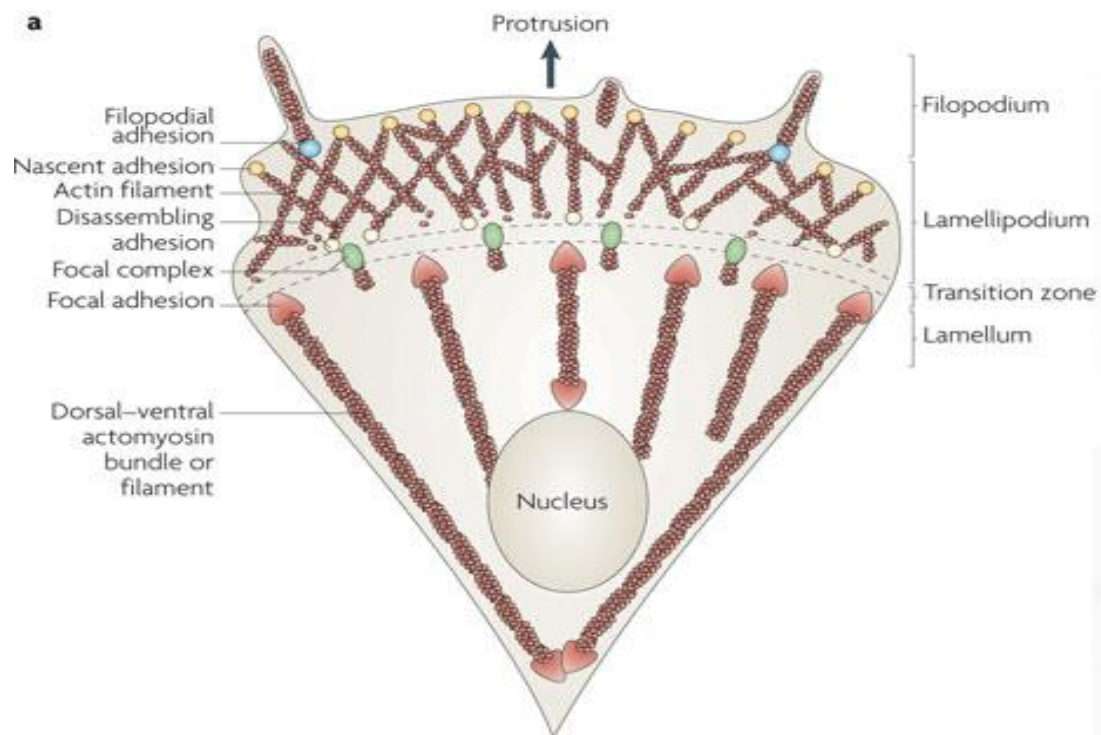
Figure 1.11 Structural elements of a migrating cell

A migrating cell forms distinct functional structures on its leading edge. These structures include filopodia and lamellipodia. Adhesion is the first step of migration, which initially from lamellipodium formation. Lamellipodium contain highly dynamic actin filaments and play an important role in the development of adhesion complexes. Filopodia are small bundles that project beyond the cell edge. Migrating cells first form transits adhering to the lamellipodium, which is mediated by cell membrane adhesion receptors. The transit adhesion then mature to large dot-like adhesion termed focal complexes. As migration progresses, focal complexes may further stabilise and mature into a relatively more stable structure- focal adhesion. Dorsal stress fibre which composed of actin filaments connect to the substrate and act as scaffold for myosin. The arrow shows the direction of cell migration.(Parsons, Horwitz and Schwartz 2010a)

Table1.3. Structural components of focal adhesion

Transmembrane		Cytoplasmic		
1. integrins	4. actin	10. zyxin	16. aciculin*	
2. syndecan IV	5. α-actinin	11. CRP	17. dystrophin*	
3. dystroglycan*	6. filamin	12. radixin	18. syntrophin*	
	7. vinculin	13. fimbrin	19. utrophin*	
	8. talin	14. profilin		
	9. tensin	15. VASP		

The table lists some structural proteins in focal adhesion. Integrins, syndecan IV and dystroglycan are located on surface of cell membrane while the rest proteins located within the cells. Cell surface proteins are involved in both anchorage and signalling transductions (for details of integrins please see section1.4.2.1). Cytoplasmic proteins are known to promote interaction of transmembrane proteins such as integrins to the cytoskeleton, among which talin, vinculin, kindlins and α-actinin are the most well studied and therefore characterised. Talin is another member of ERM protein family, which serves as a linker between integrins and actin. Vinculin is actin binding protein which masks the binding sites for talin and actin. α-actinin belongs to spectrin superfamily and is considered as an actin cross-linking protein. (Burridge and Chrzanowska-Wodnicka 1996)

1.5.2 Regulation mechanism of cell migration.

The promotion of actin polymerisations in migrating cells are controlled by the Rac, Cdc42 and Rho which are members of GTPases family. Rho GTPases are cell membrane proteins that act as molecular switches. The functions of Rho GTPases have been well studied; Rac is known to be involved in control of microfilament organisation, which in turn regulates lamellipodia formation on the leading edge of migrating cells. Rho is involved in regulation of stress fibre formation, while Cdc 42 is known to be involved in control of filopodia formation. Studies have shown that Rac and Cdc42 are activated at the leading edge of migrating cells (Kurokawa, et al. 2005), while RhoA is activated both at the cell rear and the leading edge (Kurokawa

and Matsuda 2005). Activated Cdc42 was observed at sites of filopodia formation, while activated Rac was expressed only in lamellipodia (Tapon and Hall 1997). Activation of Cdc42 seems to regulate and control the direction of cell migration; cells can form a leading edges when transfected with a dominant negative Cdc42 but do not migrate in the right direction (Lodish, H. et al. 2007).

Activated Rac and CDC42 regulate actin polymerization through activation of the other two scaffolding proteins Wiskott–Aldrich syndrome protein (WASP) and WASP-family verprolin-homologous protein (WAVE), which in turn interact with ARP2/3.   Studies have also shown that H-Ras (a subset of the Ras protein family) inhibits activation of β1 and β3 integrins in Chinese hamster ovary cells (Kinashi, et al. 2000). Accumulation of the activated GTP state of Rac1 in membrane ruffles in live cells was observed (Nobes and Hall 1995). Rap1 meanwhile regulates the integrin high affinity state in lymphoid and ECs (Nolz, et al. 2008).

1.6 The Urokinase Receptor (uPAR).

1.6.1 The basic structure of uPAR.

Urokinase receptors, multi-domain glycoproteins, are the other important cell membrane-associated adhesive receptors, which belong to the lymphocyte antigen 6(Ly-6) superfamily (Ploug and Ellis 1994). uPAR contains a peripheral glycosyl-phosphatydil-insositol (GPI) tail and three LU (Ly-6 and uPAR domains) referred as D1, D2 and D3. uPAR is attached to the cell membrane by the glycosyl-phosphatydil-insositol (GPI) tail at the Gly 283 residue at the C terminus (Kjaergaard, et al. 2008). However, unlike integrins, which have trans-membrane domains and intracellular tails, this GPI domain does not span cell membrane (figure 1.12).   uPAR is a heterogeneously glycosylated single polypeptide chain that

contains 313 amino acid residues. From the beginning of the N-terminus, this single polypeptide is arranged into folded homologous, almost globular, structures; D1, D2 and D3 domains. These domains exist as β-pleated sheets arranged into the three finger structures, ending with a small C-terminal loop (Llinas, et al. 2005). Domain 1 and the D1-D2 bind contain a vitronectin binding site while D1 and D3 contain uPA binding sites. As these binding sites are distinct, uPAR are able to bind both ligands simultaneously (Huai, et al. 2008). Furthermore, due to crosstalk between these ligands, the affinity of vitronectin to uPAR is increased by binding of uPA to uPAR (Gårdsvoll and Ploug 2007a).
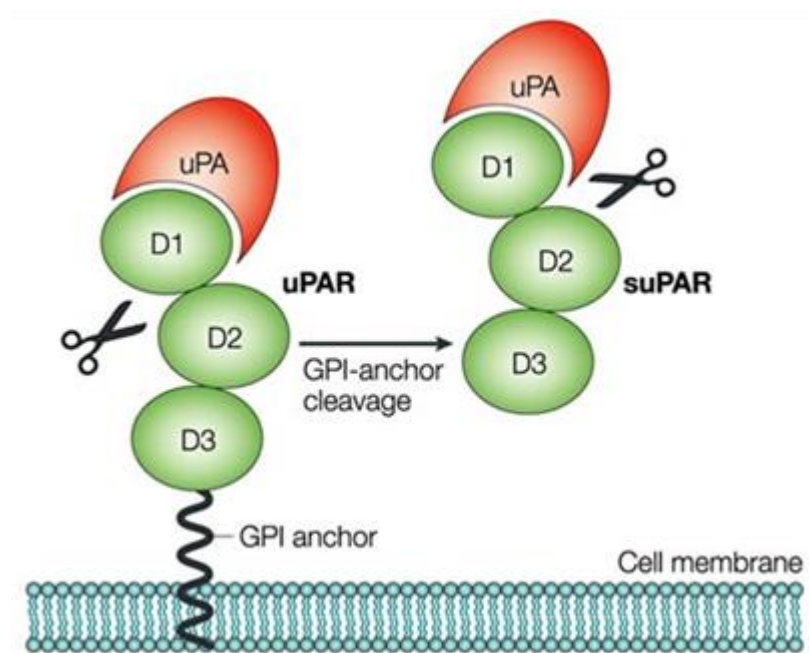
Figure1.12 uPAR structure

The urokinase receptor contains three domains termed D1, D2 and D3. They are attached by an internal disulphide bond. uPAR is anchored to the cell membrane by the glycosyl-phosphatydil-insositol (GPI) tail. Domain 1 and the D1-D2 bond contain a vitronectin binding site, while D1 and D3 contain uPA binding sites. Soluble uPAR is released from the cell membrane by cleavage of the GPI anchor. (Blasi and Carmeliet 2002a)

1.6.2 The function of uPAR.

The functions of uPAR can be classified in three distinct ways; anchorage, protease and signaling. As an anchorage receptor, uPAR is able to attach to many extracellular matrices, such as vitronectin, which in turn regulate cell motility and proliferation. As a protease, uPAR is responsible for converting pro-urokinase into urokinase. uPAR is also involved in activation of plasminogen, which produces plasmin. Both of these enzymes are required in proteolysis and fibrinolysis which are essential mechanisms to release the attachment of migrating cell from ECM and are also important elements during blood clot proteolysis. As it is less of a cytoplasmic domain, uPAR mediates signals through other membrane receptors, such as integrin, receptor tyrosine kinase (RTKS) and G protein coupled receptors for outside-in signal transduction (Blasi and Carmeliet 2002). Among these receptors, integrins are the best studied and characterized. Previous studies have shown that uPAR interacts with a number of the integrin family, specifically the heterodimers containing the β1, β2, β3 and β5 integrin subunits (Ragno 2006). Most recently, attention has focused on a less well characterized member of the integrin family-αvβ6, and its interaction with uPAR (Saldanha, et al. 2007). αvβ6 is thought to play a pivotal role in the metastasis and intra/extravasion of cancer cells via its interaction with uPAR (Ahmed, et al. 2002). It is also thought to play a role in the activation of Latency Associated Peptide (LAT or pro-TGF-β) and in epithelial-Mesenchymal Transition (EMT) (Wei, et al. 1996).

Although the direct binding of uPA with integrins is controversial, accumulating evidence demonstrated the requirement of integrins in uPAR signaling. The interaction of uPAR with its agonists promotes integrin-mediated cell motility as well as cell proliferation (Blasi 1997) (Chapman 1997) (Degryse, et al. 1999). α5β1 was demonstrated to be involved in uPA-uPAR-mediated migration in chinese hamster ovary cells. The vitronectin binding receptors, αvβ3, αvβ5, are other

integrins that are associated with uPAR (Montuori, et al. 2001).

Urokinase is a single chain enzyme, with a molecular weight of 54 kDa. The inactive state of urokinase is referred to as pro-uPA which can be activated by binding to uPAR (Prager, et al. 2004). Activated urokinase is comprised of two chains and is referred to as high molecular weight urokinase. The association of urokinase to uPAR results in plasminogen activation, which then promotes cell migration by enhanced ECM proteolysis (Estreicher, et al. 1990).

D2A and SRSRY peptides allow us investigate the interacting partner of urokinase receptor. D2A was first synthesized by Bernard Degryse and his colleagues (*Bernard Degryse, et al 2005*). Derived from the sequence of Domain 2, D2A peptides (H-Lle-Gln-Glu-Gly-Glu-Glu-Gly-Arg-Pro-Lys-Asp-Asp-Arg-OH) have been shown to interact laterally with αvβ3 integrin and induce cell migration, via outside-in signalling. SRSRY (Ser-Arg-Ser-Arg-Tyr) is another chemotactic peptide, derived form an uPAR sequence, which localized in the D1-D2 linker region. SRSRY peptides bind specifically to fMLP- a seven-transmembrane domain G-coupled receptor, and promote cell migration in this manner (Lucia Gargiulo, et al, 2005).

1.7 A brief summary

Cardiovascular disease (CVD) refers to a group of diseases that involve dysfunction of heart and blood vessels, and consequently include heart failure, arrhythmia, angina, hypertension, high cholesterol, and stoke amongst others. According to the World Health Organisation (WHO), CVD is the leading cause of global death (http://www.who.int/mediacentre/factsheets/fs317/en/). It is also estimated that 17.3 million people died from CVD around the world in 2008; a figure that represents

30% of all global deaths. This number is projected to increase to 23.6 million by 2030. In Ireland, this figure is even higher; approximately 10,000 people die from CVD (coronary heart disease, stroke and other circulatory diseases) annually. CVD is the most common cause of death in Ireland, and accounts for 36% of all deaths. The largest number of these deaths relate to CHD - mainly heart attack - at 5,000. 22% of premature deaths (under age 65) are due to CVD (http://www.irishheart.ie/iopen24/about-us-t-1.html). Globally, CVD are a heavy burden for the health care system, costing approximately €192 billion in the European Union in 2008 alone (Allender, et al. 2008). There are, therefore, significant socio- economic reasons, as well as medical, to further our knowledge of the underlying causes of CVD. This will contribute to overall knowledge and assist in developing efficient preventive (primary, secondary and tertiary) strategies for CVD.

The pathophysiology of CVD is varied and complex, hence there are many cellular and molecular mechanisms which contribute to the disease. General risk factors of CVD include unhealthy diet (high cholesterol diet and salt intake), physical inactivity, and over-consumption of alcohol and tobacco. Prolonged exposure to such unhealthy habits leads to intermediate risk factors, which include high blood pressure, high serum cholesterol and raised blood glucose levels and obesity. These serve to increase the chances of developing CVD in the future.

Our research mainly focused on atherosclerosis, a disease characterized by thickening and loss of elasticity of arterial wall. Atherosclerosis normally occur at large and medium-sized muscular elastic arteries, such as the aorta, coronary and cerebra. It is especially prevalent at sites of arterial bifurcations and regions of high curvature that result in complex blood flow patterns (Hahn and Schwartz 2009). At such sites, disturbed blood flow occurs, and this leads to susceptibility towards the formation of atherosclerotic plaques. These, in turn, cause narrowing of blood

vessels and luminal occlusion, or even wall rupture at advanced stages (Orr, et al. 2006a).

The endothelium is the inner, mono layer of blood vessels. Due to their functional nature, blood vessels are constantly and directly subject to various stimuli, including haemodynamic forces manifested in the form of cyclic strain and shear stress. Endothelial cells sense and convert these mechanical forces into biochemical signals − known as bio-mechanotransduction- which, in turn, alters EC functions. Thus, within the inner layer of blood vessels, vascular endothelial cells undergo acute and prolonged adaptations in order to maintain vascular health. EC morphology and phenotypic change is considered to be the first sign of dysfunction, which leads to development and progression of cardiovascular disease. EC morphology is maintained by actin cytoskeleton (a filamentous protein network in endothelial cells) and is comprised of microfilaments, microtubules and intermediate filaments. Actin polymerization is a complex process that plays an important role in maintaining endothelial integrity. This process requires the recruitment of numerous proteins, including both extra-cellular (e.g. ECMs) and cytosolic proteins (e.g. filamentous proteins). Over the past three decades, studies (including those carried out within our laboratory) have highlighted the importance of ERM proteins in the regulation of cytoskeleton organisation. They appear to function widely as linker proteins that serve to connect microfilaments to the plasma membrane. Our previous work demonstrated that one member of ERM family, Moesin, is critically involved in EC functions, such as migration, angiogenesis, and barrier integrity.

1.8 The overall hypotheses and study aims

1.8.1. Hypothesis

In this thesis, we focused on a relatively new member of ERM family-Merlin. Merlin is another member of the ERM protein family that has been well characterized as a linker protein of cytoskeleton and cell membrane proteins. Mutation of Merlin (NF2 gene) contributes to development of neural tumors such as schwannomas, meningiomas, and ependymomas. However, the role of Merlin in the regulation of actin cytoskeleton within the vasculature is poorly understood. Therefore, in this study, we sought to determine if Merlin is a mechanically-induced actin-binding protein essential to cellular adaptation and function. We believe that merlin is a hemodynamically regulated protein, which plays a crucial role in cytoskeletal dynamic in Human Aortic Endothelial Cells. Merlin plays an important role in regulation of HACE motility through $\alpha v \beta 3$ integrins mediated pathway. We also hypothesis that uPAR, another cell surface receptor, is involved during merlin-integrin mediated mechanno-transduction.

1.8.2 Study Objectives:

In conclusion, maintenance of endothelial integrity is critical to normal blood homeostasis, and as an actin skeleton and cell membrane linker, the role of Merlin in maintaining endothelial integrity is unknown. We therefore look to examine:

- If physiologically relevant levels of laminar and disturbed shear affect the morphology of HAECs and If Merlin is a mechanically-regulated protein in the vasculature. The HAECs therefore will be exposed to haemodynamic forces both in forms of shear stress and cyclic strain via in vitro models. The merlin protein expression level and the merlin mRNA level after

simulate by haemodynamic forces will be examed by using western-blot and QRT-PCR. This examination will determine whether the transcriptional and translational expression level of merlin is mechano-regulated by vascular haemodynamic forces.

- The role of merlin in regulation of HAECs motility. Merlin protein will be knocked-down by mean of transfection of merlin siRNA into HAECs using micropration. The efficiency of transfection will be examed by western-blot to ensure the 70-80% transfection efficiency. The comparison of merlin knock-down HAECs and scrambled control HAECs motility both in form of adhesion and migration will be monitored using real time system xCelligence.

- By using various ECM (including fibronectin, fibrinogen, laminin and vitronectin), RGD inhibitors (including RGD1,RGD2 and RGD3) and peptide (such as D2A and SRSRY) to exam through which mechanism merlin regulates HAECs motility.

Chapter Two

Materials & Methods

2.1 Materials.

2.1.1 Reagents and Chemicals.

Abcam, Cambridge, UK

Primary antibodies: Rabbit polyclonal to NF2/Merlin, Rabbit monoclonal (EP1863Y) to Moesin, Mouse monoclonal to Rac, Chicken polyclonal to cdc42, Mouse monoclonal to GFP, Mouse monoclonal to GAPDH (HRP), Rabbit polyclonal to Beta-Actin.

Secondary antibodies: Rabbit polyclonal to Chicken IgY H&L (HRP), Goat polyclonal to Chicken IgG H&L (CY5).

Aktiengeselischaft and Company, Numbrecht, Germany:

Micro-tubes (0.5ml; 30x8mm); Micro-tubes (1.5 ml; 39x10mm); 6, 24 and 96-well plates; 2, 5, 10, and 25 ml serological pipettes; 2 ml aspirator pipettes; 15 and 50ml tubes; cell scrapers; 58 cm^2, 152 cm^2 tissue culture dishes.

Ambion Inc., Tx, USA:

Silencer$^®$ pre-designed Merlin siRNA, Silencer$^®$ pre-designed Moesin siRNA.

Anachem UK

Tips: 1-20 µl, 10-200, µl 100-1000 µl;

Filtered tips: 1-20 µl, 10-200 µl, 100-1000 µl.

Applied Biosystems, CA, USA

Scrambled control siRNA, High-Capacity cDNA Reverse Transcription Kits, Fast optical 96-well reaction plates (with adhesive covers),

Barloworld-Scientific (London, UK)

White flat-bottomed 96-well plates.

Bachem AG (Switzerland)

RGD inhibitors (H7630, 3164 and 3964)

BioRad (CA, USA)

10X Tris/Glycine/SDS transfer buffer, Coomassie stain, Goat monoclonal to Mouse IgG (HRP) secondary antibody, Thick mini trans-blot filter paper, Laemelli sample buffer, IScript cDNA synthesis kit, Precision plus protein marker.

Cell signalling Technology Inc, MA,USA

Primary antibodies: Rabbit polyclonal to Phospho-Merlin (Ser5180), Rabbit polyclonal to Phospho-Ezrin (Thr567)/Radixin (Thr564)/Moesin (Thr558).

Secondary antibodies: Goat anti-rabbit IgG H+L (HRP).

Cytoskeleton Inc, CO, USA

Rac1, RhoA, cdc42 pull-down assay.

DAKO, CA, USA:

Fluorescent mounting media.

Dunn Labortechnik GmBH, Asbach, Germany:

6-well Bioflex plates.

Eppendorf, Cambridge, UK:

50X TAE Buffer

Eurofins MWG Operon (Ebersberg, Germany)

Primer sets: NF2/Merlin, Moesin, 18s (human).

Fermentas, York, UK:

DNA Ladder, Protein Ladder.

Invitrogen, CA, USA:

Alexa Fluor$^®$ 488 F(ab")2 fragment of goat anti-rabbit IgG (H+L), DH5α E-coli competent cells, DNase, RNase free distilled water, Phosphate buffered saline (PBS), SyberSafe$^®$, Trizol.

Integrated BioDiagnostics (ibidi), Martinsried, Germany:

µ-slide I, µ-slide y-shaped.

Labtech (East Sussex, UK)

ADAMTM Counter kit, Microporation kit, Microporator tubes, solution E buffer, solution R buffer, 10 and 100 µl gold tips.

Lennox Laboratory Supplies LTD, Dublin, Ireland

100% Industrial Methylated Spirits (IMS), 100% Ethanol

Medical Supply Company (Dublin, Ireland)

0.2 ml and 0.5 ml PCR tubes.

Merck Bioscience, CA, USA:

Proteoextract subcellular proteome kit,

Millipore, MA, USA:

Primary antidodies: Rabbit polyclonal to FAK antibody, Rabbit polyclonal to GAPDH antibody, Mouse monoclonal to β1 Integrin active conformations (HUTS-4) antibody,

Secondary antibodies: Goat anti-rabbit IgG H & L (HRP).

Mirus (WI, USA)

TransIT$^®$-2020 reagent, TransIT-siQUEST$^®$ reagent.

Nunc, Rochester, NY, USA:

Cryovials.

Pall Life Science, NY, USA:

Acrodisc 32 mm syringe filter with 0.2 μm super membrane, nitrocellulose membrane.

Pierce Biotechnology, IL, USA:

Bicinchoninic acid (BCA) assay kit, Restore stripping buffer, Supersignal west pico chemiluminescent substrate.

Promocell, Heidelberg, Germany:

Endothelial cell growth medium MV, Endothelial cell growth medium MV Supplement mix, Endothelial cell basal medium MV, Endothelial Cell Growth Supplement/Heparin (ECGS/H) 0.4% (v/v), Fetal Calf Serum (FCS) 5.0% (v/v), Endothelial Growth Factor (EGF) 10 ng/ml and Hydrocortisone 1 µg/ml. Cryo-SFM serum-free medium for cryopreservation, Human Aortic Endothelial Cells (HAECs).

Qiagen, West Sussex, UK:

DNase, HiSpeed Midi-prep kit.

Roche Diagnostics, Basal, Switzerland:

CIM-plates, E-plates, SYBR green (ROX), Protease inhibitor cocktail.

R&D Systems, MN, USA

Recombinant D2A and SRSRY peptides.

Santa Cruz, USA

Primary antibodies: Rabbit polyclonal to Merlin, Rabbit polyclonal to GAPDH.

Sarstedt (Drinagh, Wexford, Ireland)

2 ml aspirator pipettes, 10 cm cell culture dishes, 6-well cell culture plates, 96-well cell culture plates, cell scrapers, 0.2 ml eppendorf tubes, 1.5 ml eppendorf tubes, 2 ml eppendorf tubes, 5 ml pipettes, 10 ml pipettes, 25 ml pipettes.

Sigma Chemical Company Ltd, Dorset, UK:

2,3-diaminonaphthalene, autoradiography developing and fixer solutions, acetone, agarose, ammonium persulfate, ampicillin sodium salt, bradykinin, bromophenol blue, DAPI, DMSO, DNAse kit, EDTA, fetal bovine serum, FITC-dextran (40 kDa), glucose, glycerol, HEPES, LB agar, LB broth, magnesium sulphate, monopotassium phosphate, PBS tablets, penicillin-streptomycin (100X), Ponceau S solution, phosphoramidon, RPMI-1640 medium, sodium bicarbonate, sodium chloride, sodium deoxicholate, sodium dodecyl sulphate, sodium fluoride, sodium phosphate, sucrose, TEMED, trypsin-EDTA solution (10X), Triton® X-100, trizma base, tryptone, Tween®20.

Matrices: Fibronection, fibrinogen, Laminin and Vitronectin.

Star Labs, Milton Keynes, UK:

1μl (P2), 10 μl (P10), 20 μl (P20), 200 μl (P200) and 1000 μl (P1000) tips.

Thermo Fisher Scientific, Leicestershire, UK:

BCA reagent kit, BSA, glycine, isopropanol, Pierce Antibody Clean-up Kit, Pierce Co-IP kit, Super signal western-blot enhancer, trizmabase, weigh boats, RNase Away.

VWR International Ltd. (West Sussex, UK)

Methanol.

2.1.2. Instrumentation.

Applied Biosystems, CA, USA

Applied Biosystems 7500 Real Time PCR system with sequence detection software (SDS).

Bennett Scientific Ltd., Devon, UK

Clifton Duo Water Bath

Bio-Rad, Hercules, CA, USA

MJ-Mini gradient thermocycler. Mini-PROTEAN Tetra Cell system (4-gel system, which includes electrode assembly, Electrophoresis PowerPak®, companion running module, tank, lid with power cables, mini cell buffer dam, Transfer module)

BioTEK, VT, USA

Microplate Reader.

Eppendorf, Cambridge, UK:

Centrifuge5810R, Centrifuge 5430R.

Flexcell International Corp, NC, USA

Flexercell® tension plus™ FX-4000T system.

Global Medical Instrumentation Inc., MN, USA

Mikro 200R micro-centrifuge.

Integrated BioDiagnostics (Ibidi), Martinsried, Germany

Ibidi$^®$ pump and flow system, Incubator.

Labtech (East Sussex, UK)

ADAM MC ™ Counter, Nikon$^®$ Eclipse TS100 phase-contrast microscope.

Mason tech (Dublin, Ireland)

Nanodrop 1000™ system

Millipore, MA, USA

Guava EasyCyte HT System.

Nalgene, Rochester, NY, USA

Cryo-freezing container.

Olympus Inc., PA, USA

Phase contrast microscope (Ck30).

Roche Diagnostics, Basal, Switzerland

xCELLigence$^®$ system.

Stuart Scientific Ltd, Staffordshire, UK

Vortex, Orbital Shakers (SSL1, SSM1), See-Saw Rocker, Block Heater, Rotator.

Syngene, Cambridge, UK:

G-Box fluorescence and chemi-luminescence gel documentation and analysis system.

Taylor-Wharton, USA

Liquid nitrogen cryo-freezer unit.

Thermo Fisher Scientific, Leicestershire, UK

Holten LaminAir laminar flow cabinet

VWR International Ltd. (West Sussex, UK)

Nalgene Mr Frosty® Freezing Container for cryotubes, Haemocytometer

2.1.3 Preparation of stock solutions and buffers.

2.1.3.1 Immuno-blotting.

RIPA Cell Lysis Buffer Stock (1.28X)

HEPES, pH7.5	64 mM
NaCl	192 mM
Triton X-100	1.28% (v/v)
Sodium Deoxycholate	0.64% (v/v)
SDS	0.128% (w/v)
dH$_2$O to final volume	500 ml

RIPA Cell Lysis Buffer (1X)

1.28X RIPA Stock	1X
Sodium Fluoride	10 mM
EDTA, pH8	0.5 mM
Sodium Phosphate	10 mM
Sodium Orthovanadate	1 mM
Protease Inhibitors	1X

Sample Solubilisation Buffer (4X)

Tris-HCl, pH6.8	250 mM
SDS	8% (w/v)
Glycerol	40% (v/v)
β-Mercaptoethanol	4% (v/v)
Bromophenol Blue	0.008% (w/v)

Running Buffer (1X)

Tris-HCl	25 mM
Glycine	192 mM
SDS	0.1%

Transfer Buffer (1X)

Tris-HCl	25 mM
Glycine	192 mM
SDS	0.1%
Methanol	20%

TBS wash Buffer

Tris-HCl, pH7.4	50 mM
NaCl	150 mM

Coomassie Stain

Coomassie Brilliant Blue R250	0.25 g
Methanol:dH_2O (1:1 v/v)	90 ml
Glacial Acetic acid	10 ml

(Filter the Coomassie stain using a 0.25 μm filter)

Coomassie Destain Solution

Methanol : Acetic acid, mixed in a 50:50 ratio

Stripping Buffer

Tris-HCl, pH6.8	62.5 mM
SDS	2% (w/v)
B-Mercaptoethanol	100 mM

2.1.3.2 Molecular Biology Buffers and Medium.

SOC Media

Tryptone	2% (w/v)
Yeast Extract	0.5% (w/v)
NaCl	10 mM
KCl	2.5 mM
$MgCl_2$	10 mM
$MgSO_4$	10 mM
Glucose	20 mM

Luria-Bertani (L.B) Media

Tryptone	1% (w/v)
Yeast Extract	0.5% (w/v)
NaCl	171 mM

Luria-Bertani (L.B) Agar (1L)

Agar   15 g

Made up to 1L with L.B. media

Antibiotics

Antibiotic	Solvent	Final Concentration(µg/ml)
Ampicillin	dH_2O	100
Kanamycin	dH_2O	50

Antibiotics dissolved with dH_2O were sterilised using a 0.25 µm filter.

DNA Loading Buffer

Sucrose	40% (w/v)
Bromophenol Blue	0.25% (w/v)

2.2 Methods

2.2.1 Cell Culture Techniques

2.2.1.1 Culture of human aortic endothelial cells (HAECs)

HAECs were purchased from PromoCell GmbH (Heidelberg, Germany) and all HAEC culturing techniques were conducted in a highly clean and sterile environment using a Holten Lamin Air laminar flow cabinet. Cells were visualized using a Nikon Eclipse TS100 phase-contrast microscope. Cells were maintained in endothelial cell growth medium MV, supplemented with a separate SupplementMix$^®$ of growth factors containing ECGS/H 0.4% (v/v), FBS 5.0% (v/v), EGF 10 ng/ml, hydrocortisone 1 μg/ml, 100 U/ml penicillin and 100 g/ml streptomycin. Cells between passages 10-12 were used for experimental purposes and were maintained in a humidified atmosphere of 5% CO^2/95% air at 37 °C.

2.2.1.2 Trypsinisation of cells

As HAECs are a strongly adherent cell line, trypsinisation was required for the purposes of sub-culturing. For trypsinisation, HAECs were passaged at 70-90% confluence. In preparation, PBS trypsin and growth medium were warmed to 37 °C in a water bath. Growth medium was removed from culture dishes, and cells gently washed 2-3 times in sterile PBS to remove macroglobulin and other trypsin inhibitors present in the culture medium serum. Approximately 100 μl of trypsin-EDTA (10% (v/v) in PBS) per cm^2 of culture dish surface was subsequently added to the cells and incubated at 37 °C for 5 min. When approximately 50% of cells appeared loose, the cell culture dish was gently tapped on the side to remove cells from the culture surface. Trypsinisation was inactivated upon addition of fresh growth medium containing FBS, and cells collected from suspension by centrifugation at 100x g for 5 minutes at room temperature. Cells were

re-suspended in growth medium and counted using either a Neubauer chamber haemocytometer or ADAM MC™ cell counter. Cells were typically split at a 1 in 3 ratio.

2.2.1.3 Cryogenic preservation and recovery of cells

For long term storage, HAECs were maintained in a liquid nitrogen cryo-freezer unit (Taylor-Wharton, USA). Following trypsinisation, HAECs were centrifuged at 100x g for 5 minutes at room temperature and the supernatant removed. The cell pellet was re-suspended in 5.4 ml of freezing medium containing 20% (v/v) FBS, dimethylsulphoxide (DMSO) 10% (v/v) and 1% (v/v) penicillin/streptomycin. 1.8 ml aliquots were transferred to sterile cryo-vials and frozen in a −80 ℃ freezer at a rate of −1 ℃/minute using a Mr Freeze$^®$ cryo-freezing container. Following overnight freezing at −80 ℃, cryo-vials were transferred to the cryo-freezer unit.

For recovery of cells, cryo-vials were thawed rapidly in a 37 ℃ water bath and added to a 58 cm^2 cell culture dish containing 5 ml of pre-warmed (37 ℃) growth medium to dilute the DMSO. After 24 hours incubation the medium was removed, cells were washed once in sterile PBS, and 7 ml of fresh growth medium added.

2.2.1.4 Cell counting
2.2.1.4.1 Haemocytometer

For some experimental purposes and healthy cell growth, cells were seeded at precise numbers and densities. This was achieved using a Neubauer chamber haemocytometer following trypan blue staining of which selectively color the dead cells. In preparation, approximately 20 μl of trypan blue was added to 100 μl of cell

suspension and 20 μl of this mixture loaded into the counting chamber of the haemocytometer. Cells were visualized by phase contrast microscopy. Viable cells excluded the dye, whilst dead cells stained blue due to compromised cell membranes. Under a 10X objective lens, viable cells in the four squares (G1-G4) in each corner were counted (Fig 2.1). Cells touching the top and right lines of a square were not counted, while cells on the bottom and left side were counted. The number of cells was calculated using the following equation:

$$Cell\ number\ per\ ml\ =\ (\frac{G_1\ +\ G_2\ +\ G_3\ +\ G_4}{4})\ (1.2)\ (10^4)$$
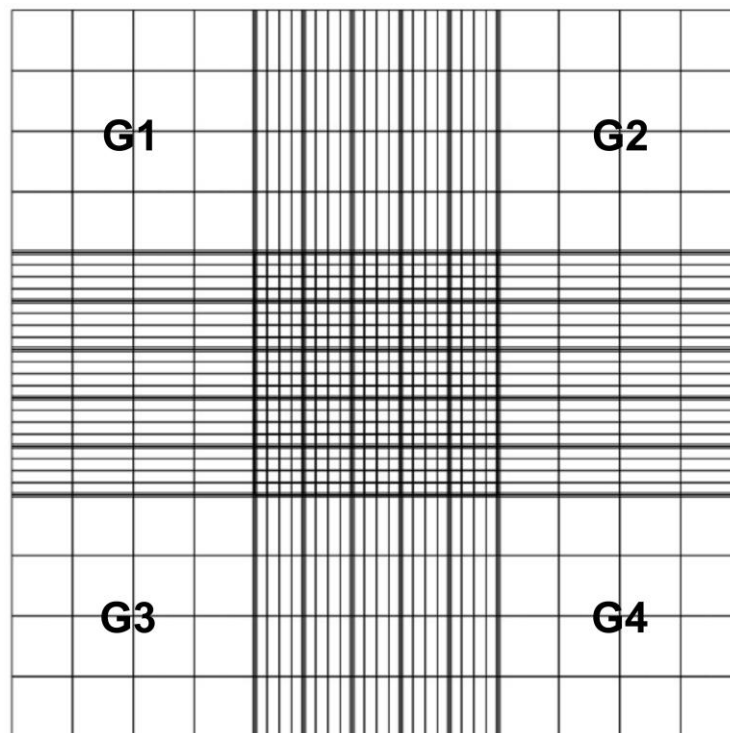
Fig 2.1: Haemocytometer counting chambers.

Under a 10X objective lens, viable cells in the four squares (G1-G4) in each corner of the counting chamber were counted. Cells touching top and right lines of a square were not counted, while cells on the bottom and left side were counted. This procedure prevented the accidental double-counting of cells (this figure is adapted from:
 http://www.microbehunter.com/2010/06/27/the-hemocytometer-counting-chamber/).

2.2.1.4.2 ADAM MC™ Cell Counter

Cell counts were also performed using an automated cell counter (ADAM MC™ cell counter, Digital Bio, Korea) (Fig 2.2), an instrument that utilizes fluorescent cell staining to determine total and viable cell count in a given sample. The ADAM MC™ unit contained fluorescence optics and image analysis software. The optics obtained 40-60 fluorescent images, each read by moving automatic X and Y stages. Image analysis software then determined both total and viable cell numbers simultaneously. The commercially supplied kit used two reaction reagents, solutions T and N. Solution T stained both viable and non-viable cells while Solution N stained only viable cells. In brief, two 12 μl aliquots of a cell sample were taken; one aliquot was mixed with 12 μl of Solution N Accustain and the second with 12 μl Solution T Accustain. 20 μl of each cell mixture was then loaded into the appropriately-labeled chamber in an AccuChip. The AccuChip was then loaded into the ADAMTM counter where 40-60 images were taken of the cell chambers and average cell number and viability calculated using the integrated image analysis software.
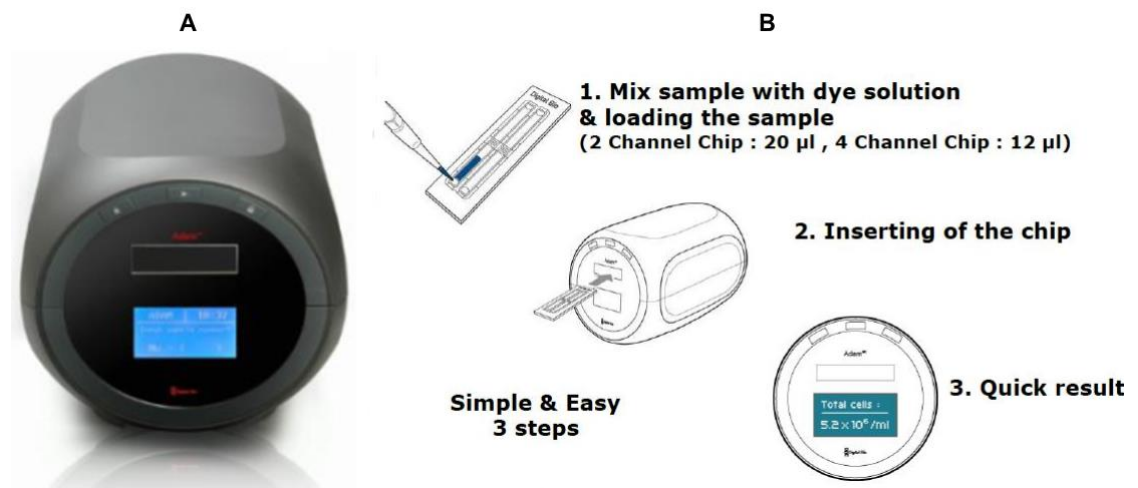
Figure 2.2: (A) The ADAMTM counter and (B) loading of an AccuChip.

To count cells, cell suspensions were mixed with both solutions at a 1:1 ratio and 20 μl of each mixture loaded into an AccuChip cell count chip. Once inside the ADAMTM instrument, the chip was then processed, with the result displayed on the LCD screen (this figure is adapted from: http://www.labtech.ie/automated-cell-counter-stock-clearance).

2.2.2 Shear stress experiments

2.2.2.1 Orbital rotation

For laminar shear stress studies, orbital rotation was applied as per published protocol (Hendrickson, et al. 1999b). HAECs were seeded into 6-well plates at a density of 10^5 cells/cm^2 for confluent studies and 10^4 cells/cm^2 for sub-confluent studies and then allowed to adhere for 24 hours. Culture medium was then removed, and 4 ml of fresh medium with growth serum was added. HAECs were then sheared at 10 dyne/cm^2 for 24 hours using an orbital rotator (Stuart Scientific Mini Orbital Shaker, Staffordshire, UK) set to the appropriate speed as determined by the following equation (Hendrickson, et al. 1999a).

$$Shear\ stress\ =\ \alpha\sqrt{pn(2\pi f)^3}$$

Where:

α = radius of rotation (cm) ρ = density of liquid (g/l)

$n = 7.5 \times 10^{-3}$ (dynes/cm2 at 37 ℃) f = rotation per second

Control plates containing un-sheared "static" endothelial cells were cultured in the same incubator, but on a different shelf to avoid vibrations caused by the orbital rotator. Following shearing experiments, cells were either: (i) harvested for Real-Time PCR measurement of mRNA expression levels; (ii) harvested for Western blotting to determine protein expression levels; (iii) transplanted either into 96 wells cell culture plate, or E-plates for adhesion assay; or into CIM-plates for migration assay.
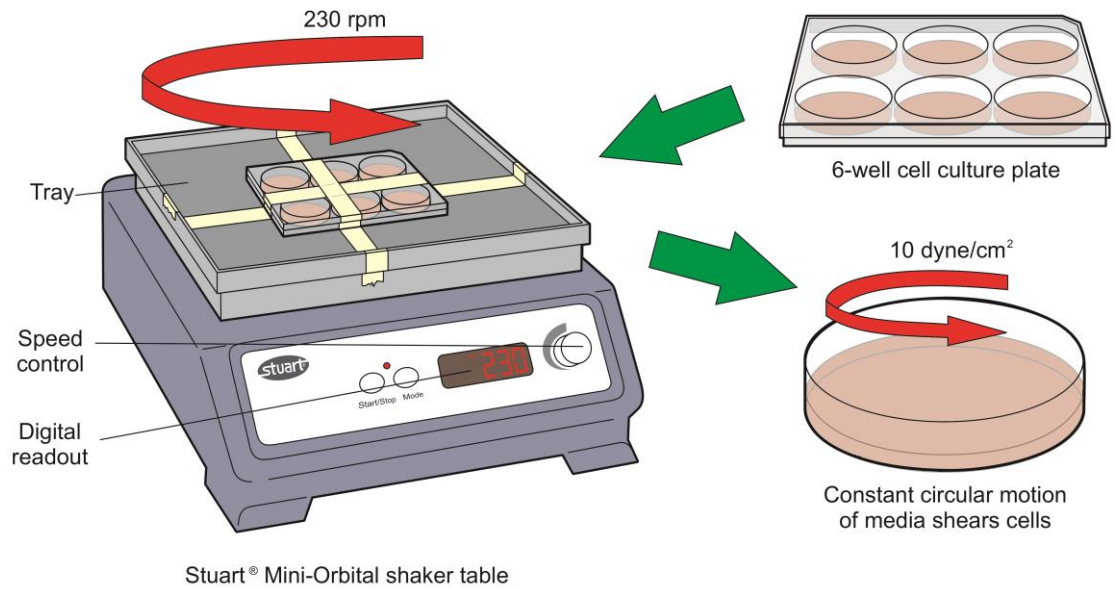
Fig. 2.3: Illustration of the orbital shaker and its operation during shear stress studies

2.2.2.2 Ibidi® (Integrated BioDiagnostics) flow system

The Ibidi® pump system is a perfused flow system used to expose ECs to precisely controlled continuously shear stress on Ibidi® μ-slides. This allows either harvest of cells for Real-Time PCR measurement of mRNA expression levels experiments or fixation for immunocytochemical staining under flow conditions. The system was microscope-friendly allowing for live imaging. There are two forms of μ-slides: Y-shaped which can be used for disturbed shear stress study and straight shaped μ-slides which can be used for laminar shear stress study. For cell seeding, slides, tubes and medium were equilibrated overnight at 37 ℃. Meanwhile, HAECs were diluted to a density of 1×10^6 cells/ml, with 200 μl of this dilution applied into the hollow chambers of each slide. HAECs were permitted time to adhere and grow to confluency (normally takes 24 hours), before μ-slides were connected to the pump system via its luer connectors in accordance with manufacturer's instructions (Fig. 24.). During this procedure, care was taken to

avoid the introduction of air bubbles into the system, which could have resulted in damage to seeded cells.   Cells were subsequently exposed to laminar shear stress at 10 dyne/cm^2 for 24 hours. Control slides containing un-sheared "static" endothelial cells were cultured in the same incubator.   Following experiments, both sheared and static slides were fixed and ready for immunocytochemical staining.
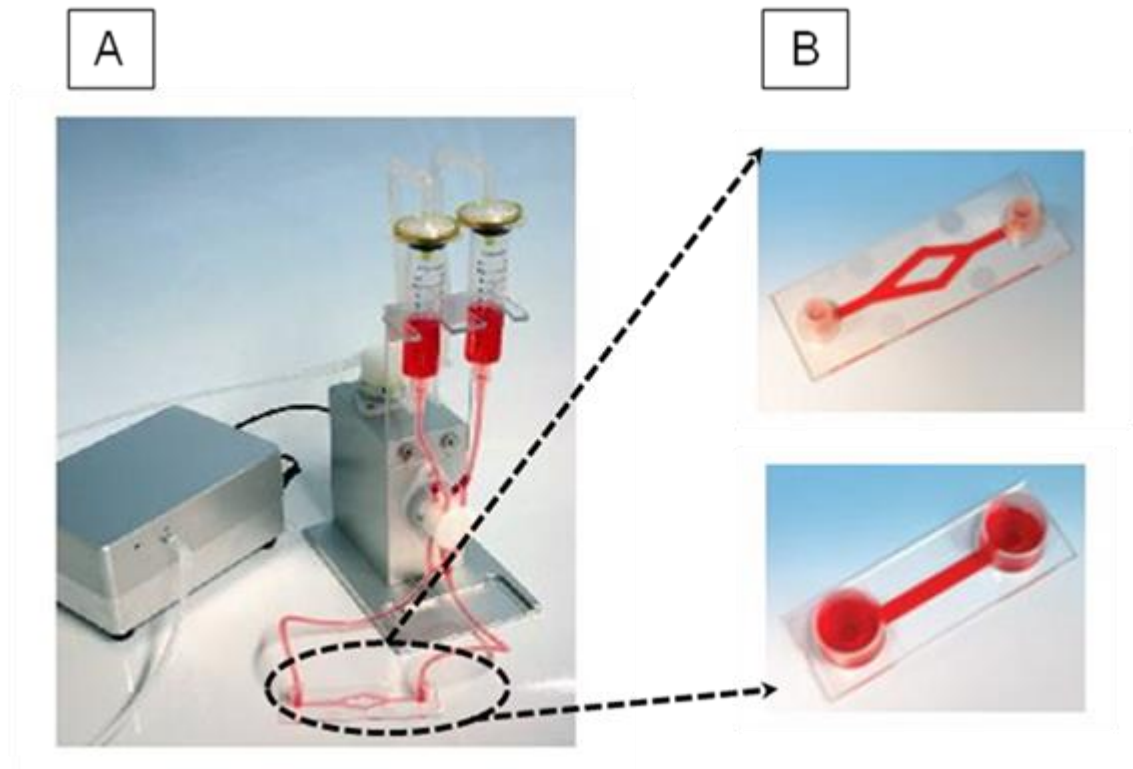
Fig.2.4: Ibidi$^®$ flow system used in laminar shear studies.

A) Ibidi$^®$ pressure pump connected to Ibidi$^®$ flow unit and Y-shaped slide.

B) Illustration of Y-shaped and straight Ibidi$^®$ μ-slides, which allow different forms of shear stress to be investigated (http://www.biophysics.com/ibidi/Instruments/ibidiPUMP.html).

2.2.2.3. Cyclic Strain

For cyclic strain studies, HAECs were seeded into 6-well Bioflex plates (Dunn Labbortechnik GmBH – Asbach, Germany) at a density of 10^5 cells/cm^2. Bioflex$^{™}$ plates contained a pronectin-coated silicon membrane bottom which enabled precise

deformation of cultured cells by a microprocessor-controlled vacuum. Once seeded, cells were then allowed to adhere and grow to confluence over a 24 hours period. Following this incubation period, Culture medium was removed, and 2 ml of fresh medium added to each well. A Flexercell Tension Plus™ FX-4000T™ system (Flexcell International Corp., Hillsborough, NC) (Figure 2.5) was used to apply different cyclic strain regimen to each plate (0%, 5% and 10% strain, 60 cycles/minute). Strain was applied for 24 hours. Cyclic strain is described as the circumferential force/wall tension generated by blood pressure causing a physical stretch in the vessel wall. The relationship between cyclic strain and vessel simension can be defined by Laplace's Law (Laplace, 1899).

$$T=Pr/h$$

Where: T = wall tension (force per unit length of the vessel), P = blood pressure, r = vessel radius and h = thickness of the vascular wall. In this thesis 5% cyclic strain is defined as physiological condition while 10% is defined as pathological condition.

Cells were also acutely stretched to 20% and induced at 1 minute, 5 minutes and 10 minutes intervals. Following strain experiments, cells were either: (i) harvested for Real-Time PCR measurement of mRNA expression levels; (ii) harvested for Western blotting to determine protein expression levels; (iii) transplanted either into 96 well cell culture plates, or E-plates for adhesion assays; or into CIM-plates for migration assays.
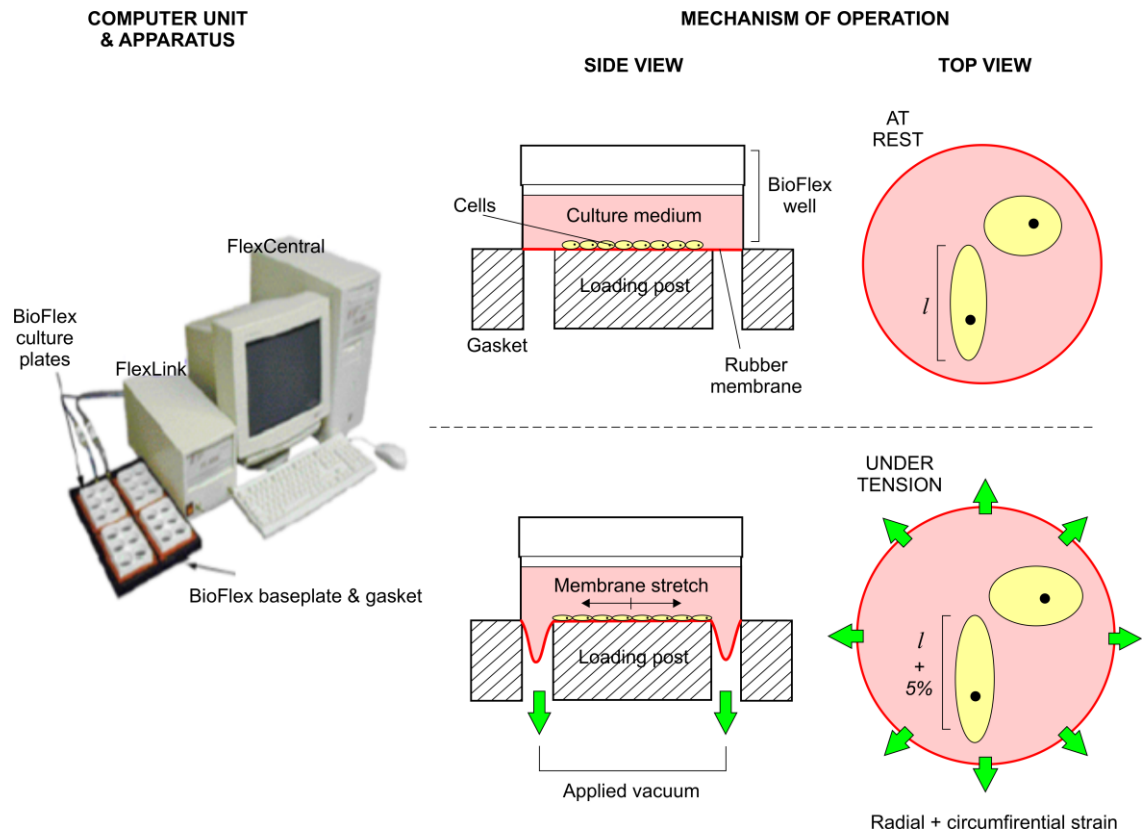
Figure 2.5: Illustration of the computer-controlled Flexercell Tension Plus™ FX-4000T™ system apparatus, and its mechanism of operation in vascular cyclic strain simulation (this figure is adapted from:

http://webpages.dcu.ie/~vhrc/Novel_Technologies.htm).

2.2.3 Immunodetection techniques

2.2.3.1 Western blotting studies

2.2.3.1.1 Preparation of whole cell lysates

To prepare cell lysate for Western blotting, cells were harvested at 4 °C; culture medium removed and cells gently washed three times in ice-cold PBS solution. Following complete aspiration of PBS, 50 μl of 1X radioimmunoprecipitation assay (RIPA) lysis buffer (20 mM Tris, 150 mM NaCl, 1 mM Na2EDTA, 1 mM EGTA, 1% Triton X-100 (v/v), 2.5 mM sodium pyrophosphate, 1 mM β-glycerophosphate,

1 mM sodium orthovanadate, 1 μg/ml leupeptin) was added into each well of the 6-well cell culture plate, then harvested using a cell scraper. Lysate was transferred into an eppendorf tube and rotated at 4 ℃ for 30-40 minutes. After 30-40 minutes rotation, lysate was centrifuged at 10,000 rpm for 20 minutes at 4 ℃. Cell lysate samples were either stored at -80 ℃ for later analysis, or used immediately in a Bicinchoninic acid (BCA) assay or Western blot.

2.2.3.1.2 Bicinchoninic acid (BCA) protein microassay

The BCA assay (also known as the Smith assay) is a biochemical assay used to determine total protein concentration in a solution. The assay relies on two reactions; firstly, peptide bonds in protein reduce Cooper (Cu^{2+}) ions to Cu^{1+} which, in turn, reacts with bicinchoninic acid to form a complex (purple) which strongly absorbs light at 562 nm. Two separate reagents were supplied in this commercially available assay kit (Pierce Chemicals, Cheshire, UK); (A) alkaline bicarbonate solution and (B) copper sulphate solution. Reagent solution was freshly prepared as follows; solution B was mixed into solution A at a ratio of 1:50, with 200 μl of this mixture added to 10 μl of protein lysate and BSA standards (standard curve in the range 0-2 mg/ml) in a 96-well plate. Each protein lysate sample and BSA standard were assayed in triplicate. Following 30minutes incubation at 37 ℃, absorbance was read at 560 nm using an ELx800 microplate reader (BioTek, VT, USA).

2.2.3.1.3 SDS-polyacrylamide gel electrophoresis of proteins

SDS-polyacrylamide gel electrophoresis (PAGE) is a technique used to separate proteins based on their charge. 10% (v/v) acrylamide resolving gels and 4% (v/v)

stacking polyacrylamide gels were used throughout all experiments. Individual volumes of each component required to make gel is shown in the following tables:

Table 2.1: 10% SDS-PAGE resolving gel and (4%) SDS-PAGE Stacking gel composition

(10%) SDS-PAGE resolving gel

Distilled H_2O	4.00 ml
1.5 M Tris-HCl, pH 8.8	2.50 ml
Acrylamide/Bis-acrylamide (30%)	3.33 ml
10% SDS	100 µl
10% Ammonium persulfate	50 µl
TEMED	5 µl
Total volume	10 ml

(4%) SDS-PAGE Stacking gel

Distilled H_2O	6.10 ml
1.5 M Tris-HCl, pH 6.8	2.5 ml
Acrylamide/Bis-acrylamide (30%)	1.30 ml
10% SDS	100 µl
10% Ammonium persulfate	100 µl
TEMED	10 µl
Total volume	10 ml

Approximately 6-8 ml of resolving gel mixture was poured gently between two glass plates, with care taken to avoid bubbles. 1 ml of 70% (v/v) ethanol was then poured

on top (forming alayer) to remove any surface air bubbles and to give an even, isolated surface to the gel. Following 30-45 minute incubation at room temperature, ethanol was poured off and the top of the resolving gel carefully washed using tap-water to remove all remaining ethanol traces. The space between plates was then dried using filter paper. Approximately 1-2 ml of 4% stacking gel mixture was then added on top of the acrylamide stacking gel and the comb carefully inserted. Stacking gel was allowed to polymerise for 15 minutes at room temperature.

Protein samples were prepared as follows; 4X sample buffer (8% SDS (w/v), 20%-mercaptoethanol (v/v), 40% glycerol (v/v), Brilliant Blue R in 0.32 M Tris pH 6.8) was added to the appropriate quantity of protein samples (the ratio was determined by BCA assay). Protein mixtures were boiled at 95 ℃ for 5 minutes to denature. Prior to loading, samples were placed on ice for 5 minutes 20 μl samples were loaded into appropriate lanes along with 3 μl of PageRuler™ Plus Pre-stained Protein Ladder (Fermantas). Protein ladder and samples were electrophoretically separated for 120 minutes at 100V.

2.2.3.1.4 Electrotransfer

To transfer proteins from gel to a membrane, a Mini PROTEAN® Trans Blot Module (BioRad, CA, USA) was employed. Following SDS-PAGE electrophoresis, gels were removed from glass plates and the stacking gel discarded. The resolved gel, membrane and filter paper were then soaked for 10 minutes in ice-cold transfer buffer (25 mM Tris, 192 mM Glycine, 20% methanol) to remove any SDS complexes bound to the gel. Following gel and membrane pre-soakings, the transfer cassette was assembled and sealed tightly, avoiding any air bubbles (as shown in Figure 2.6 below):
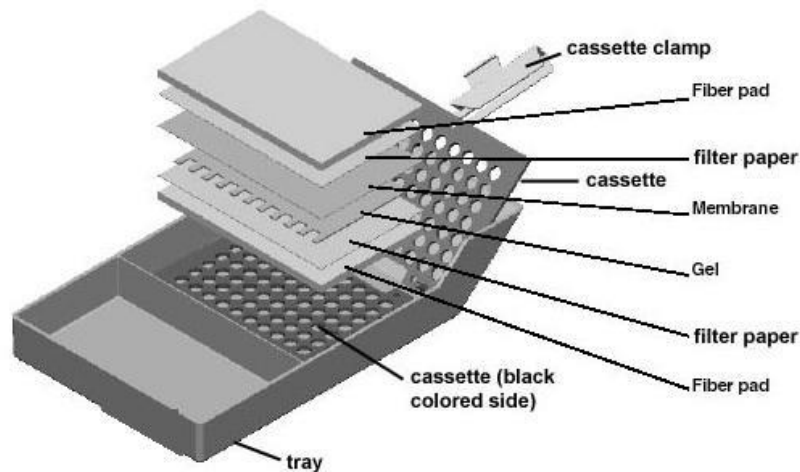
Figure 2.6: Wet transfer cassette assembly

The cassette was inserted into the Trans Blot Module with the black side facing to the same colour. Proteins were transferred at 100 V for 2 hours or overnight at 4 ℃ in a cold room at 50V while stirring.

2.2.3.1.5 Ponceau S staining

Ponceau S solution (Sigma-Aldrich, Dorset, UK) was used to visually confirm transfer of protein to membrane. In brief, mitrocellulose membrane was soaked in 20 ml Ponceau S solution and incubated for 3 minutes with constant agitation.   The membrane was then visualised using G-box analysis and washed with PBS several times until the red stain was completely removed.

2.2.3.1.6 Immunoblotting and chemiluminescence band detection

Following protein transfer, membranes probed phos-Merlin protein were blocked for 60 minutes at room temperature or overnight at 4 ℃ in blocking solution (5% (w/v) BSA in Tris Buffered Saline (TBS), 10 mM Tris pH 8.0, 150 mM NaCl). Membranes probed Merlin protein were blocked for 60 minutes at room temperature or overnight at 4 ℃ in blocking solution (5% (w/v) Milk in Tris Buffered Saline

(TBS), 10 mM Tris pH 8.0, 150 mM NaCl). After blocking, membranes were incubated for 2 hours at room temperature or overnight at 4 ℃ with primary antibody (Table 2.2) whilst rocking.

Table 2.2: Antibody dilutions for Western blot analysis.

Primary Antibody	Primary Dilution	Secondary Antibody	Secondary Dilution
Merlin/NF2 (Santa Cruz)	1:500	Goat (Cell Signalling)	1:1000
Phos-Merlin (Cell Signalling)	1:1000	Goat (Cell Signalling)	1:1000
GAPDH (Santa Cruz)	1:1000	Goat (CellSignalling)	1: 3000

Following primary incubation, membranes were washed 3 times for 5 minutes in wash buffer (0. 1% Tween-TBS). Membranes were subsequently incubated with appropriate horseradish peroxidase (HRP) conjugated secondary antibody in TBST (1% BSA (w/v)) for 1 hour with gentle rocking at room temperature.   Membranes were washed an additional three times using the same conditions as described above.

Supersignal® West Pico (Pierce, Cheshire, UK) was used to detect HRP-conjugated secondary antibodies.   The membrane was incubated with 0.5-1 ml of West Pico for 3-5 minutes, where upon completion of the incubation, excess substrate was removed and chemilluminescent signal were detected by G-Box fluorescence and chemi-luminescence gel documentation and analysis system (Syngene, Cambridge, UK).   The results were then saved as jpg format pictures which can be further analyzed by imagine J software for band intensity change.

2.2.3.1.7 Coomassie gel staining

To visualize protein bands on SDS-PAGE gels, Coomassie gel staining was used. This is a useful technique used to ensure that transfer was executed as expected. The technique includes two steps; firstly, SDS-PAGE gel was immersed with filtered (0.25 μm) coomassie solution whilst rocking for approximately 4 hours. The gel was then de-stained with methanol:acetic acid (50:50) solution until the protein bands were distinctly clear from background. De-stain solution required frequent changing.

2.2.4. Immunocytochemistry

In order to determine the localization of Merlin and its association with actin, HAECs were prepared for immunocytochemical analysis on Ibidi® y-shaped slides (Ibidi®, Germany). HAECs were washed 3 times in PBS and fixed with 3% (v/v) formaldehyde for 15 minutes. Permeabilised cells were subsequently washed in PBS 3 times; with 0.2% (v/v) Triton X-100 for 15 minutes, following which, cells were again washed 3 times. Cells were blocked for 30 minutes in PBS containing 5% (w/v) BSA solution. After blocking, cells were incubated with primary Merlin antibody (Santa Cruz, USA) diluted 1:50 in the blocking buffer for 2 hours at room temperature whilst rocking. This was followed by 3 washes in PBS and 1 hour incubation with 1:00 Alexa Fluor 488 anti-Rabbit secondary antibody. Again, cells were washed 3 times in PBS, after which, nuclear DAPI staining was performed by incubating cells with 500 ng/ml DAPI for 3 minutes. HAECs were also co-stained with F-actin by adding 1 in 40 diluted Rhodamine Phalliodin (Invetrogen) for 20 minutes. Samples were then washed for a final time and were visualised by standard fluorescent microscopy (Nikon Eclipse Ti, Tokyo, Japan).

2.2.5 mRNA preparation and analysis

2.2.5.1 RNA preparation

Total RNA isolation was carried out using the Trizol® method, developed by Chomczynski and Sacchi *(Chomczynski and Sacchi 1987)*. Following haemodynamic stimulus, cells were lysed directly in culture plates by addition of 1 ml of Trizol® per 10 cm^2. Total RNA was harvested by physical removal from the plate using a cell scraper. Samples were then incubated for 5 minutes at room temperature to allow complete dissociation of nucleoprotein complexes. Following incubation, 0.2 ml of chloroform was added per 1 ml of Trizol® reagent used, shaken vigorously for 15 seconds and then centrifuged at 7,000 x g for 15 minutes at 4 ℃. The clear top layer containing RNA was carefully collected and transferred to a fresh, sterile tube. RNA was then precipitated out of solution by addition of 0.5 ml isopropanol per 1 ml Trizol® used. Samples were inverted 5-8 times and incubated for 10 minutes at room temperature and centrifuged at 7,000 x g for 10 minutes at 4 ℃. Supernatant was carefully removed and pellet washed with 1 ml 75% ethanol per 1 ml of Trizol® used. Upon completion of centrifugation at 7,000 x g for 5 minutes at 4 ℃, the resultant pellet was air-dried for 5-10 minutes, before being re-suspended in DEPC-treated water. This was then incubated for 10 minutes at 60 ℃. Following examination of RNA concentration by NanoDrop®, samples were stored at −80 ℃.

2.2.5.2 NanoDrop® ND-1000 Spectrophotometer

To determine the amount of total RNA in each sample, a NanoDrop® ND-1000 Spectrophotometer (Thermo Scientific) was used. After the instrument was blanked with RNase-free water, an undiluted 1.2 µl sample was pipetted onto the end

of a fiber optic cable (Receiving fibre).   (The gap is computer-controlled to both 1 mm and 0.2 mm paths).   Samples were read at wavelengths of 260 nm and 280 nm and analysed by determining the ratio between the two (ABS 260/ABS 280).   A ratio of 1.9 to 2.0 was regarded as highly purified RNA.   Purification of RNA samples was achieved using a DNase treatment kit (Sigma-Aldrich, Dorset, UK).

2.2.5.3 Reverse transcription Polymerase Chain Reaction (RT-PCR)

To reverse transcribe mRNA into cDNA, a high capacity cDNA reverse transcription kit (Applied Biosystems, CA, USA) was used.   The volume of each component is shown below (20 μl was required for each reaction):

RT Buffer (10X)	2 μl
dNTP mix (100 mM)	0.8 μl
Random Primers (10X)	2 μl
MultiScribe Reverse Transcriptase	1 μl
Nuclease-free H_2O	4.2 μl

Reagents were mixed with 1000 ng RNA, and were diluted in 10 μl nuclease-free water.   Samples were then transferred into 0.2 ml PCR tubes and placed into a desktop PCR instrument and run at 25 °C for 10 minutes, 37 °C for 120 minutes and finally 85 °C for 5 minutes.   Total concentration of cDNA product was measured by NanoDrop®.

2.2.5.4 Design of PCR primer set

Merlin/NF2 DNA primers were designed using the online software programme,

Primer3 (http://frodo.wi.mit.edu/). Briefly, the full sequence of Merlin/NF2 on NCBI/BLAST website was chosen. From this sequence, highly conserved areas were copied to Primer3. The primers were designed using this software. Primers which contained 50% GC content or higher and an annealing temperature between 55-60℃ were then chosen. House-keeping genes used were 18s (purchased from Ambion). The primer sequences, lengths and annealing temperatures are shown in the table below:

Table 2.3:   Primer sequences, product size and annealing temperature used for PCR and qPCR

Gene	Primer	Sequence (5'….3')	Product Length (bp)	Annealing Temperature (℃)
Merlin	Forward	ACC GTT GCC TCC TGA CAT AC	234	59.4
	Reverse	TCG GAG TTC TCA TTG TGC AG		57.3
18s	Forward	CAG CCA CCC GAG ATT GAG CA	324	60.0
	Reverse	TAG TAG CGA CGG GCG GTG TG		60.0

2.2.5.5 Polymerase chain reaction (PCR)

Desktop PCR was used to check if newly designed primers were operational before use on Quantitative real-time polymerase chain reaction (QRT-PCR). Each PCR reaction required 25 μl of total final volume, with mixtures prepared as follows:

Forward primer (10 μM)------------------------------1- μl

Reverse primer (10 μM)------------------------------1- μl

cDNA sample--1-µl

Reaction buffer (10X)------------------------------2.5-µl

dNTP (10 mM)--2-µl

MgCl2 (25 mM)-------------------------------------1.5-µl

Taq Polymerase---------------------------------------0.25-µl

RNase free water---------------------------------15.75-µl

This mixture was then placed into an MJ Mini thermal cycler with hot-lid (Bio-Rad, CA, USA). Samples were then subjected to the following cycling conditions:

Table 2.4:   Desktop PCR cycling conditions

Steps		Temperature (°C)	Time
Denaturation		95	5 minutes
Cycling	Denaturation	95	15 seconds
	Annealing	55-60	30 seconds (40 cycles)
	Extension	72	15 seconds
	Extension	72	5 minutes
	Hold	4	Infinite

PCR products were examined by agarose gel electrophoresis, described below.

2.2.5.6 Quantitative real-time polymerase chain reaction (qPCR)

Newly designed primers could be used in qPCR after they were optimized. Quantitative PCR is a technique used to amplify and simultaneously quantify a targeted DNA sequence.   This technique follows the general principle of RT-PCR, with amplified DNA quantified in real-time as it accumulates during the reaction.

This quantification was facilitated using SYBR Green, a dye that fluoresces only when bound to double strand DNA.   Therefore, an increase in DNA product during PCR leads to a quantifiable increase in fluorescence intensity. Quantitative PCR is more precise and accurate then desktop PCR as the amplification fluorescence is read at the end of every cycle, and the amount of cDNA product formed during the PCR cycles can be quantified in real time and graphed.

Quantitative PCR was carried out using an Applied Biosystems 7900HT Fast real-time PCR instrument.   Each reaction was set up in triplicate as follows:

Table 2.5:   Components of Quantitative real-time polymerase chain reaction (qPCR)

Component	Volume (μl)	Final concentration
Forward primer	1.0	300 nM
Reverse primer	1.0	300 nM
cDNA	2.0	10 ng
SYBR Green	12.5	1X
RNase-free water	8.5	
Fianl volume	25.0	

Samples were subjected to an initial denaturation step of 95 ℃ for 10 minutes, followed by 40 cycles at 95 ℃ for 15 seconds and a primer-specific temperature of between 55-60 ℃ for 1 minute.

2.**2.5.7 Agarose gel electrophoresis**

All DNA gel electrophoresis was carried out using GibcoBRL Horizon 20.25 Gel Electrophoresis Apparatus in accordance with the manufacturer's instructions. Briefly, agarose gels were prepared by boiling 1 g of agarose in 100 ml of 1X TAE

buffer (40 mM Tris-Acetate pH 8.2, 1 mM EDTA) using a microwave oven (700 mHz) at full power for 5 minutes to make a 1% gel. Following sufficient cooling (to approximately 60 ℃), 10 μl of SYBR Safe (Invitrogen, The Netherlands) was added to the gel, mixed by swirling and poured into a casting rig. A comb was then inserted in order to form wells. The gel was allowed to cool and polymerise before filling the chamber with 1X TAE and comb removal.

As the 10X buffer in the RT-PCR reaction already contained a loading and tracking dye, 15 μl of PCR product was loaded directly into the wells of the gel. A 1 Kb DNA ladder was also added to one well as a molecular weight marker for reference. The gel was run at constant voltage (5 V/cm, usually 100 V), for 1 to 2 hours. Samples were then visualized using the transilluminator settings on GBOX (Syngene, UK). Images were saved for later densitometric analysis.

2.2.6 Transfection methods

For the purposes of experiments involving siRNA, the predesigned and validated Melin (NF2) siRNA (Cat: s194647) and Moesin siRNA (Cat: s8984) were purchased form Ambion USA, while the scambled control siRNA is commercially available from Applied Biosystems, USA.

2.2.6.1 TransIT-siQUEST® transfection reagent

TransIT-siQUEST® (Mirus) is a highly efficient transfection reagent which allows siRNA delivery into cells and knock-down of the target gene. Transfection was performed following manufacturer's instructions.

HAECs were seeded in 6-well plates prior to transfection, and allowed sufficient

time to adhere, and come to 60-80% confluency.   Once achieved, both full growth and serum-free medium were warmed to 37 °C and TransIT-siQUEST® warmed to room temperature. 250 µl of the pre-warmed serum-free medium was then added into a sterile 1.5 ml micro-centrifuge tube. 7 µl of TransIT-siQUEST® reagent and the required concentration of siRNA were added to the medium and gently mixed by pipetting up and down.   This mixture was incubated at room temperature for 20 minutes.   Meanwhile, fresh medium was added to cells (2 ml per well) and up to the completion of incubation, transfection suspension was added to each well. Cells were placed into a 37 °C incubator for 48 hours, with experiments carried out after this time.

2.2.6.2 Microporation

Microporation is an efficient technique for facilitating transfection, creating effective channels which allow delivery of numerous nucleic acid types (cDNAs, siRNAs e.g.) into mammalian cells.   The microporator unit consisted of a control unit and gold-tip electroporation chamber which allowed generation of a uniform electric field, with minimal heat generation, metal ion dissolution, pH variation and oxide formation (consistent difficulties encountered with conventional electrophoration protocols). Microporation was carried out using a microporation solution kit in accordance with the manufacturer's instructions.

The HAECs were centrifuged at 100 g for 2 minutes at room temperature following washing and trypsinising steps.   The remaining pellet was washed using PBS (Mg2+, Ca2+ free).   Cells were then counted, re-suspended and divided into aliquots containing a final density of 500,000 cells/100 µl.   Aliquots of cell suspension were centrifuged at 100 g for 5 minutes at room temperature.   The appropriate number of wells in a 6-well plate was prepared by pre-incubating 2 ml of culture media, containing serum without antibiotics, in a humidified 37 °C/5%

CO^2 tissue culture incubator. Aliquoted cell pellets were re-suspended in 110 μl/transfection of Buffer R. Re-suspended cells were transferred to a 1.5 ml eppendorf tube and 1-100 nM siRNA/500,000 cells were added. Upon addition of 3 ml Buffer E, the microporation tube was inserted into the pipette station to form the microporation unit (Labtech, East Sussex, UK) (Figure 2.9). The suspension was then pipetted into a 100 μl gold-tip using the microporator pipette. Desired pulse conditions were set; 1000 V, 30 pulse width (ms) and 3 pulse number. Following microporation, each 100 μl sample was transferred to an individual well of the 6-well plate, each containing 2 ml pre-incubated culture medium. Cells were allowed to recover overnight, after which period, the culture medium was changed.

Figure 2.9: Microporator apparatus

A) The base unit generates electrical parameters necessary for transfection of DNA and siRNA into cells.

B) The apparatus utilises a tube (containing the electroporation buffer) and custom pipette used to deliver the electroporation parameters to the cells suspended within a gold-plated pipette tip.

C) The microporation kit containing the necessary microporation solutions, tips and microporation tubes. *(www.microporator.com)*

2.2.7 Migration and Adhesion Assay

2.2.7.1 Cell-Matrix Adhesion

2.2.7.1.1 Coating Cell Adhesion Plates

To investigate cell-matrix adhesion, 96-well plates were coated with either extracellular matrix (ECM) of fibronectin, vitronectin, laminin and fibrinogen. The matrices were made up to a concentration of 10 μg/ml with Ca^{2+} and Mg^{2+} free PBS and sterilised by filtration (0.25μm). Briefly, following washing and moistening by addition of 100 μl PBS, 100 μl of the appropriate matrix was added to wells of the 96-well plate ensuring the well surface was fully covered with no air bubbles present. The plate was then incubated overnight at $4^{o}C$. The following day, 5% BSA was freshly prepared using PBS, denaturation by boiling at $60^{o}C$ for 30 minutes, and filtration (0.25 μm) to remove insoluble material. The matrix was then carefully aspirated and the wells washed twice with 200 μl PBS before the addition of 500 μl BSA to each well, ensuring no air bubbles were present. The wells were then incubated for 1 hour at room temperature, or overnight at $4^{o}C$.

2.2.7.1.2 Cell Adhesion Protocol.

Adhesion assay preparation required pre-coating of 96-well plates, with an additional wash using 200 μl PBS. Serum-starved HAECs were washed with 5 ml PBS and detached using 1 ml of versene (Invitrogen) at 37 ^{o}C. The versene reaction was halted by the addition of 3 ml full culture media. Cells were then counted and re-suspended at a density of 300,000 cells/ml in serum-free media. Cells were then allowed to recover by incubation at $37^{o}C$ for 30 minutes. 100 μl of cells were plated onto the appropriate matrix after incubation, and allowed to adhere for 0-90 minutes at $37^{o}C$. At the end of each time point, unattached cells were removed by aspiration and adhered cells washed twice with 200 μl PBS and fixed

with 3.75% (v/v) paraformaldehyde in PBS for 15 minutes at room temperature. The fixed cells were then rinsed twice with PBS and stained with 0.5% (w/v) crystal violet in 20% methanol for 10 minutes at room temperature.   Once stained, wells were washed three times with 500 μl PBS. Crystal violet was then released by addition of 50 μl 2% SDS for 30 minutes at room temperature whilst rocking.   The absorbance of each well was measured using a spectrophotometer at 562 nm. Samples were run in triplicate, and background staining measured by plating no cells and continuing the protocol as normal.

2.2.7.2 xCELLigence® adhesion assay

The xCELLigence® system (Roche, Basal, Switzerland) is a novel system that allows monitoring of cell migration, adhesion and proliferation in real time without any labeling (Figure2.7).   The system measures electrical impedance across micro-electrodes integrated on the bottom of tissue culture E-Plates. The attachment of the cells with the electrodes affects the local ionic environment at the electrode/solution interface, leading to an increase in the electrode impedance. The more cells present the higher increases in electrode impedance. Briefly, for Merlin knock-down adhesion assays, each 16-well E-plate was pre-coated with fibronectin, fibrinogen, laminin and vitronectin at a concentration of 10 μg/ml (plate coating procedures as described on 2.2.7.3.1); while for adhesion studies, plain 16-well E-plates were used. 100 μl of medium was added into each well to wet the surface and the plate allowed incubating for 30 minutes at room temperature.   During this time, cells were trypsinised and counted. Upon completion of incubation, E-plate background was scanned and 30,000 cells per condition were then added per well in a 16-well E-Plate.   This was then incubated for another 30 minutes at room temperature.   Initial adhesion of cells was then measured at 5 minutes intervals from 0-24 hours.

2.2.7.3 xCELLigence® migration assay

For migration assays, CIM-plates were disassembled according the manufacturer's instructions. 160 µl of serum-free medium was added into the lower chamber, and the upper chamber then placed onto it. Another 50 µl of serum-free medium was added into each well ensuring the surface of the well was fully covered and no air bubbles were present. The plate was then allowed to incubate for 30 minutes. Meanwhile, cells were trypsinised and counted. Upon completion of incubation, the CIM-plate background was scanned. 30,000 cells per condition were then added per well into the upper chamber of CIM-Plate. The CIM-plate was then incubated for another 30 minutes at room temperature. Initial migration of cells was then measured at 5 minute intervals from 0-24 hour.

Fig 2.7   xCELLigence® system

The xCELLigence® system (Roche, Basal, Switzerland) is a novel system that allows monitoring of cell migration, adhesion and proliferation in real time without any labeling

A)   xCELLigence® system used for cell adhesion and migration assays.

B)   CIM- plate for migration assay.

C)   E-plate for adhesion and proliferation assay.

(ww.medgadget.com/2010/06/roche_xcelligence_system_reduces_the_need_for_animal_testing_lab_rats_rejoice.html)

2.2.8 Co-immunoprecipitation (Co-IP)

2.2.8.1 Lysate Preparation

CO-IP is a technique used to isolate target protein complexes out of solution using specific binding antibodies by means of precipitation or pull-out. Complexes of target proteins were then examined by mass spectrometry to monitor possible binding partners. Our studies focused on Merlin and were carried out using a Pierce CO-Immunoprecipitation kit (Thermo UK) in accordance with the manufacturer's instructions. To begin with, HAECs were washed once with ice-cold 1X Modified Dulbecco's PBS and then lysed using ice-cold IP Lysis/Wash Buffer provided in the kit at a ratio of 500 µl per 10 cm^2 growth areas. The mixture was incubated on ice for 5 minutes, with periodic mixing. Upon completion of incubation, lysate was transferred into a 1.5 ml eppendorf tube and centrifuged at 13,000 $\times$ g for 10 minutes. The clear supernatant was transferred into a new tube and stored at -80^oC for further analysis.

2.2.8.2 Resin Preparation

This process was used for coupling affinity-purified antibody to a coupling resin, allowing precipitation of the target protein out of lysate. To begin with, the AminoLink Plus Coupling Resin and reagents were equilibrated to room temperature, with 50 µl of the resin slurry added into a Pierce Spin Column. This was then placed into a microcentrifuge tube and centrifuged at 1000 g for 1 minute. Following two washes (200µL of 1X coupling buffer), centrifugation and discarding of flow-through, approximately 20 µg of affinity-purified Merlin antibody diluted in 200 µl of 1X coupling buffer was added directly onto the resin in the spin column. In a fume hood, 3µl of the Sodium Cyanoborohydride Solution was added for every 200 µl of reaction volume. The screw cap was attached to the column and

incubated on a rotator or mixer at room temperature for 90-120 minutes, ensuring that the slurry remained suspended during incubation. The Merlin-antibody coupled resin was again washed twice using 200 µl of 1X coupling buffer following incubation. Following two more washes using 200 µl of quenching buffer, 3µl of Sodium Cyanoborohydride Solution was added in a fume hood and incubated for 15 minutes with end-over-end mixing. The resin was then washed twice with 200 µl of 1X coupling buffer and followed by six more washes with 150 µl of wash solution. At this piont, the resin was ready to proceed with CO-IP step or it could be washed twice with 200 µl of 1X coupling buffer and filled with 200 µl of 1X coupling buffer for short term storage at 4 ℃. For long-term storage, sodium azide was added to obtain a final concentration of 0.02%. For control studies, the resin was coupled with 80 µl control quenching buffer or using the control resin which was supplied within the kit.

2.2.8.3 Protein precipitation

Protein precipitation steps were performed at 4 ℃ unless otherwise indicated. Following preparation of whole-cell lysate as described in section above, briefly, lysate containing 200 µg of protein was pre-cleared using the control agarose resin slurry coupled resin in accordance with the manufacturer's introductions. Pre-cleared protein mixture was diluted in IP lysis/wash buffer to make a final concentration of 200 µg/500 µl. Prior to adding the protein mixture, resins were washed twice by adding 200 µl of IP lysis/wash buffer. Resin that contained protein mixture was incubated with gentle mixing overnight at 4 ℃. The following day, resins were washed three times with 200 µl of IP lysis/wash buffer. The CO-IP samples were eluted by the addition of 10 µl elution buffer. Samples were stored at - 80 ℃ for further Mass spectrometric analysis or subsequent Western blot analysis.

2.2.9 Transformations

2.2.9.1 Transformation of competent cells

Transformation is a technique that allows introduction of foreign cDNA into competent cells by combining it into a plasmid vector used to facilitate rapid replication and subsequent purification of high quantities of the plasmid DNA. The Merlin-GFP plasmid was purchased from Origen and DH5α competent cells purchased from Invitrogen. The transformation protocol was carried out in the following manner:

Approximately 50 ng of purified DNA plasmid was added to 50 μl of competent bacterial cells. This DNA-bacterial mix was incubated on ice for 30 minutes. Competent cells were then heat shocked by incubation at 42°C for 30 seconds, followed by subsequent incubation on ice for 2 minutes. Following this step, 500 μl of room temperature SOC media which contains 20% tryptone, 5% yeast extract, 0.5% NaCl, 1% 0.25M KCl, 2% 1 M glucose was added and cells were incubated once again for 30 minutes at 37°C while shaking at 150 rpm. Transformant cells were spread on two L.B. agar plates containing the appropriate selective antibiotic in volumes of 50 μl and 500 μl. Spread plates were then inverted and incubated at 37°C overnight, with transformed colonies selected the next day. Non-transformed competent cells were also plated out as a negative control. Only transformed colonies contained the selective antibiotic resistance gene, and therefore were able to grow on the selective antibiotic -containing agar plates. A single colony, therefore, was transferred to a 50 ml sterile tube containing 5 ml of LB broth (1% tryptone, 0.5% yeast extract, 1.0% NaCl). This primary culture was then incubated at 37°C with agitation of 200 rpm for 8 hours. 400 μl of culture was transferred to a 250 ml sterile conical flask containing 50 ml broth and incubated overnight at 37°C with agitation of 200 rpm. DNA mini-preparation was then carried out on this

secondary culture as described below. The remainder of the 5 ml primary culture was used for glycerol stocks.

2.2.9.2 Plasmid purification protocol

Plasmid DNA was purified using the QIAGEN-tip HiSpeed$^®$ system from Qiagen, according to the manufacturer's instructions. In brief, the bacterial cells were pelleted at 6000 x g for 15 minutes at 4^0C and the supernatant discarded by inverting the tube. The bacterial pellet was re-suspended by vortexing in 6 ml chilled P1 buffer. As recommended, 6 ml P2 buffer was then added to lyse re-suspended cells and this mixture was vigorously mixed by shaking for 30 seconds, and subsequently incubated at room temperature for 5 minutes. A further 6 ml of chilled P3 buffer was added to neutralise the lysis activity of P2 and once again the tube was shaken vigorously for 30 seconds. This cell lysate was poured into the barrel of a QIA midi-cartridge and incubated at room temperature for 10 minutes in order to allow settling of cell debris. Using the QIA filter, cell lysate was filtered into a previously equilibrated hispeed midi-prep tip where the DNA was allowed to bind to the resin column. Bacterial cell proteins were removed by washing the column with 20 ml of QC buffer. The DNA was eluted from the column with 5 ml of QF buffer and precipitated by the addition of 3.5 ml room temperature isopropanol. The tube was gently mixed by inversion a few times. DNA was allowed to precipitate at room temperature for 5 minutes. The isopropanol mixture was then added to the QIA-precipitator and filtered through. Plasmid bound to the precipitator was then washed with 2 ml, 70% (v/v) ethanol, air dried by flushing air through and eluted into a 1.5 ml micro-centrifuge tube by the addition of 700 µl sterile TE-buffer. Finally, eluted DNA was flushed through the precipitator once again to remove any unbound DNA and quantified by spectrometric analysis.

2.2.9.3 DNA Quantitation and Storage

In order to determine the concentration of DNA in a sample obtained from the Qiagen plasmid midi kit, the sample was analyzed using a NanoDrop® ND-1000 Spectrophotometer (Thermo Scientific) using TE to blank the instrument. Samples were read at wavelengths of 260 and 280 nm, and the concentration of the DNA calculated out as follows;

$$(Abs\ 260\ nm)\ (dilution\ factor)\ (50)\ =\ DNA\ concentration\ in\ \mu l/ml$$

DNA purity was determined by calculating the ratio of absorbance at 260 nm to 280 nm, the value of which should be greater than 1.6. All samples were tested in triplicate and kept on ice at all times during the experiment. DNA samples were then stored at -20°C for use in transient transfections.

2.2.10. Treatment with Pharmacological inhibitors.

RGD inhibitors allow elucidating the effect of vaiorus RGD peptides, each with specificity for different classes of integrins, on HAEC adhesion. RGD inhibitors were purchased from Bachem Swizland; the details of each inhibitor are listed below:

Table 2.6 The details of RGD inhibitors

	Sequences	Targets	References
RGD1 (H7630)	H-Gly-Arg-Gly-Asp-Ser-Pro-OH	FN and VN	*R.Pytela et al, 1986.* *M.Leptin,1986.* *F.D.Yelian et al, 1993.*
RGD2 (H3164)	H-Gly-Arg-Gly-Asp-D-Ser-Pro-OH	FN	*J.V.Jester et al, 1999.* *M.H.Wu et al, 2001.*
GRD3 (H3964)	H-Gly-Pen-Gly-Arg-Gly-Asp-Ser-Pro-Cys-Ala-OH	VN	*J.E.Mogford et al, 1996.* *K.J.Bayless et al, 2000.*

D2A and SRSRY peptides allow us investigate the interacting partner of urokinase receptor. D2A was first synthesized by Bernard Degryse and his collegues (*Bernard Degryse, et al 2005*). Derived from the sequence of Domain 2, D2A peptides (H-Lle-Gln-Glu-Gly-Glu-Glu-Gly-Arg-Pro-Lys-Asp-Asp-Arg-OH) have been shown to interact laterally with αvβ3 integrin and induce cell migration, via outside-in signalling. SRSRY (Ser-Arg-Ser-Arg-Tyr) is another chemotactic peptide, derived form an uPAR sequence, which localized in the D1-D2 linker region. SRSRY peptides bind specifically to fMLP- a seven-transmembrane domain G-coupled receptor, and promote cell migration in this manner (Lucia Gargiulo, et al, 2005).

To study the effect of D2A and SRSRY on Merlin phosphorylation, HAECs on 6-well plates were grown to confluency, after which the culture media was removed and cells washed twice with sterile PBS. D2A and SRSRY were diluted in serum-free culture media supplemented with antibiotics. The concentrations were optimised by Dr. Bernard Degryse in our laboratory and are shown below:

SRSRY	100 nM
D2A	1 nM

HAECs were exposed to D2A and SRSRY acutely for time intervals of 1, 3, 5, 15 and 30 minutes. Cells were lysed and stored at -80°C for further Western blot studies.

In order to study migration and adhesion, HAECs were grown to confluency, after which growth media was removed and cells washed twice in PBS. Cells were then trypsinised and counted as normal. Inhibitors were diluted in serum-free medium supplemented with antibiotics. The concentrations are given below:

uPA	100 nM
SRSRY	100 nM
D2A	1 nM
VN	1μg/ml
RGD1 inhibitors	0.5mM
RGD2 inhibitors	0.5mM
RGD3 inhibitors	0.5mM

For migration assays, inhibitors were added into the lower chamber of CIM plates and 30,000 cells then added into the upper chamber. For adhesion assays, 30,000 cells and inhibitors were mixed together to make a final volume of 200 μl. The migration and adhesion of HAECs were monitored using the xCELLigence® System.

2.2.11. FACS analysis

Following transfection of HAEC's with GFP-encoding plasmid constructs, cells were monitored by fluorescent activating cell sorting (FACS, GUAVA, Millipore) to detect GFP and assess transfection efficiency. Approximately 24 hours after GFP transfection, HAEC monolayers were washed twice with sterile PBS and harvested by trypsinisation. Cells were pelleted by centrifugation at 700 rpm for 5 minutes at room temperature and the resulting supernatant removed. Cell pellets were then washed with 1 ml of ice-cold PBS supplemented with 0.1% w/v bovine serum albumin (BSA) and centrifuged once again. Following removal of the supernatant, the cell pellets were re-suspended with 1 ml of ice-cold PBS (0.1% w/v BSA) and placed on ice. Samples were analysed by flow cytometry, following the instructions of the manufacturer.

2.2.12. Statisticla Analysis

Results are expressed as mean ±SEM and experiments were performed at least in triplicate (n=3) unless otherwise stated. Statistical comparisons between controls and treated groups were assessed using two-way ANOVA. P-values≤0.05were considered statistically significant. All results were analysed using the GraphPad Prism software.

Chapter Three:

Investigation of Haemodynamic Regulation of Merlin Expression and Co-localisation.

3.1: Introduction

It has long been known that physical levels of hemodynamic force are important in maintaining normal endothelial function. Nearly two hundred years ago, the pathologist, Virchow, pointed out that atherosclerotic lesions emerging at regions within large arteries might relate to the different pattern of blood flow occurring with them (Virchow 1989). In 1969, Caro further illustrated the role of blood flow in atherogenesis (Aoki, et al. 1969). Recent studies have also provided a further substantial evidence of this relationship between atherosclerosis and hemodynamic force.   Due to their functional nature, blood vessels are constantly and directly subject to various stimuli, including haemodynamic forces manifested in the form of cyclic strain and shear stress.   Endothelial cells sense and convert these mechanical forces into biochemical signals which, in turn, alter EC fate and functions (Orr, et al. 2006a).   Thus, within the inner layer of blood vessels, vascular endothelial cells undergo acute and prolonged adaptations in order to maintain vascular health (Furchgott and Zawadzki 1980). These adaptations include morphological change and increased secretion of both cytokines and growth factors *(Gimbrone, M., Kume, N. and Cybulsky, M.I. 1993).*   These, in turn, alter EC functions such as permeability, migration, adhesion and proliferation (De Caterina, Massaro and Libby 2007). Haemodynamic forces achieve these alterations through re-organization of actin in stress fibres, establishments and turnover of focal contacts, redistribution of focal adhesion and re-assembly of cell-cell junctional complexes (McCue, et al. 2006a).   Endothelial cells elongate in the direction of blood flow (McCue, et al. 2006b) which is critical to maintaining endothelial integrity, disruption of which, may lead to dysfunction of ECs and initiation of atherosclerosis. Previous *in vitro* studies have also demonstrated that haemodynamic forces can change expression of genes involved in several actin polymerization functions. This further highlights the importance of hemodynamic forces in regulation of EC functions (Kris, Kamm and Sieminski 2008).

EC motility is a complex process, which requires the recruitment of many proteins. These proteins include both extra-cellular (eg. ECMs) and cytosolic proteins (eg. filamentous proteins). During the last three decades, studies (including those carried out within our laboratory) have highlighted the importance of ERM proteins in the regulation of cytoskeleton organisation. They appear to function widely as linker proteins that serve to connect microfilaments to the plasma membrane. The C-terminal domain attaches to the actin filaments, and the N-terminal FERM domain attaches to the cytosolic face of trans-membrane proteins, including CD44, CD43, ICAM2 (McClatchey and Fehon 2009) and integrins (Bretscher, Edwards and Fehon 2002b). ERM is known to be involved in development (Saotome, Curto and McClatchey 2004b), differentiation (Doi, et al. 1999b), mitosis (Kunda, et al. 2008), epithelial morphogenesis (Pilot, et al. 2006) and metastasis (Christofori 2006). Previous works performed in our laboratory have also indicated that the protein, Moesin, is critically involved in EC functions such as migration, angiogenesis, and barrier integrity.

3.1.1. Hypothesis

This study will focus on a relatively new family member of ERM, Merlin. Although the functions of Merlin have been intensively studied since it was discovered 20 years ago, its role in the regulation of actin cytoskeleton organisation in endothelium remains unknown. Therefore, this study will investigate whether Merlin, a pivotal tumour suppressor protein of the ERM family, is a mechanically-induced actin-binding protein essential to cellular adaptation or if it is a reinforcement response to continuous haemodynamic assault. We believe that haemodynamic forces such as laminar shear stress altering HAECs morphology and HAEC modify its morphology through promoting actin polymerisation which requires regulate the expression of many actin adapter proteins including merlin. We deduce that merlin is a hemodynamically regulated protein, which plays a

crucial role in cytoskeletal dynamic in Human Aortic Endothelial Cells and localise at many functional structures such as focal adhesion, stress fibre and the leading edge of migrating cells.

3.1.2 Study Aims:

In conclusion, maintenance of endothelial integrity is critical to normal blood homeostasis, and as an actin skeleton and cell membrane linker, the role of Merlin in maintaining endothelial integrity is unknown.   We therefore look to examine:

- If physiologically relevant levels of laminar and disturbed shear affect the morphology of HAECs;
- If Merlin is a mechanically-regulated protein in the vasculature;
- Localization of Merlin in HAECs under mechanical stimulation;
- Examination of the effect of shear stress on action polymerization and co-localisation of Merlin protein with F-actin.

3.2 Results

3.2.1 Characterisation of Human Aortic Endothelial Cell

3.2.1.1 Human Aortic Endothelial cell morphology

In this study, we initially investigated the morphology of HAECs and the effect of laminar shear stress on HAECs' morphological alteration. Under physiological static conditions, HAECs present a smooth "cobblestone" morphology that realigns in the direction of laminar shear stress *(Cines et al, 1998; Gimbrone, 1987).* For these initial studies, HAECs were seeded into Y-shaped micro-slides (Ibidi®), and were grown to confluency. After exposure to LSS (10 dyne/cm^2, 24 hours), the cells were then fixed and monitored by phase-contrast microscopy for characteristic growth patterns and this typical "cobblestone"-shaped morphology. Results clearly showed the realignment of HAECs in the direction of flow in comparison with static controls under LSS, in which no uniform realignment was observed under DSS at regions of bifurcations and curvature.
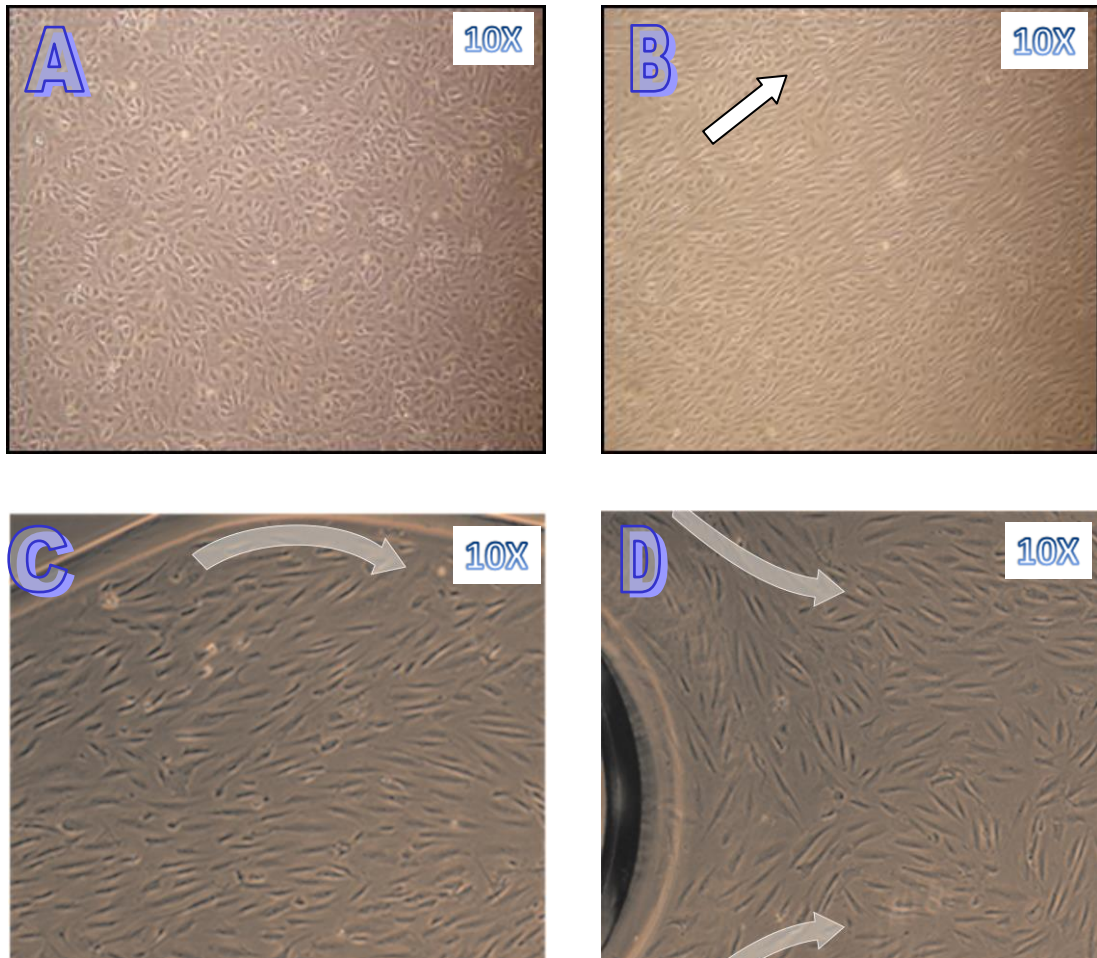
Figure 3.1: Human Aortic Endothelial cell (HAECs) morphological alterations in response to LSS and DSS compared to static control cells.

HAECs were sheared at 10 dynes for 24 hours. using the Ibidi® system.   B) Compared with the static control (A), HAECs realigned in the direction of LSS. White arrows indicate the direction of flow.   No uniform HAEC realignment was observed under DSS conditions. Images are representative.   C) Site of curvature.   D) Site of bifurcation.

3.2.1.2 F-actin realignment in response of laminar shear stress

F-actins, a major component of the cytoskeleton, are involved in many functional cellular substructures, including stress fibres, focal adhesions and adherens junctions. Polymerisation of F-actins is the initial step in HAEC response to haemodynamic forces. Therefore, we investigated the effect of LSS on F-actin realignment in HAECs. As before, HAECs were seeded into μ-slides (Ibidi[®]), and grown to confluency. Following exposure to LSS (10 dyne/cm^2, 24 hours), cells were then fixed and stained with phalloidin stain for F-actin. Cells were monitored by confocal microscopy for F-actin realignment. From the fluorescent images obtained, we observed that F-actin realigned in the direction of flow compared with static controls under LSS.
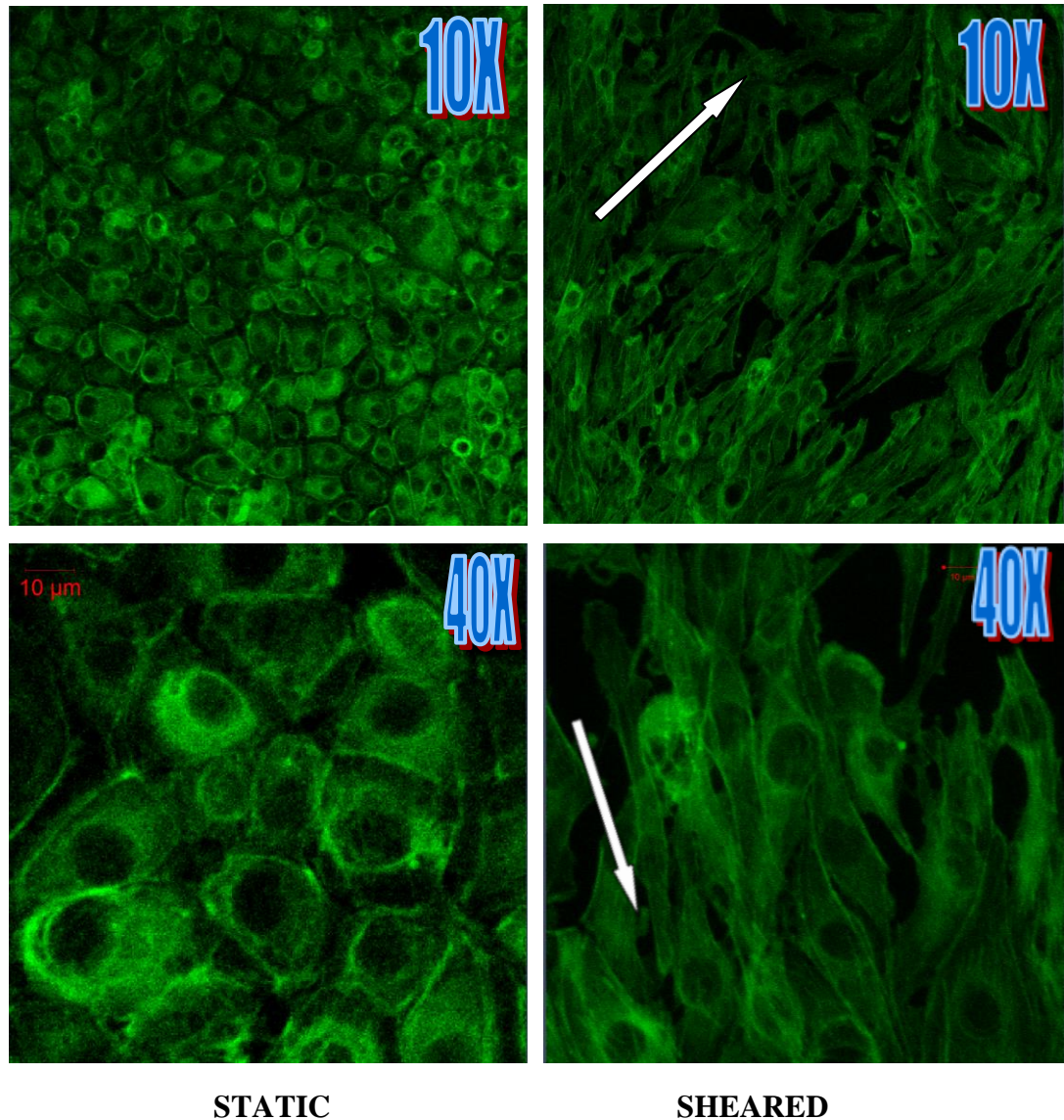
Figure 3.2: F-actin staining of HAEC's, with and without shear.

Confluent HAECs were exposed to LSS (10 dynes/cm^2, 24 hours), and monitored for F-actin realignment using confocal microscopy (Alexa Fluor 488® phalloidin (Invetrogen) stain for F-actin). Results indicated that HAEC F-actin filaments realigned in the direction of flow under shear stress. White arrows show direction of LSS.

3.2.2 The effect of haemodynamic forces on Merlin expression

3.2.2.1 The effect of shear stress on Merlin protein expression

It has been previously shown from work carried out in this laboratory by Mishan Britto (publication in preparation) that Moesin protein expression in HAECs is down-regulated by LSS (10 dyne/cm^2, 24 hours). Therefore, the same protocol was carried out to investigate the effect of shear stress on Merlin protein expression. HAECs were seeded into 6-well plates at a density of 10^5cells/cm^2 for confluent studies and 10^4cells/cm^2 for sub-confluent studies and subsequently permitted to adhere for 24 hours in order to reach confluency and 80% confluency respectively. HAECs were then sheared at 10 dyne/cm^2 for 24 hours using an orbital rotator. Control plates containing un-sheared "static" endothelial cells were cultured in the same incubator, but on a different shelf in order to avoid vibrations produced by the orbital rotator in operation. Following shearing experiments, cells were lysed and Merlin protein expression changes were monitored by Western blot analysis. 20 μg of each sample was loaded into each lane of 10% SDS-PAGE polyacrylamide gel. From the results, it was observed that Merlin protein expression in sub-confluent HAECs decreased by approximately 34% relative to the static control, while only 13% decrease was observed in confluent HAECs (Figure 3.3).
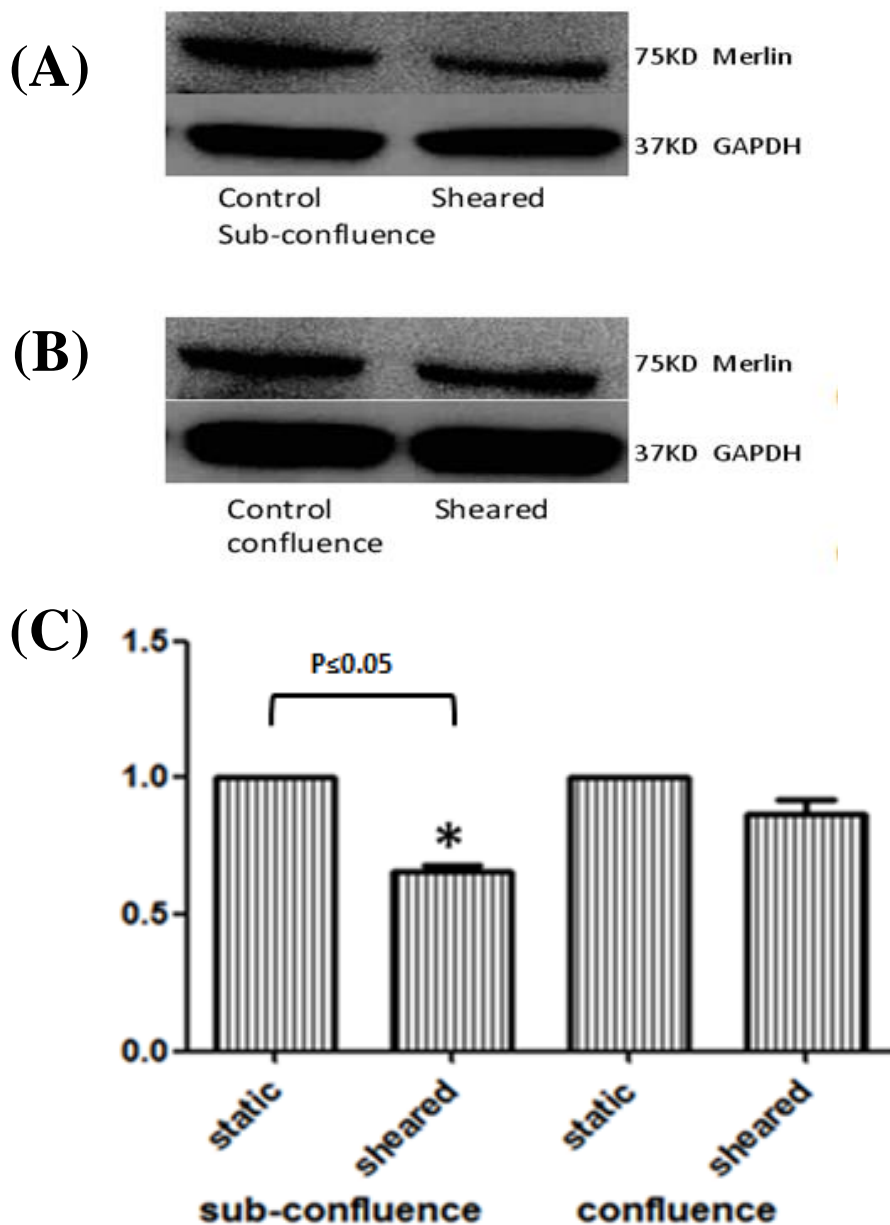
(A)

75KD Merlin

37KD GAPDH

Control   Sheared
Sub-confluence

(B)

75KD Merlin

37KD GAPDH

Control   Sheared
confluence

(C)

$P \leq 0.05$

static   sheared   static   sheared
sub-confluence   confluence

Figure 3.3:   The effect of shear stress on Merlin protein expression

Following exposure of 10 dyne/10cm^2 of physiological, laminar, shear stress over a 24 hours time period using the orbital rotator, cell lysates were analysed by Western blot. A) were conducted on sub-confluent cells seeded at 10^4 cells/cm^2.   B) were conducted on fully-confluent cells seeded at a density of 10^5 cells/cm^2.   C) Histograms represent fold change in band intensity relative to un-sheared controls.   All values were controlled for equal loading by equalising for corresponding GAPDH protein. Results are averaged from three independent experiments $\pm$SEM and each experiment was performed in triplicate; *P $\leq$0.05 vs control.

3.2.2.2 The effect of shear stress on Phosphorylation state of Merlin

The same protocol was carried out in order to investigate the effect of shear stress on phosphorylation state of Merlin. HAECs were seeded into 6-well plates at a density of 10^5 cells per cm^2 for confluent studies and 10^4 cells per cm^2 for sub-confluent studies and then allowed to adhere for 24 hours before reaching confluency and 80% confluency separately. HAECs were then sheared at 10 $dyne/cm^2$ for 24 hours using an orbital rotator. Control plates containing un-sheared "static" endothelial cells were cultured in the same incubator, but on a different shelf to avoid vibrations caused by the orbital rotator. Following shearing experiments, cells were lysed and phosphorylation state of Merlin was monitored by Western-blot. Phosphorylation state of Merlin in sub-confluent HAECs was found to increase by approximately 2.37 fold relative to total merlin protein, while only 1.44 fold increase in confluent HAECs (Figure 3.4).
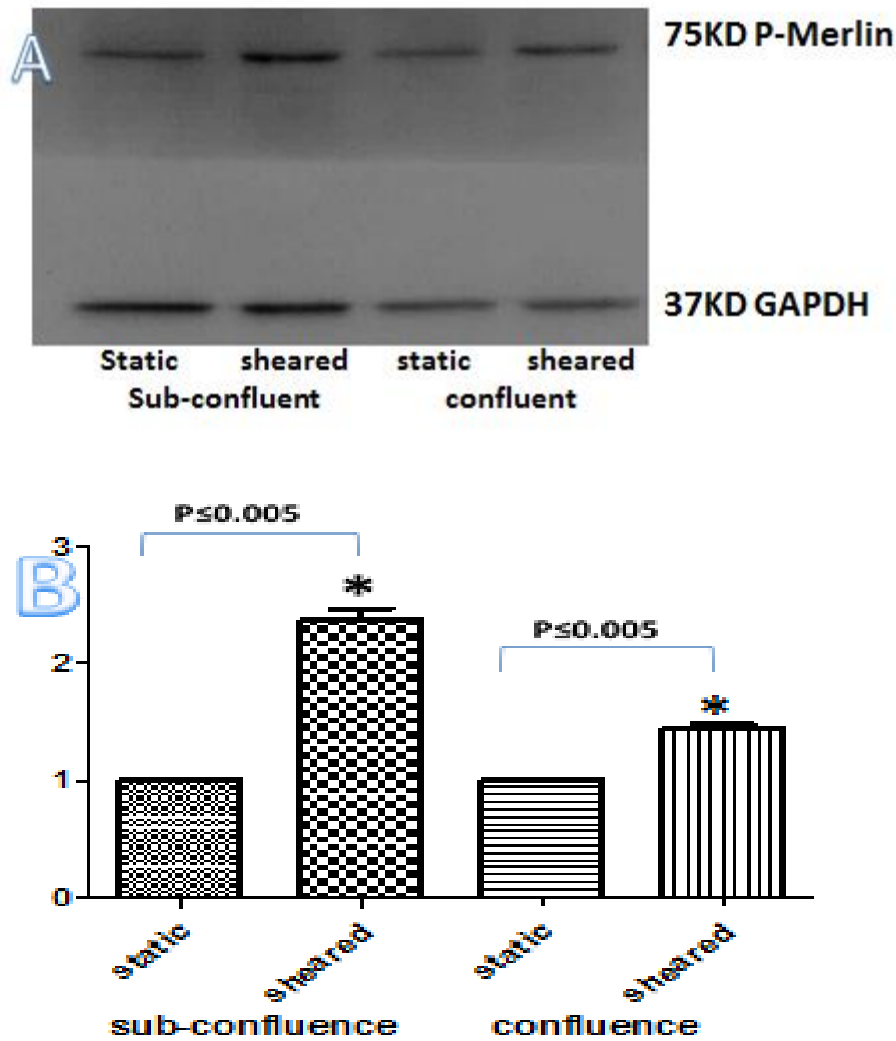
Figure 3.4: The effect of shear stress on Phosphorylation state of Merlin

Following exposure of to 10 dyne/10cm^2 of laminar shear stress over a 24 hour time period using an orbital rotator, both sub-confluent cells (seeded at 10^4 cells/cm^2) and fully-confluent cells (seeded at 10^5 cells/cm^2) were lysed and analysed by Western blotting. A) Western blot analysis to generate phosphorylated merlin protein band. B) Histograms represent fold change in band intensity relative to total merlin protein. All values were controlled for equal loading by equalising for corresponding GAPDH protein. Results are averaged from three independent experiments $\pm$ SEM and each experiment was performed in triplicate; *P$\leqslant$0.005 vs control.

3.2.2.3 The effect of cyclic strain on Merlin protein expression

For cyclical strain studies, HAECs were seeded into 6-well Bioflex plates (Dunn Labbortechnik GmBH – Asbach, Germany) at a density of 10^5 cells per cm^2. Bioflex^{TM} plates contained a pronectin-coated silicon membrane bottoms, enabling precise deformation of cultured cells by microprocessor-controlled vacuum. Once seeded, cells were allowed to adhere and grow to confluence over a 24 hour period. Following this incubation period, culture medium was removed, and 2 ml of fresh medium added to each well. A Flexercell Tension Plus^{TM} FX-4000T^{TM} system (Flexcell International Corp., Hillsborough, NC) was employed to apply different cyclic strains. Following exposure of HAECs to cyclic strain at static (0%), physiological (5%) and pathogenic (10%) levels over a 24 hour time period, Merlin protein expression was monitored by Western blotting. Protein expression of Merlin was found to have decreased by approximately 25% in HAECs at 5% cyclic strain relative to the static control. Reaching pathogenic levels of cyclic strain, Merlin was observed to have decreased by approximately 34% in HAECs (Fig 3.5).
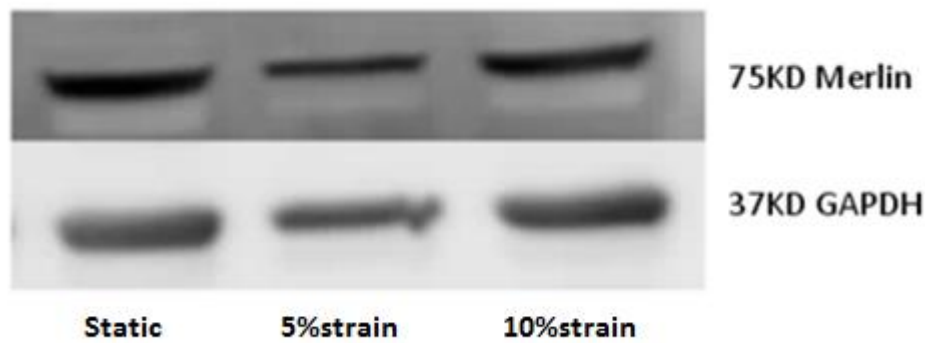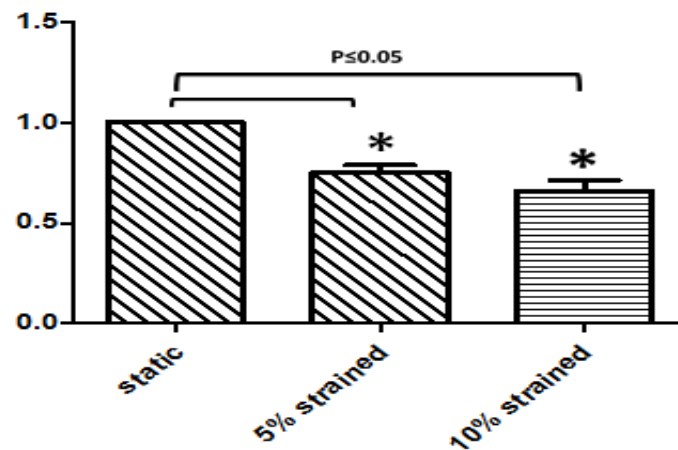
Figure 3.5:   The effect of cyclic strain on Merlin protein expression

Following exposure of to 5% and 10% cyclic strain over a 24 hour time period using the Flexercell Tension Plus™ FX-4000T™ system, cell lysates were analysed by Western blotting.   Histograms represent fold change in band intensity relative to un-strained controls. Western blot band analysis Merlin protein (75KD) expression change in HAECs following 24 hours cyclic strain.   All values were controlled for equal loading by equalising for corresponding GAPDH. Results are averaged from three independent experiments ±SEM and each experiment was performed in triplicate; *P≤0.05 vs control.

3.2.2.4 The effect of cyclic strain on phosphorylation state of Merlin

Again, HAECs were seeded into 6-well Bioflex plates (Dunn Labbortechnik GmBH – Asbach, Germany) at a density of 10^5 cells per cm^2.   Cells were then allowed to adhere and grow to confluence over a 24 hour period.   After this incubation period, culture medium was removed, and 2 ml of fresh medium added to each well. Following exposure of HAECs to cyclic strain at static (0%), physiological (5%) and pathogenic (10%) levels over a 24 hour time period, phosphorylation state of Merlin was monitored by Western blotting. Phosphorylation state of Merlin was found to have increased by approximately 1.85 fold in HAECs at 5% cyclic strain relative to the total merlin protein.   Reaching pathogenic levels of cyclic strain, Merlin was observed to have increased by 2.51 fold in HAECs (Fig 3.6) relative to the total merlin protein.
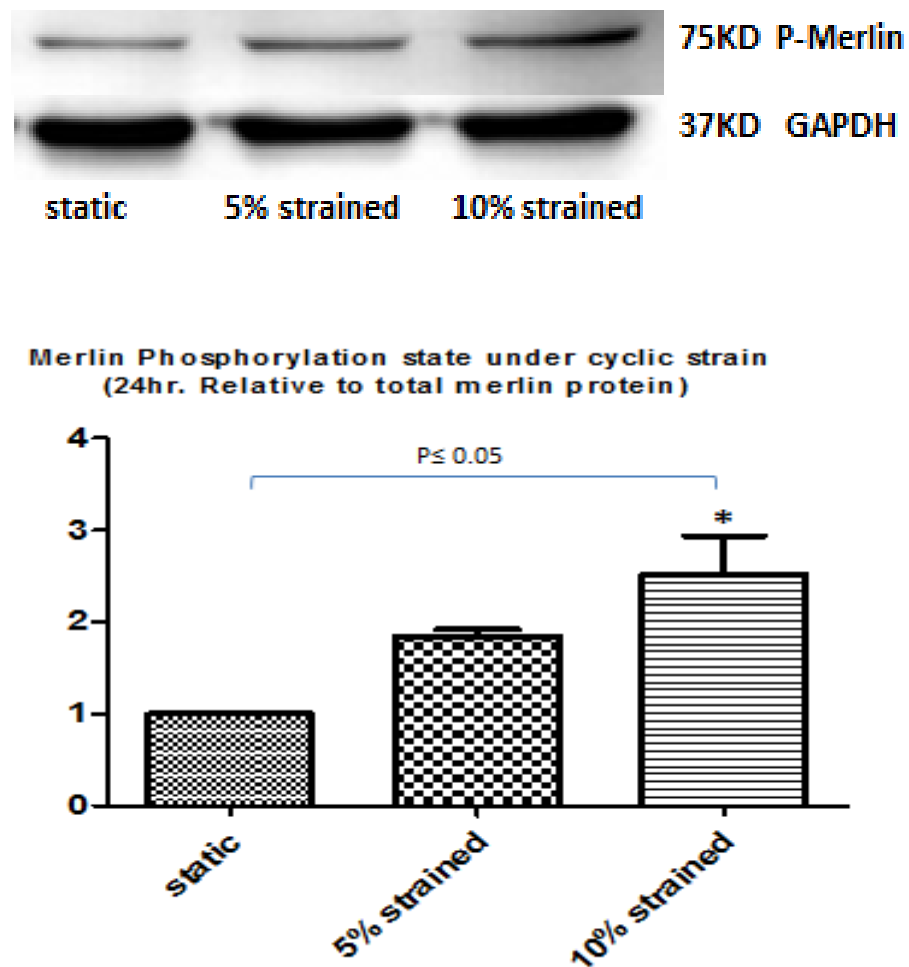
Figure 3.6: **The effect of cyclic strain on Phosphorylation state of Merlin**

Following exposure of to 5% and 10% cyclic strain over a 24 hour time period using a Flexercell Tension Plus™ FX-4000T™ system, cell lysates were analysed by Western blot. Western blot band analysis phosphorylated merlin protein after expose to cyclic strain for 24 hours. Histograms represent fold change in band intensity relative to total merlin protein. All values were controlled for equal loading by equalising for corresponding GAPDH protein. Results are averaged from three independent experiments $\pm$ SEM and each experiment was performed in triplicate; *P$\leqslant$ 0.05 vs control.

3.2.2.5 The effect of acute stretch on phosphorylation state of Merlin

HAECs were also exposed to 20% stretch for various time periods (1 minute, 5 minute and 10 minute) in order to investigate acute Merlin phosphorylation state. HAECs were seeded into 6-well Bioflex plates (Dunn Labbortechnik GmBH – Asbach, Germany) at a density of 10^5 cells per cm^2. Cells were then allowed to adhere and grow to confluence over a 24 hour period. Following this incubation period, culture medium was removed, and 2 ml of fresh medium added to each well. Cells were then acutely stretched to 20% and induced at 1 minute, 5 minute and 10 minute intervals using the Flexercell Tension Plus™ FX-4000T™ system. Phosphorylation states of Merlin was significantly decreased by 56% at 1 minute of stretch, 52% decrease at 5 minute of stretch and 60% at 10 mintes of stretch respectively compare to un-stretched control (Figure.3.6).
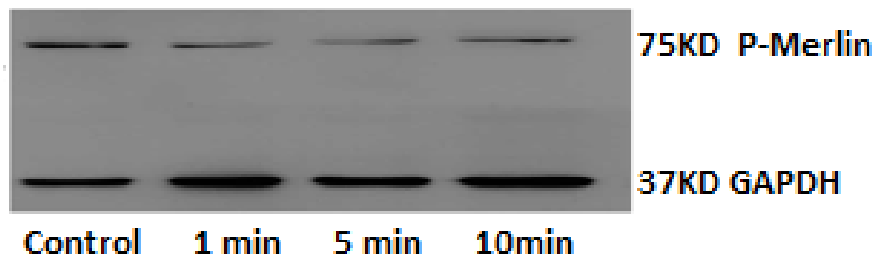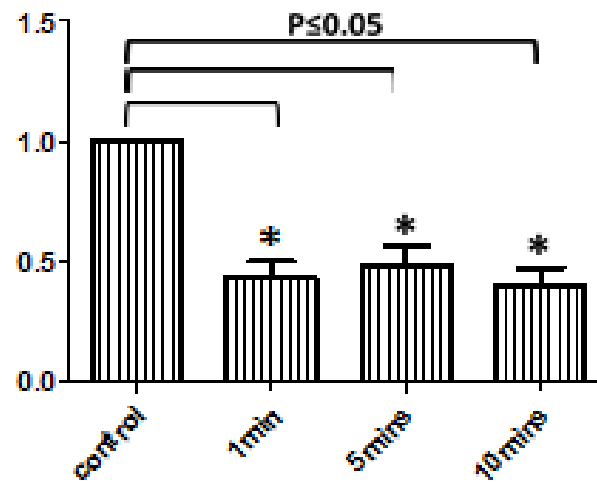
Figure 3.7: The effect of 20% cyclic stretch on Phosphorylation state of Merlin

Following exposure of 20% cyclic stretch at time point of 1 minute, 5 minute and 10 minute using the Flexercell Tension Plus™ FX-4000T™ system, cell lysates were analysed by Western blot. Western blot analysis of Phosphorylation state of Merlin (75KD) in HAECs after exposure to 20% cyclic strain at different time points. Histograms represent fold change in band intensity relative to un-stretched controls. All values were controlled for equal loading by equalising for corresponding GAPDH. Results are averaged from three independent experiments ±SEM and each experiment was performed in triplicate; *P≤ 0.05 vs control.

3.2.2.6 The effect of haemodynamic forces on Merlin mRNA expression

Previous results show that Merlin protein expression and phosphorylation state are regulated by haemodynamic forces. Therefore, we commenced an investigation to further examine mRNA levels which reflect Merlin gene expression under various haemodynamic forces. Briefly, following exposure of HAECs to cyclic strain at static (0%), physiological (5%) and pathogenic (10%) levels over a 24 hour time period, and exposure of both fully-confluent and sub-confluent HAECs to laminar shear stress (10 dynes/cm^2; 24 hour), total RNA isolation was carried out using the Trizol® method, developed by Chomczynski and Sacchi (Chomczynski and Sacchi, 1987). Messenger RNA was then reverse transcribed into complimentary DNA (cDNA) using a high capacity cDNA reverse transcription kit (Applied Biosystems, CA, USA). Merlin primers were designed using the online software programme, Primer3 (http://frodo.wi.mit.edu/) and Desktop PCR used to ensure that newly designed primers were operational before use in Quantitative real-time polymerase chain reaction (QRT-PCR) experiments. QRT-PCR products were tested on a 1% agarose gel to ensure that only one clear band at the expected product size was visualised. Merlin mRNA changes were examined using an Applied Biosystems 7900HT Fast real-time PCR instrument following Quantitative real-time PCR Experiment (MIQE) guidelines (Bustin, et al., 2009). The house keeping gene, 18s, was used for all qPCR normalisation.

Messenger RNA levels were reflective of these protein quantities, with Merlin increasing expression significantly by 71% relative to the static control in sub-confluent HAECs exposed to laminar shear stress at 10 dyne/cm^2 for 24 hours In contrast, only a 24% increase in confluent HAECs was determined under the

same conditions (Figure 3.8 (A)). Under 5% cyclic strain for 24 hours, Merlin mRNA levels only increased by approximately 15%, while a significant increase (approximately 89%) was found under 10% strain for 24 hours (Figure 3.8 (B)).
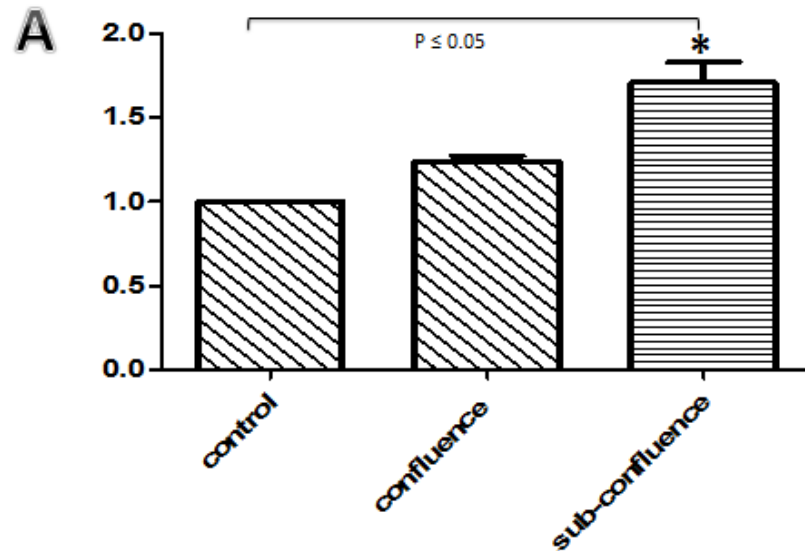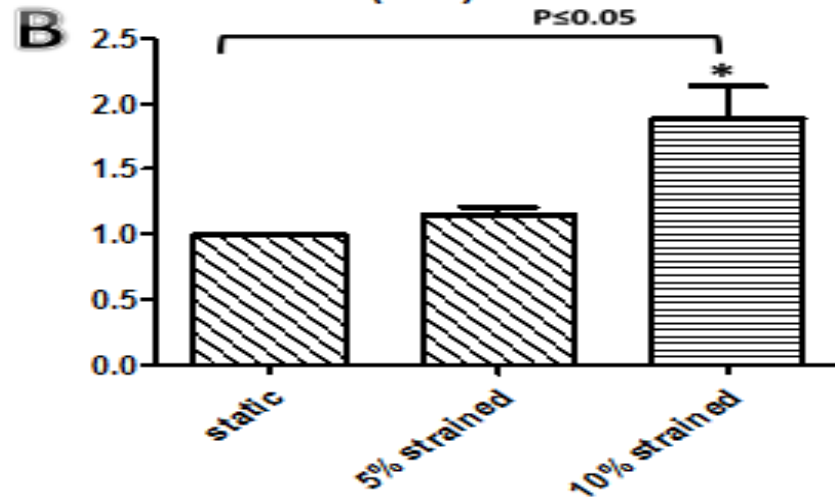
Figure 3.8: Merlin mRNA expression change under haemodynamic stimulus.

A) Following exposure of 10 dyne/$10 cm^2$ of laminar shear stress over a 24 hour time period using the orbital rotator, and B) following exposure of 5% and 10% cyclic strain over a 24 hour time period using the Flexercell Tension Plus™ FX-4000T™ system, Merlin mRNA was extracted and a two-step QRT-PCR carried out using specific primer sets for the measurement of Merlin gene expression. Results were normalised to the housekeeping gene, 18s, and histograms represent normalised values relative to the un-sheared control. Results are averaged from three independent experiments ±SEM and each experiment was performed in triplicate; *P ≤ 0.05 vs control.

3.2.2.7 Immunocytochemical analysis of Merlin co-localisation under shear

In order to study Merlin co-localisation under shear, HAECs were diluted to a density of $1\text{x}10^6$ cells/ml, with 200 μl of this dilution introduced into an Ibidi$^®$ Y-shape μ slide. HAECs were permitted time to adhere and grow to confluency, and then sheared using the Ibidi$^®$ pump system. Merlin co-localization with F-actin after 10 dyne/cm^2 shear stress for 24 hours was examined by staining cells with rhodamine phalloidin (Figure 3.9). In comparison with static controls, HAECs re-aligned in the direction of shear stress and the co-stain with F-actin revealed Merlin association with dynamic actin at the site of stress fibres (Figure 3.10(A)), focal adhesions (Figure 3.10(B)), at sites of cell-cell contact (Figure 3.10(C)) and at the leading cell edge, lamellipodial regions in particular (Figure 3.10(D)).
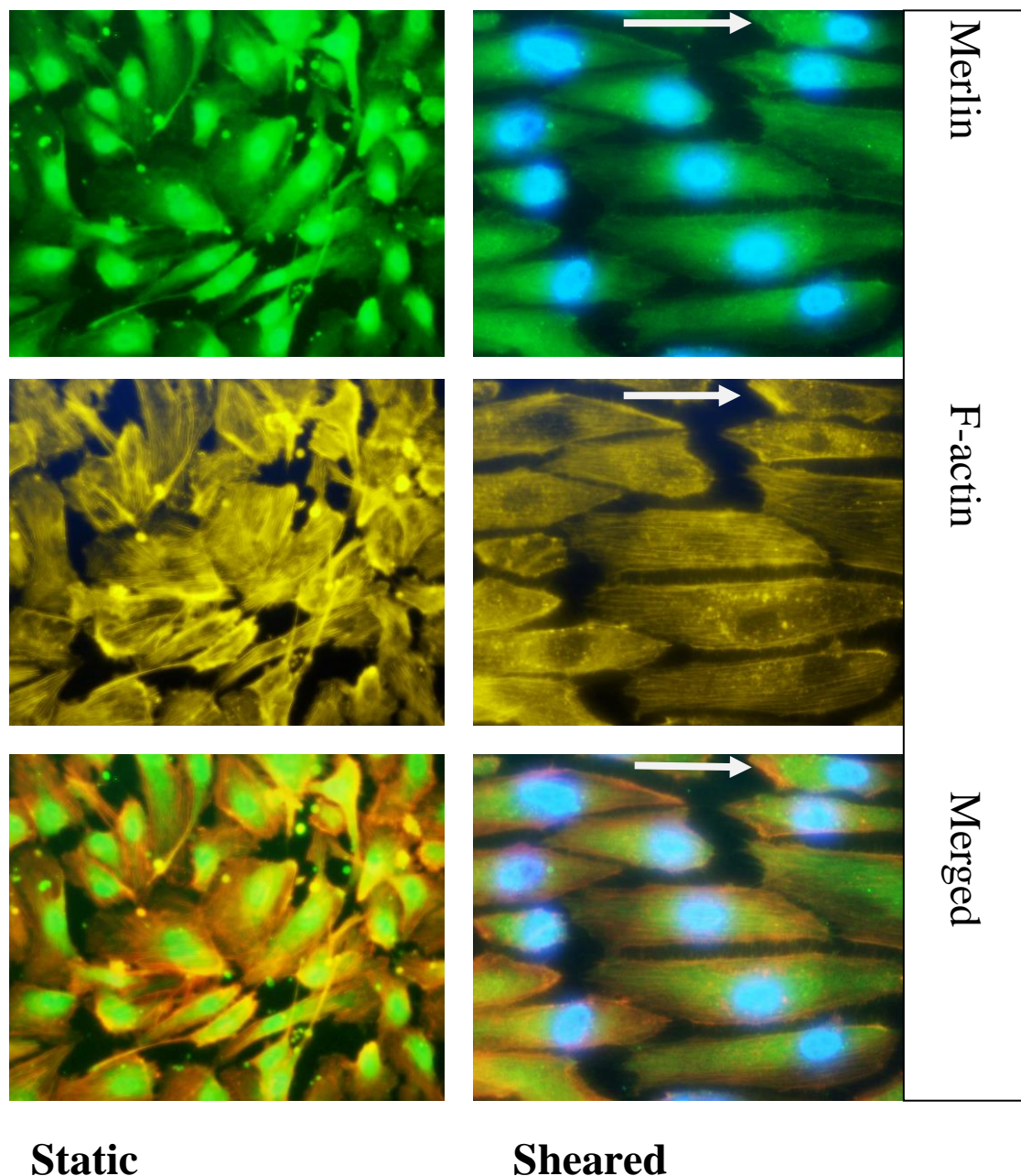
Figure 3.9: The effect of shear stress on vascular endothelial cells and Merlin co-localisation with F-actin

HAECs were exposed to static and 10 dyne/cm^2 laminar shear stress for 24 hours. Cellular localisation of Merlin was analysed by immunofluorescent imaging, co-staining for F-actin and monitoring of Merlin (green) with F-actin (yellow) by standard fluorescent microscopy.   HAEC F-actin filaments realigned in the direction of flow under LSS while and no F-actin filaments realignments were observed under static conditions.   (Arrow showing the direction of blood flow)

Figure 3.10: Merlin localisation by immunofluorescence microscopy.

Cellular localisation of Merlin was analysed by immunofluorescent imaging. Images show the association of merlin with dynamic actin strictures within the cells. Arrows indicate Merlin localisation at the site of stress fibres (A), focal adhesions (B), cell-cell junction (C), and lamellipodia leading edges (D). Imagine A has taken from static control sample and imagine B-D have taken from sheared samples.

3.3 Discussion

According to the World Health Organisation (WHO), CVD is the leading cause of death across the world, including America, Europe and Asia. The lesions of atherosclerosis contribute enormously to this large death toll. It is now well known that endothelium is critical in maintaining vascular homeostasis, the dysfunction of which contributes many different CVD, including atherosclerosis. As a direct stimulus, blood flow alters many EC functions, including morphology (Nerem, Levesque and Cornhill 1981), protein and gene expression, permeability (Förstermann and Münzel 2006) (Vita and Keaney 2002), adhesion and migration (Figure 3.11). The alignment in direction of blood flow and formation of long spindle morphology is the first adaptation of endothelium under shear stress. This is achieved by alteration of its actin polymerisation. However, this uniform alignment does not appear at sites of bifurcations and curvature (Langille and Adamson 1981). At such sites more complicate forms of shear stresses such as oscillated and disturbed shear stress are formed which contribute the initiation and progression of atherosclerosis.

Under physiological conditions, the value of shear stress is 10-15 dynes/cm^2 (Lehoux and Tedgui, 2003) and the value of cyclic strain is 5-7.5% (Fujiwara K.2003. Debes JC, Fung YC. 1995). The level of health shear stress in this thesis is chosen a protocol of 10 dynes/cm^2. The level of health cyclic strain is chosen a protocol of 5%. 10% and 20% of cyclic strain were also used to mimic the state of hypertension. 10% cyclic strain was used for chronic studies while 20% stretch was only used for acute studies as HAECs cannot withstand for 20% stretch more than few hours. These values were also optimised by previous works in our laboratory using biomarkers which particularly represent the pathological and physiological ranges of haemodynamic forces for HAECs (unpublished data).

In this study, we first examined if haemodynamic forces affect HAECs morphology. We compared the effect of both patterns of laminar and disturbed shear stress on HAECs morphologies, particularly at sites of bifurcations and curvature, where there exists a high risk of developing atherosclerosis. From the results obtained, we have successfully demonstrated that HAECs realign in the direction of flow compared with static control under LSS, but no uniform realignment was observed under DSS at regions of bifurcations and curvature. These results indicated that shear stress plays a critical role in regulation of HAEC morphology; consequently, the primary questions which must be answered are through which mechanism haemodynamic forces achieve regulation of HAEC functions, and whether or not Merlin plays a role in this mechanism.

Many studies show that in response to shear stress, endothelial cells change their morphology through reorganisation of its cytoskeleton. In the process, actin filament re-polymerises and forms different functional structures such as stress fibre bundles which provide an internal structural frame work for EC themselves (Wong, Pollard and Herman 1983) (Wechezak, Viggers and Sauvage 1985). As a cytoskeleton adaptor protein, Merlin is responsible for regulation of cell morphology, in addition to such functions as adhesion and migration (Reed and Gutmann 2001). Lallemand, et al have discovered that both merlin protein expression level and phosphorylation states are regulated by cell density, growth factor withdraw and cell-ECM detachment (Lallemand, et al. 2003). Their studies demonstrated that deficiency of merlin lost the ability of cellular contact-dependent inhibition of growth. Increased merlin protein expression was observed in primary rat Schwann cells (Morrison, et al. 2001). Many studies have also illustrated that merlin is activated or phosphorylated in cell-cell contact manner (Shaw, McClatchey and Jacks 1998) (Morrison, et al. 2001b) (Herrlich, et al. 2000). Furthermore our laboratory demonstrated the persistent increase of moesin with cyclic strain in sub-confluent HAECs. Meanwhile, the comparison of confluent and sub-confluent

cell culture conditions allow us to mimic the endothelial injury models which may indicates the role of merlin in control of cell migration and growth.
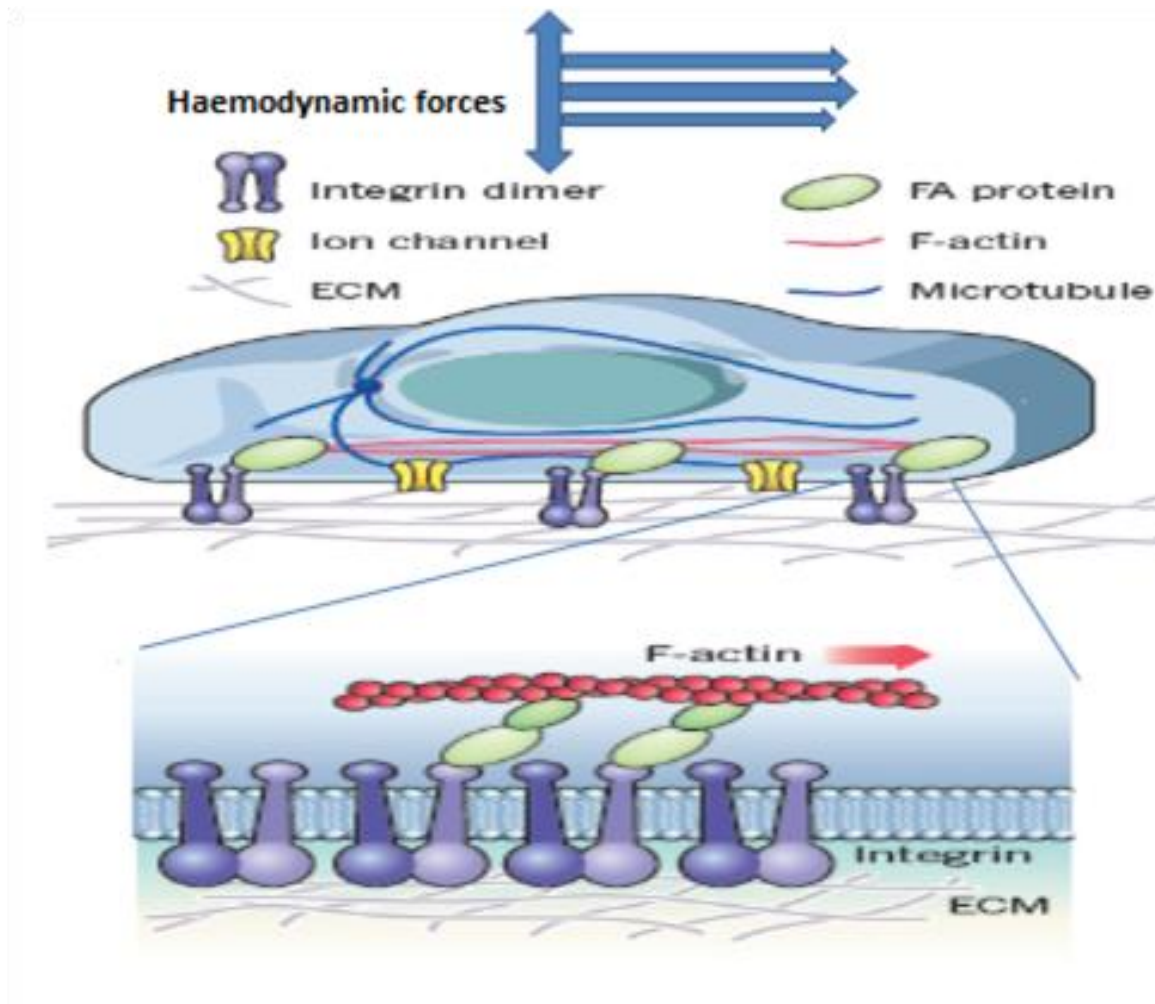
Figure 3.11: The application of haemodynamic force to endothelial cell

HAECs expose to multiple haemodynamic forces in the vasculature including the shear stress of blood flow and generate myosin-dependent contractile and actin polymerisation mediated tensile forces through ECM. The close-up of a FA showing the actin stress fibre binding into focal adhesion complex which anchored to the ECM through integrins. Diagram modified from (Hoffman, Grashoff and Schwartz 2011).

We, therefore firstly, focused on the effects of physiological shear stress levels on Merlin protein in both confluent and sub-confluent HAEC cultures.   We found that after continuous exposure to 10 dynes; 24 hours shear, only a slight decrease in Merlin protein expression in confluent HAECs was observed.   In contrast, however, a dramatic decrease in sub-confluent HAECs compared with static control occurred. We also discover the similar results in a comparison study between static and physiological (5%) levels and pathological (10%) levels of cyclic strain.   Merlin protein expression underwent only subtle decreases while significant decreases were observed following pathogenic levels.

Activation of Merlin is inhibited by the phosphorylation of Ser518, located on the C-terminal, preventing its ability to bind to actin (Sherman, et al. 1997). We can see that after 10 dyne/cm^2; 24 hours shear, only a slight increase in phosphorylated Merlin protein expression in confluent HAECs occurred.   In contrast, however, a dramatic increase in sub-confluent HAECs compared with total merlin protein was observed.   Again, similar results were found in a comparison between static and physiological (5%) levels and pathological (10%) levels of cyclic strain. Phosphorylated Merlin protein expression underwent only subtle increases while significant increases were observed following exposure to pathogenic levels. Results suggested that Merlin activation is inhibited under physiological conditions that allow ECs to undergo active modulation.

The above results have confirmed that Merlin protein expression and phosphorylation states are indeed regulated by haemodynamic forces.   Therefore, further examination of the mRNA levels that reflect Merlin quantities under haemodynamic forces was carried out.   In brief, experiments under the same haemodynamic force conditions in HAECs were repeated for Merlin mRNA expression.   Interestingly, it was found that mRNA levels increased with both shear

stress and cyclic strain, and did not correspond to Merlin protein expression. This phenomenon was also observed by previous works in our laboratory while studying the other ERM family protein, Moesin, under the same conditions. This may indicate the regulation of haemodynamic forces on merlin protein functions. There are generally three ways to regulate merlin activity. First, HAECs can alter merlin protein expression rate. The rate of merlin protein synthesis is controlled by the rate at which the merlin DNA encoding the protein is converted to mRNA. This process may involve microRNA mediated transcript degradation and translational suppression of which decrease the synthesis of merlin protein. MicroRNA (miRNA) are short non-coding single stranded RNA molecules usually 19-25 nucleotides in length. MicroRNA was discovered by Lee et al in 1993 on the nematode Caenorhabditis *elegans* (Lee, Feinbaum and Ambros 1993). It functions in many different biological processes, such as gene silencing (Bartel 2009). Intensive studies have shown that microRNA are involved in cardiac development and cardiovascular functions that are well described in Eric M. Small and Eric N. Olson's review (Small and Olson 2011). Saydam O, et al., have also demonstrated the role of miR-7's tumour suppressor function in schwannomas (Saydam, et al. 2011). Second, HAECs can change the activity of protein such as affinity of substrate binding. Last, HAECs may transport merlin proteins into different locations thus alter the cytoplasmic protein concentration. However, the exact way that HAECs control merlin functions is still poorly understood, and will be investigated in depth in future studies.

Our previous works have shown that cyclic strain increase HAECs motility both at adhesion and migration. As I mentioned before, cell adhesion and migration are two related processes. This process requires involvement of many actin adaptor proteins. The migrating cell first form distinct functional structures at its leading edge which then attach the cell to the ECM. Response to haemodynamic forces, cell can start adhesion as quick as few minutes. Therefore we want to investigate if merlin is

163

required in cyclic strain induced both HACEs adhesion and migration at molecular levels. The phosphorylation of merlin disable it form inhibition of cell adhesion and migration. In consequence, investigation of phosphorylation state of merlin will reflect its function during the process. The acute impact of cyclic stretch on Merlin phosphorylation states in HAECs was examined by exposure to 20% stretch for various time periods (1 minute, 5 minute and 10 minute) using the Flexercell Tension Plus™ FX-4000T™ system. Phosphorylation states of Merlin were monitored by Western blot analysis. We observed that phosphorylation states of Merlin were significantly decreased by 56% at 1 minute of stretch, 52% decrease at 5 minute of stretch and 60% at 10 minutes of stretch respectively compare to un-stretched control (Figure.3.6). Dephosphorylation of merlin is an important acute adaptive response mechanism to haemodynamic force. Phosphorylation of merlin is the other important regulatory mechanism of its function. Merlin inactivation occurs by phosphorylation at serine 518 in the C-terminal by either p21-activated kinase (PAK) or cAMP dependent protein kinase A (PKA) resulting in disassociation of the C-terminal from FERM *(Kissil, et al. 2002)*.
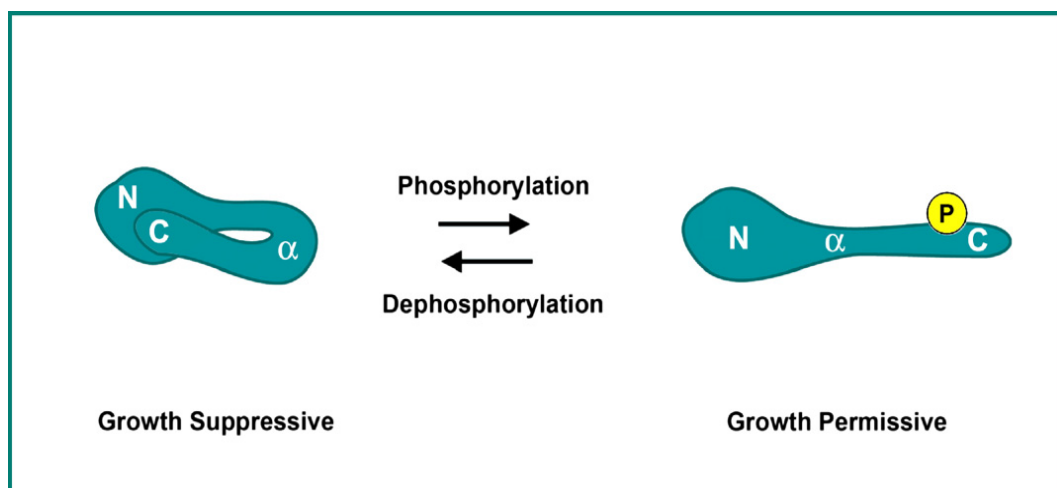
Figure 3.12: Merlin phosphorylation.

Merlin inactivation occurs by phosphorylation at serine 518 in the C-terminal by either p21-activated kinase (PAK) or cAMP dependent protein kinase A (PKA). The phosphorylation of merlin leads to de-association of its C-terminal from N-terminal which promote cell growth. (Scoles 2008).

Like other ERM proteins, Merlin is a critical component involved in regulating cell morphology and motility by binding to the actin cytoskeleton (Reed and Gutmann 2001b). Studies show that Merlin is located at many dynamic functional regions, such as microspikes and membrane ruffles (Bretscher, Edwards and Fehon 2002a) (Gonzalez-Agosti, et al. 1996). In order to investigate Merlin co-localisation with F-actin, HAECs were exposed to 10 dynes shear stress for 24 h. and stained with rhodamine phalloidin.   In comparison with static controls, HAECs re-aligned in the direction of shear stress and the co-stain with F-actin revealed Merlin association with dynamic actin at the site of stress fibres, focal adhesions, at sites of cell-cell contact and, in particular, the leading cell edge in lamellipodial regions. Importantly, this indicated its involvement with actin polymerisation.

From the above studies, we can conclude that Merlin, an endogenous protein in HAECs, is highly responsive to mechanical stimuli.   Merlin was also observed in numerous functional sites of dynamic action activity such as cell-cell communication, cell adhesion, cell migration and actin polymerization.

Chapter Four:

The Role of Mechano-Regulated Merlin in Cell-Matrix Adhesion and Migration.

4.1 Introduction

Cell adhesion and migration are two related processes which are crucial in maintaining cell morphogenesis; indeed, abnormal cell migration contributes many human diseases, including cancer, immunodeficiency disorders and cardiovascular disease. Cell movement has traditionally classified by four steps: 1) formation of functional region on the leading edge of the migrating cell, 2) protrusion and adhesion of the leading edge to ECM, 3) cell body translocation, 4) detachment of rear adhesion (Huttenlocher, Sandborg and Horwitz 1995) (Ridley, et al. 2003).

Cellular migration is driven by a number of factors; the gradient of growth factors or chemokines, ECM proteins (e.g. collogen and fibronectin), and electrochemical gradients (Parsons, Horwitz and Schwartz 2010b). It is now well known that the mechanical forces is the other crucial factor that maintaining the organisation of focal adhesion and cytoskeleton polymerisation that in turn regulate endothelial cell adhesion and adhesion. In response to extracellular stimuli, protrusive cells form distinct functional regions (e.g. lamellipodia, filopodia) at their leading edge by actin polymerization (Katoh and Negishi 2003). This functional leading edge then stretch out towards to the cues, and then stabilised by adhesion. Cellular adherence to ECM is therefore also considered as the first step of cell migration (Parsons, Horwitz and Schwartz 2010a). Many cell surface receptors such as integrins, cadherins, proteoglycans and cell adhesion molecules are involved in cell motility, among which integrins are the best characterized. Integrin mediated cell adhesion adheres specifically to ECM proteins which is determined by extracellular ECM binding domains (Figure 4.1). For example αvβ3 specifically binding fibronectin while α2β1 only bind to laminin. In turn, the variety of these different integrin mediated adhesion affect the dynamic of cell motility and activation of different cell signalling pathway which regulates cell response to stimuli. For example, αvβ3 mediated

adhesion is more stable than α5β1 mediated adhesion (Huttenlocher and Horwitz 2011).
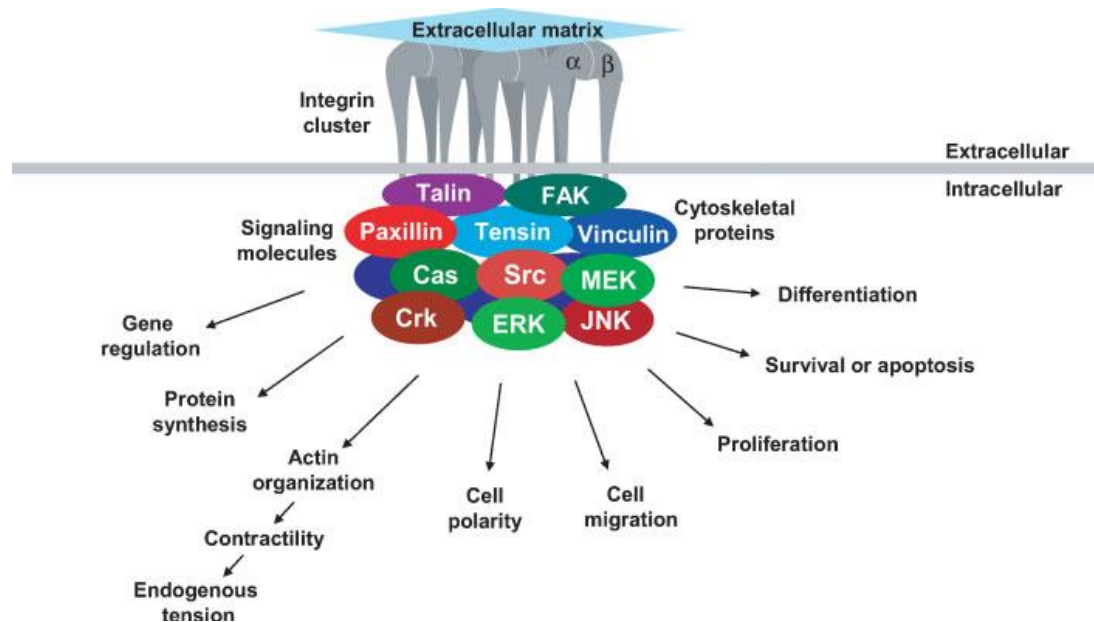
Figure 4.1: Cell–matrix adhesions and their downstream regulation.

Cell-ECM adhesions mediated by numerous integrins and recruit many cytoplasmic proteins. The recruitment of different cytoplasmic proteins leads to various downstream signalling cascades which regulate diverse cell fates (Allison L. Berrier, and Kenneth M. yamada, 2007).

The nascent integrin mediated adhesions by binding to ECM are matured and form a "dot- like adhesions" termed as focal complex which can be further stabilised to focal adhesion by associate with many actin binding scaffolding proteins. Over 150 proteins have been identified to involve in focal adhesion and this number is still expending (Zaidel-Bar and Geiger 2010). Among these proteins, vinculin, talin, kindlins and α-actinin have been intensively studied. Both talin and α-actinin promote the maturation of focal complex. Calderwood has shown the ability of talin interact with β-integrin cytoplasmic domains to increase its binding affinity to ECM (Calderwood 2004), and absent of talin or α-actinin significant effect on cell

adhesion (Zhang, et al. 2008) (Choi, et al. 2008). Both talin and α-actinin can interact with vinculin (Ziegler, Liddington and Critchley 2006), but Xu et al have shown that vinculin does not play critical role in adhesion formation (Xu, Baribault and Adamson 1998).

Many studies have revealed that Merlin interaction occurs with β1-integrin (Obremski, Hall and Fernandez- Valle 1998a), actin (Bashour, et al. 2002) and microtubules (Muranen, et al. 2007) and L.Hemmings et al have also demonstrated that talin contains a N-terminal binding site of ERM that indicating that Merlin may play an important role in regulation of endothelium cell functions such as adhesion and migration (Hemmings, et al. 1996).

4.1.1. Hypothesis

The investigation of merlin interacting proteins will reveal potential therapeutic targets and help us understand by which mechanism merlin involved in regulate vascular functions. The previous results have shown that merlin present at many functional structures in HAECs. Therefore we expect to see that merlin will binding to cytoskeleton proteins such as actin and microtubulin. We also believe that merlin, as a member of the ERM family, plays an important role in regulation of HACE motility through αvβ3 integrins mediated pathway. The knock-down of merlin will affect HACEs motilities under haemodynamic forces.

4.1.2. Study Aims:

From the previous studies, we concluded that Merlin is endogenously expressed in HAECs and is highly responsive to mechanical stimuli.   Merlin is also involved in

numerous cell functions such as cell-cell communication, cell adhesion, cell migration and actin polymerization. In order to further confirm these conclusions and to investigate if Merlin affects cell-matrix adhesion and cell migration he following studies were carried out:

- The investigation of the binding proteins of Merlin using Proteomics Mass Spectrometric analyse.

- The investigation of the effect of siRNA mediated merlin knock-down HAECs on cell adhesion using the real time cell analysis system xCelligence.

- The investigation of the effect of haemodynamic forces on Merlin knock-down HAEC motility using xCELLigence system.

4.2 Results.

4.2.1 Mass Spectrometric analyse of Merlin binding proteins

From chapter 3, we observed that Merlin localise at numerous functional sites of dynamic action activity such as cell-cell communication, cell adhesion, cell migration and actin polymerization. The results implicate Merlin play an important role in regulation of haemodynamic regulated actin polymerisation. This regulation may involve in many Merlin binding partner proteins which we will first investigate at this chapter.

CO-IP is carried out using Pierce Co-Immunoprecipitation Kit (Thermo Scientific). In brief, the HAECs were lysed according the manufacturer's instructions. Lysate was then immunoprecipitated using a purified Merlin antibody coupled resin. Two control studies were performed along the experiments. One is the Quenched Resin Control is prepared by adding a 200 μl of quenching buffer to the resin column, which stops the resin from binding. Another inactivated Resin control is supplied within the kit which is composed of the same support material as the co-IP resin, but it is not activated. The elution sample of CO-IP was analysed both western blot and Mass Spectrometric methods (the elutions were sent and analysed by Dr Paul Dowling' laboratory in National Institute for Cellular Biotechnology, DCU).

Before analysis using the Mass Spectrometer, the CO-IP elution samples were validated by Western blot. From Fig 4.1, we can observe a clear band in the eluted Merlin protein sample, while no band is visible in either control resin samples. Samples were then examined using Mass Spectrometry. Results were interesting, and pointed to the fact that compared with controls, Merlin protein bound to many functional proteins including tubulin, myosin light chain 6B, annexin and actin.

This result verified our last co-localisation study that Merlin is present at numerous functional sites of stress fibres, focal adhesion, at sites of cell-cell contact and the leading cell edge in lamellipodial regions.

Control Quenched Resin   **Control Inactivated Resin**   **Merlin**
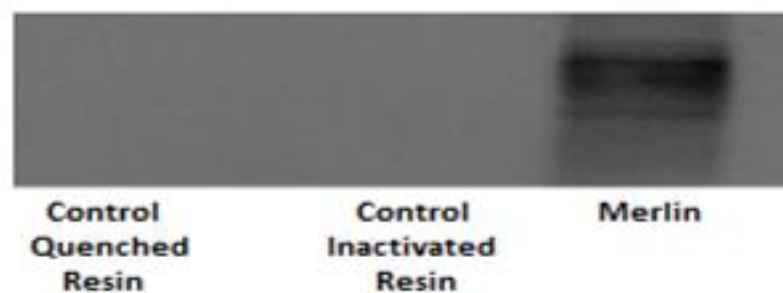
Figure 4.2 Validation of Immunoprecipitated Merlin by Western blot.

Following the immunoprecipitation of Merlin from Human Aortic Endothelial Cell lysate, a portion of the precipitated sample was tested on a Western blot to verify the elution contained Merlin.   A clear band is observed in the eluted Merlin protein sample, while no band can be seen in either control resin samples.

Table 4.1 Mass Spectrometry results of control CO-IP elution samples from HAECs.

sp|P62158|CALM_HUMAN **Calmodulin** OS=Homo sapiens GN=CALM1 PE=1 SV=2 [MASS=16838]
sp|P11142|HSP7C_HUMAN **Heat shock cognate 71 kDa protein** OS=Homo sapiens GN=HSPA8 PE=1 SV=1 [MASS=70898]
sp|P68104|EF1A1_HUMAN **Elongation factor 1-alpha 1** OS=Homo sapiens GN=EEF1A1 PE=1 SV=1 [MASS=50141]
sp|P08670|VIME_HUMAN **Vimentin** OS=Homo sapiens GN=VIM PE=1 SV=4 [MASS=53651]
sp|P51991|ROA3_HUMAN **Heterogeneous nuclear ribonucleoprotein A3** OS=Homo sapiens GN=HNRNPA3 PE=1 SV=2 [MASS=39595]
sp|P35268|RL22_HUMAN **60S ribosomal protein L22** OS=Homo sapiens GN=RPL22 PE=1 SV=2 [MASS=14787]
sp|P11021|GRP78_HUMAN **78 kDa glucose-regulated protein** OS=Homo sapiens GN=HSPA5 PE=1 SV=2 [MASS=72332]
sp|P62258|1433E_HUMAN **14-3-3 protein epsilon** OS=Homo sapiens GN=YWHAE PE=1 SV=1 [MASS=29174]
sp|P62805|H4_HUMAN **Histone H4** OS=Homo sapiens GN=HIST1H4A PE=1 SV=2 [MASS=11367]
sp|P14618|KPYM_HUMAN **Pyruvate kinase isozymes M1/M2** OS=Homo sapiens GN=PKM2 PE=1 SV=4 [MASS=57937]

This table displays the results of non-specific binding proteins in the inactivated Resin control CO-IP elution sample.

Table 4.2 Mass Spectrometry results of Immunoprecipation of Merlin from HAECs

sp|Q8NBS9|TXND5_HUMAN **Thioredoxin domain-containing protein 5** OS=Homo sapiens GN=TXNDC5 PE=1 SV=2 [MASS=47629]
sp|P68104|EF1A1_HUMAN **Elongation factor 1-alpha 1** OS=Homo sapiens GN=EEF1A1 PE=1 SV=1 [MASS=50141]
sp|P62736|ACTA_HUMAN **Actin, aortic smooth muscle** OS=Homo sapiens GN=ACTA2 PE=1 SV=1 [MASS=42009]
sp|P02786|TFR1_HUMAN **Transferrin receptor protein 1** OS=Homo sapiens GN=TFRC PE=1 SV=2 [MASS=84871]
sp|P07355|ANXA2_HUMAN **Annexin A2** OS=Homo sapiens GN=ANXA2 PE=1 SV=2 [MASS=38604]
sp|P21980|TGM2_HUMAN **Protein-glutamine gamma-glutamyltransferase 2** OS=Homo sapiens GN=TGM2 PE=1 SV=2 [MASS=77328]
sp|P14649|MYL6B_HUMAN **Myosin light chain 6B** OS=Homo sapiens GN=MYL6B PE=1 SV=1 [MASS=22764]
sp|P62269|RS18_HUMAN 40S **ribosomal protein S18** OS=Homo sapiens GN=RPS18 PE=1 SV=3 [MASS=17719]
sp|P68371|TBB2C_HUMAN **Tubulin beta-2C chain** OS=Homo sapiens GN=TUBB2C PE=1 SV=1 [MASS=49831]
sp|P11021|GRP78_HUMAN **78 kDa glucose-regulated protein** OS=Homo sapiens GN=HSPA5 PE=1 SV=2 [MASS=72332]
sp|P50454|SERPH_HUMAN **Serpin H1** OS=Homo sapiens GN=SERPINH1 PE=1 SV=2 [MASS=46440]
sp|Q13885|TBB2A_HUMAN **Tubulin beta-2A chain** OS=Homo sapiens GN=TUBB2A PE=1 SV=1 [MASS=49907]

This table displays the results of Merlin CO-IP elution sampled. The results pointed that compared with controls, Merlin protein binding to many proteins include tubulin, myosin light chain 6B, annexin and actin. This result future confirmed our last co-localisation study that Merlin present at numerous functional sites of stress fibres, focal adhesion, at sites of cell-cell contact and the leading cell edge in lamellipodial regions.

4.2.2. Merlin siRNA optimisation

Merlin knock-down HAECs allowed us to further evaluate the role of Merlin in HAECs motility. In order to achieve this goal, Merlin was knocked-down by introducing Merlin siRNA into HAECs. HAECS were transfected by two different methods: Microporation (Digital Bio) and TransIT-siQUEST® (Mirus) to determine the most appropriate method of siRNA delivery.

Initial optimization of each system required fine tuning of electrical parameters and cell numbers. Once achieved, both systems were compared for cell viability and transfection efficiency. HAECs were monitored by phase contrast microscopy. Analysis 48 hour post transfection revealed noticeably better cell viability (and morphology) with Microporation compared to siQUEST. HAECs were then transfected with different concentrations of Merlin siRNA (10-40 nM), to determine the optimum amount of siRNA with highest transfection efficiency and lowest toxicity. Same amount of scrambled siRNA was used as a control. After transfection, cells were allowed to recovery for 48 hours and transfection efficiency monitored by Western blot. Results of these experiments showed that Merlin protein expression is down-regulated by 77% after HAECs were transfected with 40 nM of Merlin siRNA at 48 hour time point. As a result, all subsequent transfections were performed using microporation at the same concentration of siRNA and the same incubation times.
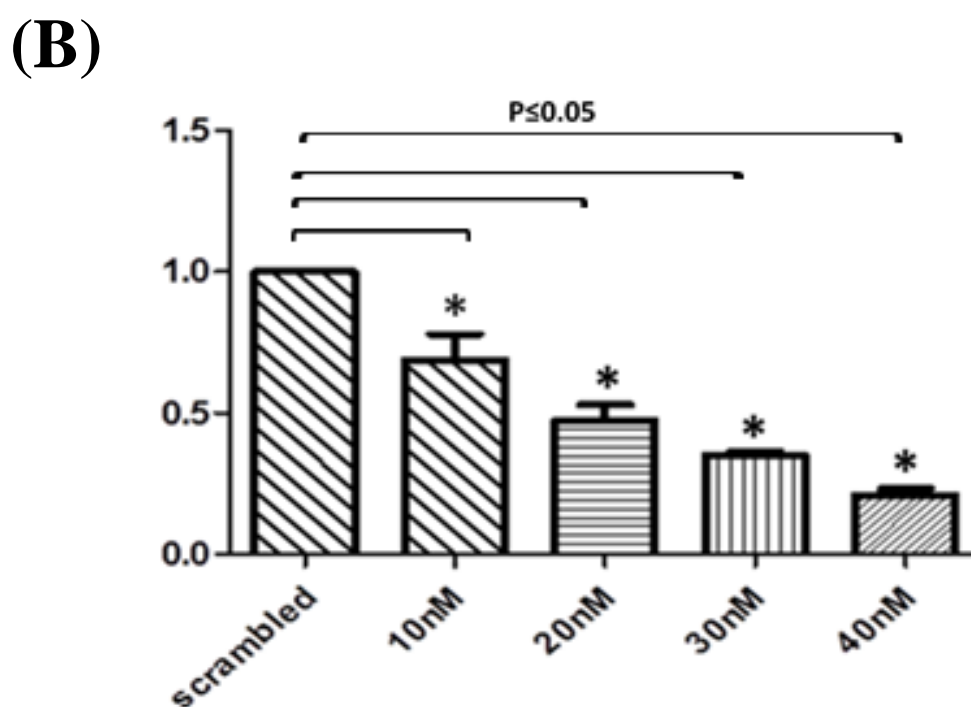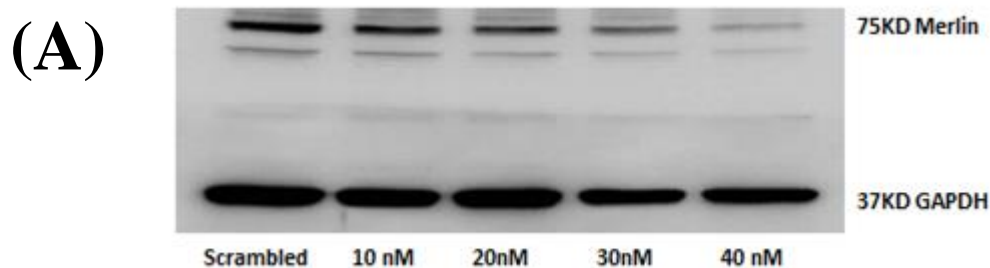
(A)

75KD Merlin

37KD GAPDH

Scrambled   10 nM   20nM   30nM   40 nM

(B)

Figure 4.3:   Optimisation of Merlin siRNA concentrations.

HAECs were transfected with Merlin siRNA at different concentrations using a Microporator (Digital Bio).   Cells were then incubated at $37^{\circ}C$ for 48 hour.   Cell lysates were analysed by Western blot.   A) Western blot analysis of Merlin (75 KD) expression change after transfected with siRNA.   B) Histograms represent fold change in band intensity relative to scrambled controls.   All values were controlled for equal loading by equalising for corresponding GAPDH. Results are averaged from three independent experiments $\pm$ SEM and each experiment was performed in triplicate; $*P \leqslant 0.05$ vs control.

4.2.3. The effect of Merlin knock-down on HAECs adhesion to various ECM.

In the previous studies highlighted in chapter 3, we discovered that Merlin was present at sites focal adhesion, stress fibres and the leading edges of lamellipodia using immune fluorescent images (figure 3.10), and in addition, using a proteomic approach we illustrated that Merlin binding occurs to the cytoskeleton proteins, actin and tubulin (Table 4.2). We hypothesised that Merlin is critical in regulation of HACEs adhesion and migration. In order to investigate the effect of Merlin in HAEC adhesion, and to evaluate by which mechanism Merlin is involved, several different ECM were introduced. Merlin knock-down HAECs were subsequently plated into E-plates pre-coated with various extracellular matrices, consisting of fibronectin, vitronectin, fibrinogen or laminin. Cell-matrix adhesion was monitored by xCelligence®. Results indicated that relative to none coating controls, in Merlin knock-down HAECs, cell-matrix adhesion was greatly increased (figure 4.4). Also in the Merlin knock-down, increased levels of attachment of vitronectin was approximately 1.9-fold, while an approximate 1.66-fold increase to fibronectin compared to laminin (0.1%) and fibrinogen (8%) was observed (figure 4.3).
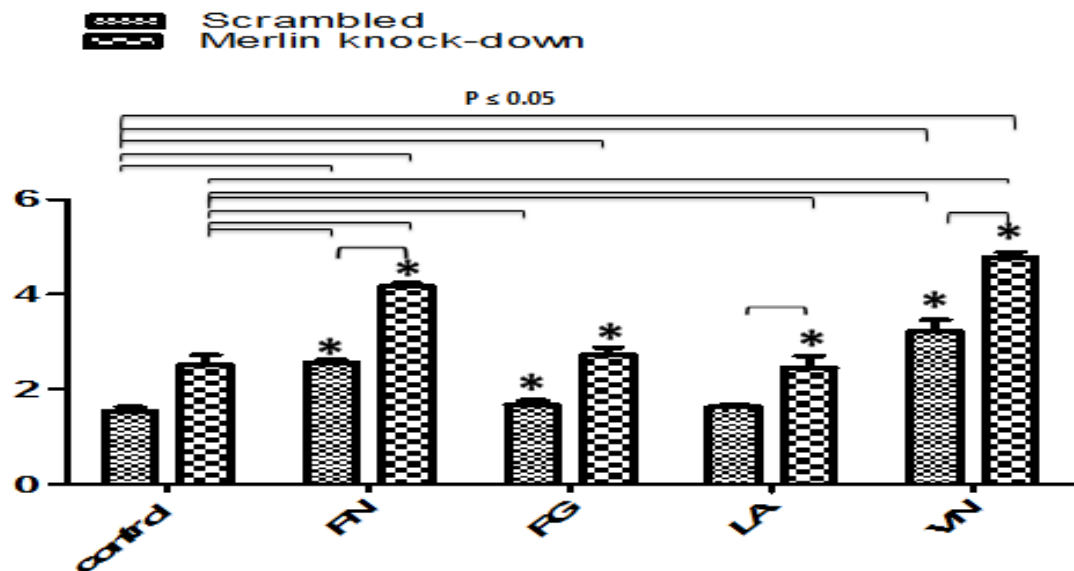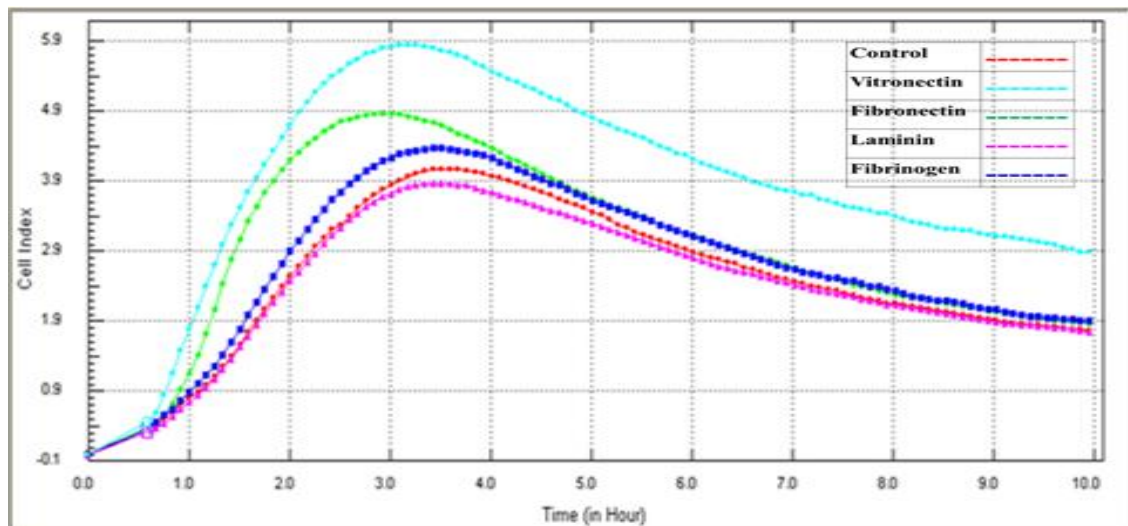
Fig 4.4 the effect of Merlin knock-down on HAEC adhesion to various ECMs

The effect of Merlin knock-down on HAEC adhesion was studied using the xCELLigence® system. Merlin knock-down HAECs were seeded into E-plates pre-coated with fibronectin (Green), fibrinogen (Blue), Laminin (Pink) and Vitronectin (Cyan), at a concentration of 30,000 cells per well. Plates with none coating (Red) were set as controls. Results appear to indicate that Merlin-absent HAECs exhibited preferential adhesion to VN and FN. Histograms represent slope changes according with CI value of ECMs related to no-coating controls. Results are averaged from three independent experiments ±SEM and each experiment was performed in triplicate; *P≤ 0.05 vs control.
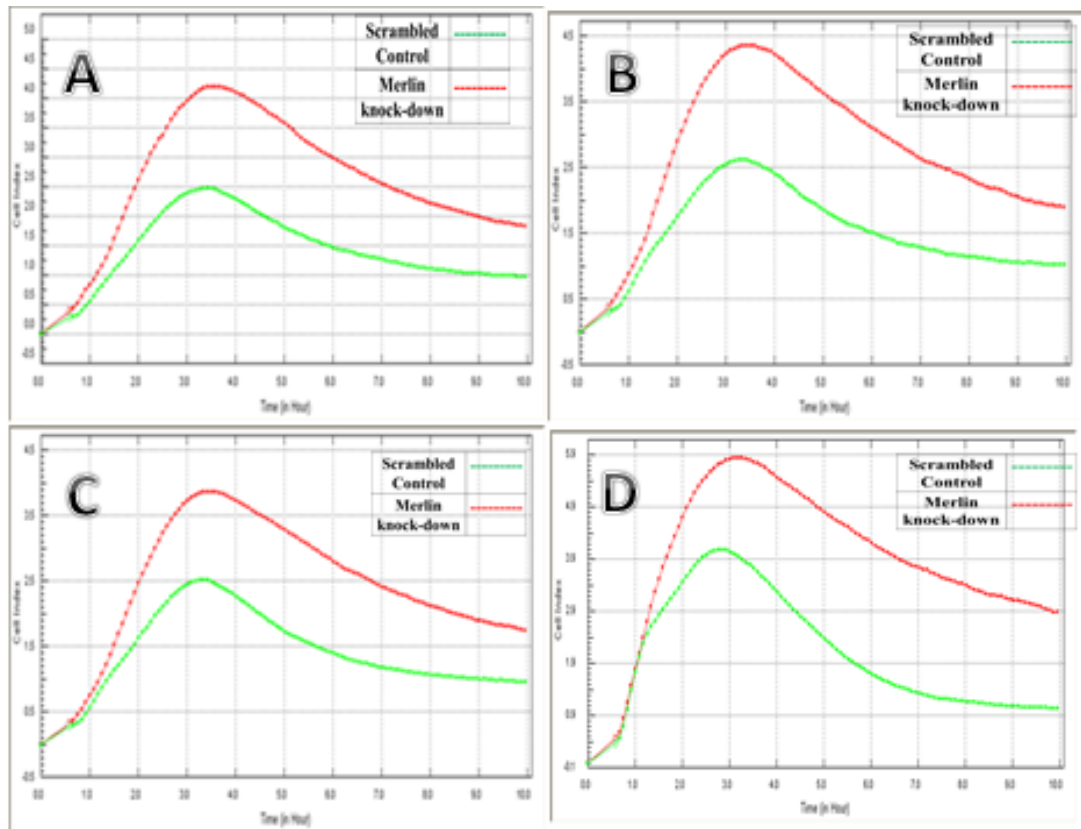
Fig 4.5 The role of Merlin knock-down on HAEC–ECM adhesion.

The role of Merlin knock-down on HAEC –ECM adhesion was studied using the xCELLigence® system. Merlin knock-down HAECs were seeded into E-plates which were pre-coated with fibronectin (A), fibrinogen (B), Laminin (C) and Vitronectin (D), at a concentration of 30,000 cells per well. Graphs illustrate that the absence of Merlin (Red) increased HAEC adhesion to all ECM compared with the scrambled control (Green).

4.2.4. The role of Merlin knock-down on HAEC migration

Again, to investigate the role of Merlin in HAEC migration, the same protocol was followed. Following knock down by transfecting Merlin siRNA, HAECs were subsequently plated into the upper chambers of CIM-plates at a concentration of 30,000 cells per well. Cell migration was then monitored by Real Time Cell Analysis System xCELLigence®. Results indicate that the knock-down of Merlin (Green) increased HAEC migration (approximately 1.76 fold) compared with scrambled controls.

Fig 4.6 The role of Merlin knock-down on HAEC migration.

The role of Merlin absence on HAECs migration was studied using xCELLigence system. Merlin knock-down HAECs were seeded into CIM-plate at a concentration of 30,000 cells per well. Graphs illustrate that absent of Merlin (Green) increase HAECs migration compared with scrambled control (Blue). Histograms represent slope change according with CI values related to scrambled control. Results are averaged from three independent experiments ±SEM and each experiment was performed in triplicate.

4.2.5 The effect of laminar shear stress on Merlin knock-down HAECs' adhesion.

As mentioned previously, under physiological conditions, ECs realign in the direction of blood flow in order to maintain healthy hemostasis. The previous chapter showed that Merlin is highly responsive to mechanical stimuli, and also from section 4.2.3 and section 4.2.4, it was observed that the Merlin knock-down greatly affects HAEC motility. Therefore, we wanted to further elucidate the effect of laminar shear stress on Merlin-absent HAEC motility.

We first investigated the effect of laminar shear stress on Merlin knock-down HAEC adhesion. HAECs were transfected with Merlin siRNA. Cells were then incubated for 48 hours at 37°C. Cells were harvested after incubation and transfection efficiency monitored by Western blot to ensure an approximate 80% knock-down of Merlin was achieved. Both Merlin knock-down HAECs and scrambled control cells were exposed to LSS (10 dyne/cm^2 for 24 hours). Cells were then trypsinised and seeded into E-plates at a concentration of 30,000 cells/well. The cell adhesions were monitored by the Real Time Cell Analysis System xCELLigence$^®$.

Results indicated that relative to static controls, the level of adherance of HAECs was significantly increased by 1.4-fold after exposure to LSS. In the Merlin knock-down, the level of adherence was further increased to 1.69-fold over wild type cells, after exposure to LSS compared with static controls.
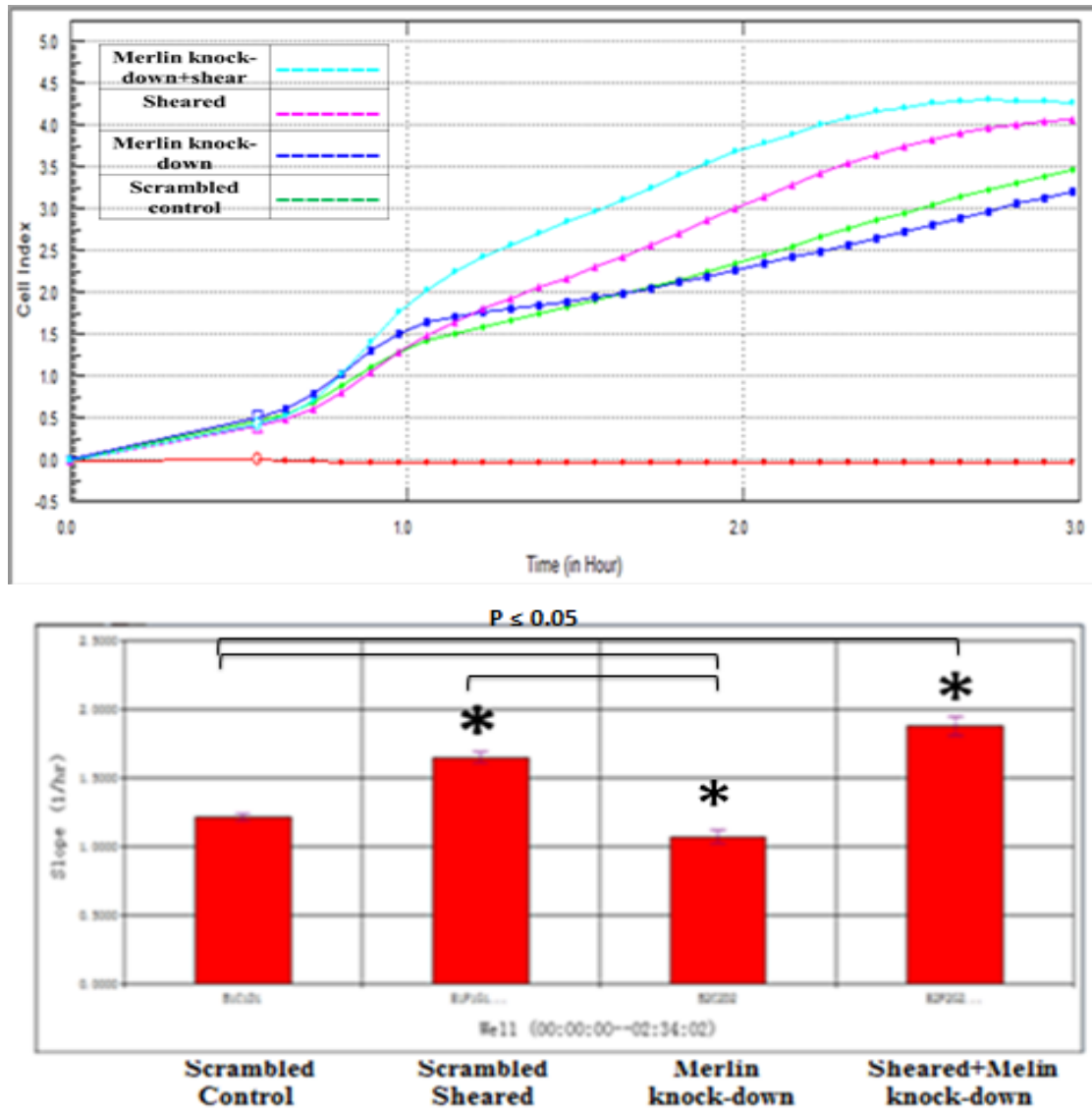
Figure 4.7 The role of laminar shear stress on Merlin knock-down HAEC adhesion.

The role of laminar shear stress on HAEC adhesion was studied using xCELLigence system. Following 10 dyne/cm² 24 hours shear, both scrambled and Merlin knock-down cells were seeded into E-plates at a concentration of 30,000 cells per well. Graphs illustrate the effect of LSS on merlin knock-down HAEC adhesion. Green: scrambled control; Blue: Merlin knock-down; Pink: sheared; Cyan: Merlin knock-down+sheared. Histograms represent slope change according with CI values. Results are averaged from three independent experiments ± SEM and each experiment was performed in triplicate; *P≤ 0.05 vs control.

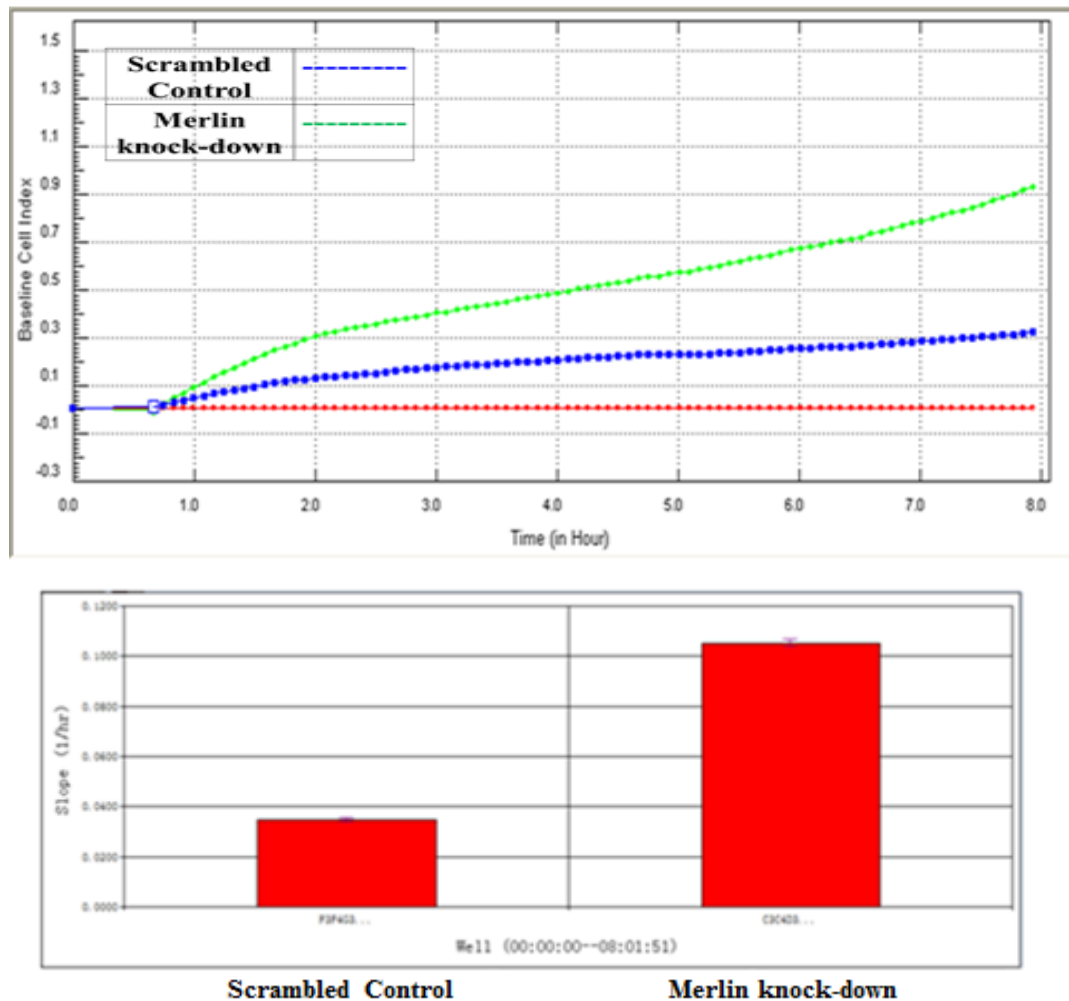## 4.2.6 The effect of laminar shear stress on Merlin knock-down HAEC migration.

In order to investigate the effect of laminar shear stress on Merlin-absent HAEC migration, HAECs were transfected with Merlin siRNA. Cells were then incubated for 48 hours, at 37°C. Cells were then harvested following incubation, and transfection efficiency was monitored by Western blot to ensure about 80% knock-down of Merlin was achieved. Both Merlin knock-down HAECs and scrambled control cells were exposed to LSS (10 dyne/cm^2 for 24 hours). Cells were then trypsinised and seeded into CIM-plates at concentration of 30,000 cells per well. Cell migration was monitored by Real Time Cell Analysis System xCELLigence$^{®}$.

Results indicate that relative to static controls, the level of HAEC migration was non-significantly increased by 1.7-fold after exposure to LSS. In the Merlin knock-down, the level of migration further increased to 3.4-fold after exposure to LSS compared with static controls.
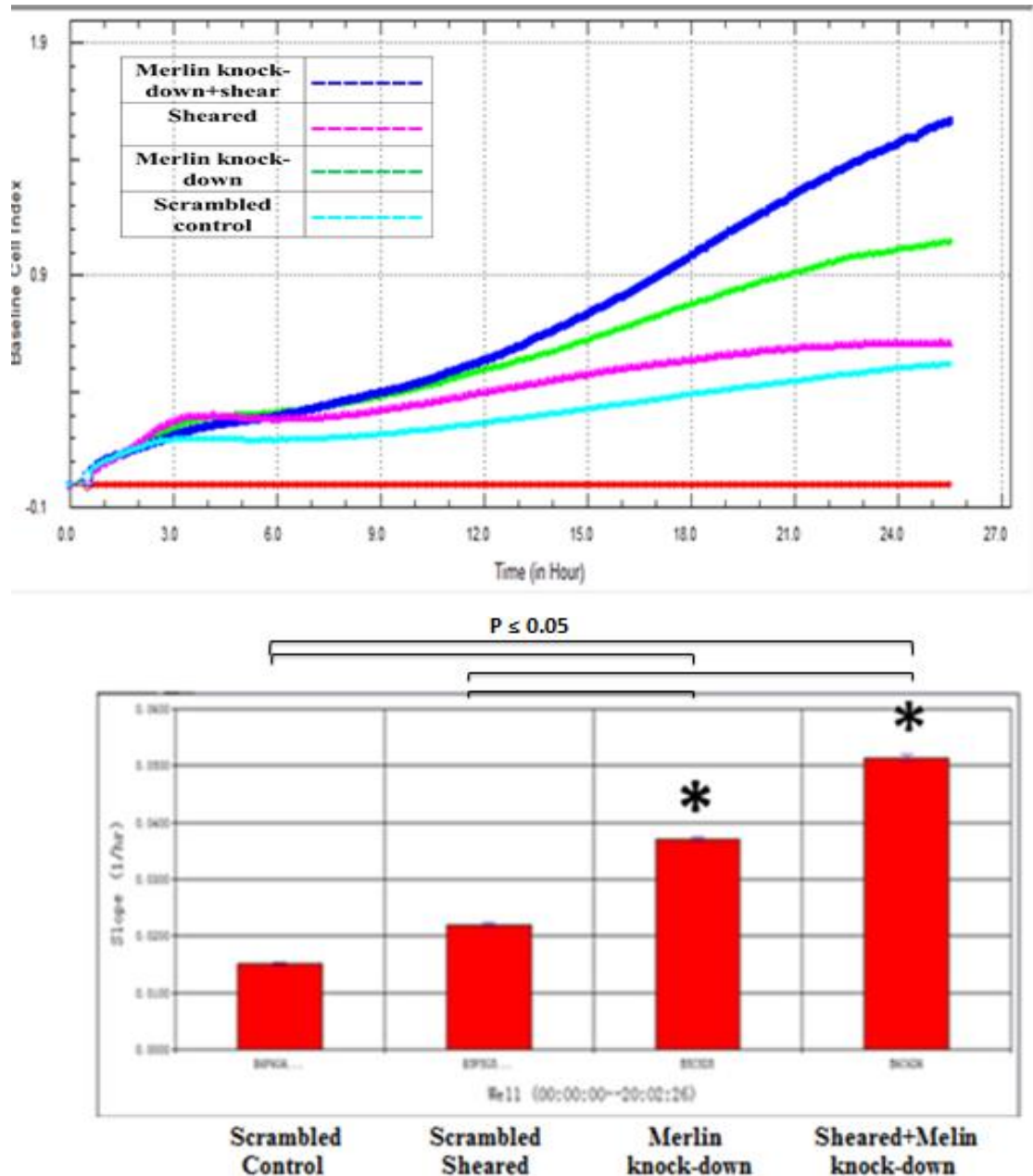
Figure 4.8   The role of laminar shear stress on Merlin knock-down HAEC migration.

The role of laminar shear stress on HAEC adhesion was studied using xCELLigence® system.   Following 10 dyne/cm^2 24 hours shear, both scrambled and Merlin knock-down cells were seeded into E-plates at concentration of 30,000 cells per well. Graphs illustrate the effect of LSS on HAEC migration in the absence of Merlin.   Cyan: scrambled control; Pink: sheared; Green: Merlin knock-down; Blue: Merlin knock-down+sheared. Histograms represent slope change according with CI values. Results are averaged from three independent experiments $\pm$ SEM and each experiment was performed in triplicate and each experiment was performed in triplicate; *P$\leqslant$ 0.05 vs control.

4.2.7 The effect of cyclic strain on Merlin knock-down HAEC adhesion.

To investigate the effect of cyclic strain on Merlin knock-down HAEC adhesion, HAECs were transfected with Merlin siRNA. Cells were then incubated for 48 hours at 37°C. The cells were harvested after incubation and transfection efficiency was monitored by Western blot to ensure that approximately 80% knock-down of Merlin was achieved. Both Merlin knock-down HAECs and scrambled control cells were then exposed to cyclic strain (10% for 24 hours). Cells were then trypsinised and seeded into E-plates at a concentration of 30,000 cells per well. HAEC adhesion was monitored using the Real Time Cell Analysis System xCELLigence$^{®}$.

Results indicate that relative to static controls, the level of adherence of HAECs was increased by 1.38-fold after exposure to 10% cyclic strain. Significantly, in the Merlin knock-down, the level of adherence significantly increased to 2.25-fold after exposure to 10% cyclic strain compared with static controls.
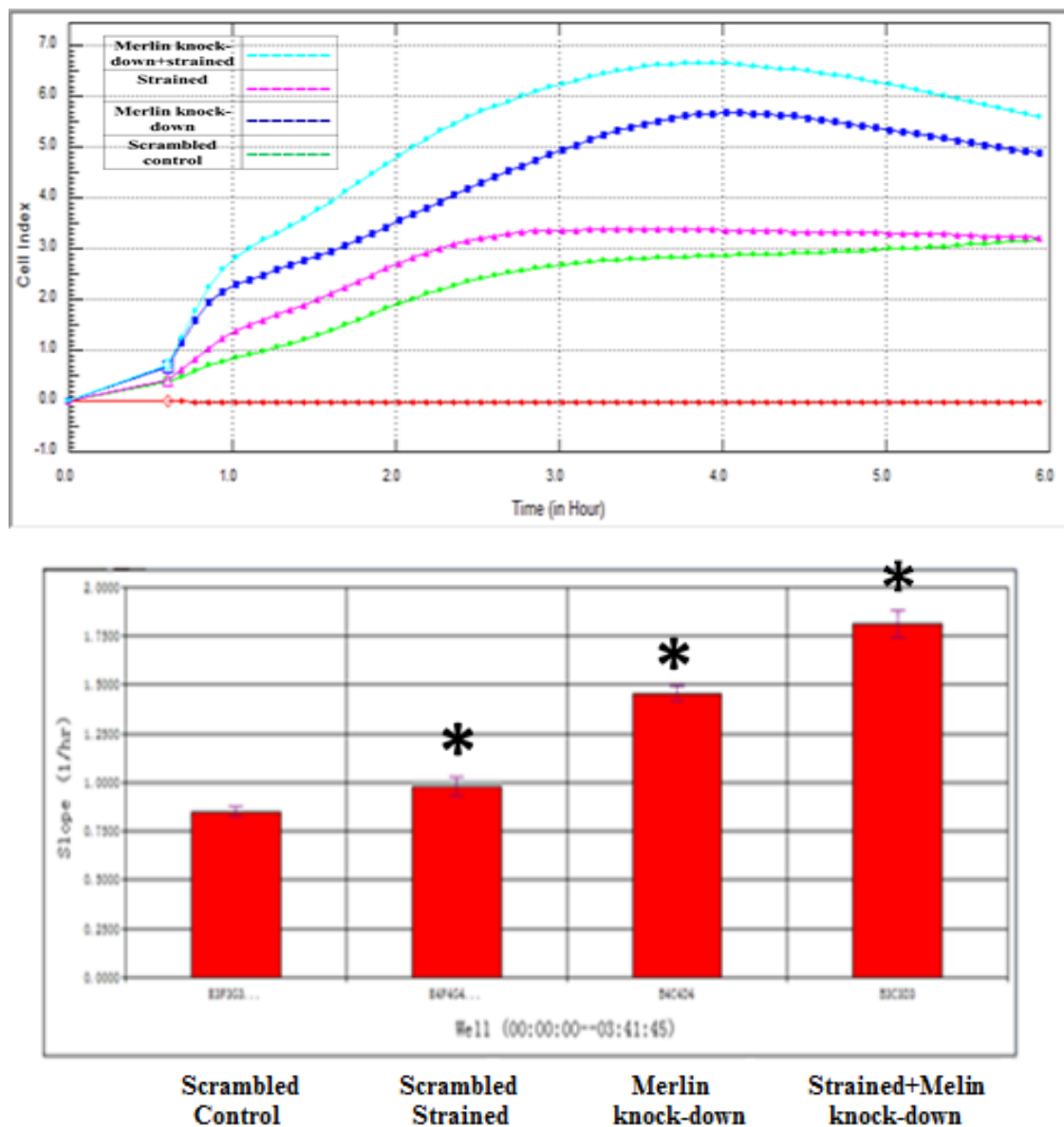
Figure 4.9 The role of cyclic strain on Merlin knock-down HAEC adhesion.

The role of cyclic strain on HAEC adhesion was studied using the xCELLigence® system. Following 10% 24 hours strain, both scrambled and Merlin knock-down cells were seeded into E-plates at a concentration of 30,000 cells per well. The above graphs illustrate the effect of cyclic strain on Merlin absent HAEC adhesion: Green: scrambled control; Blue: Merlin knock-down; Pink: strained; Cyan: Merlin knock-down+sheared. Histograms represent the slope change according to the CI value. Results are averaged from three independent experiments $\pm$SEM and each experiment was performed in triplicate; P$\leqslant$ 0.05 vs control.

4.2.8 The effect of cyclic strain on Merlin knock-down HAEC migration.

In order to investigate the effect of cyclic strain on Merlin knock-down HAEC migration, HAECs were transfected with Merlin siRNA.   Cells were then incubated for 48 hours at 37°C.   Cells were harvested following incubation, and transfection efficiency was monitored by Western blot to make sure that about 80% knock-down of Merlin was achieved.   Both Merlin knock-down HAECs and scrambled control cells were exposed to cyclic strain (10% for 24 hours). The cells were then trypsinised using EDTA and then seeded into CIM-plates at concentration of 30,000 cells per well.   Cell adhesions were monitored by the Real Time Cell Analysis System xCELLigence$^{®}$.

Results indicate that relative to static controls, the level of migration of HAECs was increased by 1.25-fold after expose to 10% cyclic strain.   When Merlin was knocked-down, migration levels was significantly increased to 2.17-fold after exposure to 10% cyclic strain compared with static controls.
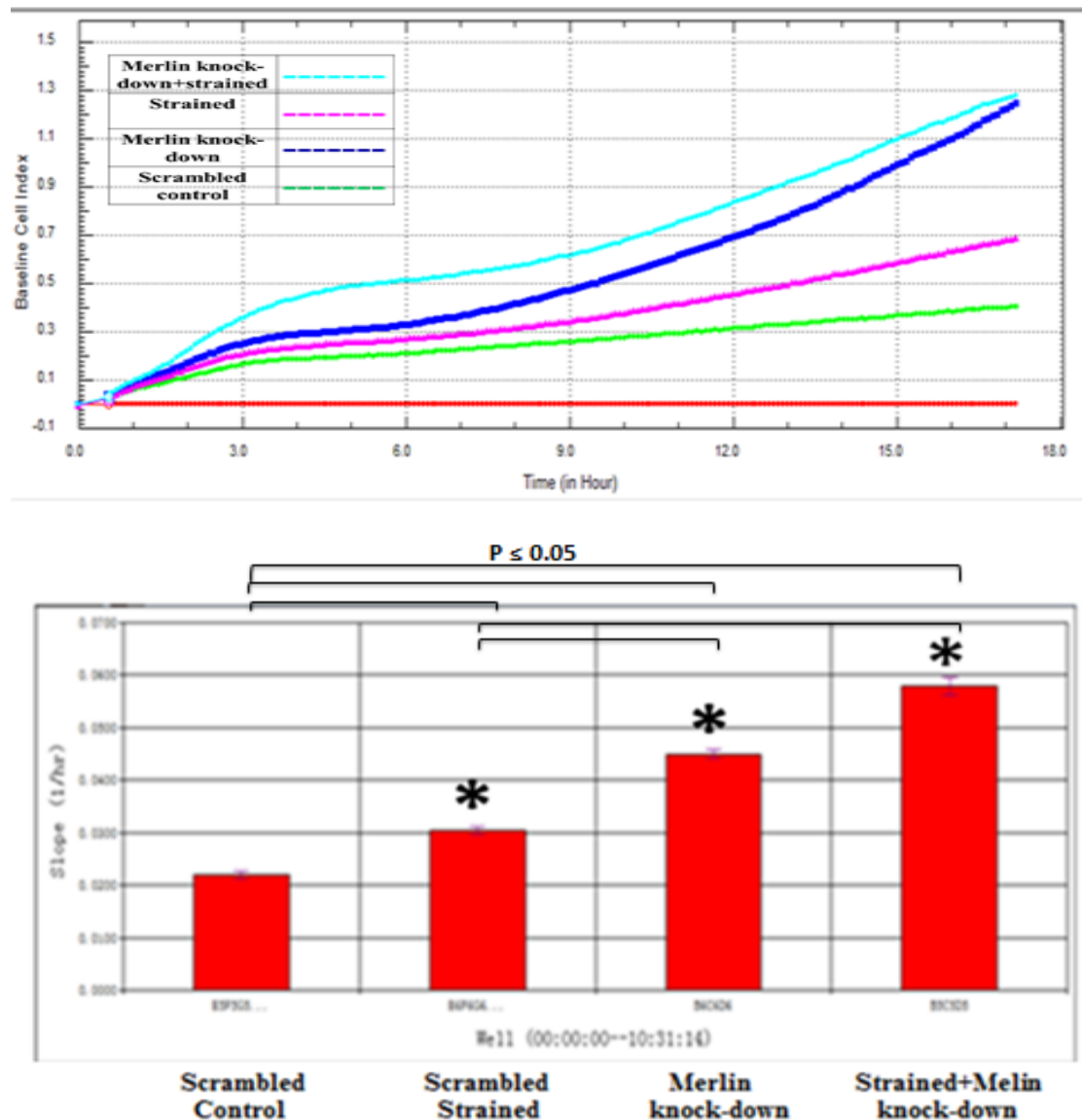
Figure 4.10 The role of cyclic strain on Merlin knock-down HAEC migration.

The role of cyclic strain on HAEC adhesion was studied using the xCELLigence® system. Following 10% 24 hours strain, both scrambled and Merlin knock-down cells were seeded into E-plates at a concentration of 30,000 cells per well. Graphs illustrate the effect of cyclic strain on Merlin-absent HAEC migration: Green: scrambled control; Blue: Merlin knock-down; Pink: strained; Cyan: Merlin knock-down+sheared. Histograms represent the slope change according to the CI value. Results are averaged from three independent experiments ±SEM and each experiment was performed in triplicate; *P≤ 0.05 vs control.

4.3. Discussion

Intensive studies have been carried out since the discovery of Merlin in 1993, due to its tumour suppressor function and its close structural similarity to ERM proteins. It has been widely reported that Merlin affects the stabilization of membrane-cytoskeleton interaction. Over 30 proteins so far have been known to interact with Merlin (Table 4.3) (Scoles 2008c). All these interacting proteins critically regulate Merlin structure and function. For example, Merlin may be phosphorylated at serine 518 by interacting with p21-activated kinases (PAKs) (Kissil, et al. 2002b). Merlin is well known as a linker protein between the membrane and cytoskeleton. However, unlike other ERM family members, Merlin contains both an F-actin binding domain and FERM domain in the N-terminal (Sainio, et al. 1997) (Xu and Gutmann 1998b) which may indicate the merlin exists for different functions. Interestingly, our IP results discovered the interaction of merlin with microtubules. Xu HM has also demonstrated that Merlin contains a microtubule-binding domain in the N-terminal, which can be closed by self-association form (Figure 4.11) (Xu and Gutmann 1998b). Xu demonstrated that merlin binding to polymerized actin at its N-terminal domain mapping to residues 178–367. This interaction is not affected folding of merlin which is considered as "close conformation". The "closed conformation" may serve as a docking site that allows merlin interacts with its critical effector proteins. In contrast, interaction of merlin with microtubules exists in an ''open conformation". Merlin is unable to associate with microtubules in the ''closed conformation", due to the losses of the correct conformation necessary for this association. The interaction of merlin with microtubules may also implicate the cross talk between tubulin and actin (Figure 4.12). As one of the major component of cytoskeleton, microtubule has long been known to be essential for cell polarization, vesicle transport and cell division. It is also play a critical role in cell migration (Scliwa and Höner 1993) (Small, et al. 2002). Vasiliev et al were first reported that microtubules were required during cell migration in 1970 (Vasiliev, et al. 1970). Concentrated microtubules were observed

at the leading edge of lamellipodia (Rinnerthaler, Geiger and Small 1988). Furthermore, Kaverina demonstrated the presence of microtubules at FA in fibroblast (Kaverina, Rottner and Small 1998). Stabilization of plus end enable microtubules re-orient towards the leading edge and constitute a highly dynamic cytoskeleton filament system. Microtubules are considered to control disassemble of FA (Rid, et al. 2005). The polymerization of microtubule filament requires helps of many scaffolding proteins, such as paxillin (Efimov, et al. 2008). However, the role of merlin plays in microtubule polymerization is poorly understood and requires a further investigation.
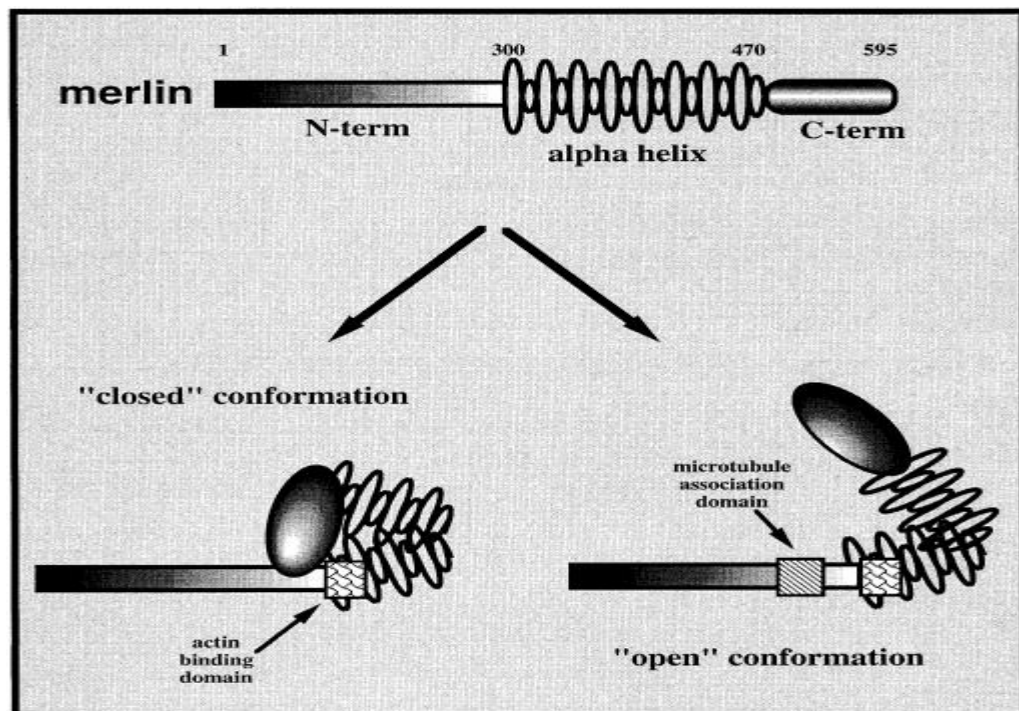
Figure 4.11 The model of merlin "open and close conformation".

Xu demonstrated that merlin binding to polymerized actin at its N-terminal domain mapping to residues 178–367. This interaction is not affected folding of merlin which is considered as "close conformation". The "closed conformation" may serve as a docking site that allows merlin interacts with its critical effector proteins that fail of merlin growth suppressor function. In contrast, interaction of merlin with microtubules exists in an ''open conformation''. Merlin is unable to associate with microtubules in the "closed conformation〞, due to the losses of the correct conformation necessary for this association. (Xu, Huamei 1998)

The CO-IP results indicated that Merlin protein bound to many functional proteins including tubulin, myosin light chain 6B, annexin and actin. This result verified our last co-localisation study that Merlin is present at numerous functional sites of stress fibres, focal adhesion, at sites of cell-cell contact and the leading cell edge in lamellipodial regions. However, our CO-IP results also unveiled some other Merlin interacting proteins, including transferrin receptor protein 1, annexin A2 and myosin light chain 6B. Transferrin receptor protein is involved in regulate the intaking of irons into cell (Qian ZM, Li H, Sun H, Ho K,. 2002), while annexin is cellular protein that is involved in control cellular processes including cell motility. The diversity of merlin binding protein may indicate its broad cellular functions. As these proteins have not been reported as interacting with Merlin in other studies, a further investigation will carried out to determine if these proteins are directly interact with Merlin.
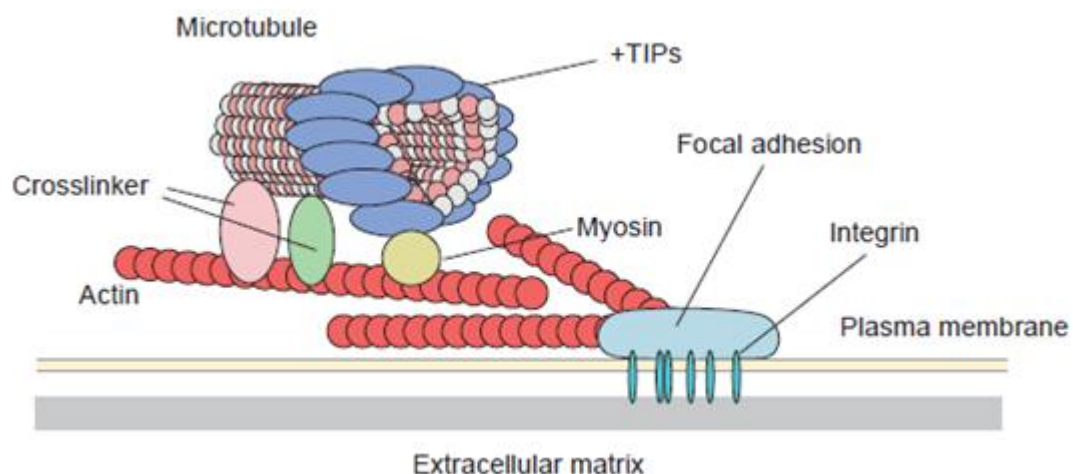
Figure 4.12 Crosstalk between actin filaments and microtubule, and their interaction with focal adhesion.

Microtubules are stabilized at the plus ends and oriented towards to the leading edge of migrating cell where it interacts with FA. Several proteins are involved in the processes, including cross-linker proteins which possess both actin- and microtubule-binding domains and actin-based motor protein myosins. The local targeting of microtubules modulates the activities of Rho family GTPases, resulting in the regulation of focal adhesion turnover. (Watanabe, Noritake and Kaibuchi 2005)

As Merlin was originally identified as a tumour suppressor, mutations to NF2 gene related to many cancers, including schwannomas, meningiomas, melanoma and thyroid cancer (Evans, et al. 1992) (Gutmann, et al. 1997) (Xiao, Chernoff and Testa 2003) (Bianchi, et al. 1994). Many studies have shown that Merlin is critical in regulating in cell growth and motility (LaJeunesse, McCartney and Fehon 1998) (Sherman, et al. 1997b) (Ikeda, et al. 1999). Absence of Merlin interrupts embryonic development and also initiates tumour metastasis (McClatchey, et al. 1997) (McClatchey, et al. 1998). Our studies have also revealed that merlin knock-down significantly increases HACE motility in terms of both adhesion and migration. In order to investigate what role Merlin plays in cell-matrix and cell-cell adhesion and how this might be regulated, a series of cell adhesion experiments were performed using a variety of ECMs, including fibronection, fibrinogen, laminin and vitronectin. Results indicated that relative to scrambled controls, Merlin-absent cells bound preferentially to vitronectin (VN) and fibronectin (FN). It is well documented that both of VN and FN contain the adhesive sequence: Argenine-Glycine-Aspartic acid (RGD) which selectively binds to $\alpha v\beta 3$ and $\beta 1$ integrin (Redick, et al. 2000). High expression of these ECMs is related to endothelial injury or inflammation. Apart from these RGD sequences, FN also contains two other actin-binding domains: Pro-His-Ser-Arg-Asn (PHSRN) and Ile-Asp-Ala-Pro-Ser (IDAPS). It is documented in literature that the PHSRN domain is recognised by $\alpha 5\beta 1$ while the IDAPS domain activates $\alpha 4\beta 1$ (Vogel 2006) (Pierschbacher and Ruoslahti 1984) (Mould and Humphries 1991). As mentioned previously, Obremski, Hall and Fernandez have revealed that Merlin also interacts with $\beta 1$-integrin (Obremski, Hall and Fernandez-Valle 1998b). From the attachment data, we can speculate on the important role played by Merlin in control of HAEC adhesion and migration. Furthermore, it may act to regulate HAEC motility by interacting with $\alpha v\beta 3$ and $\beta 1$ integrin.

Our previous data also show down-regulation of Merlin protein expression by various hemodynamic forces including shear stress and cyclic strain (figure 3.3 and figure 3.5). The effects of hemodynamic force on EC functions have long been investigated and the one of the historical discoveries is the realignment of ECs in the direction of a steady shear flow (Davies and Tripathi 1993). The process is then followed by EC migration. Both steps involved in cytoskeleton reorganization and formation of focal adhesion require the recruitment of many proteins. Many laboratories, including those of our colleagues in DCU, have shown the effects of cyclic strain and shear stress on EC migration (Von Offenberg Sweeney, et al. 2005). In this regard, we proposed that prolonged exposure of hemodynamic force would change HAEC functions, such as motility through the down-regulation of Merlin protein. Figure 4.6 to figure 4.9 elegantly illustrates how both shear stress and cyclic strain increased HAEC adhesion and migration, and how these increases were even more enhanced when Merlin was knocked-down. These results clearly implicate the negative role of Merlin in regulation of HAEC motility. However, we observed that merlin knock-down increased adhesion in Figure 4.5 but no effect in Figure 4.7. The effect of merlin knock-down on HAEC adhesion in figure 4.5 was performed on ECM coated plate while the experiments on figure 4.7 were performed on none-coating plate. This may alter the HAEC's attachment.

Table 4.3 Merlin interacting proteins

Interacting protein	Function	Interacting region (amino acids)
Merlin	Multifunctional tumor suppressor	8–121 binds 200–300 302–308 binds 580–595
Activators and suppressors of merlin function		
PAK	Merlin kinase	1–313 (PAK1)
PKA	Merlin kinase	Not determined
MYPT-1-PP1δ	Merlin phosphatase	312–341
Calpain	Merlin cleavage	Not determined
Structural proteins supporting merlin function		
βII-spectrin	Cytoskeletal structuring, focal adhesions	469–590
Actin	Cytoskeletal structuring	178–367
Microtubles	Cytoskeletal structuring	122–302
Growth activators suppressed by merlin		
Ezrin	Cytoskeleton-membrane interactions	1–313
Radixin	Cytoskeleton-membrane interactions	Not determined
Moesin	Cytoskeleton-membrane interactions	1–332
CD44	Hyaluronan signaling, focal adhesions	1–50
Layilin	Focal adhesions, hyaluronan signaling	1–332
TRBP	Protein translation	288–595
elF3c	Protein translation	1–304
PIKE	P13-kinase signaling	1–332
Syntenin	Axon growth, IL-5Rα signaling, endosomal localization	566–595
NHERF	NHE and cMAP signaling, AJ formation	1–332
RalGDS	Small GTPase signaling	1–288
EG1/Magicin	Small GTPase signaling	340–590/595
HEI10	Cell cycle regulation	306–339
N-WASP	Actin polymerization	1–332
Growth inhibitors that function with merlin		
MAP	Small GTPase signaling	288–595
RhoGDI	Small GTPase signaling	1–341
Paxillin	Focal adhesions	50–70 and 425–450
HRS	Endoctytic trafficking	453–557
DCC	Cell adhesion and neurite outgrowth	1–341
NGB	Tumor suppressor, GTPase	1–52 and 288–344
Drosophila expanded	Mediates control of fly development	522–635
Role in merlin suppression of growth unclear		
CRM1/exportin	Nuclear export	539–551
RIβ	PKA function, myelination, learning, memory	463–480
Caspr/paranodin	Myelination, βI integrin signaling	1–314
SCHIP-1	Unknown	1–27 and 280–323

(Scoles 2008e)

Chapter Five

The role of Merlin in the regulation of the uPAR-integrin signalling nexus

5.1 Introduction

The extracellular matrix (ECM), not only provides physical support for tissue, but is also pivotal in both interaction with and activation of cell plasma membrane receptors, and thus cytoplasmic signal transduction. Some of the cell fate and functions that are regulated by such processes include cell adhesion and migration. Interaction between ECM and cell membrane receptors plays an important role in vascular remodelling and EC repair. Alteration of the physical property or composition of ECM results in hypertensive heart disease (HHD) which is one of the major causes of stroke and heart failure (Berk, Fujiwara and Lehoux 2007). The deposition of fibronectin and fibrinogen into the subendothelial ECM is the early sign of progression of atherosclerosis. A. Wayne Orr et al have showed the interaction of subendothelial ECM with flow activates endothelial cell integrins, which in turn trigger nuclear factor-κB activation (Tzima, et al. 2001).

The urokinase type plasminogen activator receptor, uPAR, is one of the cell membrane adhesive receptors that play a crucial role in a number of cellular processes, including proteolysis and fibrinolysis. uPAR is an essential component of the activation machinery that converts and activates plasminogen into the protease plasmin. It also facilitates the pro-urokinase into urokinase (uPA). Both of these enzymes are essential in proteolysis and fibrinolysis. uPAR is anchored to cell membrane by its GPI domain (peripheral glycosyl-phosphatydil-insositol) which can also be cleaved and release the soluble uPAR (Figure 1.12). The GPI tail located at the Gly 283 residue which does not span the membrane. Due to its lack of a cytoplasmic domain, uPAR must interact with other trans-membrane receptors, such as integrin and G-coupled receptors, for outside-in signal transduction (figure 5.1) (Blasi and Carmeliet 2002b). Among these receptors, integrins are the most well studied and characterised. Previous studies have shown that uPAR interacts with a

number of the integrin family, specifically the heterodimers containing the β1, β2, β3 and β5 integrin subunits (Ragno 2006). Most recently, attention has focused on a less well characterised member of the integrin family-αvβ6, and its interaction with uPAR (Saldanha, et al. 2007). αvβ6 is thought to play a pivotal role in the metastasis and intra/extravasion of cancer cells via its interaction with uPAR (Ahmed, et al. 2002). It is also thought to play a role in the activation of Latency Associated Peptide (LAT or pro-TGF-β) and in epithelial-Mesenchymal Transition (EMT) (Wei, et al. 1996).

Integrins have been the focus of intense study due to their role in a multitude of cellular functions and their ability to "integrate" signals into and out of the cell in a bi-directional manner (Schwartz and Assoian 2001b) (Harris, Wild and Stopak 1980). They have been well studied for their ability to transduce these "inside-out" and "outside-in" signals which are capable of influencing cytoskeletal dynamics and subsequent, cell adhesion and migration. Although the direct binding of uPA with integrins is controversial, accumulating evidence demonstrated the requirement of integrins in uPAR signalling. The interaction of uPAR with its agonists promotes integrin-mediated cell motility as well as cell proliferation (Blasi 1997) (Chapman 1997) (Degryse, et al. 1999). α5β1 was demonstrated to be involved in uPA-uPAR-mediated migration in chinese hamster ovary cells. The vitronectin binding receptors, αvβ3, αvβ5, are other integrins that are associated with uPAR (Montuori, et al. 2001).

Urokinase is a single chain enzyme, with a molecular weight of 54 kDa. The inactive state of urokinase is referred to as pro-uPA which can be activated by binding to uPAR (Prager, et al. 2004). Activated urokinase is comprised of two chains and is referred to as high molecular weight urokinase. The association of urokinase to uPAR result in plasminogen activation, which then promotes cell

migration by enhanced ECM proteolysis (Estreicher, et al. 1990). Many studies have also demonstrated that uPAR promotes cell migration and proliferation through the activation of FAK and Rho families signalling pathways (JA 2002) (Vial, Sahai and Marshall 2003) (Kjøller and Hall 2001a).

Wei, et al. were the first to describe the binding interaction between uPAR and vitronectin (Wei, et al. 1996). It is now well established that vitronectin interacts with many integrin family members, including αvβ1, αvβ3, αvβ5 and αIIβ3, which all contain a RGD motif (Hynes 1992) (Pytela, Pierschbacher and Ruoslahti 1985a) (Pytela, Pierschbacher and Ruoslahti 1985b) (Preissner and Jenne 1991). The vitronectin binding site on uPAR is located on the D1 and the D1-D2 linker regions (Gårdsvoll and Ploug 2007). Sidenius, N. et al. demonstrated that the interaction between urokinase and uPAR enhance the binding ability of vitronectin with uPAR (Alfano, et al. 2002). Vitronectin can also be observed at the sites of focal adhesions (Ciambrone and McKeown-Longo 1992) (Kjøller and Hall 2001b) and specifically at the site of interaction between vitronectin and FA which is involved in re-arrangement of FA components (Kjøller and Hall 2001b).
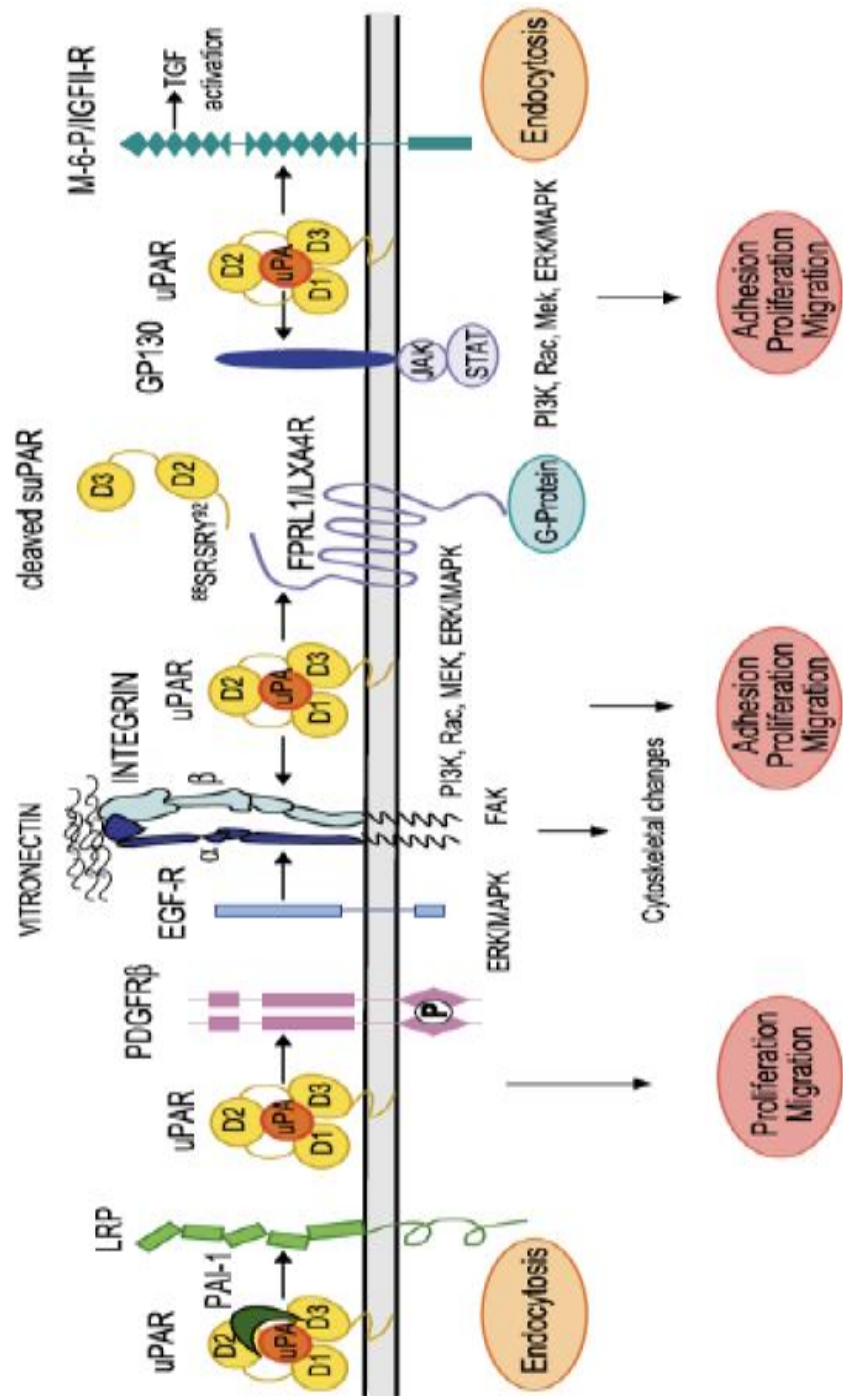
Figure 5.1:   uPA-uPAR and their interacting receptors

(Binder, Mihaly and Prager 2007)

5.1.1 Study Aims

5.1.1.1 Background

Previous work in our laboratory has demonstrated that uPAR to be found involved in strain-induced tube formation, and that uPA is critical in cyclic strain regulated cell migration and tube formation in ECs (Von Offenberg Sweeney et al., 2005). Intensive studies in our laboratory have also indicated that Moesin, another ERM family member, is critically involved in chemotaxis, angiogenesis and endothelial barrier integrity. Therefore, the work undertaken set out to investigate if uPAR is involved in EC adhesion and migration, and by which mechanisms these uPAR mediated functions are controlled.

5.1.1.2 Hypothesis

We postulated that merlin regulates HACE adhesion and migration through a specific integrin-$\alpha v \beta 3$, and the interaction of $\alpha v \beta 3$ with uPAR is required in this cellular mechanism.

5.1.1.3 Specific Aims

The overall aims of this chapter include:

- Based on the results of the cell-ECM adhesion and migration assays, investigate integrin inhibition (i.e. integrins that bind to RGD-containing ECM) alter cell migration.

  - Using urokinase (uPA) to activate of uPAR, and using integrin ($\alpha v \beta 3$) and G-coupled receptor (fMLly) activating peptides (e.g. D2A and SRSRY) to investigate the role of uPAR on endothelial cell migration, and to identify which membrane receptor is the principle play in this process i.e. migration.

- Using siRNA mediated knock-down techniques, investigate if Merlin is involved in uPAR- integrin mediated cell-matrix adhesion and migration.

- To investigate whether Merlin phosphorylation is modulated by uPAR using signalling.

5.2 Results

5.2.1 The effect of various RGDs inhibitory peptides on integrin mediated HAECs adhesion.

From the previous chapter, it can be seen that knock-down of merlin in HAECs preferentially promote adhesion to both VN and FN.   Both of these ECM contain a RGD sequence which selectively activates specific integrins, such as $\alpha v\beta 3$ (table 5.2). To elucidate the effect of various specific RGD peptides on integrin-mediated HAECs' adhesion, real time adhesion assays were carried out in the presence of three well characterised RGD inhibitors.   RGD1 inhibitor blocks both vitronectin and fibronectin mediated integrin interactions, RGD2 inhibitor is specific for fibronectin mediated integrin adhesion, while RGD3 blocks vitronectin mediated integrin activation.   In brief, the role of three RGDs on integrin mediated adhesion, in wild type HAEC was studied using the real time impedance based xCELLigence® system (Roche Diagnostics, Basal, Switzerland), HAECs were seeded into E-plates at a concentration of 30,000 cells per well, with the same number of untreated cells used for controls. The wells of which, had been treated with either RGD1, RGD2, or RGD3 prior to beginning the experiment.   Results illustrate that compared with untreated controls, RGD1 inhibitor significant decreased wild type HAECs' adhesion (62%), while incurring a non-significant 20% reduction in HAEC adhesion was observed with RGD2 and a non-significant 38% reduction in HACE adhesion was observed with RGD3 mediated inhibition. Furthermore, the maximal attachments of HAEC on both control and RGD inhibitors treated cells were reached at the 3 hour time point.
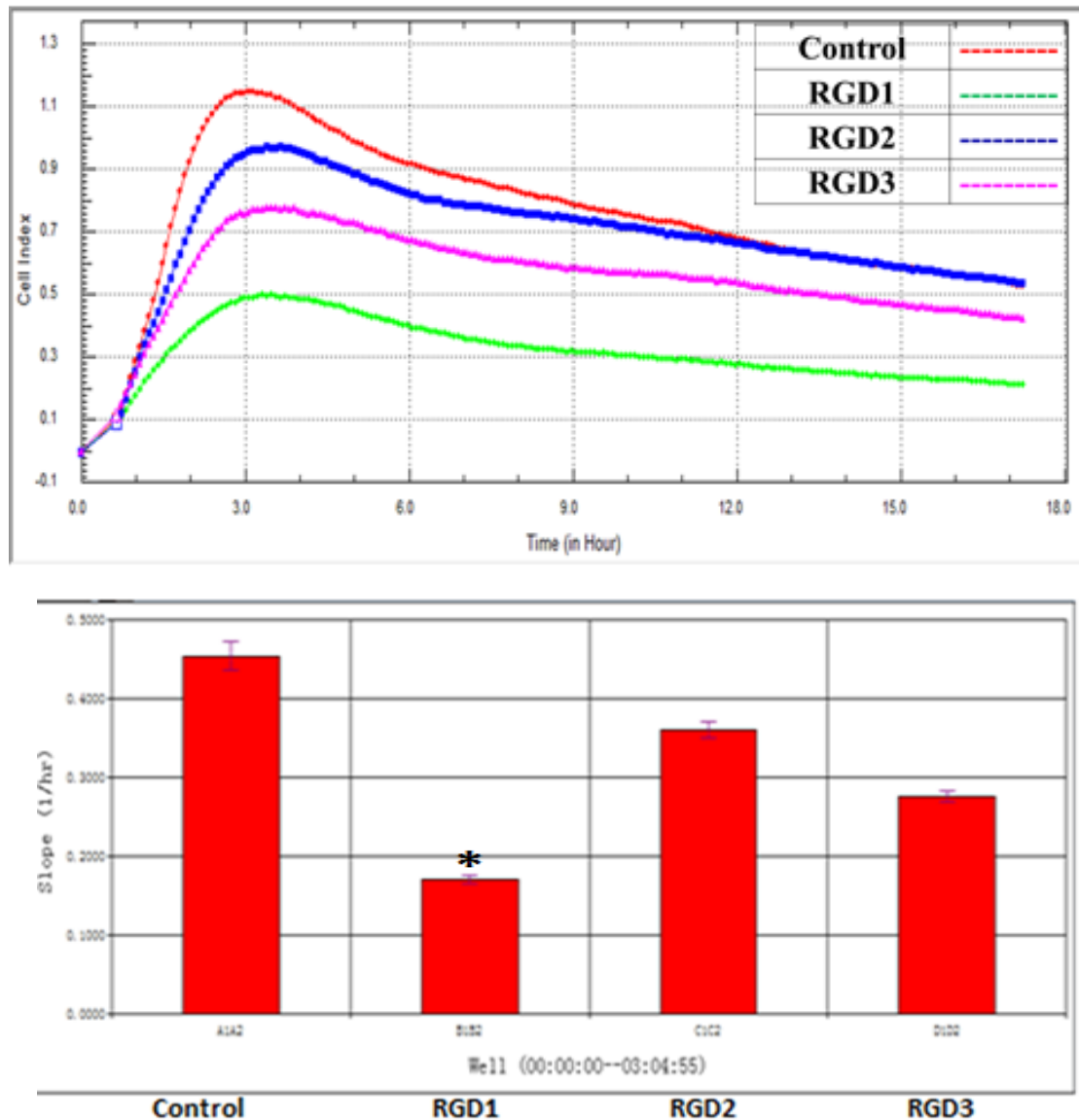
Fig 5.2: **The effect of specific RGDs inhibitors on integrin mediated HAECs' adhesion**

The role of RGD-mediated integrin inhibition on wild type HAEC adhesion was studied using the real-time xCELLigence® system. HAECs were seeded into E-plates at a concentration of 30,000 cells per well, with the same number of untreated cells used for controls. The wells of which, had been treated with either RGD1, RGD2, or RGD3 prior to beginning the experiment. Graphs illustrate that compared with untreated controls; RGD inhibitors significantly decreased HAEC adhesion as expected. The histogram represents slope changes, i.e. rate of adhesion, according with CI value change of RGD-treated HACE related to un-treated control. Results are averaged from three independent experiments $\pm$ SEM; *P$\leqslant$ 0.05 vs control.

5.2.2 Specific of RGD inhibitors and their effect on uPA mediated HAECs' adhesion.

As uPAR only contains an extracellular domain, it has to transduce extracellular signals through the interaction and synergistic association with other cell membrane receptors. Many studies have shown that integrins play important roles in uPAR mediated cell signaling. Therefore, in this section, we investigate if integrins are involved in the uPAR mediated signaling. To study the effects of RGD inhibitors on uPA stimulated HAEC adhesion, again, the xCELLigence$^®$ system was employed. Wild type HAECs were seeded into E-plates at a concentration of 30,000 cells per well. The wells of which, had been treated with uPA and either RGD1, RGD2, or RGD3 prior to beginning the experiment. For controls, untreated cells were used. The results illustrated that in comparison with untreated controls, uPA-mediated activation of uPAR increased HAEC adhesion by approximately 23% (non-significant). This increase was abrogated, significantly with treatment of RGD1 (54% decrease) and RGD3 (52% decrease). Only a non significant 24% reduction on HAEC adhesion was observed upon treatment with RGD2. Furthermore, maximal adhesion of HAECs in both control and treated cells was reached at the 3 hour time point.

Fig 5.3: The effect of specific RGD inhibitors on uPA mediated HAECs adhesion

The effect of the three specific RGD inhibitors on uPA-mediated wild type HAECs adhesion was studied using the xCELLigence® system. HAECs were seeded into E-plates at a concentration of 30,000 cells per well. The wells of which, had been treated with uPA and either RGD1, RGD2, or RGD3 prior to beginning the experiment (the concentrations are described in chapter 2). Untreated cells were used as controls. Graphs illustrate that compared with untreated controls; uPA increased HAEC adhesion, the effect of which was significantly inhibited by the addition of the RGD inhibitors. The histogram represents slope changes according with CI value change. (Red: control, Green: UPA, Blue: RGD1+UPA, Pink: RGD2+UPA, Cyan: RGD3+UPA). Results are averaged from three independent experiments $\pm$SEM; *P$\leqslant$ 0.05 vs control.

5.2.3 The effect of specific RGD inhibitors on D2A mediated HAEC adhesion.

Due to less of cytoplasmic domain, uPAR has to interact with the other transmembrane proteins such as αvβ3 and fMLP for signaling transduction. To investigate which transmembrane protein is involved in uPAR regulated HAECs motility two peptides D2A and SRSRY were employed. D2A was first synthesized by Bernard Degryse and his collegues (Bernard Degryse, et al 2005). The details of this peptide please see section 1.6.2. D2A has been shown to interact laterally with αvβ3 integrin and induce cell migration, via outside-in signalling. SRSRY (Ser-Arg-Ser-Arg-Tyr) is another chemotactic peptide, bind specifically to fMLP- a seven-transmembrane domain G-coupled receptor, and promote cell migration in this manner (Lucia Gargiulo, et al, 2005).

In order to study the effect of the RGD inhibitors on D2A mediated HAECs adhesion (i.e. αvβ3 integrin mediated), the xCELLigence$^®$ system was employed. Wild type HAECs were seeded into E-plates at a concentration of 30,000 cells per well. The wells of which, had been treated with D2A and either RGD1, RGD2, or RGD3 prior to beginning the experiment. Untreated cells were used as controls. The results illustrate that compared with untreated controls, D2A-mediated activation of αvβ3 significantly increased HAEC adhesion by approximate 23%, and was significantly decreased by treatment with RGD1 (69% decrease) and RGD3 (40% decrease), while only a 24% reduction on HAEC adhesion was observed upon treatment with RGD2. Furthermore, the maximal attachments of HAEC on both control and treated cells were reached at 3 hour time point.

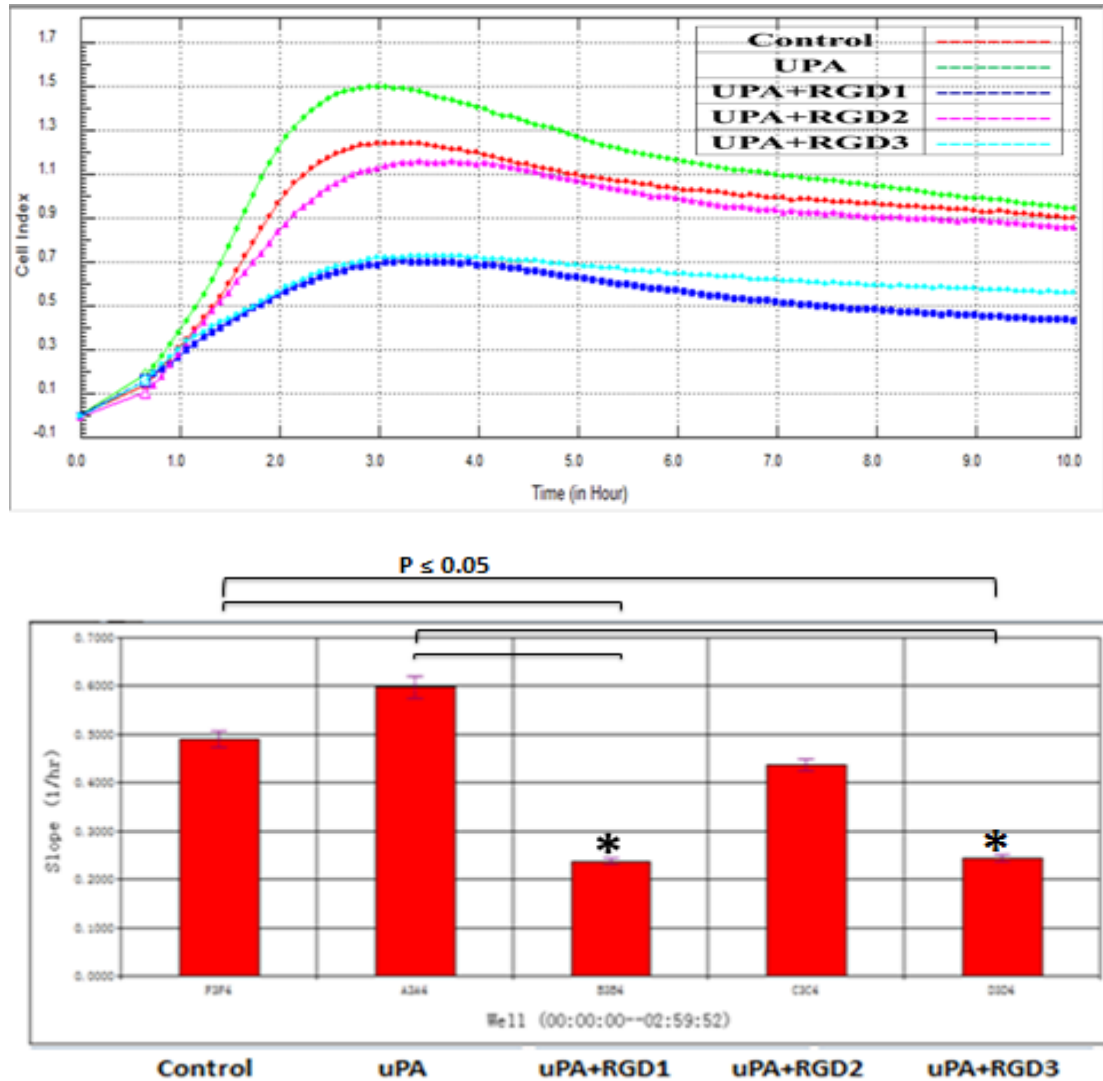**Fig 5.4: The effect of specific RGD inhibitors on D2A mediated wild type HAEC adhesion**

The effect of specific RGD inhibitors on D2A mediated wild type HAEC adhesion was studied using the xCELLigence system[®]. Wild type HAECs were seeded into E-plates at a concentration of 30,000 cells per well. The wells of which, had been treated with D2A and either RGD1, RGD2, or RGD3 prior to beginning the experiment. Untreated cells were used as controls. Graphs illustrate that compared with untreated controls D2A increased HAEC adhesion, and that this increase was significantly inhibited by the addition of RGD inhibitors. The histogram represents slope changes according with CI value change. (Cyan: control, Pink: D2A, Red: RGD1+D2A, Green: RGD2+D2A, Blue: RGD3+D2A). Results are averaged from three independent experiments $\pm$ SEM; *P$\leqslant$ 0.05 vs control.

5.2.4 The effect of specific RGD inhibitors on SRSRY mediated HAEC adhesion.

To study the effect of the three RGD inhibitors on SRSRY mediated HAECs adhesion (i.e. fMLP mediated adhesion), the xCELLigence$^{®}$ system was employed. Wild type HAECs were seeded into E-plates at a concentration of 30,000 cells per well. The wells of which, had been treated with SRSRY and either RGD1, RGD2, or RGD3 prior to beginning the experiment. Results indicate that compared with untreated controls, SRSRY mediated activation of fMLP increased HAEC adhesion by approximately 10% (non-significant), the effect of which was significantly decreased by treatment with RGD1 (67% decrease) and RGD3 (53% decrease), while only a 20% reduction on HAEC adhesion was observed upon treatment with RGD2. Furthermore, maximal adhesion of HAECs, with both control and treated cells was reached at the 3 hour time point.
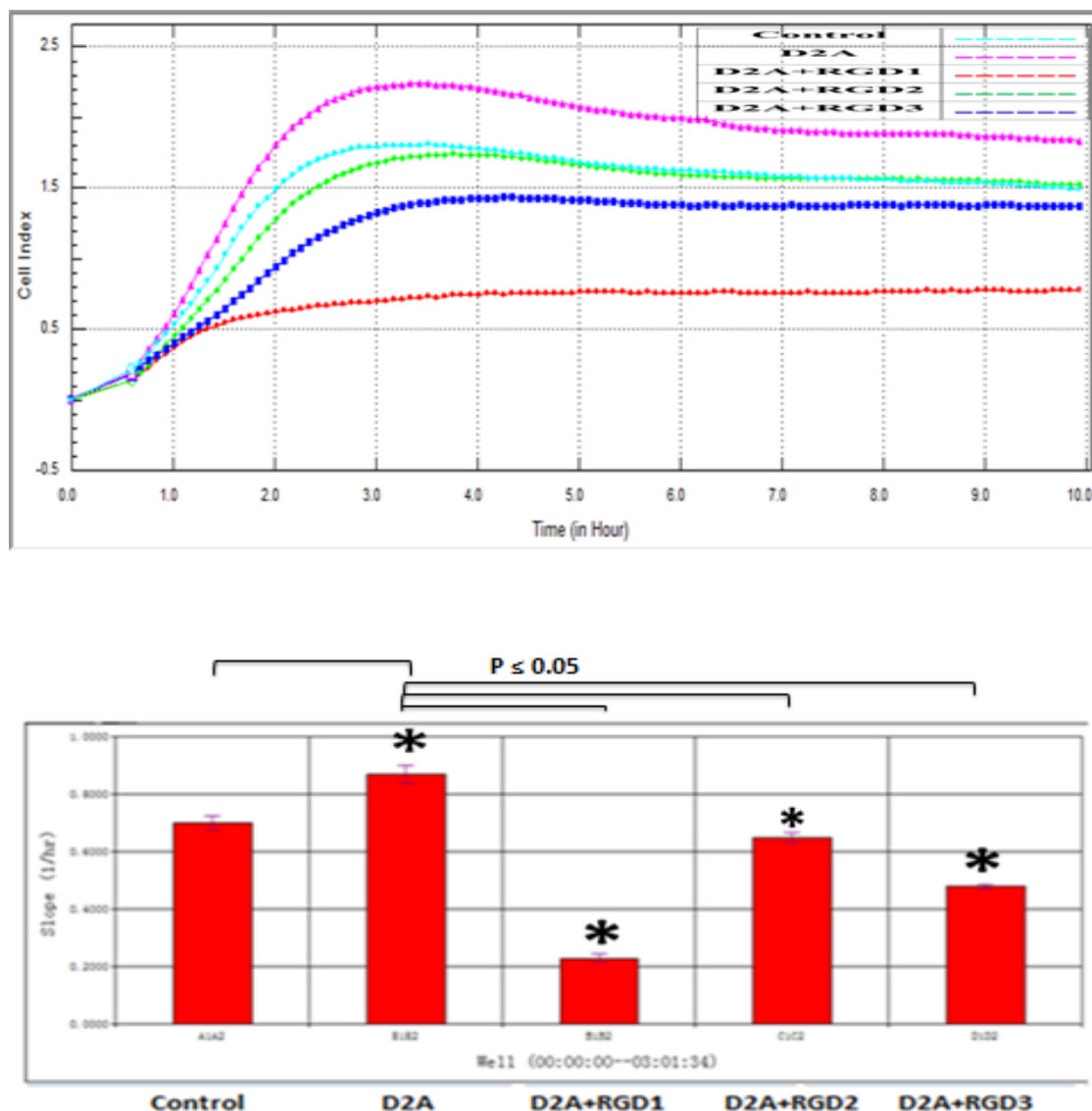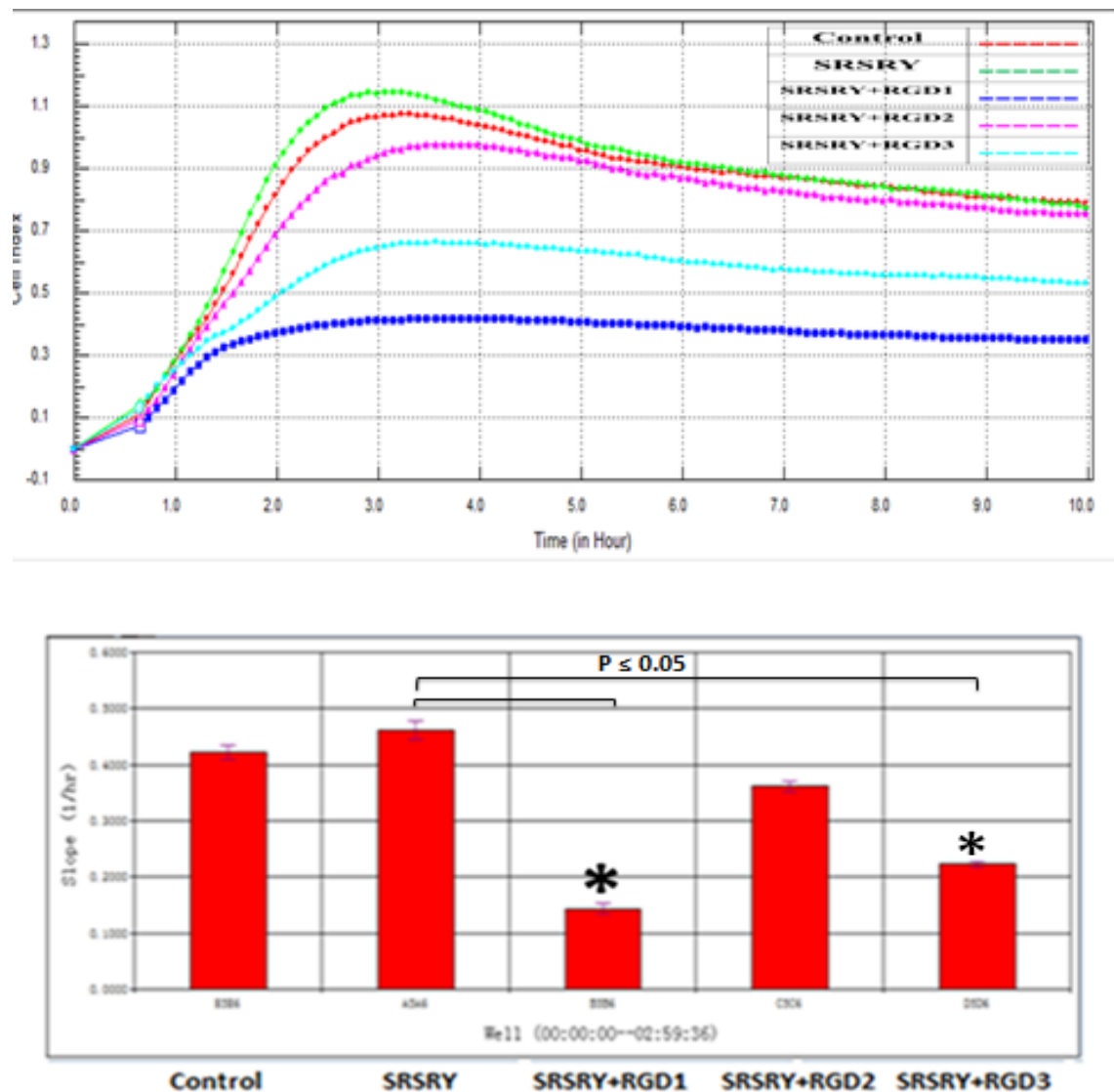
Fig 5.5: The effect of specific RGD inhibitors on SRSRY peptide mediated HAEC adhesion.

The effect of specific RGD inhibitors on SRSRY mediated adhesion in wild type HAECs, as studied using the xCELLigence® system. Wild type HAECs were seeded into E-plates at a concentration of 30,000 cells per well. The wells of which, had been treated with SRSRY and either RGD1, RGD2, or RGD3 prior to beginning the experiment. Untreated cells were used as controls. Graphs illustrate that compared to untreated controls; SRSRY increased HAEC adhesion, which was significantly inhibited by the addition of RGD inhibitors. The histogram represents slope changes according with CI value change. (Red: control, Green: SRSRY, Blue: RGD1+SRSRY, Pink: RGD2+SRSRY, Cyan: RGD3+SRSRY). Results are averaged from three independent experiments $\pm$SEM; *P$\leqslant$ 0.05 vs control.

5.2.5 The effect of the integrin inhibitor, RGD1 on HAEC adhesion in siRNA mediated merlin knockdown HAECs

From the previous studies, we concluded that uPAR transduced cell signals through the integrin mediated pathways. We then sought to investigate whether Merlin was involved in this molecular mechanism. The role of RGD1 mediated integrin inhibition on Merlin knock-down HAEC adhesion was studied using the xCELLigence® system. HAECs were first transfected with Merlin siRNA to knock-down Merlin protein expression. HAECs were also transfected with scrambled siRNA for the control study. The transfection and subsequent knock-down efficiency was monitored using western blot, to ensure a minimum of 70 to 80% knock-down of Merlin in HAECs was achieved before analysis could proceed. Both scrambled control and Merlin knock-down HAECs were seeded into E-plates at a concentration of 30,000 cells per well. The wells of which, had been treated with RGD1 prior to beginning the experiment. Untreated cells were used as controls. The results indicate that compared with scrambled controls, Merlin knock-down significantly increased HAEC adhesion by 73%. This then decreased by 63% when treated with RGD 1 inhibitors. Maximal attachments of HAECs on both control and treated cells were reached at the 4 hour time point.

Fig 5.6:   The effect of RGD1 mediated integrin inhibition on HAEC adhesion in siRNA mediated merlin knock-down cells

The effect of RGD1 mediated integrin inhibition on Merlin knock-down HAEC adhesion was studied using the xCELLigence® system.   Both Merlin knock-down (i.e. siRNA treated) and scrambled siRNA treated control HAECs were seeded into E-plates at a concentration of 30,000 cells per well. The wells of which, had been treated with RGD1 prior to beginning the experiment. Scrambled siRNA transfected HAECs were used as controls.   Graphs illustrate that compared with untreated controls, the treatment of RGD1 inhibitor significantly reduced the effect of Merlin absence on HAEC adhesion. The histogram represents slope changes according with CI value change. Results are averaged from three independent experiments $\pm$ SEM; *$P \leqslant$ 0.05 vs control.

5.2.6 The effect of the integrin inhibitor, RGD2 on HAEC adhesion in siRNA mediated merlin knockdown cells

The effect of RGD2 mediated integrin inhibition on the Merlin knock-down HAEC adhesion profile was studied in real-time, using the xCELLigence® system. HAECs were first transfected with Merlin siRNA to knock-down Merlin protein expression. HAECs were also transfected with scrambled siRNA for control studies. The transfection and subsequent knock-down efficiency was monitored using Western blot, to ensure a minimum 70 to 80% knock-down of Merlin in HAECs was achieved before analysis could proceed. Both scrambled control and Merlin knock-down HAECs were seeded into E-plates at a concentration of 30,000 cells per well. The wells of which, had been treated with RGD2 prior to beginning the experiment. Untreated cells were used as controls. Results showed that in comparison with scrambled control, Merlin knock-down significantly increased HAEC adhesion by 73%, the effect of which was decreased by 27% upon treatment by RGD2 inhibitors. Furthermore, the maximal adhesion of HAECs with both control and treated cells was reached at the 4 hour time point.
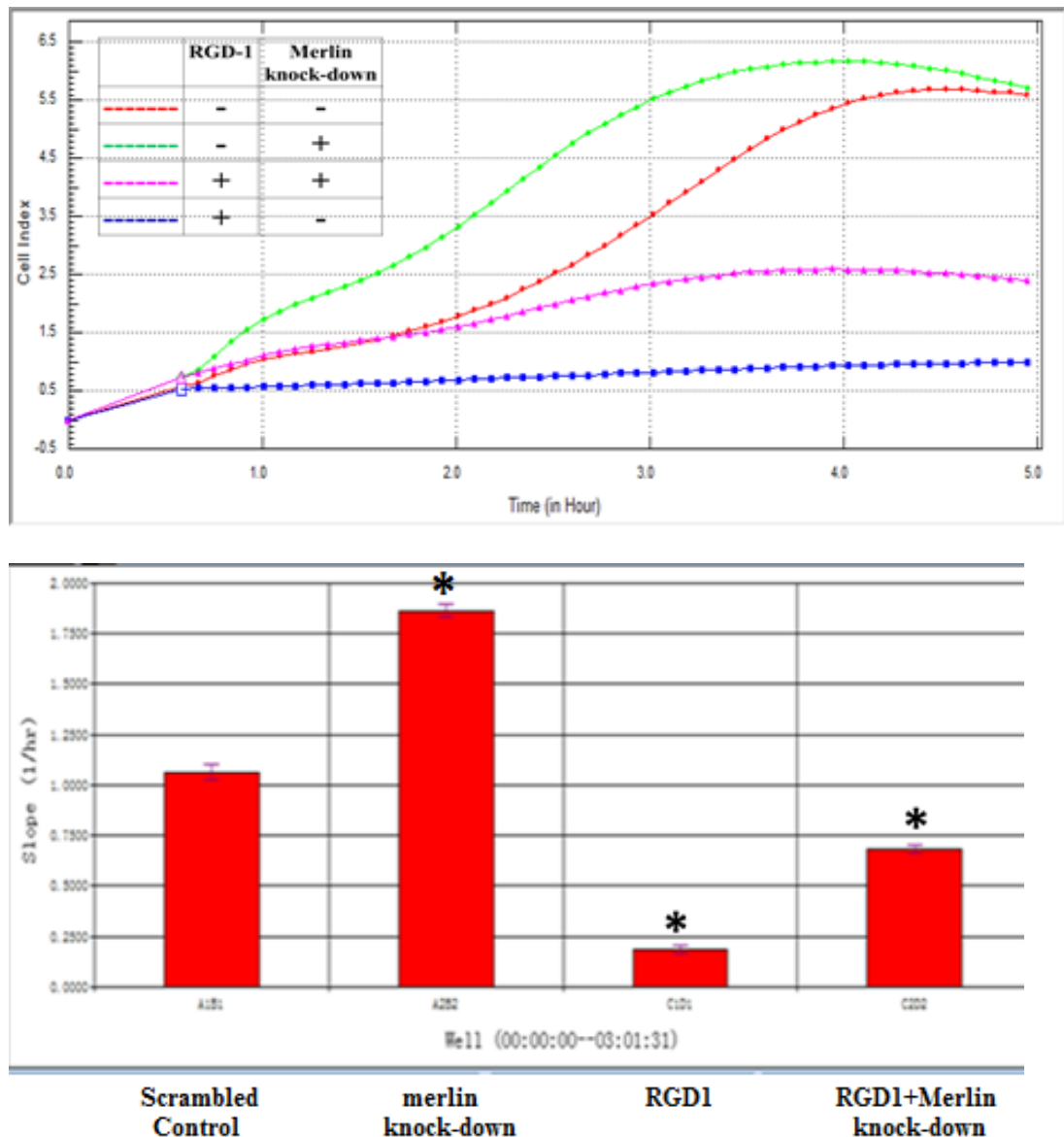
Fig 5.7: The effect of the integrin inhibitor, RGD2 on HAEC adhesion in siRNA mediated merlin knock-down cell

The effect of RGD2 mediated integrin inhibition on Merlin knock-down HAEC adhesion was studied in real time using the xCELLigence® system. Both scrambled control and Merlin knock-down HAECs were seeded into E-plates at a concentration of 30,000 cells per well. The wells of which, had been treated with RGD2 prior to beginning the experiment. Untreated scrambled control HAECs were used as controls. Graphs illustrate that compared with untreated controls, treatment of RGD2 inhibitor reduced the effect observed on Merlin knock-down on HAEC adhesion. The histogram represents slope changes according with CI value change. Results are averaged from three independent experiments $\pm$SEM; *P$\leqslant$ 0.05 vs control.

5.2.7 The effect of the integrin inhibitor, RGD3 on HAEC adhesion in siRNA mediated merlin knock-down cells

The effect of RGD3 mediated integrin inhibition on HAEC adhesion in merlin knock-down cells, was studied using real time cell analysis, the xCELLigence® system. HAECs were transfected with Merlin siRNA to knock-down Merlin expression. HAECs were transfected with scrambled siRNA for the purposes of control studies, as well as untransfected cell. The transfection and subsequent knock-down efficiency was monitored using western blot, to make sure a minimum of a 70 to 80% knock-down of Merlin in HAECs was achieved before analysis could proceed. Both scrambled control and Merlin knock-down HAECs were seeded into E-plates at a concentration of 30,000 cells per well. The wells of which, had been treated with RGD3 prior to beginning the experiment. Untreated cells were also used for controls. The findings illustrated, that compared with scrambled controls, Merlin knock-down significantly increased HAEC adhesion by 73%, the effect of which was abrogated by 74% upon treatment with RGD3 inhibitory peptides. Furthermore, maximal adhesion of HAECs on both control and treated cells were reached at the 4 hour time point.

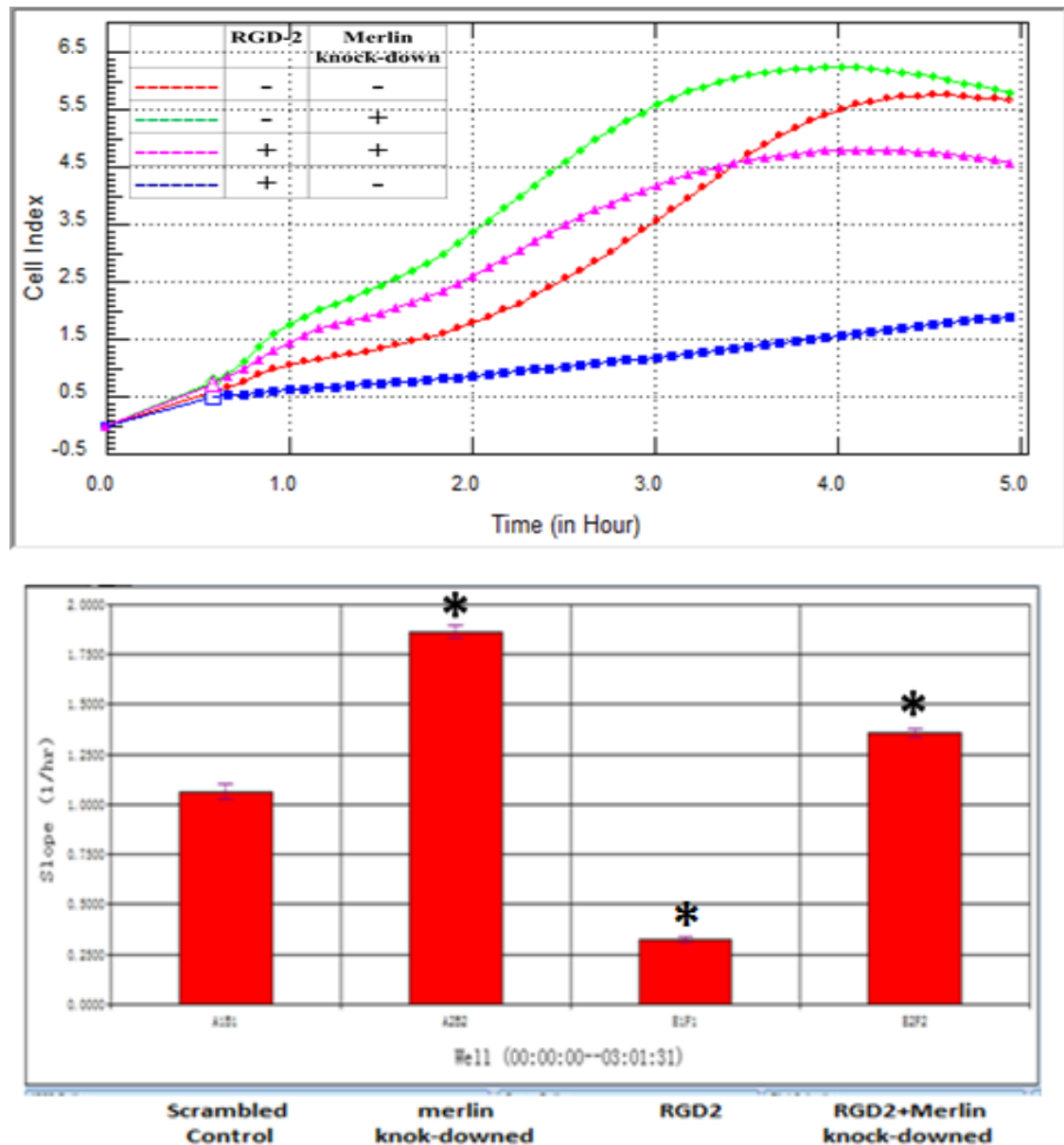**Fig 5.8:** **The effect of RGD3 mediated integrin inhibition on HAECs adhesion, in siRNA mediated merlin knock-down cells**

The effect of RGD3 mediated integrin inhibition on HAECs adhesion in merlin knock-down cell, was studied using the xCELLigence® system. Both scrambled control and Merlin knock-down HAECs were seeded into E-plates at a concentration of 30,000 cells per well. The wells of which, had been treated with RGD3 prior to beginning the experiment. Untreated scrambled control HAECs were used as controls in this experiment.   Graphs illustrate that compared with untreated controls, treatment of RGD3 inhibitor significantly reduced the impact of Merlin absence on HAEC adhesion.   The histogram represents slope changes according with CI value change. Results are averaged from three independent experiments ±SEM; *P≤ 0.05 vs control.

5.2.8 The effect of the integrin inhibitor, RGD1 on HAEC migration in siRNA mediated merlin knock-down cells

The effect of RGD1 mediated integrin inhibition on Merlin knock-down HAEC migration profile was studied in real-time, using the xCELLigence® system. HAECs were transfected with Merlin siRNA to knock down Merlin protein expression. HAECs were also transfected with scrambled siRNA for the control studies. The transfection and subsequent knock-down efficiency was monitored using Western blot to ensure a minimum of 70 to 80% knock down of Merlin in HAECs was achieved before analysis could proceed. Both scrambled controls and Merlin knock-down HAECs were then seeded into the upper chambers of CIM-plates at a concentration of 30,000 cells per well. The lower chambers of CIM plate of which, had been treated with RGD1 prior to beginning the experiment. As before, untreated cells were used as controls. The results illustrate that compared with scrambled controls, merlin knock-down significantly increased HAEC migration by 71%, the effect of which was decrease by 24% upon treatment with RGD1 inhibitors. Furthermore, the maximal migration of HAEC with both control and treated cells was reached at the 4 hour time point.
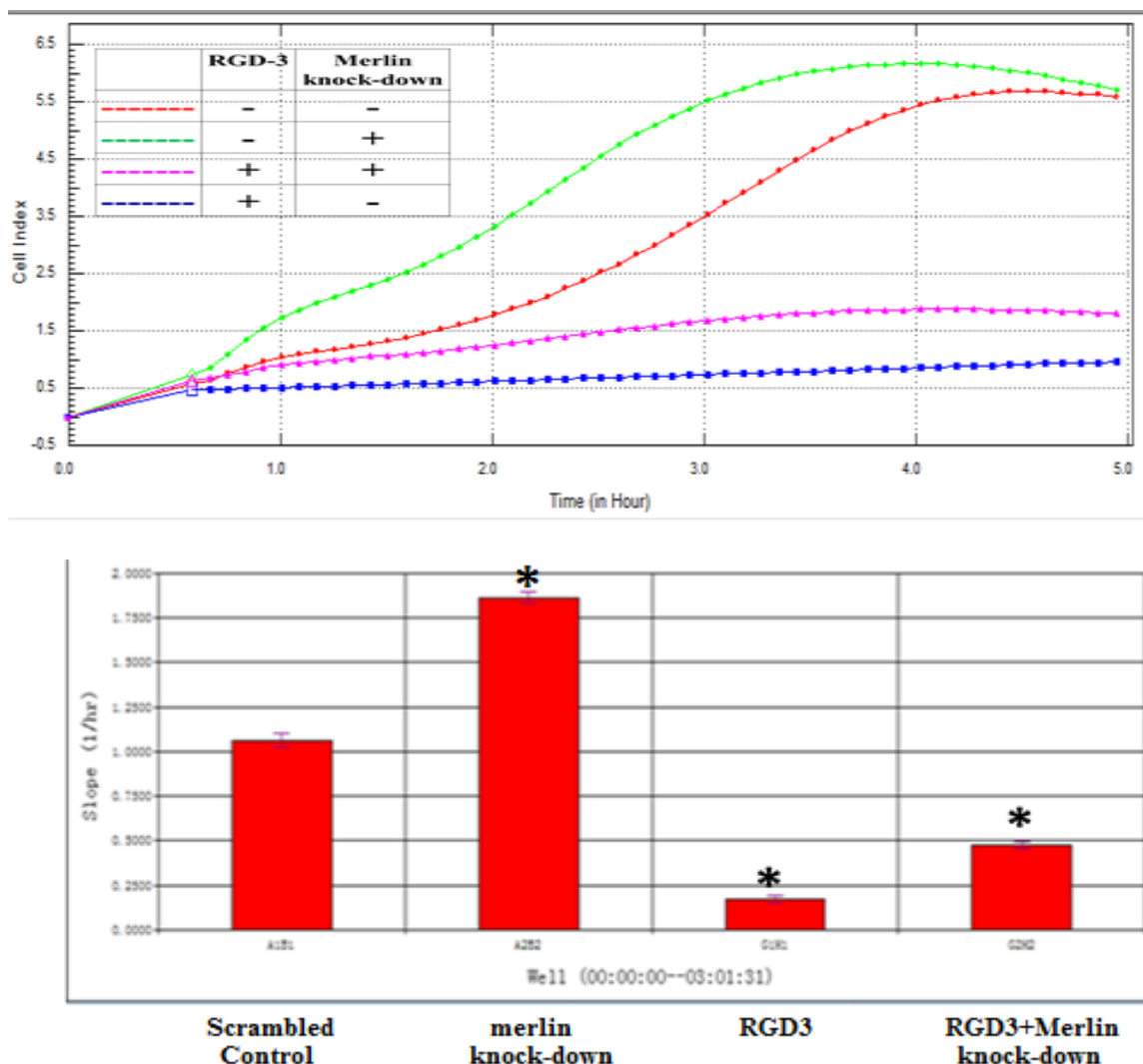
Fig 5.9: **The effect of RGD1 mediated integrin inhibition on Merlin knock-down HAEC migration**

The effect of RGD1 mediated integrin inhibition on Merlin knock-down HAEC migration was studied in real time using the xCELLigence® system. Both Merlin knock-down and scrambled control HAECs were seeded into the upper chambers of CIM-plates at a concentration of 30,000 cells per well. The lower chambers of CIM plate of which, had been treated with RGD1 prior to beginning the experiment. Graphs illustrate that compared with untreated controls, RGD1 inhibitor reduced the effect observed on Merlin knock-down HAEC migration by 24%. The histogram represents slope changes according with CI value change. Results are averaged from three independent experiments $\pm$SEM; *P$\leqslant$ 0.05 vs control.

5.2.9 The effect of the integrin inhibitor, RGD2 on HAEC migration in siRNA mediated merlin knock-down cells

The effect of RGD2 mediated integrin inhibition on Merlin knock-down HAEC migration profile was studied in real-time, using the xCELLigence® system. HAECs were transfected with Merlin siRNA to knock down Merlin protein expression. HAECs were also transfected with scrambled siRNA for the control studies. The transfection and subsequent knock-down efficiency was monitored using Western blot to ensure a minimum of 70 to 80% knock down of Merlin in HAECs was achieved before analysis could proceed. Both scrambled controls and Merlin knock-down HAECs were then seeded into the upper chambers of CIM-plates at a concentration of 30,000 cells per well. The lower chambers of CIM plate of which, had been treated with RGD2 prior to beginning the experiment. As before, untreated cells were used as controls. The results illustrate that compared with scrambled controls, merlin knock-down significantly increased HAEC migration by 71%, the effect of which was decrease by 5% upon treatment with RGD2 inhibitors. Furthermore, the maximal migration of HAEC with both control and treated cells was reached at the 4 hour time point.
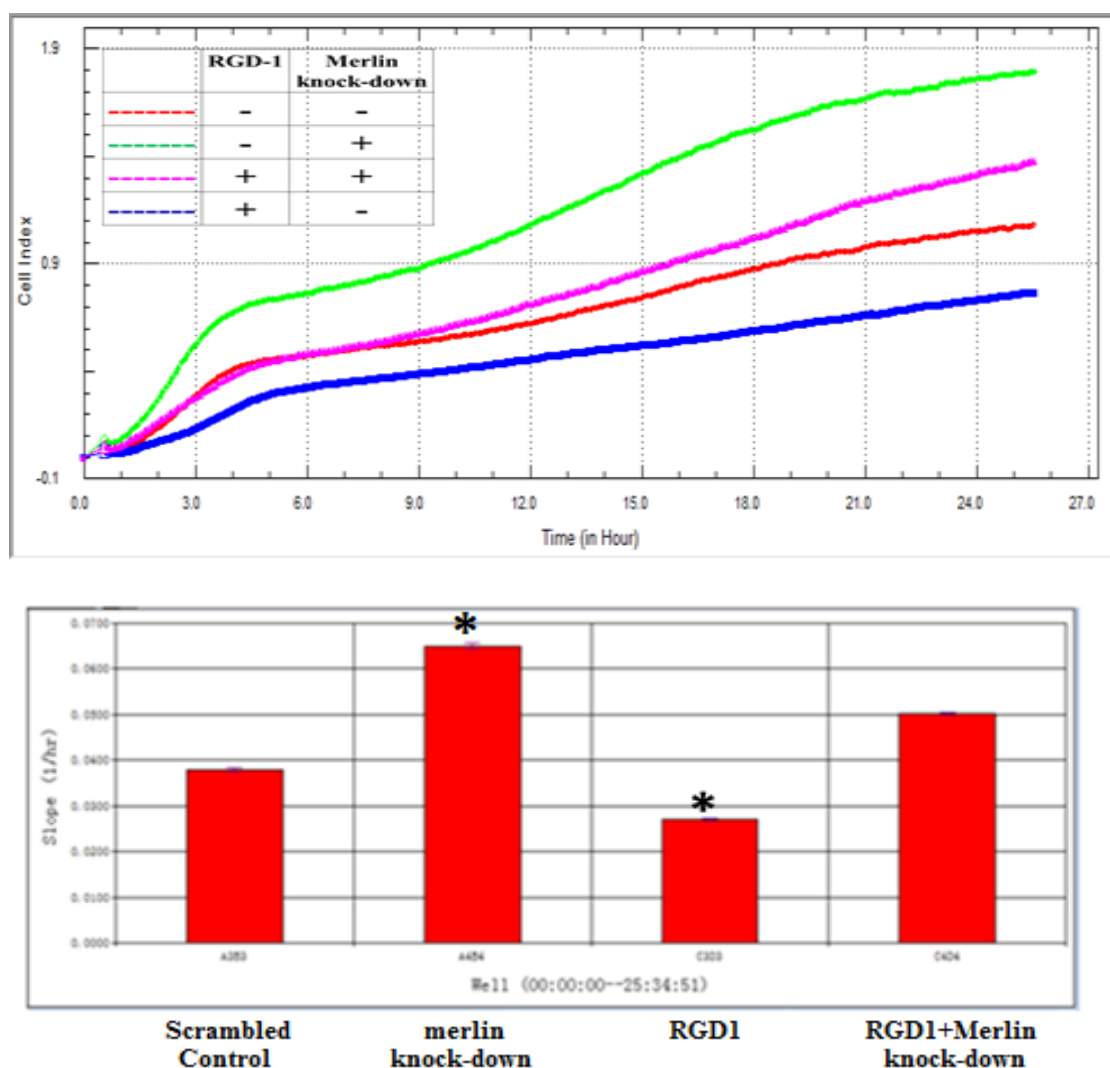
Fig 5.10: The effect of RGD2 mediated integrin inhibition on Merlin knock-down HAEC migration

The effect of RGD2 mediated integrin inhibition on Merlin knock-down HAEC migration was studied in real time using the xCELLigence® system. Both Merlin knock-down and scrambled control HAECs were seeded into the upper chambers of CIM-plates at a concentration of 30,000 cells per well. The lower chambers of CIM plate of which, had been treated with RGD2 prior to beginning the experiment. Graphs illustrate that compared with untreated controls, RGD2 inhibitor reduced the effect observed on Merlin knock-down HAEC migration by 5%. The histogram represents slope changes according with CI value change. Results are averaged from three independent experiments $\pm$SEM; *P$\leqslant$ 0.05 vs control.

5.2.10 The effect of the integrin inhibitor, RGD3 on HAEC migration in siRNA mediated merlin knock-down cells

The effect of RGD3 mediated integrin inhibition on Merlin knock-down HAEC migration profile was studied in real-time, using the xCELLigence$^®$ system. HAECs were transfected with Merlin siRNA to knock down Merlin protein expression. HAECs were also transfected with scrambled siRNA for the control studies. The transfection and subsequent knock-down efficiency was monitored using Western blot to ensure a minimum of 70 to 80% knock down of Merlin in HAECs was achieved before analysis could proceed. Both scrambled controls and Merlin knock-down HAECs were then seeded into the upper chambers of CIM-plates at a concentration of 30,000 cells per well. The lower chambers of CIM plate of which, had been treated with RGD3 prior to beginning the experiment. As before, untreated cells were used as controls. The results illustrate that compared with scrambled controls, merlin knock-down significantly increased HAEC migration by 71%, the effect of which was decrease by 70% upon treatment with RGD3 inhibitors. Furthermore, the maximal migration of HAEC with both control and treated cells was reached at the 4 hour time point.
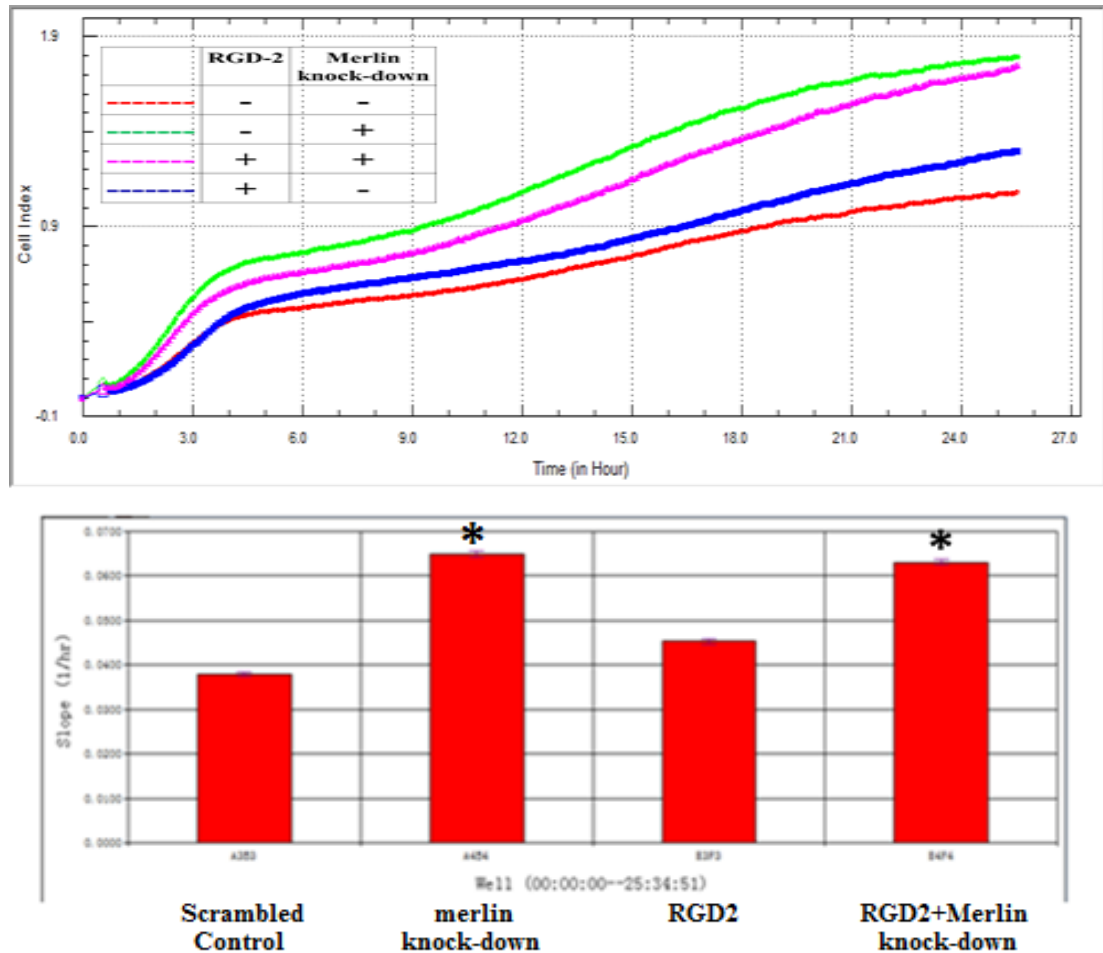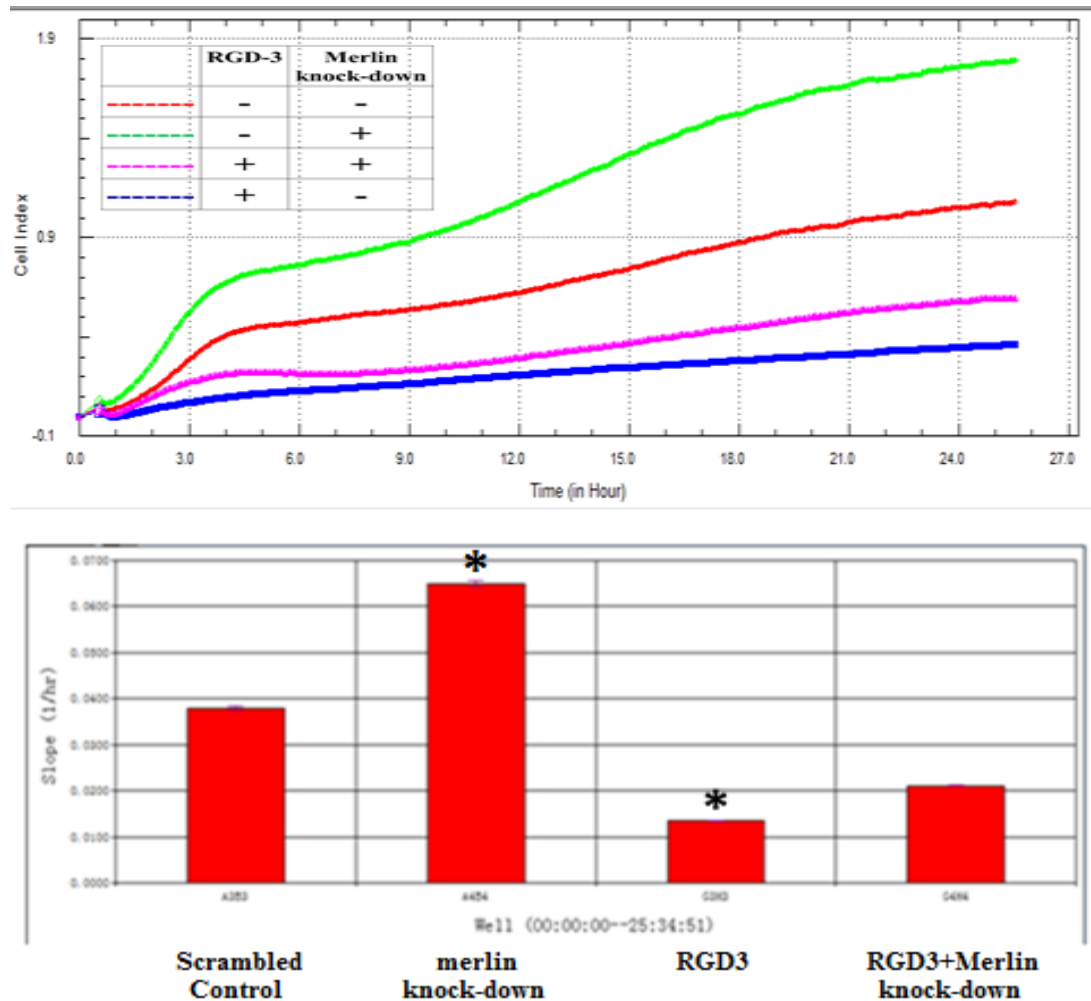
Fig 5.11: The effect of RGD3 mediated integrin inhibition on Merlin knock-down HAEC migration

The effect of RGD3 mediated integrin inhibition on Merlin knock-down HAEC migration was studied in real time using the xCELLigence® system. Both Merlin knock-down and scrambled control HAECs were seeded into the upper chambers of CIM-plates at a concentration of 30,000 cells per well.   The lower chambers of CIM plate of which, had been treated with RGD3 prior to beginning the experiment. Graphs illustrate that compared with untreated controls, RGD3 inhibitor reduced the effect observed on Merlin knock-down HAEC migration by 70%.   The histogram represents slope changes according with CI value change. Results are averaged from three independent experiments $\pm$SEM; *P$\leqslant$ 0.05 vs control.

5.2.11 The comparison of RGD inhibitors on merlin knock-down HAEC motility.

To compare the effect of RGD inhibitors on merlin knock-down HAEC motility HAECs were transfected with Merlin siRNA to knock down Merlin protein expression. HAECs were also transfected with scrambled siRNA for the control studies. The transfection and subsequent knock-down efficiency was monitored using Western blot to ensure a minimum of 70 to 80% knock down of Merlin in HAECs was achieved before analysis could proceed. Both scrambled controls and Merlin knock-down HAECs were then seeded into E-plate for adhesion studies or CIM-plate for migration assay of which had been treated with RGD inhibitors prior to beginning the experiment. The HAECs motility was monitored in real-time, using the xCELLigence® system.

The results demonstrate that compared with scrambled controls, merlin knock-down significantly increased HAEC motility, including adhesion (30%) and migration (88%). RGD1 inhibitors decreased the HAEC motility about 81% on adhesion and 52% on migration compared with scrambled control. RGD2 inhibitors decreased the HAEC motility about 71% on adhesion and 2% on migration compared with scrambled control. RGD3 inhibitors decreased the HAEC motility about 83% on adhesion and 75% on migration compared with scrambled control. RGD inhibitors have also shown the ability to decrease HAECs motility when merlin was knocked-down. The treatment of RGD1 decreased merlin knocked-down HAEC adhesion by 58% and migration 47% respectively. The treatment of RGD2 decreased merlin knocked-down HAEC adhesion by 24% and migration 16% respectively. The treatment of RGD3 decreased merlin knocked-down HAEC adhesion by 70% and migration 67% respectively.
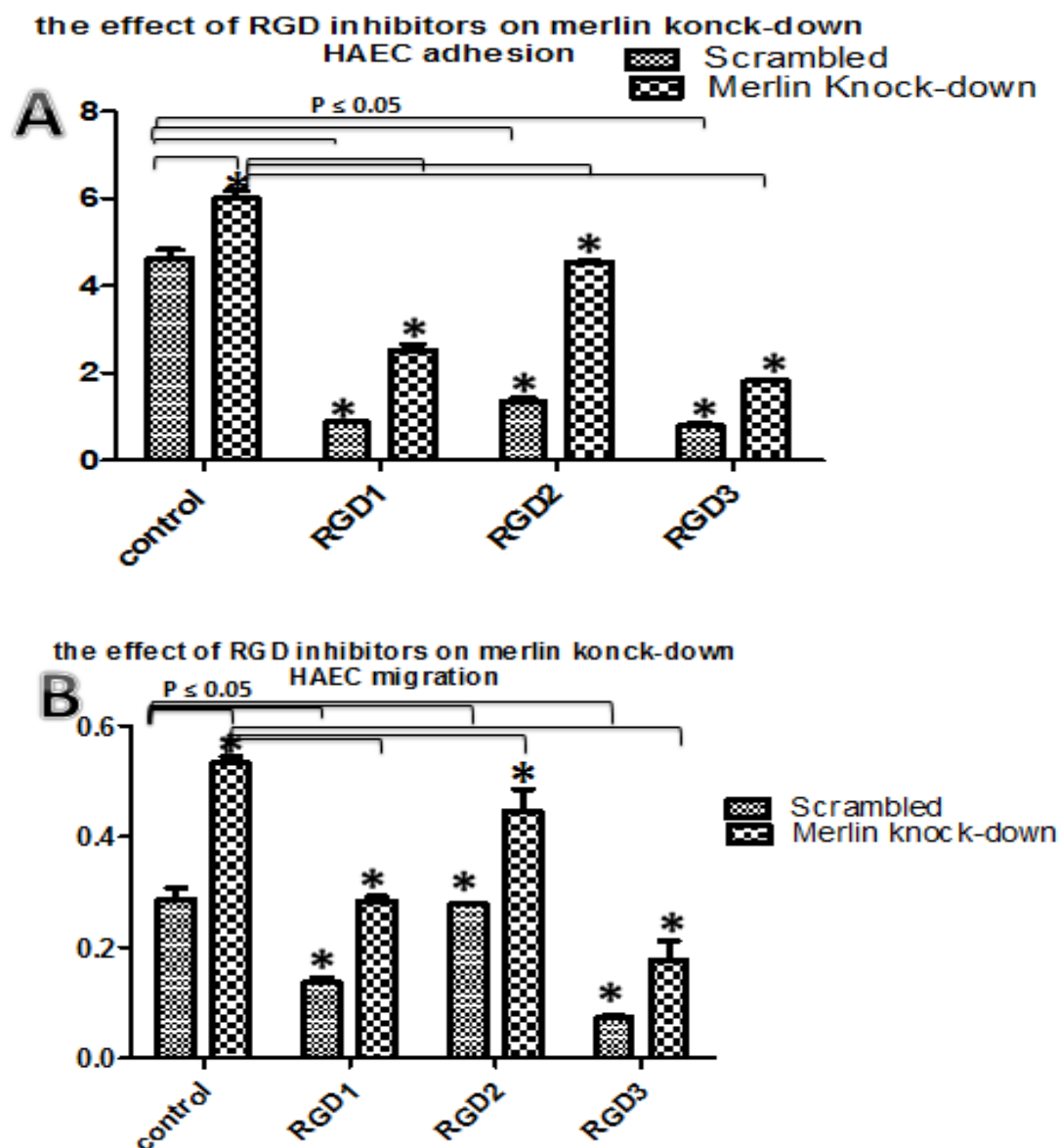
Fig 5.12: The comparison of RGD inhibitors on merlin knock-down HAEC motility.

To compare of RGD inhibitors on merlin knock-down HAEC motility, the real time and label-free monitoring system, the xCELLigence® system was employed. Both Merlin knock-down and scrambled control HAECs were seeded into E-plate for adhesion studies or CIM-plate for migration assay of which had been treated with RGD inhibitors prior to beginning the experiment at a concentration of 30,000 cells per well. The figure A represents adhesion assay and the figure B represents migration assay. Results are averaged from three independent experiments ±SEM; *P≤ 0.05 vs control.

5.2.12. The effect of D2A peptides on Merlin phosphorylation.

In summary, we have demonstrated that uPAR plays a critical role in regulation of HAEC adhesion and migration, a process mediated via integrins. Moreover we have illustrated that Merlin is involved in this integrin-mediated cellular process.   In this section, we endeavored to further investigate if the activation of αvβ3 integrin by D2A directly modulates merlin phosphorylation state.   To study the effect of D2A peptides on merlin phosphorylation state, HAECs were seeded into 6-well plates at a density of 10^5 cells per cm^2 and allowed to adhere and grow to confluence over a 24 hour period.   Cells were then exposed to 1 nM D2A acutely for time points of 1, 3, 5, 10, 30 minute.   Untreated HACEs were used as control. Cells were then lysed, and analyzed by Western blotting.   Results demonstrate that merlin phosphorylation is increased within a short time-frame, starting at the 3 minutes (eliciting 0.25-fold increase in merlin phosphorylation approximately) and this transient phosphorylation of Merlin gradually increases until in a linear fashion until it reaches peak phosphorylation at 30 minutes approximately 2.2 fold increases.
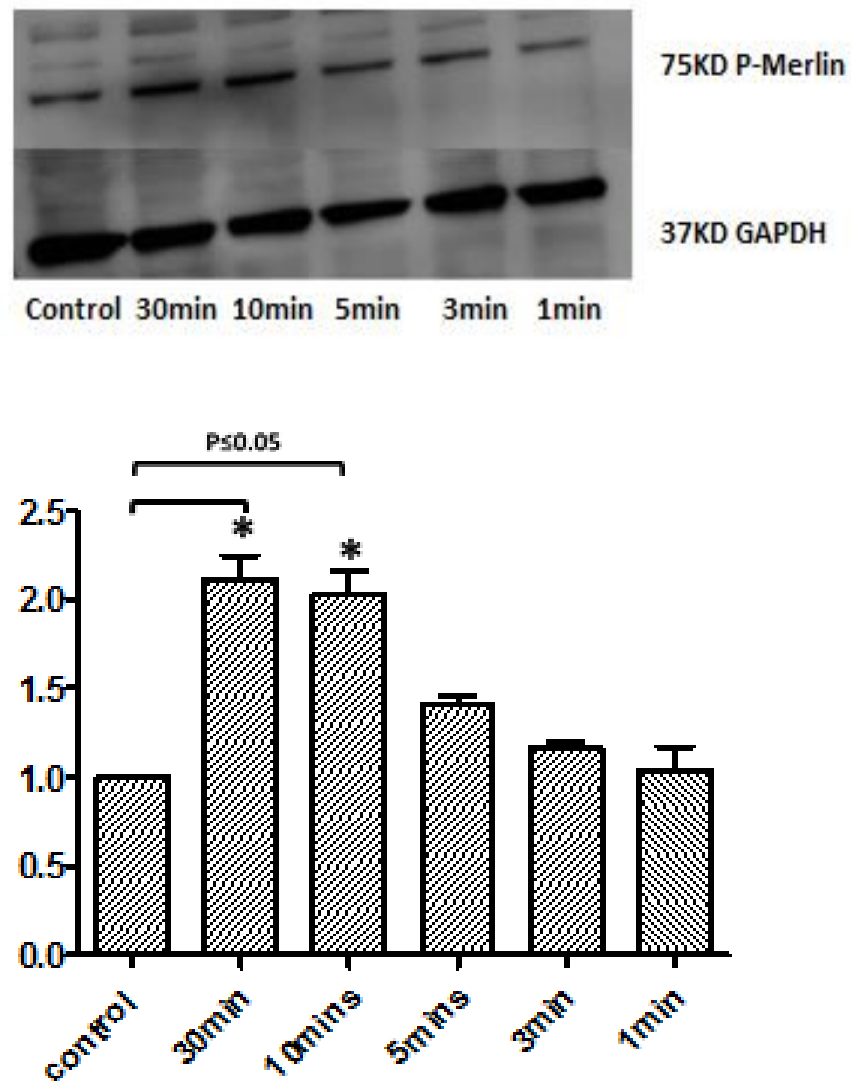
Fig 5.13: **The effect of D2A peptides on Phospho-Merlin expression.**

HAECs were seeded into 6-well plates at a density of 10^5 cells per cm^2, and allowed to adhere and grow to confluence over a 24 hour time frame. The cells were then exposed to 1 nM D2A for the times stated above. The effect of D2A peptides on phospho-merlin state was then monitored by Western blot. Histograms represent fold change in band intensity relative to untreated control. Results are averaged from three independent experiments $\pm$SEM; *P$\leqslant$0.05 vs control.

5.2.13 The effect of SRSRY peptides on merlin phosphorylation.

Again, to study the effect of SRSRY peptides on merlin phosphorylation, HAECs were seeded into 6-well plates at a density of 10^5 cells per cm^2 and allowed to adhere and grow to confluence over 24 hour time frame. The cells were then exposed to 100nM SRSRY at time intervals of 1, 3, 5, 10, 30 minute. Untreated HACEs were used as control. The cells were then lysed and analyzed by Western blot. Results indicate that Merlin phosphorylation is increased; starting at the 1 minute time point (approximately 0.2-fold increase) and this phosphorylation of Merlin gradually increases, reaching a maximum at the 10 minutes (approximately 1.65-fold increase). Then decrease slightly at the 30 minute time point (about 1.6 fold increase).
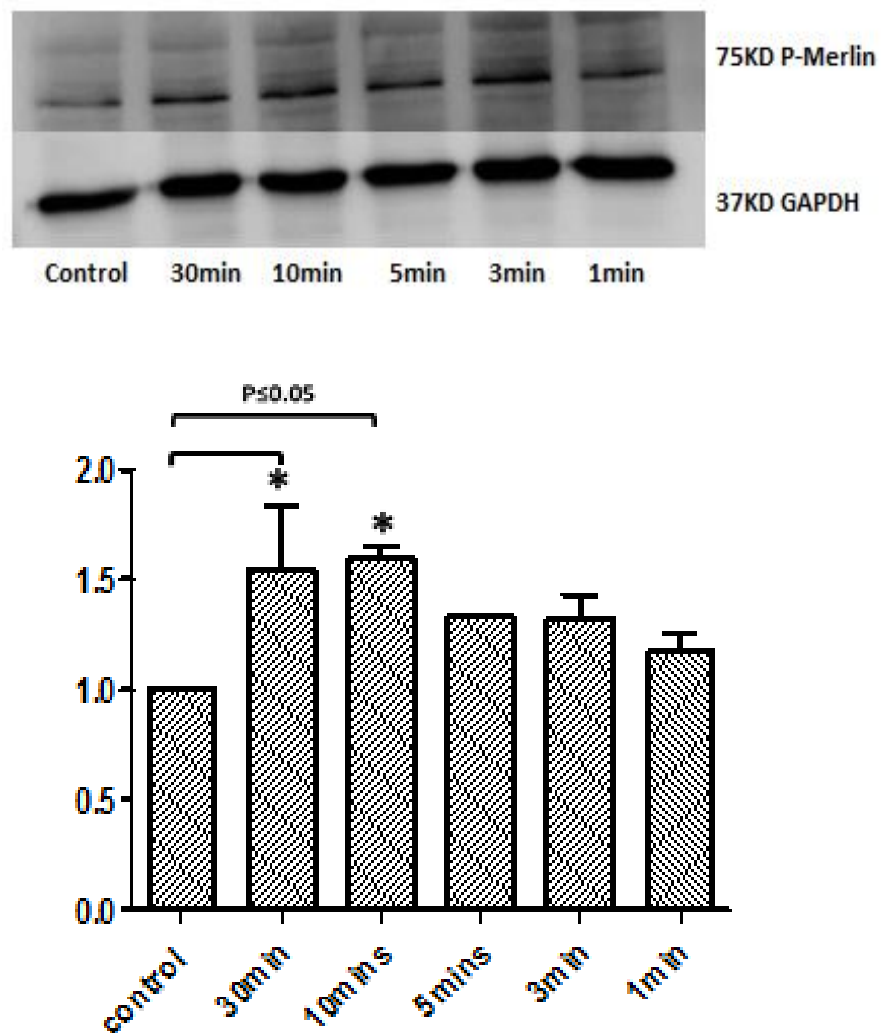
Fig 5.14:   The effect of SRSRY peptides on merlin phosphorylation.

HAECs were seeded into 6-well plates at a density of 10^5 cells per cm^2 and allowed to adhere and grow to confluence over 24 hours.   Cells were then treated with 100 nM SRSRY for the times outlined. The effect of SRSRY peptides on merlin phosphorylation state was then monitored by Western blot.   Histograms represent fold change in band intensity relative to untreated control. Results are averaged from three independent experiments $\pm$ SEM; *P$\leqslant$ 0.05 vs control.

5.3 Discussion

From the previous chapter, it can be seen that Merlin knock-down HAECs preferentially adhered to VN and FN. Both of these ECM contain a RGD sequence, which selectively interacts with specific integrins heterodimers, such as αvβ3 (for the comprehensive list of FN and VN binding integrins please check table 5.2). To elucidate the effect of various RGD peptides, each with specificity for different classes of integrins, on HAEC adhesion, a real time cell monitoring system, based on electrical impedance-xCELLigence system- was established. This allowed the dynamic monitoring of both cell adhesion and migrations over time, without the need for end-/fixed-point analysis. This allowed us to precisely monitor the rate and extent of adhesion and migration, something with is difficult to analyses with static standard assays. By investigating these cellular functions in real-time with three different, well characterized RGD peptide (for details please check Table 2.6), we were able to decipher the class of integrins involved and their overall contribution to the cellular dynamic. RGD1 inhibitor prevents both vitronectin and fibronectin mediated integrin adhesion and outside-in signaling (Pytela, et al. 1986) (Leptin 1986) (Yelian, et al. 1993), RGD2 inhibitor prevents fibronectin mediated integrin activation (Jester, et al. 1999) (Wu, Ustinova and Granger 2001), while RGD3 blocks vitronectin mediated integrin activation (J.E.Mogford et al, 1996. K.J.Bayless et al, 2000).

Results illustrated that in comparison with untreated controls; RGD1and RGD3 inhibitors significantly decreased wild type HAEC adhesion, while only a slight reduction of HAECs adhesion was observed with the use of RGD2 mediated inhibition. This finding leads to the conclusion that integrin-mediated signaling is crucial for the regulation of EC motility. The role of integrin in cell migration is well characterized elsewhere in literature (Moissoglu and Schwartz 2006). Cell

migration requires the attachment of cell surface to ECM which is mediated by many cell surface adhesion receptors including integrins, adhererins, cell adhesion molecules, syndecans and other proteoglycans. Among these receptors, integrins are is the most well studied and best characterized due to their importance in a multitude of cellular functions. Integrins contribute to cell adhesion and migration in multiple ways. The interaction between integrins and ECM can be modulated by intracellular signal which is termed "in-side out" and in turn activated integrins alter focal adhesion complex and induce intracellular signaling cascade which is called "out-side in" integrin signal. Integrins also serve as linkers that connect cytoskeleton to the ECM. Integrins are heterodimers which comprised of alpha (α) subunits and beta (β) subunits. Up to date, 24 integrins have been identified in human. Expression of integrins is in tissue specific manner. Many integrins such as αvβ3, β1, α5β1 and α6β4, play a center role in regulating endothelial integrity as well as vasculogenesis and angiogenesis (Weis 2007). Vasculogenesis is completely rely on FN mediated activation of α5β1 (Astrof and Hynes 2009). Studies also demonstrated that α5β1 is critical during vascular morphogenesis in mice with a FN dependent manner (Carlson, et al. 2008). Concentrated αvβ3 was observed at sites of wound healing and tumor growth which indicate its important role during pathologic vascularization (Brooks, Clark and Cheresh 1994b).

Furthermore, these results have also shown that this integrin mediated HAEC cell adhesion and migration is principally through the interaction with vitronectin. Many integrins have been identified interact with vitronectin, list of these integrins can be found in Table 5.1. Among these integrins, αvβ3 is endogenously expressed in endothelial cells and is involved in pathologic vascularization as mentioned above. Vitronectin is found in many connective tissues, and is involved in many physiological and pathological processes such as angiogenesis (Brooks, Clark and Cheresh 1994a) (Brooks, et al. 1995), hemostasis (Mohri and Ohkubo 1991)

(Thiagarajan and Kelly 1988) and metastasis (Juliano and Varner 1993) (Nip, et al. 1992). As a member of ECM family, vitronectin not only interacts with integrins, but also has an ability to bind uPAR (Madsen and Sidenius 2008). Studies show that uPAR is not essential in Vitronectin (VN) induces cell migration but the interaction between uPAR and integrin promote its ability to bind Vitronectin (Wei, et al. 2011). It is well known that VN increase migration by interacting with integrin αvβ3, and many studies have illustrated that uPAR also regulate cell migration and adhesion through laterally interacting with αvβ3 (Waltz and Chapman 1994) (Wei, et al. 1994) (Ossowski and Aguirre-Ghiso 2000b).

Table 5.1 The list of FN and VN binding integrins

ECM	Integrins
FN	αIIbβ3, α5β1, α8β1, αvβ1, αvβ3, αvβ6, α4β1, α4β7, αDβ2, αMβ2, αxβ2,
VN	αvβ3, αIIbβ3, α8β1, αvβ1, αvβ5, αvβ8

(Lowell and Mayadas 2012)

As uPAR only contains extracellular domains, it must transduce cellular signals across the cell membrane and into the cell through various, dynamic interactions with other cell membrane receptors. A wide range of cell membrane receptors have been identified to interact with uPAR, including integrin, G-protein coupled receptors and LDL-receptor related proteins (Resnati, et al. 1996) (Ossowski and Aguirre-Ghiso 2000a). The uPAR-integrin signaling nexus has been well studied and is well characterized. However, our picture and understanding of such interactions, and their subsequent role in cell fate decisions and functions is far from complete, warranting further expensive investigation. Indeed, these uPAR-integrin associations may be a novel therapeutic in various pathological states such as cancer, inflammation and vascular disease. A wide range of integrins have been reported

to interact with uPAR, e.g. α3β1, αmβ2, αvβ3 and α5β1 (Wei, et al. 1996) (Wei, Y. et al 2001) (Simon, et al. 2000). uPAR is suggested as a modulator in integrin mediated pathway (Xue, et al. 1997). *Wei, Y. et al,* demonstrated the direct binding of uPAR and α5β1, rather than blocking or renders fibronectin (Fn) binding by α5β1 Arg-Gly-Asp (RGD) resistant (Wei, et al. 2005). The binding sites of α5β1 and α3β1 locate at D3 domain (Wei, et al. 2005) (Simon, et al. 2000), while D2 region is corresponding binding site for αvβ3 (Degryse, et al. 2005b). The affinity of α5β1 to FN was enhanced when uPAR was introduced (Leiss, et al. 2008). Co-immunoprecipitates reveal the interaction between αvβ3 integrin and uPAR in podocytes (Wei, et al. 2007a) and activation of uPAR leading to expression of αvβ3 integrin at tumour cell surface (Schiller, et al. 2009). Similarly, uAPR expressions induced by treatment with lipopolysaccharide promote activation of αvβ3 in mouse kidney podocytes (Wei, et al. 2007b). All the evidences implicate the essential role of uPAR in integrins mediated cellular singling.

In this chapter, we therefore focus on investigating whether integrins were involved in uPAR-mediated HAEC migration, and if so what classes of integrins were involved and what were their overall contribution to this important cellular function. In order to study the effect of specific RGD inhibitors on uPA mediated HAEC adhesion, urokinase, and two peptides; D2A and SRSRY were utilized. Sensitive and responsive to a plethora of enzymes, including uPA, plasmin, metalloproteases, and trypsin, uPAR can be truncated into soluble forms, for example; c-uPAR is a soluble form of uPAR (minus the D1 domain). C-uPAR possesses potent and immediate chemotactic properties, and Fazioli, F *et al.,* discovered that the chemotactic activity attributed to the D2D3 domain did not require of uPA-uPAR interaction in uPA-/- mice (Fazioli, et al. 1997). Generation of shorter domain peptides facilitated the study of the specific binding properties of uPAR. D2A was first synthesized by Bernard Degryse and his collegues (Degryse, et al. 2005) (Kamikubo, Neels and

Degryse 2009). Derived from the sequence of Domain 2, D2A peptides have been shown to interact laterally with αvβ3 integrin and induce cell migration *via* outside-in signaling. SRSRY (Ser-Arg-Ser-Arg-Tyr) is another chemotactic peptide, derived from an uPAR sequence, which localized in the D1-D2 linker region. SRSRY peptides bind specifically to fMLP- a seven-transmembrane domain G-coupled receptor, and have been demonstrated to promote cell migration in this manner *(*Gargiulo, et al. 2005). From the results we can see that EC adhesion was increased with treatment of urokinase and D2A peptide but no significant increase was observed upon treatment with SRSRY peptide. This indicates that uPAR regulate HAEC migration through the interaction with integrins rather than fMLP. And again, αvβ3 has been demonstrated to play a major role in this process.

From above studies, we conclude that uPAR transduce cell signals through integrin mediated pathways. We then wanted to investigate if merlin is involved in this mechanism. To illustrate the role of merlin in the regulation of HAEC migration, the adhesion and migration experiments highlighted at the beginning of this chapter were repeated, but this time using siRNA mediated merlin knock-down in HAEC cells. The transfection and knock-down efficiency was evaluated using western blot to ensure a minimum 70 to 80% reduction of merlin for each experiment. The HAECs transfected with scrambled control siRNA were used as control, as well as untransfected cells. Both merlin knock-down and scrambled control HAECs were then seeded into E-plates for adhesion assay or CIM-plates for migration assay which were pre-treated with either RGD inhibitors (RGD1, 2 and 3). From the results obtained, similar data were achieved as in chapter 4, i.e. HAEC adhesion and migration are significantly increased in the absence of merlin. The treatment use of RGD1 and RGD2 inhibits both HAEC's adhesion and migration dramatically. The inhibitory effect of RGD peptides on HAEC-matrix interactions are significantly attenuated when merlin is knocked-down in the cell. This finding concludes that

merlin is critical component in regulation of HAECs adhesion and migration. And also merlin regulates HAECs adhesion and migration via vitronectin interacting integrins. The comprehensive list of the RGD binding integrins is shown below (table 5.2). Among these integrins, only $\alpha v\beta 3$, $\alpha IIb\beta 3$, $\alpha 8\beta 1$, $\alpha v\beta 1$, $\alpha v\beta 5$, $\alpha v\beta 8$ have demonstrated interact with vitronectin and furthermore, $\alpha v\beta 3$ and $\alpha IIb\beta 3$ are the only two endogenously express in endothelial cells. Combine with our previous results; we conclude that merlin regulates HAECs adhesion and migration via vitronectin interacting integrins-$\alpha v\beta 3$. HAECs adhesion and migration are significantly increased when merlin was knocked-down. The use of RGD1 and RGD2 greatly inhibits both HAEC adhesion and migration dramatically. However the treatment of RGD2 only affects HAEC's adhesion and no any inhibition on HAEC's migration was observed. This may due to technical problem or degradation of RGD2 inhibitor after long term exposure to warm atmosphere. The inhibition of RGDs on HAECs motilities are significantly reduced when merlin was knocked-down. This finding concludes that merlin is critical component in regulation of HAECs adhesion and migration.   And also merlin regulates HAECs adhesion and migration via Fibronectin interacting integrin such as $\alpha v\beta 3$.

Table 5.2 The RGD binding integrins

Integrins	Ligands	Primary sites of expression
αIIbβ3	Fibrinogen, thromobospondin, fibronectin, vitronectin, vWF, Cyr61, ICAM-4, CD40L	Platelets
α5β1	Fibronectin, osteopontin, fibrillin, thrombospondin, ADAM, COMP	Blood vessels (embryonic)
α8β1	Tenascin, fibronectin, osteoponitin, vitronectin, latent TGFβ, nephronectin	Kidney, inner ear
αvβ1	Latent TGFβ, fibronectin, osteopontin, vitronectin	Poorly defined
αvβ3	Fibrinogen, vitronectin, fibronectin, vWF, thrombospondin, fibrillin, tenascin, PECAM-1, osteopontin, ADAM, Cyr61, MMP, uPAR, uPA, ICAM-4	Osteoclasts, vascular endothelium
αvβ5	Osteopontin, vitronectin, latent TGFβ	Eye, bone
αvβ6	Latent TGFβ, fibronectin, osteopontin, ADAM	Skin, lung
αvβ8	Latent TGFβ, vitronectin	Vascular endothelium

(Lowell and Mayadas 2012)

In this chapter, we have already demonstrated that uPAR is critical in regulation of HAEC adhesion and migration *via* integrins specifically αvβ3 mediated signaling. In addition, we have illustrated that merlin is involved in this integrin mediated cell signaling pathway. Moreover, in this study, we wanted to further investigate if the activation of αvβ3 and fMLP by uPA derived peptides will directly modulate merlin phosphorylation state. In this study, HAECs were treated with chemotactic peptides D2A and SRSRY (the details of these peptides are described above) respectively. These experiments need to be performed on 6 well plates which allow us achieve significant amount of cell lysate. Due to the very high molecular weight of uPA, the

investigation of effect of uPA on merlin phosphorylation state in HAEC requires large volume of uPA. We could not afford the cost and the uPA activate uPAR is well documented somewhere else. Therefore we did not exam the effect of uPA on merlin phosphorylation. In brief, at defined points over a time-course (1, 3, 5, 10, 30 minutes), HAECs were lysed and merlin phosphorylation states were monitored using western blot. The results indicated that merlin was acutely phosphorylated when treated with D2A and SRSRY (the phosphorylation occurs as early as 1-3minute), and this phosphorylation process was transit for it reach its peak time for 10 minute for SRSRY, and 30 minute for D2A.

As I mentioned in section 1.6.2, uPAR can be activated by many extracellular matrices, such as vitronectin, which in turn promote cell motility and proliferation. As a protease, uPAR is responsible for converting pro-urokinase into urokinase and activate plasminogen to produce plasmin. Both of these enzymes are required in proteolysis which is essential mechanisms to release the attachment of migrating cell from ECM. Many extracellular cues stimulate HAECs motility including haemodynamic forces and exposure to ECM. D2A and SRSRY peptide derived from uPAR which representing the binding site of $\alpha v \beta 3$ and fMLP. The treatments of these peptides mimic the interaction of $\alpha v \beta 3$ and fMLP to uPAR which in turn activate downstream signaling cascade and promote cell motility. Both activation of $\alpha v \beta 3$ by either haemodynamic forces (see the results from chapter 3) or D2A, in turn increase the state of merlin phosphorylation which inactive its HAEC motility suppressor function. We observed that the fMLP activating peptide SRSRY which has no significant effect on HAEC motility (this results were observed at 30 minutes upto 10 hours base) also increase merlin phosphorylation state. Compared with D2A induced merlin phosphorylation state (approximately 2.2 fold increase), SRSRY promote only 1.65 fold increase of merlin phosphorylation at 10 minute time point and the effect decreased to 1.6 fold when time reach 30 minute. Which may indicate

SRSRY activation may only transiently affect HAEC motility but has no effect on long term regulation.

In summary, from our studies, we concluded that Merlin is endogenously expressed in HAECs, and is highly responsive to mechanical stimuli. As linker between actin cytoskeleton and the plasma membrane, Merlin regulates cell motilities through uPAR and integrin interaction signaling pathways. Merlin is localized predominantly at functional sites of stress fibers, filopodia, lamellipodia and focal adhesions. Through exposure to haemodynamic force or other activating factors, such as D2A and SRSRY, HAECs are able to sense environmental changes via cell surface receptors, including uPAR and integrin, and transduce the signal inside cell. This, in turn, serves to either suppress Merlin expression, or increase Merlin phosphorylation. Loss of Merlin activity results in the freeing of integrin binding sites that promote interaction between integrin and the integrin–actin linkage proteins (including talin, vinculin, Kindlins and α-actinin). This infers a role of merlin being a competitive inhibitor of integrin activation. Rac, CDC42 and Rho pathways are then activated following binding of the above proteins to integrins, which in turn leads to formation of various functional migration structures, such as filopodia, lamellipodia and stress fiber (figure 6.1).

Chapter 6:

Summary and Future Direction

6.1 Final Summary

Atherosclerosis is described as a slowly formation and progression of plaque within blood vessel which leading to narrowing and hardening the vessel wall. The causes of atherosclerosis are complicate. Hyperlipidaemia, especially high plasma concentrations of low-density lipoprotein (LDL) cholesterol, is one of the major causes of the disease. However some scientist believe atherosclerosis is an inflammatory disease due to the improvement of new therapeutic approach and change in life style to lower plasma cholesterol seem have no effect on the death toll (Ross R. 1999).

Atherosclerosis normally occur at large and medium-sized muscular elastic arteries; the aorta, coronary and cerebra, especially at the site of arterial bifurcation and regions of high curvature that results in complex blood flow patterns (Hahn and Schwartz, 2009; Lusis, 2000). At such sites, disturbed blood flow occurs and leads to formation of atherosclerotic plaques which in turn narrow the blood vessel and cause luminal occlusion or even wall rupture at advanced stages (Lusis, 2000; Orr et al., 2006). As the inner layer of blood vessel, endothelial cells play a crucial role in control vascular functions including the control of vascular tone, endothelium permeability, endothelial cell adhesion, migration and proliferation. Blood flow itself exist a strong biomechanical influence on the vessel wall. Sensing to these haemodynamic forces, endothelial cell constantly undergo adaptation to maintain homeostasis. Some paper described that EC elongate at the direction of blood flow (Cines et al, 1998: Gimbrone, 1987). EC morphology is maintained by actin cytoskeleton. Actin polymerization is a complex process that plays an important role in maintaining endothelial integrity. This process requires the recruitment of numerous actin adaptor proteins.

In this thesis, we examed the role of the actin adaptor protein merlin and its impact on endothelial cell-matrix adhesion and migration. We initially investigated the effect of shear stress on HAEC morphology, and ascertained if the expression and regulatory profile of Merlin is affected by hemodynamic forces, including shear stress and cyclic strain. The results clearly showed realignment of HAECs in the direction of flow when comparing static controls to LSS. Moreover, no uniform realignment was observed under DSS at regions of bifurcations and curvature. The results have also shown that Merlin was highly responsive to mechanical stimuli in HAECs. By using fluorescence microscopy, we observed Merlin association with dynamic actin at many functional sites, such as those at stress fibres, focal adhesions, and at sites of cell-cell contact. Merlin association was particularly apparent at the leading cell edge in lamellipodial regions, indicative of *de novo* integrin activation and attachment to the ECM.

Studies then focused on the role, and possible regulatory mechanism, of Merlin on cell-matrix adhesion and migration. We first investigated Merlin binding partners using CO-IP and proteomic analysis. Our results unveiled a number of merlin-interacting proteins, including tubulin, annexin, actin transferrin receptor protein 1, annexin A2 and myosin light chain 6B. By using siRNA-mediated knock-down, several experiments were undertaken to evaluate the effects of knock-down merlin expression in HAEC cell-matrix adhesion. Results indicate that relative to scrambled controls, in merlin knock-down HAECs, cell-matrix adhesion was greatly increased and merlin knock-down HAECs preferentially adhered to vitronectin and fibronectin compared to laminin and fibrinogen. Parallel investigations for HAEC migration were carried out under identical conditions. Merlin knock-down results indicated that relative to scrambled controls, absence of merlin greatly increased HAEC migration. Merlin knock-down HAECs were also exposed to various haemodynamic forces, including shear stress and cyclic strain, to further elucidate the effect of these forces on merlin knock-down HAEC motility.

Results indicated that both forms of haemodynamic force significantly increased HAEC motility. Furthermore, these effects were greatly enhanced by knock-down of Merlin. In this regard, it was proposed that prolonged exposure to hemodynamic force would alter HAEC functions, such as motility, through down-regulating merlin.

The above studies demonstrated that Merlin plays a pivotal role in cell motility - especially in cell-ECM adhesion and migration. Additionally, Merlin knock-down HAECs preferentially adhered to vitronectin and fibronectin. Both of these ECMs contain a RGD sequence that selectively activates specific integrins, such as $\alpha v \beta 3$. In order to determine and elucidate the mechanism of integrin-mediated HAEC adhesion, and to identify the specific integrin involved, three well characterised RGD inhibitors were introduced. RGD1 inhibitor prevents both vitronectin and fibronectin-mediated integrin activation. RGD2 inhibitor prevents fibronectin-mediated integrin activation only, and RGD3 specifically blocks vitronectin-mediated integrin activation. Experimental results illustrated that compared with untreated controls, RGD1 and RGD3 inhibitors significantly decreased wild type HAEC adhesion, while only a slight reduction in RGD2-mediated inhibition of HAECs adhesion was noted. These findings led to the conclusion that integrin-mediated signalling is crucial for regulation of endothelial cell motility and the role of integrins in cell migration.

Furthermore, results have also demonstrated that this integrin-mediated cell adhesion and migration is achieved through binding with vitronectin. As a member of the ECM family, vitronectin not only interacts with integrins, but also has the ability to bind with uPAR. As uPAR contains only extracellular domains, it must transduce cellular signals by interacting with other cell membrane receptors, such as $\alpha v \beta 3$. In order to elucidate the effect of RGD inhibitors on uPA-mediated HAEC

adhesion, urokinase and two peptides (D2A and SRSRY) were introduced. Derived from the sequence of domain 2 of uPAR, D2A peptides interact laterally with αvβ3 integrin and induce cell migration. SRSRY (Ser-Arg-Ser-Arg-Tyr) is another chemotactic uPAR derived sequence located in the D1-D2 linker region. SRSRY peptides bind specifically to fMLP, a seven transmembrane domain G-coupled receptor, and promote cell migration. Experimental data illustrated that endothelial motility increased with treatment of urokinase and D2A peptide. However, no significant increase was observed when treated with SRSRY peptide (figure 5.2-figure 5.4). This indicated that uPAR serves to regulate HAEC motility through interaction with integrins, rather than fMLP. Additionally, data pointed to αvβ3 as the major integrin involved in this pathway.

From above studies, we concluded that uPAR transduces cell signals through the integrin pathway. The investigation then turned to Merlin, to determine its involvement in the mechanism. In order to illustrate the role of Merlin in the regulation of HAEC motility, Merlin knock-down was achieved by transfection with siRNA. HAECs transfected with scrambled control siRNA were used as controls. Both Merlin-absent and scrambled control HAECs were then seeded into xCELLigence E-plates for adhesion assays or CIM-plates for migration assays, pre-treated with either RGD inhibitors (RGD1, 2 and 3). From the results, it was observed that HAEC motility- both adhesion and migration - were significantly increased after knock-down of Merlin. Treatment with RGD1 and RGD2 inhibited both HAEC adhesion and migration dramatically. However, treatment with RGD2 only affected HAEC adhesion, with no inhibition of HAEC migration observed. Inhibition of HAEC motility, using specific RGD inhibitors, was significantly abrogated with knock-down of Merlin. Thus, the conclusion of these findings was that Merlin is critical component in regulation of HAEC adhesion and migration. Moreover, it was determined that Merlin serves to regulate HAEC adhesion and migration via vitronectin-interacting integrins. Integrins including αvβ3, αIIbβ3,

241

α8β1, αvβ1, αvβ5, αvβ8, have demonstrated interact with vitronectin and furthermore, αvβ3 and αIIbβ3 are the only two endogenously express in endothelial cells. Combine with our previous results; we conclude that merlin regulates HAECs adhesion and migration via vitronectin interacting integrins-αvβ3.

In the last section, we demonstrated that Merlin was acutely phosphorylated when exposed to D2A and SRSRY (with phosphorylation beginning after 1-3 mins). This phosphorylation process was transit for it reaches its peak time for 10 min for SRSRY, and 30 mins for D2A.

In summary, from our studies, we concluded that Merlin is endogenously expressed in HAECs, and is highly responsive to mechanical stimuli. As linker between actin cytoskeleton and the plasma membrane, Merlin regulates cell motilities through uPAR and integrin interaction signalling pathways. Merlin is localised predominantly at functional sites of stress fibres, filopodia, lamellipodia and focal adhesions. Through exposure to haemodynamic force or other activating factors, such as D2A and SRSRY, HAECs are able to sense environmental changes via cell surface receptors, including uPAR and integrin, and transduce the signal inside cell. This, in turn, serves to either suppress Merlin expression, or increase Merlin phosphorylation. Loss of Merlin activity results in the freeing of integrin binding sites that promote interaction between integrin and the integrin–actin linkage proteins (including talin, vinculin, Kindlins and α-actinin). This highlights the role of merlin being a competitive inhibitor of integrin activation. Rac, CDC42 and Rho pathways are then activated following binding of the above proteins to integrins, which in turn leads to formation of various functional migration structures, such as filopodia, lamellipodia and stress fibre (figure 6.1).
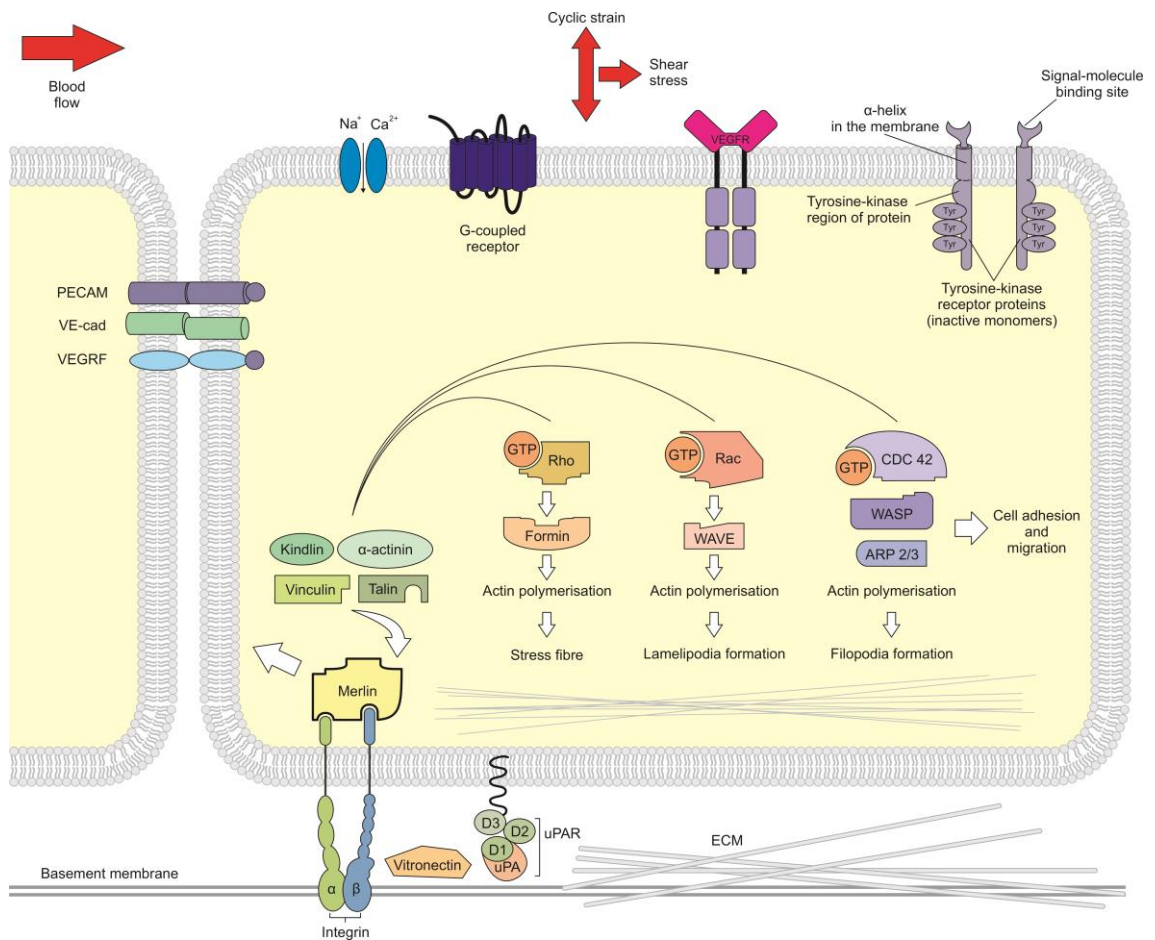
Figure 6.1 The critical role of merlin in uPAR mediated motility regulation

Through exposure to haemodynamic force or other activating factors, such as D2A and SRSRY, HAECs are able to sense environmental changes via cell surface receptors, including uPAR, integrin, ions channel, G-coupled receptor, VEGFR, TKR and transduce the signal inside cell. This, in turn, serves to either suppress Merlin expression, or increase Merlin phosphorylation. Loss of Merlin activity results in the freeing of integrin binding sites that promote interaction between integrin and the integrin–actin linkage proteins (including talin, vinculin, Kindlins and α-actinin). Rac, CDC42 and Rho pathways are then activated following the binding of these proteins to integrin, which in turn leads to the formation of various functional migration structures, such as filopodia, lamellipodia and stress fibres.

6.2 Future Directions

This thesis examined the role of the cell membrane and cytoskeleton linker protein, Merlin, on endothelial cell-matrix adhesion and migration within vasculature. We observed that Merlin expression, both at protein and mRNA levels, is altered by haemodynamic force, including cyclic strain and laminar shear stress. Interestingly, it was found that mRNA levels increased with both shear stress and cyclic strain, and did not correspond to Merlin protein expression. This phenomenon was also observed in previous studies in our lab while studying the protein, moesin, under the same conditions. This may, therefore, be indicative of the fact that Merlin mRNA is regulated by splicing, mediated through the RNA interference (RNAi) pathway. This pathway mainly involves microRNA. MicroRNA (short non-coding single strand RNA molecules, normally 19-25 nucleotides long), was discovered by Lee et al in 1993 during studies on the nematode, Caenorhabditis elegans (C. elegans), (Lee, Feinbaum and Ambros 1993). It is involved in many different biological processes, such as gene silencing (Bartel 2009). Intensive studies have shown that microRNAs are involved in cardiac development and cardiovascular functions, well described in Eric M. Small and Eric N. Olson's review (Small and Olson 2011). Saydam O, et al have also demonstrated the role of miR-7's tumour suppressor function in schwannomas (Saydam, et al. 2011). However, the role of microRNA in controlling Merlin function in ECs remains poorly understood, and forms the basis of future investigations to be carried out.

Currently, over 30 proteins have been identified that interact with Merlin (list of merlin binding proteins please see Table 4.3). Each of these interacting proteins critically regulates merlin structure and function. For example, merlin may be phosphorylated at serine 518 by interacting with p21-activated kinases (PAKs). Merlin has been identified as being involved in numerous signalling pathways, and

results in this thesis clearly demonstrate the important role of Merlin in HAEC motility regulation. In the future, more research based on CO-IP will be carried under different conditions, including under various haemodynamic conditions and knock-down and over-expression of Merlin. Interacting proteins may reveal potential pathways that regulate cell motility.

Our studies have also clearly shown Merlin association with dynamic actin at many functional sites, such as stress fibres, focal adhesions, at sites of cell-cell contact and, in particular, the leading cell edge in lamellipodial regions. We have hypothesised that the loss of Merlin activity results in freeing of integrin-binding sites that promote interaction between integrin and the integrin–actin linker proteins. These include talin, vinculin, kindlins and α-actinin. Investigating the co-localisation of Merlin and these integrin-binding proteins using confocal microscopy, would greatly enhance our knowledge of the dynamics of integrin activation, particularly the events around the cytoplasmic tails. In this study, the Ibidi® flow system would also be used to explore the effects of mechano-regulation on integrin-binding proteins under various conditions, such as over-express and knock-down of Merlin. Furthermore, the role of different ECMs on Merlin localisation will be investigated.

Bibliography

Abercrombie, M. 1980. The Croonian lecture, 1978: the crawling movement of metazoan cells. *Proceedings of the Royal Society of London.Series B, Biological Sciences,* pp.129-147.

Ahmed, N., Pansino, F., Clyde, R., Murthi, P., Quinn, M., Rice, G., Agrez, M., Mok, S. and Baker, M. 2002. Overexpression of αvβ6 integrin in serous epithelial ovarian cancer regulates extracellular matrix degradation via the plasminogen activation cascade. *Carcinogenesis,* 23(2), pp.237-244.

Aird, W.C. 2007. Phenotypic heterogeneity of the endothelium I. Structure, function, and mechanisms. *Circulation Research,* 100(2), pp.158-173.

Alfano, M., Sidenius, N., Panzeri, B., Blasi, F. and Poli, G. 2002. Urokinase–urokinase receptor interaction mediates an inhibitory signal for HIV-1 replication. *Proceedings of the National Academy of Sciences,* 99(13), pp.8862-8867.

Allender, S., Scarborough, P., Peto, V., Rayner, M., Leal, J., Luengo-Fernandez, R. and Gray, A. 2008. European cardiovascular disease statistics. *European Heart Network,* 3pp.11-35.

Allison L. Berrier, and Kenneth M. yamada, 2007. Cell–Matrix Adhesion. J. Cell. Physiol. 213: 565–573, 2007.

Ambrose, J.A., Tannenbaum, M.A., Alexopoulos, D., Hjemdahl-Monsen, C.E., Leavy, J., Weiss, M., Borrico, S., Gorlin, R. and Fuster, V. 1988. Angiographic progression of coronary artery disease and the development of myocardial infarction. *Journal of the American College of Cardiology,* 12(1), pp.56-62.

Aoki, T., Wood, H., Old, L. and Boyse, E. 1969. Arterial wall shear and distribution of early atheroma in man. *Nature,* 223(1), pp.159.

Arroyo, L.H. and Lee, R.T. 1999. Mechanisms of plaque rupture mechanical and biologic interactions. *Cardiovascular Research,* 41(2), pp.369-375.

Astrof, S. and Hynes, R.O. 2009. Fibronectins in vascular morphogenesis. *Angiogenesis,* 12(2), pp.165-175.

Ballestrem, C., Hinz, B., Imhof, B.A. and Wehrle-Haller, B. 2001. Marching at the front and dragging behind differential αVβ3-integrin turnover regulates focal adhesion behavior. *The Journal of Cell Biology,* 155(7), pp.1319-1332.

Barakat, A., Leaver, E., Pappone, P. and Davies, P. 1999. A flow-activated chloride-selective membrane current in vascular endothelial cells. *Circulation Research,* 85(9), pp.820-828.

Bartel, D.P. 2009. MicroRNAs: target recognition and regulatory functions. *Cell,* 136(2), pp.215-233.

Bashour, A., Meng, J., Ip, W., MacCollin, M. and Ratner, N. 2002. The neurofibromatosis type 2 gene product, merlin, reverses the F-actin cytoskeletal defects in primary human Schwannoma cells. *Molecular and Cellular Biology,* 22(4), pp.1150-1157.

Berk, B.C., Fujiwara, K. and Lehoux, S. 2007. ECM remodeling in hypertensive heart disease. *Journal of Clinical Investigation,* 117(3), pp.568-575.

Berryman, M., Gary, R. and Bretscher, A. 1995. Ezrin oligomers are major cytoskeletal components of placental microvilli: a proposal for their involvement in cortical morphogenesis. *The Journal of Cell Biology,* 131(5), pp.1231-1242.

Berthiaume, F. and Frangos, J.A. 1992. Flow-induced prostacyclin production is mediated by a pertussis toxin-sensitive G protein. *FEBS Letters,* 308(3), pp.277-279.

Bianchi, A.B., Hara, T., Ramesh, V., Gao, J., Klein-Szanto, A.J., Morin, F., Menon, A.G., Trofatter, J.A., Gusella, J.F. and Seizinger, B.R. 1994. Mutations in transcript isoforms of the neurofibromatosis 2 gene in multiple human tumour types. *Nature Genetics,* 6(2), pp.185-192.

Binder, B.R., Mihaly, J. and Prager, G.W. 2007. uPAR-uPA-PAI-1 interactions and signaling: a vascular biologist's view. *THROMBOSIS AND HAEMOSTASIS-STUTTGART-,* 97(3), pp.336.

Blasi, F. 1997. uPA, uPAR, PAI-I: Key intersection of proteolytic, adhesive and chemotacfic highways? *Immunology Today,* 18(9), pp.415-417.

Blasi, F. and Carmeliet, P. 2002. uPAR: a versatile signalling orchestrator. *Nature Reviews Molecular Cell Biology,* 3(12), pp.932-943.

Blessing, C.A., Ugrinova, G.T. and Goodson, H.V. 2004. Actin and ARPs: action in the nucleus. *Trends in Cell Biology,* 14(8), pp.435-442.

Bonilha, V.L., Rayborn, M.E., Saotome, I., McClatchey, A.I. and Hollyfield, J.G. 2006. Microvilli defects in retinas of ezrin knockout mice. *Experimental Eye Research,* 82(4), pp.720-729.

Brakebusch, C., Bouvard, D., Stanchi, F., Sakai, T. and Fässler, R. 2002. Integrins in invasive growth. *Journal of Clinical Investigation,* 109(8), pp.999-1006.

Bretscher, A., Edwards, K. and Fehon, R.G. 2002. ERM proteins and merlin: integrators at the cell cortex. *Nature Reviews Molecular Cell Biology,* 3(8), pp.586-599.

Brooks, P.C., Clark, R. and Cheresh, D.A. 1994. Requirement of vascular integrin alpha v beta 3 for angiogenesis. *Science,* 264(5158), pp.569-571.

Brooks, P.C., Strömblad, S., Klemke, R., Visscher, D., Sarkar, F.H. and Cheresh, D.A. 1995. Antiintegrin alpha v beta 3 blocks human breast cancer growth and angiogenesis in human skin. *Journal of Clinical Investigation,* 96(4), pp.1815.

Burridge, K. and Chrzanowska-Wodnicka, M. 1996. Focal adhesions, contractility, and signaling. *Annual Review of Cell and Developmental Biology,* 12(1), pp.463-519.

Burridge, K. and Wennerberg, K. 2004. Rho and Rac take center stage. *Cell,* 116(2), pp.167-179.

Calderwood, D.A. 2004. Integrin activation. *Journal of Cell Science,* 117(5), pp.657-666.

Carlier, M., Laurent, V., Santolini, J., Melki, R., Didry, D., Xia, G., Hong, Y., Chua, N. and Pantaloni, D. 1997. Actin depolymerizing factor (ADF/cofilin) enhances the rate of filament turnover: implication in actin-based motility. *The Journal of Cell Biology,* 136(6), pp.1307-1322.

Carlos, T.M. and Harlan, J.M. 1994. Leukocyte-endothelial adhesion molecules. *Blood,* 84(7), pp.2068-2101.

Carlson, T.R., Hu, H., Braren, R., Kim, Y.H. and Wang, R.A. 2008. Cell-autonomous requirement for β1 integrin in endothelial cell adhesion, migration and survival during angiogenesis in mice. *Development,* 135(12), pp.2193-2202.

Chapman, H.A. 1997. Plasminogen activators, integrins, and the coordinated regulation of cell adhesion and migration. *Current Opinion in Cell Biology,* 9(5), pp.714-724.

Chesarone, M.A. and Goode, B.L. 2009. Actin nucleation and elongation factors: mechanisms and interplay. *Current Opinion in Cell Biology,* 21(1), pp.28-37.

Chew, C.S., Chen, X., Parente, J.A., Tarrer, S., Okamoto, C. and Qin, H. 2002. Lasp-1 binds to non-muscle F-actin in vitro and is localized within multiple sites of dynamic actin assembly in vivo. *Journal of Cell Science,* 115(24), pp.4787-4799.

Chew, C.S., Parente, J., Chen, X., Chaponnier, C. and Cameron, R.S. 2000. The LIM and SH3 domain-containing protein, lasp-1, may link the cAMP signaling pathway with dynamic membrane restructuring activities in ion transporting epithelia. *Journal of Cell Science,* 113(11), pp.2035-2045.

Chew, C., Parente, J., Zhou, C., Baranco, E. and Chen, X. 1998. Lasp-1 is a regulated phosphoprotein within the cAMP signaling pathway in the gastric parietal cell. *American Journal of Physiology-Cell Physiology,* 275(1), pp.C56-C67.

Chien, S., Li, S. and Shyy, J.Y. 1998. Effects of mechanical forces on signal transduction and gene expression in endothelial cells. *Hypertension,* 31(1), pp.162-169.

Choi, C.K., Vicente-Manzanares, M., Zareno, J., Whitmore, L.A., Mogilner, A. and Horwitz, A.R. 2008. Actin and α-actinin orchestrate the assembly and maturation of nascent adhesions in a myosin II motor-independent manner. *Nature Cell Biology,* 10(9), pp.1039-1050.

Christofori, G. 2006. New signals from the invasive front. *Nature,* 441(7092), pp.444-450.

Ciambrone, G. and McKeown-Longo, P. 1992. Vitronectin regulates the synthesis and localization of urokinase-type plasminogen activator in HT-1080 cells. *Journal of Biological Chemistry,* 267(19), pp.13617-13622.

Cines, D.B., Pollak, E.S., Buck, C.A., Loscalzo, J., Zimmerman, G.A., McEver, R.P., Pober, J.S., Wick, T.M., Konkle, B.A. and Schwartz, B.S. 1998. Endothelial cells in physiology and in the pathophysiology of vascular disorders. *Blood,* 91(10), pp.3527-3561.

Cook, N.R., Cutler, J.A., Obarzanek, E., Buring, J.E., Rexrode, K.M., Kumanyika, S.K., Appel, L.J. and Whelton, P.K. 2007. Long term effects of dietary sodium reduction on cardiovascular disease outcomes: observational follow-up of the trials of hypertension prevention (TOHP). *Bmj,* 334(7599), pp.885.

Critchley, D.R. and Gingras, A.R. 2008. Talin at a glance. *Journal of Cell Science,* 121(9), pp.1345-1347.

Davies, P.F. and Tripathi, S. 1993. Mechanical stress mechanisms and the cell. An endothelial paradigm. *Circulation Research,* 72(2), pp.239-245.

Davignon, J. and Ganz, P. 2004. Role of endothelial dysfunction in atherosclerosis. *Circulation,* 109(23 suppl 1), pp.III-27-III-32.

De Caterina, R., Massaro, M. and Libby, P. 2007. Endothelial functions and dysfunctions. *Endothelial Dysfunctions in Vascular Disease,* pp.1-25.

Degryse, B., Resnati, M., Czekay, R., Loskutoff, D.J. and Blasi, F. 2005. Domain 2 of the urokinase receptor contains an Integrin-interacting epitope with intrinsic signaling activity generation of a new integrin inhibitor. *Journal of Biological Chemistry,* 280(26), pp.24792-24803.

Degryse, B., Resnati, M., Rabbani, S.A., Villa, A., Fazioli, F. and Blasi, F. 1999. Src-dependence and pertussis-toxin sensitivity of urokinase receptor-dependent chemotaxis and cytoskeleton reorganization in rat smooth muscle cells. *Blood,* 94(2), pp.649-662.

Doi, Y., Itoh, M., Yonemura, S., Ishihara, S., Takano, H., Noda, T., Tsukita, S. and Tsukita, S. 1999. Normal development of mice and unimpaired cell adhesion/cell motility/actin-based cytoskeleton without compensatory up-regulation of ezrin or radixin in moesin gene knockout. *Journal of Biological Chemistry,* 274(4), pp.2315-2321.

Dyche Mullins, R. and Pollard, T.D. 1999. Structure and function of the Arp2/3 complex. *Current Opinion in Structural Biology,* 9(2), pp.244-249.

Efimov, A., Schiefermeier, N., Grigoriev, I., Brown, M.C., Turner, C.E., Small, J.V. and Kaverina, I. 2008. Paxillin-dependent stimulation of microtubule catastrophes at focal adhesion sites. *Journal of Cell Science,* 121(2), pp.196-204.

Endemann, D.H. and Schiffrin, E.L. 2004. Endothelial dysfunction. *Journal of the American Society of Nephrology,* 15(8), pp.1983-1992.

Estreicher, A., Mühlhauser, J., Carpentier, J., Orci, L. and Vassalli, J. 1990. The receptor for urokinase type plasminogen activator polarizes expression of the protease to the leading edge of migrating monocytes and promotes degradation of enzyme inhibitor complexes. *The Journal of Cell Biology,* 111(2), pp.783-792.

Etienne-Manneville, S. and Hall, A. 2002. Rho GTPases in cell biology. *Nature,* 420(6916), pp.629-635.

Evans, D.G.R., Huson, S., Donnai, D., Neary, W., Blair, V., Newton, V. and Harris, R. 1992. A clinical study of type 2 neurofibromatosis. *QJM,* 84(1), pp.603-618.

Fazioli, F., Resnati, M., Sidenius, N., Higashimoto, Y., Appella, E. and Blasi, F. 1997. A urokinase-sensitive region of the human urokinase receptor is responsible for its chemotactic activity. *The EMBO Journal,* 16(24), pp.7279-7286.

Fishman, A.P. 1982. Endothelium: a distributed organ of diverse capabilities. *Annals of the New York Academy of Sciences,* 401(1), pp.1-8.

Folkow, B. 1993. Early structural changes in hypertension: pathophysiology and clinical consequences. *Journal of Cardiovascular Pharmacology,* 22pp.S1.

Förstermann, U. and Münzel, T. 2006. Endothelial nitric oxide synthase in vascular disease from marvel to menace. *Circulation,* 113(13), pp.1708-1714.

Furchgott, R.F. and Zawadzki, J.V. 1980. The obligatory role of endothelial cells in the relaxation of arterial smooth muscle by acetylcholine.

Gårdsvoll, H. and Ploug, M. 2007. Mapping of the Vitronectin-binding Site on the urokinase receptor involvement of a coherent receptor interface consisting of residues from both domain I and the flanking interdomain linker region. *Journal of Biological Chemistry,* 282(18), pp.13561-13572.

Gargiulo, L., Longanesi-Cattani, I., Bifulco, K., Franco, P., Raiola, R., Campiglia, P., Grieco, P., Peluso, G., Stoppelli, M.P. and Carriero, M.V. 2005. Cross-talk between fMLP and vitronectin receptors triggered by urokinase receptor-derived SRSRY peptide. *Journal of Biological Chemistry,* 280(26), pp.25225-25232.

Goldman, R. D., Chou, Y. H., Prahlad, V. and Yoon, M. (1999). Intermediate filaments: dynamic processes regulating their assembly, motility, and interactions with other cytoskeletal systems. FASEB J 13 Suppl 2, S261-5.

Gonsior, S.M., Platz, S., Buchmeier, S., Scheer, U., Jockusch, B.M. and Hinssen, H. 1999. Conformational difference between nuclear and cytoplasmic actin as detected by a monoclonal antibody. *Journal of Cell Science,* 112(6), pp.797-809.

Gonzalez-Agosti, C., Xu, L., Pinney, D., Beauchamp, R., Hobbs, W., Gusella, J. and Ramesh, V. 1996. The merlin tumor suppressor localizes preferentially in membrane ruffles. *Oncogene,* 13(6), pp.1239.

Grover-Páez, F. and Zavalza-Gómez, A.B. 2009. Endothelial dysfunction and cardiovascular risk factors. *Diabetes Research and Clinical Practice,* 84(1), pp.1-10.

Grunewald, T.G., Kammerer, U., Kapp, M., Eck, M., Dietl, J., Butt, E. and Honig, A. 2007. Nuclear localization and cytosolic overexpression of LASP-1 correlates with tumor size and nodal-positivity of human breast carcinoma. *BMC Cancer,* 7(1), pp.198.

Grunewald, T.G., Kammerer, U., Schulze, E., Schindler, D., Honig, A., Zimmer, M. and Butt, E. 2006. Silencing of LASP-1 influences zyxin localization, inhibits proliferation and reduces migration in breast cancer cells. *Experimental Cell Research,* 312(7), pp.974-982.

Gryglewski, R.J. 1995. Interactions between endothelial mediators. *Pharmacology & Toxicology,* 77(1), pp.1-9.

Gudi, S.R., Clark, C.B. and Frangos, J.A. 1996. Fluid Flow Rapidly Activates G Proteins in Human Endothelial Cells Involvement of G Proteins in Mechanochemical Signal Transduction. *Circulation Research,* 79(4), pp.834-839.

Gudi, S., Huvar, I., White, C.R., McKnight, N.L., Dusserre, N., Boss, G.R. and Frangos, J.A. 2003. Rapid activation of Ras by fluid flow is mediated by Gαq and Gβγ subunits of heterotrimeric G proteins in human endothelial cells. *Arteriosclerosis, Thrombosis, and Vascular Biology,* 23(6), pp.994-1000.

Gutmann, D.H., Giordano, M.J., Fishback, A.S. and Guha, A. 1997. Loss of merlin expression in sporadic meningiomas, ependymomas and schwannomas. *Neurology,* 49(1), pp.267-270.

Gutmann, D.H., Sherman, L., Seftor, L., Haipek, C., Lu, K.H. and Hendrix, M. 1999. Increased expression of the NF2 tumor suppressor gene product, merlin, impairs cell motility, adhesion and spreading. *Human Molecular Genetics,* 8(2), pp.267-275.

Hadi, H.A., Carr, C.S. and Al Suwaidi, J. 2005. Endothelial dysfunction: cardiovascular risk factors, therapy, and outcome. *Vascular Health and Risk Management,* 1(3), pp.183.

Hahn, C. and Schwartz, M.A. 2009. Mechanotransduction in vascular physiology and atherogenesis. *Nature Reviews Molecular Cell Biology,* 10(1), pp.53-62.

Hamm, H.E. 1998. The many faces of G protein signaling. *Journal of Biological Chemistry,* 273(2), pp.669-672.

Harris, A.K., Wild, P. and Stopak, D. 1980. Silicone rubber substrata: a new wrinkle in the study of cell locomotion. *Science,* 208(4440), pp.177-179.

Heath, J.P. and Holifield, B.F. 1992. On the mechanisms of cortical actin flow and its role in cytoskeletal organisation of fibroblasts. *IN: Symposia of the Society for Experimental Biology.* 47:35-56.

Hemmings, L., Rees, D., Ohanian, V., Bolton, S., Gilmore, A., Patel, B., Priddle, H., Trevithick, J., Hynes, R. and Critchley, D. 1996. Talin contains three actin-binding sites

each of which is adjacent to a vinculin-binding site. *Journal of Cell Science,* 109(11), pp.2715-2726.

Hendrickson, R.J., Cahill, P.A., Sitzmann, J.V. and Redmond, E.M. 1999. Ethanol enhances basal and flow-stimulated nitric oxide synthase activity in vitro by activating an inhibitory guanine nucleotide binding protein. *Journal of Pharmacology and Experimental Therapeutics,* 289(3), pp.1293-1300.

Herrlich, P., Morrison, H., Sleeman, J., ORIAN-ROUSSEAU, V., König, H., WEG-REMERS, S. and Ponta, H. 2000. CD44 Acts Both as a Growth-and Invasiveness-Promoting Molecule and as a Tumor-Suppressing Cofactor. *Annals of the New York Academy of Sciences,* 910(1), pp.106-120.

Hoffman, B.D., Grashoff, C. and Schwartz, M.A. 2011. Dynamic molecular processes mediate cellular mechanotransduction. *Nature,* 475(7356), pp.316-323.

Hofmann, W., Reichart, B., Ewald, A., Müller, E., Schmitt, I., Stauber, R.H., Lottspeich, F., Jockusch, B.M., Scheer, U. and Hauber, J. 2001. Cofactor Requirements for Nuclear Export of Rev Response Element (Rre)–And Constitutive Transport Element (Cte)–Containing Retroviral Rnas An Unexpected Role for Actin. *The Journal of Cell Biology,* 152(5), pp.895-910.

Huai, Q., Zhou, A., Lin, L., Mazar, A.P., Parry, G.C., Callahan, J., Shaw, D.E., Furie, B., Furie, B.C. and Huang, M. 2008. Crystal structures of two human vitronectin, urokinase and urokinase receptor complexes. *Nature Structural & Molecular Biology,* 15(4), pp.422-423.

Huang, L., Ichimaru, E., Pestonjamasp, K., Cui, X., Nakamura, H., Lo, G.Y., Lin, F.I., Luna, E.J. and Furthmayr, H. 1998. Merlin differs from moesin in binding to F-actin and in its intra-and intermolecular interactions. *Biochemical and Biophysical Research Communications,* 248(3), pp.548-553.

Humphries, J.D., Askari, J.A., Zhang, X., Takada, Y., Humphries, M.J. and Mould, A.P. 2000. Molecular basis of ligand recognition by integrin alpha5beta 1. II. Specificity of arg-gly-Asp binding is determined by Trp157 of the alpha subunit.. *Journal of Biological Chemistry,* 275(27), pp.20337-20345.

Hunt, B.J., Poston, L., Scachter, M. and Halliday, A. 2002. *An introduction to vascular biology.* Cambridge University Press. Online ISBN:9780511545948

Huttenlocher, A. and Horwitz, A.R. 2011. Integrins in cell migration. *Cold Spring Harbor Perspectives in Biology,* 3(9),

Huttenlocher, A., Sandborg, R.R. and Horwitz, A.F. 1995. Adhesion in cell migration. *Current Opinion in Cell Biology,* 7(5), pp.697-706.

Hynes, R.O. 1992. Integrins: versatility, modulation, and signaling in cell adhesion. *Cell,* 69(1), pp.11-25.

Ikeda, K., Saeki, Y., Gonzalez-Agosti, C., Ramesh, V. and Chiocca, E.A. 1999. Inhibition of NF2-negative and NF2-positive primary human meningioma cell proliferation by overexpression of merlin due to vector-mediated gene transfer. *Journal of Neurosurgery,* 91(1), pp.85-92.

JA, A.G. 2002. Inhibition of FAK signaling activated by urokinase receptor induces dormancy in human carcinoma cells in vivo. *Oncogene,* 21(16), pp.2513-2524.

Jankovics, F., Sinka, R., Lukácsovich, T. and Erdélyi, M. 2002. MOESIN Crosslinks Actin and Cell Membrane in Drosophila Oocytes and Is Required for OSKAR Anchoring. *Current Biology,* 12(23), pp.2060-2065.

Jester, J.V., Huang, J., Barry–Lane, P.A., Kao, W.W., Petroll, W.M. and Cavanagh, H.D. 1999. Transforming Growth Factorβ–Mediated Corneal Myofibroblast Differentiation Requires Actin and Fibronectin Assembly. *Investigative Ophthalmology & Visual Science,* 40(9), pp.1959-1967.

Jockusch, B.M., Schoenenberger, C., Stetefeld, J. and Aebi, U. 2006. Tracking down the different forms of nuclear actin. *Trends in Cell Biology,* 16(8), pp.391-396.

Juliano, R.L. and Varner, J.A. 1993. Adhesion molecules in cancer: the role of integrins. *Current Opinion in Cell Biology,* 5(5), pp.812-818.

Kamikubo, Y., Neels, J.G. and Degryse, B. 2009. Vitronectin inhibits plasminogen activator inhibitor-1-induced signalling and chemotaxis by blocking plasminogen activator inhibitor-1 binding to the low-density lipoprotein receptor-related protein. *The International Journal of Biochemistry & Cell Biology,* 41(3), pp.578-585.

Karagiosis, S.A. and Ready, D.F. 2004. Moesin contributes an essential structural role in Drosophila photoreceptor morphogenesis. *Development,* 131(4), pp.725-732.

Katoh, H. and Negishi, M. 2003. RhoG activates Rac1 by direct interaction with the Dock180-binding protein Elmo. *Nature,* 424(6947), pp.461-464.

Katsumi, A., Orr, A.W., Tzima, E. and Schwartz, M.A. 2004. Integrins in mechanotransduction. *Journal of Biological Chemistry,* 279(13), pp.12001-12004.

Kaverina, I., Rottner, K. and Small, J.V. 1998. Targeting, capture, and stabilization of microtubules at early focal adhesions. *The Journal of Cell Biology,* 142(1), pp.181-190.

Kikuchi, S., Hata, M., Fukumoto, K., Yamane, Y., Matsui, T., Tamura, A., Yonemura, S., Yamagishi, H., Keppler, D. and Tsukita, S. 2002. Radixin deficiency causes

conjugated hyperbilirubinemia with loss of Mrp2 from bile canalicular membranes. *Nature Genetics,* 31(3), pp.320-325.

Kinashi, Y., Sakurai, Y., Masunaga, S., Suzuki, M., Akaboshi, M. and Ono, K. 2000. Dimethyl sulfoxide protects against thermal and epithermal neutron-induced cell death and mutagenesis of Chinese hamster ovary (CHO) cells. *International Journal of Radiation Oncology* Biology* Physics,* 47(5), pp.1371-1378.

Kissil, J.L., Johnson, K.C., Eckman, M.S. and Jacks, T. 2002. Merlin phosphorylation by p21-activated kinase 2 and effects of phosphorylation on merlin localization. *Journal of Biological Chemistry,* 277(12), pp.10394-10399.

Kitajiri, S., Fukumoto, K., Hata, M., Sasaki, H., Katsuno, T., Nakagawa, T., Ito, J., Tsukita, S. and Tsukita, S. 2004. Radixin deficiency causes deafness associated with progressive degeneration of cochlear stereocilia. *The Journal of Cell Biology,* 166(4), pp.559-570.

Kjaergaard, M., Hansen, L.V., Jacobsen, B., Gardsvoll, H. and Ploug, M. 2008. Structure and ligand interactions of the urokinase receptor (uPAR). *Frontiers in Bioscience : A Journal and Virtual Library,* 13pp.5441-5461.

Kjøller, L. and Hall, A. 2001. Rac mediates cytoskeletal rearrangements and increased cell motility induced by urokinase-type plasminogen activator receptor binding to vitronectin. *The Journal of Cell Biology,* 152(6), pp.1145-1158.

Knezevic, N., Tauseef, M., Thennes, T. and Mehta, D. 2009. The G protein βγ subunit mediates reannealing of adherens junctions to reverse endothelial permeability increase by thrombin. *The Journal of Experimental Medicine,* 206(12), pp.2761-2777.

Kris, A.S., Kamm, R.D. and Sieminski, A.L. 2008. VASP involvement in force-mediated adherens junction strengthening. *Biochemical and Biophysical Research Communications,* 375(1), pp.134-138.

Kuchan, M. and Frangos, J. 1993. Shear stress regulates endothelin-1 release via protein kinase C and cGMP in cultured endothelial cells. *American Journal of Physiology-Heart and Circulatory Physiology,* 264(1), pp.H150-H156.

Kunda, P., Pelling, A.E., Liu, T. and Baum, B. 2008. Moesin controls cortical rigidity, cell rounding, and spindle morphogenesis during mitosis. *Current Biology,* 18(2), pp.91-101.

Kurokawa, K., Nakamura, T., Aoki, K. and Matsuda, M. 2005. Mechanism and role of localized activation of Rho-family GTPases in growth factor-stimulated fibroblasts and neuronal cells. *Biochemical Society Transactions,* 33(4), pp.631-634.

Kurokawa, K. and Matsuda, M. 2005. Localized RhoA activation as a requirement for the induction of membrane ruffling. *Molecular Biology of the Cell,* 16(9),pp.4294-4303.

LaJeunesse, D.R., McCartney, B.M. and Fehon, R.G. 1998. Structural analysis of Drosophila merlin reveals functional domains important for growth control and subcellular localization. *The Journal of Cell Biology,* 141(7), pp.1589-1599.

Lallemand, D., Curto, M., Saotome, I., Giovannini, M. and McClatchey, A.I. 2003. NF2 deficiency promotes tumorigenesis and metastasis by destabilizing adherens junctions. *Genes & Development,* 17(9), pp.1090-1100.

Langille, B.L. and Adamson, S.L. 1981. Relationship between blood flow direction and endothelial cell orientation at arterial branch sites in rabbits and mice. *Circulation Research,* 48(4), pp.481-488.

Laukaitis, C.M., Webb, D.J., Donais, K. and Horwitz, A.F. 2001. Differential dynamics of α5 integrin, paxillin, and α-actinin during formation and disassembly of adhesions in migrating cells. *The Journal of Cell Biology,* 153(7), pp.1427-1440.

Lee, J. and Gotlieb, A. 2002. Microtubule–actin interactions may regulate endothelial integrity and repair. *Cardiovascular Pathology,* 11(3), pp.135-140.

Lee, R.C., Feinbaum, R.L. and Ambros, V. 1993. The C. elegans heterochronic gene lin-4 encodes small RNAs with antisense complementarity to lin-14*Cell,* 75(5), pp.843-854.

Lee, T.J. and Gotlieb, A.I. 2003. Microfilaments and microtubules maintain endothelial integrity. *Microscopy Research and Technique,* 60(1), pp.115-127.

Lehoux, S. and Tedgui, A. 2003. Cellular mechanics and gene expression in blood vessels. *Journal of Biomechanics,* 36(5), pp.631-643.

Leiss, M., Beckmann, K., Girós, A., Costell, M. and Fässler, R. 2008. The role of integrin binding sites in fibronectin matrix assembly in vivo. *Current Opinion in Cell Biology,* 20(5), pp.502-507.

Leptin, M. 1986. Cell biology: The fibronectin receptor family. *Nature,* 321pp.728.

Li, B., Zhuang, L. and Trueb, B. 2004. Zyxin interacts with the SH3 domains of the cytoskeletal proteins LIM-nebulette and Lasp-1. *Journal of Biological Chemistry,* 279(19), pp.20401-20410.

Lin, Y.H., Park, Z., Lin, D., Brahmbhatt, A.A., Rio, M., Yates, J.R. and Klemke, R.L. 2004. Regulation of cell migration and survival by focal adhesion targeting of Lasp-1. *The Journal of Cell Biology,* 165(3), pp.421-432.

Llinas, P., Le Du, M.H., Gårdsvoll, H., Danø, K., Ploug, M., Gilquin, B., Stura, E.A. and Ménez, A. 2005. Crystal structure of the human urokinase plasminogen activator receptor bound to an antagonist peptide. *The EMBO Journal,* 24(9), pp.1655-1663.

Lodish,H. Berk, A. Kaiser C, Krieger, M. Scott, M. Bretscher, A. Ploegh, H. Matsudaira, P. (2007). Molecular Cell Biology. 6th ed. USA: W.H. Freeman and Company. p748-751.

Loscalzo, J. and Welch, G. 1995. Nitric oxide and its role in the cardiovascular system. *Progress in Cardiovascular Diseases,* 38(2), pp.87-104.

Lowell, C.A. and Mayadas, T.N. 2012. Overview: studying integrins in vivo *IN:* Anonymous*Integrin and Cell Adhesion Molecules.* Springer, pp.369-397.

Madsen, C.D. and Sidenius, N. 2008. The interaction between urokinase receptor and vitronectin in cell adhesion and signalling. *European Journal of Cell Biology,* 87(8), pp.617-629.

Mallavarapu, A. and Mitchison, T. 1999. Regulated actin cytoskeleton assembly at filopodium tips controls their extension and retraction. *The Journal of Cell Biology,* 146(5), pp.1097-1106.

Mangeat, P., Roy, C. and Martin, M. 1999. ERM proteins in cell adhesion and membrane dynamics. *Trends in Cell Biology,* 9(5), pp.187-192.

Martinac, B. 2004. Mechanosensitive ion channels: molecules of mechanotransduction. *Journal of Cell Science,* 117(12), pp.2449-2460.

McClatchey, A.I. and Fehon, R.G. 2009. Merlin and the ERM proteins–regulators of receptor distribution and signaling at the cell cortex. *Trends in Cell Biology,* 19(5), pp.198-206.

McClatchey, A.I., Saotome, I., Mercer, K., Crowley, D., Gusella, J.F., Bronson, R.T. and Jacks, T. 1998. Mice heterozygous for a mutation at the Nf2 tumor suppressor locus develop a range of highly metastatic tumors. *Genes & Development,* 12(8), pp.1121-1133.

McClatchey, A.I., Saotome, I., Ramesh, V., Gusella, J.F. and Jacks, T. 1997. The Nf2 tumor suppressor gene product is essential for extraembryonic development immediately prior to gastrulation. *Genes & Development,* 11(10), pp.1253-1265.

McCue, S., Dajnowiec, D., Xu, F., Zhang, M., Jackson, M.R. and Langille, B.L. 2006. Shear stress regulates forward and reverse planar cell polarity of vascular endothelium in vivo and in vitro. *Circulation Research,* 98(7), pp.939-946.

McGough, A., Way, M. and DeRosier, D. 1994. Determination of the alpha-actinin-binding site on actin filaments by cryoelectron microscopy and image analysis. *The Journal of Cell Biology,* 126(2), pp.433-443.

Mohri, H. and Ohkubo, T. 1991. How vitronectin binds to activated glycoprotein IIb-IIIa complex and its function in platelet aggregation. *American Journal of Clinical Pathology,* 96(5), pp.605.

Moissoglu, K. and Schwartz, M.A. 2006. Integrin signalling in directed cell migration. *Biology of the Cell,* 98(9), pp.547-555.

Montecucco, F. and Mach, F. 2009. Atherosclerosis is an inflammatory disease. *IN: Seminars in immunopathology.* Springer.

Montuori, N., Mattiello, A., Mancini, A., Santoli, M., Taglialatela, P., Caputi, M., Rossi, G. and Ragno, P. 2001. Urokinase-type plasminogen activator up-regulates the expression of its cellular receptor through a post-transcriptional mechanism. *FEBS Letters,* 508(3), pp.379-384.

Morrison, H., Sherman, L.S., Legg, J., Banine, F., Isacke, C., Haipek, C.A., Gutmann, D.H., Ponta, H. and Herrlich, P. 2001. The NF2 tumor suppressor gene product, merlin, mediates contact inhibition of growth through interactions with CD44. *Genes & Development,* 15(8), pp.968-980.

Mould, A. and Humphries, M. 1991. Identification of a novel recognition sequence for the integrin alpha 4 beta 1 in the COOH-terminal heparin-binding domain of fibronectin. *The EMBO Journal,* 10(13), pp.4089.

Muranen, T., Grönholm, M., Lampin, A., Lallemand, D., Zhao, F., Giovannini, M. and Carpén, O. 2007. The tumor suppressor merlin interacts with microtubules and modulates Schwann cell microtubule cytoskeleton. *Human Molecular Genetics,* 16(14), pp.1742-1751.

Nerem, R.M., Levesque, M.J. and Cornhill, J.F. 1981. Vascular endothelial morphology as an indicator of the pattern of blood flow. *Journal of Biomechanical Engineering,* 103(3), pp.172-176.

Nip, J., Shibata, H., Loskutoff, D.J., Cheresh, D.A. and Brodt, P. 1992. Human melanoma cells derived from lymphatic metastases use integrin alpha v beta 3 to adhere to lymph node vitronectin. *Journal of Clinical Investigation,* 90(4), pp.1406.

Nobes, C. and Hall, A. 1995. Rho, rac and cdc42 GTPases: regulators of actin structures, cell adhesion and motility. *Biochemical Society Transactions,* 23(3), pp.456-459.

Nolz, J.C., Nacusi, L.P., Segovis, C.M., Medeiros, R.B., Mitchell, J.S., Shimizu, Y. and Billadeau, D.D. 2008. The WAVE2 complex regulates T cell receptor signaling to integrins via Abl-and CrkL–C3G-mediated activation of Rap1. *The Journal of Cell Biology,* 182(6), pp.1231-1244.

Obremski, V.J., Hall, A.M. and Fernandez-Valle, C. 1998. Merlin, the neurofibromatosis type 2 gene product, and β1 integrin associate in isolated and differentiating Schwann cells. *Journal of Neurobiology,* 37(4), pp.487-501.

Ohno, M., Gibbons, G.H., Dzau, V.J. and Cooke, J.P. 1993. Shear stress elevates endothelial cGMP. Role of a potassium channel and G protein coupling. *Circulation,* 88(1), pp.193-197.

Olave, I.A., Reck-Peterson, S.L. and Crabtree, G.R. 2002. Nuclear actin and actin-related proteins in chromatin remodeling. *Annual Review of Biochemistry,* 71(1), pp.755-781.

Olesen, S., Claphamt, D. and Davies, P. 1988. Haemodynamic shear stress activates a K current in vascular endothelial cells. *Nature,* 331(6152), pp.168-170.

Orr, A.W., Helmke, B.P., Blackman, B.R. and Schwartz, M.A. 2006. Mechanisms of mechanotransduction. *Developmental Cell,* 10(1), pp.11-20.

Ossowski, L. and Aguirre-Ghiso, J.A. 2000. Urokinase receptor and integrin partnership: coordination of signaling for cell adhesion, migration and growth. *Current Opinion in Cell Biology,* 12(5), pp.613-620.

Papadaki, M. and Eskin, S.G. 1997. Effects of fluid shear stress on gene regulation of vascular cells. *Biotechnology Progress,* 13(3), pp.209-221.

Parsons, J.T., Horwitz, A.R. and Schwartz, M.A. 2010. Cell adhesion: integrating cytoskeletal dynamics and cellular tension. *Nature Reviews Molecular Cell Biology,* 11(9), pp.633-643.

Pierschbacher, M.D. and Ruoslahti, E. 1984. Variants of the cell recognition site of fibronectin that retain attachment-promoting activity. *Proceedings of the National Academy of Sciences,* 81(19), pp.5985-5988.

Pilot, F., Philippe, J., Lemmers, C. and Lecuit, T. 2006. Spatial control of actin organization at adherens junctions by a synaptotagmin-like protein. *Nature,* 442(7102), pp.580-584.

Ploug, M. and Ellis, V. 1994. Structure—function relationships in the receptor for urokinase-type plasminogen activator Comparison to other members of the Ly-6 family and snake venom α-neurotoxins. *FEBS Letters,* 349(2), pp.163-168.

Polesello, C., Delon, I., Valenti, P., Ferrer, P. and Payre, F. 2002. Dmoesin controls actin-based cell shape and polarity during Drosophila melanogaster oogenesis. *Nature Cell Biology,* 4(10), pp.782-789.

Pollard, T.D. and Beltzner, C.C. 2002. Structure and function of the Arp2/3 complex. *Current Opinion in Structural Biology,* 12(6), pp.768-774.

Pottiez, G., Sevin, E., Cecchelli, R., Karamanos, Y. and Flahaut, C. 2009. Actin, gelsolin and filamin-A are dynamic actors in the cytoskeleton remodelling contributing to the blood brain barrier phenotype. *Proteomics,* 9(5), pp.1207-1219.

Prager, G.W., Breuss, J.M., Steurer, S., Mihaly, J. and Binder, B.R. 2004. Vascular endothelial growth factor (VEGF) induces rapid prourokinase (pro-uPA) activation on the surface of endothelial cells. *Blood,* 103(3), pp.955-962.

Preissner, K.T. and Jenne, D. 1991. Vitronectin: a new molecular connection in haemostasis. *Thrombosis and Haemostasis,* 66(2), pp.189-194.

Pytela, R., Pierschbacher, M.D., Ginsberg, M.H., Plow, E.F. and Ruoslahti, E. 1986. Platelet membrane glycoprotein IIb/IIIa: member of a family of Arg-Gly-Asp--specific adhesion receptors. *Science,* 231(4745), pp.1559-1562.

Pytela, R., Pierschbacher, M.D. and Ruoslahti, E. 1985a. A 125/115-kDa cell surface receptor specific for vitronectin interacts with the arginine-glycine-aspartic acid adhesion sequence derived from fibronectin. *Proceedings of the National Academy of Sciences,* 82(17), pp.5766-5770.

Pytela, R., Pierschbacher, M.D. and Ruoslahti, E. 1985b. Identification and isolation of a 140 kd cell surface glycoprotein with properties expected of a fibronectin receptor. *Cell,* 40(1), pp.191-198.

Ragno, P. 2006. The urokinase receptor: a ligand or a receptor? Story of a sociable molecule. *Cellular and Molecular Life Sciences CMLS,* 63(9), pp.1028-1037.

Ramesh, V. 2004. Merlin and the ERM proteins in Schwann cells, neurons and growth cones. *Nature Reviews Neuroscience,* 5(6), pp.462-470.

Ratnikov, B., Partridge, A. and Ginsberg, M. 2005. Integrin activation by talin. *Journal of Thrombosis and Haemostasis,* 3(8), pp.1783-1790.

Redick, S.D., Settles, D.L., Briscoe, G. and Erickson, H.P. 2000. Defining fibronectin's cell adhesion synergy site by site-directed mutagenesis. *The Journal of Cell Biology,* 149(2), pp.521-527.

Redmond, E.M., Cahill, P.A. and Sitzmann, J.V. 1998. Flow-mediated regulation of G-protein expression in cocultured vascular smooth muscle and endothelial cells. *Arteriosclerosis, Thrombosis, and Vascular Biology,* 18(1), pp.75-83.

Reed, N. and Gutmann, D.H. 2001. Tumorigenesis in neurofibromatosis: new insights and potential therapies. *Trends in Molecular Medicine,* 7(4), pp.157-162.

Resnati, M., Guttinger, M., Valcamonica, S., Sidenius, N., Blasi, F. and Fazioli, F. 1996. Proteolytic cleavage of the urokinase receptor substitutes for the agonist-induced chemotactic effect. *The EMBO Journal,* 15(7), pp.1572.

Resnick, N., Yahav, H., Shay-Salit, A., Shushy, M., Schubert, S., Zilberman, L.C.M. and Wofovitz, E. 2003. Fluid shear stress and the vascular endothelium: for better and for worse. *Progress in Biophysics and Molecular Biology,* 81(3), pp.177-199.

Rid, R., Schiefermeier, N., Grigoriev, I., Small, J.V. and Kaverina, I. 2005. The last but not the least: the origin and significance of trailing adhesions in fibroblastic cells. *Cell Motility and the Cytoskeleton,* 61(3), pp.161-171.

Ridley, A.J., Schwartz, M.A., Burridge, K., Firtel, R.A., Ginsberg, M.H., Borisy, G., Parsons, J.T. and Horwitz, A.R. 2003. Cell migration: integrating signals from front to back. *Science,* 302(5651), pp.1704-1709.

Rinnerthaler, G., Geiger, B. and Small, J. 1988. Contact formation during fibroblast locomotion: involvement of membrane ruffles and microtubules. *J.Cell Biol,* 106pp.747-760.

Ross, R., 1999. Atherosclerosis--an inflammatory diseas. N Engl J Med. 1999 Jan 14;340(2):115-26.

Rouleau, G.A., Merel, P., Lutchman, M., Sanson, M., Zucman, J., Marineau, C., Hoang-Xuan, K., Demczuk, S., Desmaze, C. and Plougastel, B. 1993. Alteration in a new gene encoding a putative membrane-organizing protein causes neuro-fibromatosis type 2. Nature 363, 515 - 521 (10 June 1993); doi:10.1038/363515a0

Rubanyi, G.M., Romero, J.C. and Vanhoutte, P.M. 1986. Flow-induced release of endothelium-derived relaxing factor. *American Journal of Physiology-Heart and Circulatory Physiology,* 250(6), pp.H1145-H1149.

Sainio, M., Zhao, F., Heiska, L., Turunen, O., den Bakker, M., Zwarthoff, E., Lutchman, M., Rouleau, G.A., Jaaskelainen, J. and Vaheri, A. 1997. Neurofibromatosis 2 tumor suppressor protein colocalizes with ezrin and CD44 and associates with actin-containing cytoskeleton. *Journal of Cell Science,* 110(18), pp.2249-2260.

Saldanha, R.G., Molloy, M.P., Bdeir, K., Cines, D.B., Song, X., Uitto, P.M., Weinreb, P.H., Violette, S.M. and Baker, M.S. 2007. Proteomic identification of lynchpin urokinase plasminogen activator receptor protein interactions associated with epithelial cancer malignancy. *Journal of Proteome Research,* 6(3), pp.1016-1028.

Saotome, I., Curto, M. and McClatchey, A.I. 2004. Ezrin is essential for epithelial organization and villus morphogenesis in the developing intestine. *Developmental Cell,* 6(6), pp.855-864.

Sato, N., Funayama, N., Nagafuchi, A., Yonemura, S. and Tsukita, S. 1992. A gene family consisting of ezrin, radixin and moesin. Its specific localization at actin filament/plasma membrane association sites. *Journal of Cell Science,* 103(1), pp.131-143.

Saydam, O., Senol, O., Würdinger, T., Mizrak, A., Ozdener, G.B., Stemmer-Rachamimov, A.O., Yi, M., Stephens, R.M., Krichevsky, A.M. and Saydam, N. 2011. miRNA-7 attenuation in Schwannoma tumors stimulates growth by upregulating three oncogenic signaling pathways. *Cancer Research,* 71(3), pp.852-861.

Schiller, H.B., Szekeres, A., Binder, B.R., Stockinger, H. and Leksa, V. 2009. Mannose 6-phosphate/insulin-like growth factor 2 receptor limits cell invasion by controlling αVβ3 integrin expression and proteolytic processing of urokinase-type plasminogen activator receptor. *Molecular Biology of the Cell,* 20(3), pp.745-756.

Schoenenberger, C., Buchmeier, S., Boerries, M., Sütterlin, R., Aebi, U. and Jockusch, B. 2005. Conformation-specific antibodies reveal distinct actin structures in the nucleus and the cytoplasm. *Journal of Structural Biology,* 152(3), pp.157-168.

Schreiber, V., Moog-Lutz, C. and RÃ, C. 1998. Lasp-1, a novel type of actin-binding protein accumulating in cell membrane extensions. *Molecular Medicine,* 4(10), pp.675.

Schwartz, M.A. and Assoian, R.K. 2001. Integrins and cell proliferation regulation of cyclin-dependent kinases via cytoplasmic signaling pathways. *Journal of Cell Science,* 114(14), pp.2553-2560.

Scliwa, M. and Höner, B. 1993. Microtubules, centrosomes and intermediate filaments in directed cell movement. *Trends in Cell Biology,* 3(11), pp.377-380.

Scoles, D.R. 2008. The merlin interacting proteins reveal multiple targets for NF2 therapy. *Biochimica Et Biophysica Acta (BBA)-Reviews on Cancer,* 1785(1), pp.32-54.

Shaw, R.J., McClatchey, A.I. and Jacks, T. 1998. Regulation of the neurofibromatosis type 2 tumor suppressor protein, merlin, by adhesion and growth arrest stimuli. *Journal of Biological Chemistry,* 273(13), pp.7757-7764.

Sherman, L., Xu, H.M., Geist, R.T., Saporito-Irwin, S., Howells, N., Ponta, H., Herrlich, P. and Gutmann, D.H. 1997. Interdomain binding mediates tumor growth suppression by the NF2 gene product. *Oncogene,* 15(20), pp.2505-2509.

Shimizu, T., Seto, A., Maita, N., Hamada, K., Tsukita, S., Tsukita, S. and Hakoshima, T. 2002. Structural basis for neurofibromatosis type 2. *Journal of Biological Chemistry,* 277(12), pp.10332-10336.

Sima, A.V., Stancu, C.S. and Simionescu, M. 2009. Vascular endothelium in atherosclerosis. *Cell and Tissue Research,* 335(1), pp.191-203.

Simon, D.I., Wei, Y., Zhang, L., Rao, N.K., Xu, H., Chen, Z., Liu, Q., Rosenberg, S. and Chapman, H.A. 2000. Identification of a urokinase receptor-integrin interaction site promiscuous regulator of integrin function. *Journal of Biological Chemistry,* 275(14), pp.10228-10234.

Small, E.M. and Olson, E.N. 2011. Pervasive roles of microRNAs in cardiovascular biology. *Nature,* 469(7330), pp.336-342.

Small, J.V. 1994. Lamellipodia architecture: actin filament turnover and the lateral flow of actin filaments during motility. *IN: Seminars in cell biology.* Elsevier.

Small, J.V., Geiger, B., Kaverina, I. and Bershadsky, A. 2002. How do microtubules guide migrating cells? *Nature Reviews Molecular Cell Biology,* 3(12), pp.957-964.

Speck, O., Hughes, S.C., Noren, N.K., Kulikauskas, R.M. and Fehon, R.G. 2003. Moesin functions antagonistically to the Rho pathway to maintain epithelial integrity. *Nature,* 421(6918), pp.83-87.

Springer, T.A. 1994. Traffic signals for lymphocyte recirculation and leukocyte emigration: the multistep paradigm. *Cell,* 76(2), pp.301-314.

Stamenkovic, I. and Yu, Q. 2010. Merlin, a "magic" linker between the extracellular cues and intracellular signaling pathways that regulate cell motility, proliferation, and survival. *Current Protein & Peptide Science,* 11(6), pp.471.

Stoneman, V.E. and Bennett, M.R. 2004. Role of apoptosis in atherosclerosis and its therapeutic implications. *Clinical Science,* 107(4), pp.343-354.

Stossel, T.P., Condeelis, J., Cooley, L., Hartwig, J.H., Noegel, A., Schleicher, M. and Shapiro, S.S. 2001. Filamins as integrators of cell mechanics and signalling. *Nature Reviews Molecular Cell Biology,* 2(2), pp.138-145.

Takada, Y., Ye, X. and Simon, S. 2007. The integrins. *Genome Biol,* 8(5), pp.215.

Tamura, A., Kikuchi, S., Hata, M., Katsuno, T., Matsui, T., Hayashi, H., Suzuki, Y., Noda, T., Tsukita, S. and Tsukita, S. 2005. Achlorhydria by ezrin knockdown defects in the formation/expansion of apical canaliculi in gastric parietal cells. *The Journal of Cell Biology,* 169(1), pp.21-28.

Tapon, N. and Hall, A. 1997. Rho, Rac and Cdc42 GTPases regulate the organization of the actin cytoskeleton. *Current Opinion in Cell Biology,* 9(1), pp.86-92.

Thiagarajan, P. and Kelly, K.L. 1988. Exposure of binding sites for vitronectin on platelets following stimulation. *Journal of Biological Chemistry,* 263(6), pp.3035-3038.

Toffoletto, E. 1965. *Discorso sul Malpighi.* Editrice Nigrizia.

Tomasetto, C., Moog-Lutz, C., Régnier, C.H., Schreiber, V., Basset, P. and Rio, M. 1995. Lasp-1 (MLN 50) defines a new LIM protein subfamily characterized by the association of LIM and SH3 domains. *FEBS Letters,* 373(3), pp.245-249.

Traub, O. and Berk, B.C. 1998. Laminar shear stress mechanisms by which endothelial cells transduce an atheroprotective force. *Arteriosclerosis, Thrombosis, and Vascular Biology,* 18(5), pp.677-685.

Trofatter, J.A., MacCollin, M.M., Rutter, J.L., Murrell, J.R., Duyao, M.P., Parry, D.M., Eldridge, R., Kley, N., Menon, A.G. and Pulaski, K. 1993. A novel moesin-, ezrin-, radixin-like gene is a candidate for the neurofibromatosis 2 tumor suppressor. *Cell,* 72(5), pp.791-800.

Tzima, E., del Pozo, M.A., Shattil, S.J., Chien, S. and Schwartz, M.A. 2001. Activation of integrins in endothelial cells by fluid shear stress mediates Rho-dependent cytoskeletal alignment. *The EMBO Journal,* 20(17), pp.4639-4647.

Vanhoutte, P., Shimokawa, H., Tang, E. and Feletou, M. 2009. Endothelial dysfunction and vascular disease. *Acta Physiologica,* 196(2), pp.193-222.

Vasiliev, J.M., Gelfand, I., Domnina, L., Ivanova, O.Y., Komm, S. and Olshevskaja, L. 1970. Effect of colcemid on the locomotory behaviour of fibroblasts. *Journal of Embryology and Experimental Morphology,* 24(3), pp.625-640.

Vial, E., Sahai, E. and Marshall, C.J. 2003. ERK-MAPK signaling coordinately regulates activity of Rac1 and RhoA for tumor cell motility. *Cancer Cell,* 4(1), pp.67-79.

Viel, A. and Branton, D. 1996. Spectrin: on the path from structure to function. *Current Opinion in Cell Biology,* 8(1), pp.49-55.

Virchow, R. 1989. As Based upon Physiological and Pathological Histology. *Nutrition Reviews,* 47(1), pp.23-25.

Vita, J.A. and Keaney, J.F. 2002. Endothelial function a barometer for cardiovascular risk? *Circulation,* 106(6), pp.640-642.

Vogel, V. 2006. Mechanotransduction involving multimodular proteins: converting force into biochemical signals. *Annu.Rev.Biophys.Biomol.Struct.,* 35pp.459-488.

Von Offenberg Sweeney, N., Cummins, P.M., Cotter, E.J., Fitzpatrick, P.A., Birney, Y.A., Redmond, E.M. and Cahill, P.A. 2005. Cyclic strain-mediated regulation of vascular endothelial cell migration and tube formation. *Biochemical and Biophysical Research Communications,* 329(2), pp.573-582.

Waltz, D.A. and Chapman, H.A. 1994. Reversible cellular adhesion to vitronectin linked to urokinase receptor occupancy. *Journal of Biological Chemistry,* 269(20), pp.14746-14750.

Watanabe, T., Noritake, J. and Kaibuchi, K. 2005. Regulation of microtubules in cell migration. *Trends in Cell Biology,* 15(2), pp.76-83.

Wechezak, A., Viggers, R. and Sauvage, L. 1985. Fibronectin and F-actin redistribution in cultured endothelial cells exposed to shear stress. *Laboratory Investigation; a Journal of Technical Methods and Pathology,* 53(6), pp.639-647.

Wei, C., El Hindi, S., Li, J., Fornoni, A., Goes, N., Sageshima, J., Maiguel, D., Karumanchi, S.A., Yap, H. and Saleem, M. 2011. Circulating urokinase receptor as a cause of focal segmental glomerulosclerosis. *Nature Medicine,* 17(8), pp.952-960.

Wei, C., Möller, C.C., Altintas, M.M., Li, J., Schwarz, K., Zacchigna, S., Xie, L., Henger, A., Schmid, H. and Rastaldi, M.P. 2007. Modification of kidney barrier function by the urokinase receptor. *Nature Medicine,* 14(1), pp.55-63.

Wei, Y., Czekay, R., Robillard, L., Kugler, M.C., Zhang, F., Kim, K.K., Xiong, J., Humphries, M.J. and Chapman, H.A. 2005. Regulation of α5β1 integrin conformation and function by urokinase receptor binding. *The Journal of Cell Biology,* 168(3), pp.501-511.

Wei, Y., Lukashev, M., Simon, D.I., Bodary, S.C., Rosenberg, S., Doyle, M.V. and Chapman, H.A. 1996. Regulation of integrin function by the urokinase receptor. *Science,* 273(5281), pp.1551-1555.

Wei, Y., Waltz, D.A., Rao, N., Drummond, R.J., Rosenberg, S. and Chapman, H.A. 1994. Identification of the urokinase receptor as an adhesion receptor for vitronectin. *Journal of Biological Chemistry,* 269(51), pp.32380-32388.

Weis, S.M. 2007. Evaluating integrin function in models of angiogenesis and vascular permeability. *Methods in Enzymology,* 426pp.505-528.

Wieland, T. and Mittmann, C. 2003. Regulators of G-protein signalling: multifunctional proteins with impact on signalling in the cardiovascular system. *Pharmacology & Therapeutics,* 97(2), pp.95-115.

Wong, A.J., Pollard, T.D. and Herman, I.M. 1983. Actin filament stress fibers in vascular endothelial cells in vivo. *Science,* 219(4586), pp.867-869.

Wu, M.H., Ustinova, E. and Granger, H.J. 2001. Integrin binding to fibronectin and vitronectin maintains the barrier function of isolated porcine coronary venules. *The Journal of Physiology,* 532(3), pp.785-791.

Xiao, G., Chernoff, J. and Testa, J.R. 2003. NF2: the wizardry of merlin. *Genes, Chromosomes and Cancer,* 38(4), pp.389-399.

Xu, H. and Gutmann, D.H. 1998. Merlin differentially associates with the microtubule and actin cytoskeleton. *Journal of Neuroscience Research,* 51(3), pp.403-415.

Xu, W., Baribault, H. and Adamson, E.D. 1998. Vinculin knockout results in heart and brain defects during embryonic development. *Development,* 125(2), pp.327-337.

Xue, W., Mizukami, I., Todd, R.F. and Petty, H.R. 1997. Urokinase-type plasminogen activator receptors associate with $\beta 1$ and $\beta 3$ integrins of fibrosarcoma cells: dependence on extracellular matrix components. *Cancer Research,* 57(9), pp.1682-1689.

Yelian, F.D., Edgeworth, N.A., Dong, L., Chung, A.E. and Armant, D.R. 1993. Recombinant entactin promotes mouse primary trophoblast cell adhesion and migration through the Arg-Gly-Asp (RGD) recognition sequence. *The Journal of Cell Biology,* 121(4), pp.923-929.

Zaidel-Bar, R. and Geiger, B. 2010. The switchable integrin adhesome. *Journal of Cell Science,* 123(9), pp.1385-1388.

Zhang, X., Jiang, G., Cai, Y., Monkley, S.J., Critchley, D.R. and Sheetz, M.P. 2008. Talin depletion reveals independence of initial cell spreading from integrin activation and traction. *Nature Cell Biology,* 10(9), pp.1062-1068.

Zhou, J., Chew, M., Ravn, H.B. and Falk, E. 1999. Plaque pathology and coronary thrombosis in the pathogenesis of acute coronary syndromes. *Scandinavian Journal of Clinical & Laboratory Investigation,* 59(S230), pp.3-11.

Ziegler, W.H., Liddington, R.C. and Critchley, D.R. 2006. The structure and regulation of vinculin. *Trends in Cell Biology,* 16(9), pp.453-460.

Zimerman, B., Volberg, T. and Geiger, B. 2004. Early molecular events in the assembly of the focal adhesion-stress fiber complex during fibroblast spreading. *Cell Motility and the Cytoskeleton,* 58(3), pp.143-159.